



Microévolution des déterminismes sexuels chez le poisson Tétra Mexicain, *Astyanax mexicanus*

Boudjema Imarazene

► To cite this version:

Boudjema Imarazene. Microévolution des déterminismes sexuels chez le poisson Tétra Mexicain, *Astyanax mexicanus*. Génétique animale. Université de Rennes, 2020. Français. NNT : 2020REN1B042 . tel-03899641v2

HAL Id: tel-03899641

<https://theses.hal.science/tel-03899641v2>

Submitted on 15 Dec 2022

HAL is a multi-disciplinary open access archive for the deposit and dissemination of scientific research documents, whether they are published or not. The documents may come from teaching and research institutions in France or abroad, or from public or private research centers.

L'archive ouverte pluridisciplinaire **HAL**, est destinée au dépôt et à la diffusion de documents scientifiques de niveau recherche, publiés ou non, émanant des établissements d'enseignement et de recherche français ou étrangers, des laboratoires publics ou privés.

THESE DE DOCTORAT DE

L'UNIVERSITE DE RENNES 1

ECOLE DOCTORALE N° 600

Ecole doctorale Ecologie, Géosciences, Agronomie et Alimentation

Spécialité : « *Génétique, Génomique et bioinformatique* »

Par

« Boudjema IMARAZENE »

« Microévolution des déterminismes sexuels chez le poisson Tétra Mexicain, *Astyanax mexicanus* »

Thèse présentée et soutenue à « Rennes », le « 14 décembre 2020 »

Unité de recherche : INRAE, UR 1037 Laboratoire de Physiologie et Génomique des Poissons (LPGP)

Rapporteurs avant soutenance :

Jean-François Baroiller
Odile Bronchain

DR, CIRAD, ISEM, Montpellier, France
MC, Univ Paris-Saclay, UMR9197, CNRS, Gif-sur-Yvette, France

Composition du Jury :

Président : Gilles Salbert
Examinateurs : Jean-François Baroiller
Odile Bronchain
Astrid Böhne
Amaury Herpin
Dir. de thèse : Yann Guiguen
Co-dir. de thèse : Sylvie Rétaux

Pr, UMR 6290, Université de Rennes 1, Rennes, France
DR, CIRAD, ISEM, Montpellier, France
MC, Univ Paris-Saclay, UMR9197, CNRS, Gif-sur-Yvette, France
DR, Research Museum Alexander Koenig, Bonn, Allemagne
CR, UR 1037 LPGP, INRAE, Rennes, France
DR, UR 1037 LPGP, INRAE, Rennes, France
DR, NeuroPsi, CNRS, Gif-sur-Yvette, France

A mon Frère Nourdine, ce géant

« Tout obstacle renforce la détermination. Celui qui s'est fixé un but n'en change pas. »

Léonardo De Vinci (1452 – 1519)

Soutien financier

Ce projet de thèse a été co-financé en partie par l'université de Rennes 1 (l'école doctorale EGAAL) ainsi que l'INRAE et le CNRS

Remerciements

Je tiens tout d'abord à adresser mes plus sincères remerciements aux rapporteurs, Jean-François Baroiller et Odile Brochain ainsi que les membres du jury, Astrid Böhne et Gilles Salbert, pour avoir accepté d'évaluer mon travail de thèse. J'attends vos critiques et remarques avec impatience.

Je remercie Julien Bobe, de m'avoir accueilli au sein de son laboratoire.

Je voudrai remercier mes directeurs de thèse, Yann Guiguen et Sylvie Rétaux, pour m'avoir proposé ce projet de thèse et pour leur confiance. Je vous remercie pour votre enthousiasme, pour les conseils scientifiques, l'encadrement technique, ainsi que le temps et l'énergie que vous avez consacré à ce manuscrit. Je vous remercie également pour m'avoir offert l'opportunité de présenter mes travaux en France, à Hawaii et au Mexique. Ces quatre années et toutes nos discussions m'ont permis de grandir scientifiquement ! Sylvie, j'en profite pour te réitérer mes sincères remerciements de m'avoir fait confiance en m'ouvrant les portes de ton labo dans les moments les plus durs de ma thèse Merci, Merci, Merci !!!

Je remercie également Amaury Herpin, pour son encadrement technique et scientifique.

Je tiens à exprimer ma gratitude à Didier Casane et Frédéric Véruynes, pour avoir accepté de faire partie de mon CSI et de suivre mon projet de thèse de si près. Je les remercie pour toutes les discussions et remarques pertinentes lors de mes comités de thèse. Didier, un grand merci pour l'intérêt que tu as montré à mon projet de thèse lors de mes différentes présentations à Rennes et à Gif. Frédéric, je te remercie également pour l'ensemble de ta contribution à ce travail et tout particulièrement pour les caryotypes.

Je voudrai remercier Laure Ponticelli, d'avoir cru en moi lorsque je n'arrivais même pas à aligner deux phrases correctes. Merci de m'avoir fait comprendre qu'il n'y a pas plus utile que la recherche inutile. Merci de m'avoir pousser à donner le meilleur de moi-même. Et merci d'avoir tout fait pour que je puisse finir ma thèse dignement. C'est aussi grâce à ta confiance que le rêve de faire une thèse devient réalité.

J'en profite par la même occasion pour remercier Charles Le Pabic, pour être le précurseur de mon admiration pour la recherche. J'étais arrivé au mauvais moment, mais les deux heures que tu me consacrais une fois toutes les deux semaines étaient suffisantes pour m'inspirer de toi et de ton autonomie. Un grand merci !

Réaliser ma thèse au sein de deux laboratoires, a été "malgré tout" une expérience extrêmement riche, scientifiquement et humainement. Ainsi, j'ai eu l'opportunité de rencontrer des personnes exceptionnelles avec qui j'ai partagé des moments simples mais mémorables. Cette thèse a été également riche en collaborations, et sans qui je n'ose même pas imaginer ce qu'elle aurait contenu. Alors comment ne pas remercier toutes ces personnes.

Un très grand merci à toi Julie (Perez), pour ton accueil à Montpellier et ta contribution précieuse à mes travaux. Je te remercie pour avoir accepté de venir à Rennes pour les manipes, et de rester jusqu'à pas d'heure pendant cette de semaine de folie. Ce fut un grand plaisir de te rencontrer et de collaborer avec toi.

Je remercie toute la Team Deca à Gif, de m'avoir fait une place parmi eux. Maryline pour son sourire permanent et sa disponibilité, Julien pour son aide précieuse pour les in situ, et Jorge pour m'avoir initié aux injections et les spoils de « Game of Thrones ». Je remercie également Camille et Louise de m'avoir accepté dans leur cercle de VIP « cubicule club » et pour toutes les pauses café. Une rencontre que je ne suis pas prêt d'oublier, Guillaume, grâce à qui j'ai appris la « classe » des mots. Un petit clin d'œil à Naomie pour sa bonne humeur de tous les jours. Merci également à Stéphane pour toutes les discussions que nous avons eues. Je n'oublie certainement pas François, qui trouve toujours une blague même là où il n'y en a pas mais aussi pour les discussions scientifiques toujours intéressantes. Merci aussi à Maxime pour son aide avec R et pour tous les moments rigolo vécus au Mexique. D'ailleurs, un grand merci à Sylvie et toute l'équipe pour cette très belle découverte « les poissons dans leurs grottes » mais pas que...ce qui se passe au Mexique reste au Mexique. Je n'oublie pas de remercier Constance pour toutes les rigolades et les moments sympathiques avec l'équipe. Le « Bousier scarabée » arrive enfin au bout de son chemin. Mon tit chou et mon lapin, Victor, j'ai été plus que ravi de collaborer avec toi dès mes débuts, mais surtout de t'avoir rencontré. Tu as été le premier à en avoir marre de moi puisque je faisais des commandes de 2000 poissons toutes les semaines. Lucie, toi aussi tu as été d'une aide précieuse avec les CRISPR. Grâce à toi j'avais réussi à générer mes premiers mutants. Je n'oublie pas non plus que tu as été là pour moi quand ça

n'allait pas trop. Pour tout ça, je voudrai tous vous remercier pour ces quelques mois qui m'ont aider à tenir. Merci à tous, vous êtes les meilleurs !

Un grand merci à tous les membres de l'ancienne équipe AMAGEN. Merci particulièrement à Laurent pour sa bonne humeur et son aide lors de mes divers envois de poissons.

Cette thèse a été avant tout, des démarches administratives (installation au labo, fonctionnement, congés, congrès, déplacements et bien d'autres). À ce titre, je tiens à remercier Céline Deslandes, Nathalie Huet et plus récemment Emilie Le Brun pour leur soutien administratif tout au long de cette thèse. Je vous remercie pour votre sourire permanent.

Je tiens à remercier tout particulièrement Patricia Dubois, ou plutôt “notre concierge” pour son aide précieuse et particulièrement pour les billets de train de dernière minute. Patricia, je te remercie également pour ton soutien infaillible, les petits mots que tu collais à chacun de mes “Bulletins de paie”, d’être toujours à l’écoute au labo quand ça n’allait pas, de trouver les bons mots pour me remonter le moral mais aussi pour tous les moments joyeux pendant nos pauses. Arrivé le confinement, tu nous as accompagné pendant des mois avec ton talent de poète. Pour ma part, tu as rendu mes journées plus joyeuses. C’était un plaisir de te lire et de découvrir ce que notre concierge a fait de son week-end de confinée (entre Dressing, rangement, ménage, lecture..). Je ne te remercierai jamais assez d’être notre repère pendant des mois !

J’adresse mes sincères remerciements à Agnès, Maryse, Sylvie et Guylène, pour leur gentillesse, pour nos discussions et l’appui administratif.

Je voudrai exprimer ma gratitude à Pierre-Yves Rescan pour ses encouragements. Je le remercie également pour toutes nos discussions scientifiques ou politiques.

Cette thèse a été un challenge pour moi dès mon arrivée sur Rennes. Sans poissons, rien n’aurait été possible ou du moins très compliqué. Il a donc fallu mettre en place l’élevage très rapidement et dans les meilleures conditions possibles. Pour tout le travail qui a été fait, je tiens à remercier de manière générale tous les collègues, anciens et actuels, des expérimentations animales qui veillent sur nos poissons. Si je dois résumer l’équipe en un mot, je dirai que vous êtes le “Moteur” du labo.

De manière plus personnelle, Amélie et Pierre-Lô, je vous remercie pour tout ce que vous avez fait pour mes Astyanax et pour moi aussi... Je vous remercie particulièrement pour toutes les fois (vous n’avez sûrement pas compté mais moi si !) où vous vous êtes déplacés, soit à la

station totale, soit à la gare pour chercher ou me déposer des poissons. Je n'oublierai jamais ça ! J'ai été plus que ravi de collaborer avec vous. Amélie, je te remercie d'être à l'écoute !!

Fred, je te remercie pour l'énergie que tu as investi dans la mise en place des élevages très rapidement après mon arrivée, pour ta disposition à toute discussion et ton ouverture à toutes mes propositions, bien évidemment dans la limite du raisonnable. Je te remercie pour tous les colis suspects que nous avions confectionnés ensemble. C'était clair que je ne passais pas inaperçu et grâce à toi j'ai eu l'honneur de m'expliquer avec les flics à plusieurs reprises ;). Je te remercie d'avoir partagé ton expertise en élevage, ton sourire permanent et tes blagues toutes pourri (tes) qui me faisaient pleurer de rire quand même. Je garderai précieusement ton conseil "on peut rigoler de tout mais pas avec tout le monde". Merci également pour tous les autres moments en dehors du labo. J'espère qu'on pourra trouver une petite semaine dans un futur proche pour vous faire visiter mon pays!

Alizée, je te remercie d'avoir donné de toute ton énergie et de ta créativité afin de perfectionner les élevages d'*Astyanax*. Il t'aurait fallu quelques mois de plus pour les faire reproduire. J'ai été ravi de te rencontrer, de collaborer avec toi et d'être ton ami "je n'oublie pas ton Lolo bien sûr ;)".

Merci à Cécile Duret qui a commencé cette aventure *Astyanax* avec moi "je n'oublierai pas le jour où on a trouvé 40 cadavres dans un seul aquarium en l'espace d'un week-end". On a très vite compris à qui on avait affaire. Merci de ta gentillesse et de ton implication.

Je remercie également Jean-Marc et Guillaume pour leur implication et les discussions toujours intéressantes. Merci pour toutes les fois où vous êtes venus m'apporter de l'aide aux IEs et m'accompagner dans mes délires. C'était toujours un plaisir d'interagir avec vous.

Je tiens à remercier Romain Feron pour sa contribution inestimable à mon projet de thèse !

Séverine, je te remercie pour ta contribution immense à mon projet de thèse même si ça n'a pas été toujours facile pour toi avant de trouver tes marques. Ce que tu as fait pour ce projet est juste énorme ! Alors pour ça et pour tout le reste Merci !

Elodie, tu as été ma sauveuse et j'en suis conscient ! Je ne trouve même pas les mots pour décrire ça mais laisse-moi te remercier encore et encore pour tout ce que tu as fait pour ce projet de thèse. Grâce à ton efficacité, le projet est là où il est aujourd'hui. Merci de m'avoir formé également à certaines manipes à mes débuts au labo !

Je tiens à remercier également mes voisines de bureau, Thao et Anne Sophie pour toutes les discussions que nous avons eues et pour le soutien moral (Thao) !

Steph, je ne sais même pas par où commencer, mais une chose est sûre, Merci n'est définitivement pas suffisant pour t'exprimer ce que je ressens. Ton soutien infaillible m'a certainement aidé à m'accrocher au labo et à rêver de ce jour où je déposerai enfin. Un immense merci d'être restée toi-même. Elles sont rares les personnes comme toi !

Manon (Thomas), je te remercie pour ta contribution à ma thèse et pour le soutien moral au labo. J'ai été content de te retrouver au labo après notre rencontre à Gif et j'en profite pour m'excuser encore pour les derniers mois (tu sauras de quoi je parle) !

Claudiane, je te remercie pour ton soutien également et pour tous les moments en dehors du labo. Merci de nous avoir toujours ouvert votre maison. J'ai toujours apprécié les moments qu'on a passé chez vous et vivement qu'on vous retrouve encore.

Je remercie tous les membres de l'équipe socs avec qui j'ai interagi, soit sur de la science ou autres (Violette Thermes et Violaine Colson). Je voudrai souhaiter une très bonne chance aux doctorants de l'équipe, Manon L, Antoine, Emilien et Aude. Je vous souhaite toute la réussite dans vos recherches. Je n'oublie pas non plus Jessica. Merci à Ming et Miya qui ont partagé le bureau avec moi ! Je remercie également Hélène Rime pour sa gentillesse !

Merci également à Elisabeth Sambroni pour sa gentillesse et son sourire si contagieux !

Je n'oublie pas de remercier Laurent Collin pour son aide à chaque fois que je le sollicite ainsi que pour les cafés de 7 h du matin avec toute la team des « lèves-tôt ».

J'adresse mes sincères remerciements à Adèle Branthonne et Béatrice Porcon pour toute l'aide apportée en histologie.

Patrick, Isabelle et Sandrine, je vous remercie de m'avoir fait une place parmi vous, de me prendre sous vos ailes et de m'apporter votre soutien au labo ainsi qu'en dehors labo. Aujourd'hui, c'est à mon tour de prendre la navette et je suis déjà en train de nous revoir sur cette plage aux caraïbes. Oups, je voulais dire « nous imaginer » mais comme on dit INCHALLAH un jour ce sera à nous... Merci pour tous les moments qu'on a passé ensemble. On est les winners !!!!

La thèse c'est aussi les amis. Je voudrai tous les remercier pour les moments sympa qu'on a passé ensemble et pour leur soutien durant ces 4 années. Je pense notamment à Marion et Alex que j'ai retrouvé (ou trouvé) à Rennes et avec qui nous avons passé des moments très joyeux même par Skype. Merci Alex d'avoir relu mon intro même si c'était de l'Arabe pour toi ;). Merci pour tout, les « chopains » ! Je remercie également Amélie, Marine, Ben, Morgane et Shani pour tous les moments d'évasions que nous avions passé ensemble. J'arrive enfin au bout et on va pouvoir respirer autre chose que cette thèse! J'ai même hâte de commencer les cours de fitness sur Facebook live ;). Merci à Aline et Ivan pour les tous les moments bien plus que sympathiques à Paris, Rennes et chez vous au bled. Bientôt ce sera la teuf avec l'huile d'olives...Enfin, ça c'est si on compte sur Abdarezak tout comme pour l'anti-thèse d'ailleurs ☺.

Un grand merci à mon frérot Ahmed ou « habibou », je préfère ! Tu as été d'un immense soutien depuis le début jusqu'à la fin. On a passé des moments magiques. Tu arrivais deux heures en retard à nos soirées à chaque fois mais tu repartais toujours 3 plus tard que prévu. En même temps avec du « Jus » qui se boit tout seul on oublie très vite l'heure. J'en garde des très bons souvenirs et j'espère qu'on se retrouvera dans un futur proche (sûrement pas dans le sud mais pourquoi pas en Bretagne héhé). Merci pour ton aide pour rassembler les morceaux de ce manuscrit. Tanmirt-Ik agma !!

Un grand merci à tous les blédards du village, tonton Ferhat, Nassim, Menad et Ziad pour les soirées bien plus qu'agréables. Avec vous, je replonge à chaque fois dans une époque où l'insouciance n'avait pas de place. Tellement de phrases qui me reviennent en tête mais j'en garde deux en particulier : « Tu coupes par-là et t'exploses là-bas » ou encore « Je suis passé comme un éclair » disait-il Ferhat.

Merci à toute ma famille. Mes parents et Nana Baya qui ne comprennent toujours pas ce que je fais et à qui je n'arrête jamais de penser ! Si j'en suis là aujourd'hui, c'est grâce à votre éducation et les valeurs que vous m'aviez inculquées. À mes sœurs Rachida, Samra, Nassima et Fatima et à Mes frères Jugurtha et Moh Said qui me soutiennent depuis des années même à distance. Merci pour vos encouragements tout au long de ces 8 années. Je remercie mon frère Bachir qui a toujours été présent depuis mon arrivée en France et sans qui tout ça n'aurait pas été possible ! Merci pour tout ce que vous avez fait pour moi toi et Tarkia. Cette thèse est sûrement la mienne mais j'aimerai tellement la partager avec vous. Un merci ne suffirait pas !

Je remercie aussi ma deuxième famille en France « Alain » et « Kiki » de m'avoir accepté de faire partie de la famille. Je ne vous remercierai jamais assez pour ce que vous faites pour nous depuis quelques années déjà. Cette année n'a pas été facile, je sais, mais j'espère que bientôt on rattrapera tous les moments perdus.

Un grand merci à Marc et Dany, pour leur soutien depuis notre première rencontre et pour tous les moments agréables partagés ensemble.

Enfin, la plupart garde le ou la meilleur(e) pour la fin mais toi, tu n'es pas seulement la meilleure. Toi, tu n'es pas qu'un simple soutien et tu n'es pas non plus juste la moitié. Toi, tu es le tout depuis 7 ans maintenant. Tu as cru en moi et tu m'as toujours poussé à aller de l'avant depuis le début. Des moments compliqués, j'en ai eu depuis mon arrivée en France mais grâce à toi, j'ai su me relever à chaque fois. Merci d'être à mes côtés, d'être ma force et ma joie de vivre. Merci de m'avoir supporté pendant tout ce temps et surtout ces dernières années ! Déborah (<3), tu fais que la vie est belle !!

SOMMAIRE

SOMMAIRE	1
TABLE DES FIGURES	3
INTRODUCTION.....	4
I. LA DÉTERMINATION DU SEXE CHEZ LES POISSONS TÉLÉOSTÉENS	7
I.1. La détermination environnementale du sexe	7
I.2. La détermination génétique du sexe	9
I.2.1. La détermination génétique monofactorielle du sexe.....	11
I.2.1.1. Émergence des déterminants majeurs du sexe.....	12
I.2.1.2. Déterminants majeurs du sexe.....	13
I.2.2. La détermination polygénique du sexe.....	17
I.2.3. La détermination génétique extra-chromosomique du sexe.....	18
II. LES CHROMOSOMES B : UNE ÉNIGME	18
II.1. La distribution des chromosomes B chez les eucaryotes	19
II.2. La structure des chromosomes B.....	20
II.3. Composition moléculaire et fonction des chromosomes B.....	22
II.4. Les mécanismes de transmission des chromosomes B	23
II.5. L'origine et l'évolution des chromosomes B	24
II.5.1. L'origine interspécifique	24
II.5.2. L'origine intraspécifique	25
II.6. Les chromosomes B et le déterminisme du sexe.....	26
III. LE MODÈLE ASTYANAX MEXICANUS	29
III.1. <i>Astyanax mexicanus</i> : une seule espèce, plusieurs populations	29
III.2. Les formes cavernicoles d' <i>Astyanax mexicanus</i> ont-elles une origine unique ou multiple ? .	31
III.3. <i>Astyanax mexicanus</i> : une seule espèce, des environnements contrastés	33
III.4. <i>Astyanax mexicanus</i> : l'adaptation convergente à un environnement extrême.....	34
III.5. La diversité génétique et phénotypique dans un contexte d'une évolution répétée chez <i>Astyanax mexicanus</i>	36
III.6. Mais qu'en est-il de la détermination du sexe et de son évolution chez <i>Astyanax mexicanus</i> ?	38
III.7. <i>Astyanax mexicanus</i> : un modèle pour les études comparatives à une échelle micro-évolution	39

PROJET DE THÈSE	41
Contexte scientifique de la thèse.....	42
Objectifs et stratégie de la thèse.....	43
RÉSULTATS	45
Publication 1 : <i>Primordial germ cell migration and histological and molecular characterization of gonadal differentiation in Pachón cavefish <i>Astyanax mexicanus</i>.....</i>	48
Publication 2 : <i>A supernumerary “B-sex” chromosome controls sex determination in the Pachón cave, <i>Astyanax mexicanus</i></i>	86
Publication 3 : <i>Evolution of sex determination in <i>Astyanax mexicanus</i> morphotypes and populations</i>	145
DISCUSSION	178
BIBLIOGRAPHIE	191
ANNEXES.....	213
Annexe 1 :	214
Annexe 2 :	235
Annexe 3 :	237

TABLE DES FIGURES

Figure 1. Diversité des systèmes de détermination du sexe chez les vertébrés basée sur l’analyse de 2145 espèces.

Figure 2. Évolution et diversité des gènes déterminants du sexe chez les vertébrés, avec un focus particulier sur les poissons téléostéens.

Figure 3. Distribution des chromosomes B dans les principaux groupes d'eucaryotes.

Figure 4. Origine multi-chromosomique du chromosome B chez *Astatotilapia latifasciata*.

Figure 5. Les différentes formes d'*Astyanax mexicanus* et la distribution géographique des populations cavernicoles.

Figure 6. Les formes de surface et cavernicoles d'*Astyanax mexicanus* et leurs environnements respectifs.

Figure 7. Exemples de différences majeures entre les poissons de surface (SF) et les poissons cavernicoles (CF).

Figure 8. Dimorphisme sexuel chez l'*Astyanax mexicanus*.

Figure 9. Représentation schématique illustrant les facteurs moléculaires et les principaux changements morphologiques au cours du développement des gonades chez *Astyanax mexicanus*.

INTRODUCTION

INTRODUCTION GENERALE

La reproduction sexuée est un processus très répandu dans le règne animal et particulièrement conservé chez les vertébrés (Otto & Lenormand, 2002). Cette stratégie de reproduction est basée sur l'existence de sexes différenciés, mâles et femelles. Ces derniers vont eux-mêmes produire des gamètes différenciés, spermatozoïdes et ovules, dont la fécondation produira les individus de la génération suivante. Les mécanismes qui conduisent à cette sexualisation sont très complexes et ont engendré des dimorphismes (sexuels) à plusieurs niveaux. Il s'agit par exemple de la mise en place de dimorphismes phénotypiques tels que des patrons de coloration différents entre des individus de sexes différents, ou des différences dans le comportement reproducteur, les stratégies de recherche et le choix d'un partenaire.

Parmi ces nombreux dimorphismes, les dimorphismes phénotypiques visibles (ou caractéristiques sexuelles secondaires) ne sont en fait que le reflet de différences physiologiques et anatomiques internes qui sont généralement mises en place très précocement lors du développement embryonnaire. Cette sexualisation précoce est la résultante tout d'abord, d'un processus de détermination sexuelle qui peut être vu comme le commutateur central, puis d'un processus de différenciation sexuelle qui va sexualiser, sous le contrôle initial du commutateur central, l'ensemble des structures anatomiques spécialisées en particulier les gonades embryonnaires (Mank & Avise, 2009).

La différenciation gonadique est donc définie comme l'ensemble des événements physiologiques, moléculaires et cellulaires, par lesquels une gonade indifférenciée bipotente va se développer en un testicule ou un ovaire. La détermination du sexe, est quant à elle, le processus initial qui induit la cascade de différenciation gonadique, et qui va définir l'identité sexuelle de l'individu en tant que mâle ou femelle (Hayes, 1998).

Au cours de ces dernières décennies, l'étude des mécanismes de détermination et de différenciation du sexe chez les vertébrés a suscité un intérêt majeur tant d'un point de vue de la recherche fondamentale que de la recherche appliquée avec par exemple :

- Des applications dans le domaine médical du fait de problèmes congénitaux ayant pour conséquences des perturbations du sexe gonadique et / ou des caractéristiques sexuelles secondaires (maladies connues sous le terme de “disorder of sex development” ou DSD).

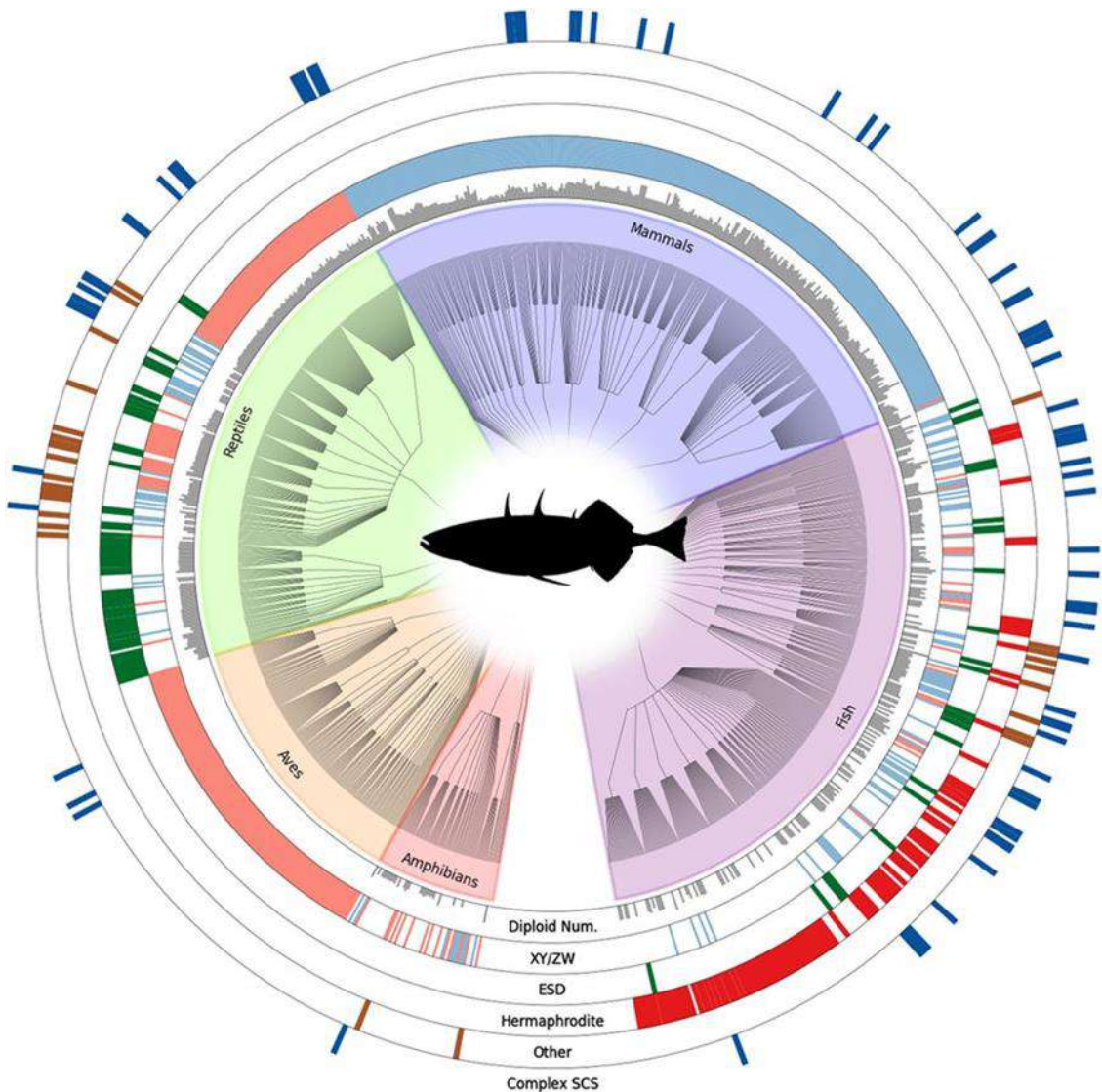


Figure 1. Diversité des systèmes de détermination du sexe chez les vertébrés basée sur l'analyse de 2145 espèces. Le cercle central correspond aux différents groupes des vertébrés représentés par des couleurs différentes (orange : amphibiens (173 espèces) ; jaune : oiseaux (195 espèces) ; vert : reptiles (593 espèces) ; mauve : mammifères (479 espèces) ; violet : poissons (705 espèces)). Les correspondances des autres cercles sont présentées à la base de chacun des cercles qui indique la présence ou l'absence de l'attribut associé. Les hauteurs des barres grises dans le cercle interne représentent le nombre de chromosomes à l'état diploïde “Diploid Num”. Le cercle correspondant à la case “XY/ZW” représente les espèces ayant une hétérogamétie de type XX/XY (en bleu) ou de type ZZ/ZW (en rose). ESD : déterminisme environnemental du sexe. Hermaphrodite : représente les espèces hermaphrodites de chaque groupe. Others : regroupe les espèces qui se reproduisent par parthénogénèse, gynogénèse et hybridogénèse. Complex SCS : correspond aux systèmes chromosomiques complexes (X1X2Y). D'après (Tree of Sex Consortium, 2014).

- Des applications dans le domaine de l'agriculture pour favoriser l'élevage contrôlé de populations dont le sexe présente un avantage en agronomie.

La quantité substantielle de données qui a été produite révèle une remarquable plasticité dans les mécanismes de détermination du sexe chez les vertébrés, à l'inverse de certains processus développementaux tels que la formation des axes embryonnaires (antéro-postérieur et dorso-ventral) ou la spécification de l'œil, qui sont tous deux régis par des réseaux géniques assez conservés (Capel, 2017).

Ainsi, les mécanismes de détermination du sexe varient considérablement d'un groupe à l'autre et ont été divisés en 3 catégories principales : (1) la détermination génétique du sexe ou (GSD, pour Genetic Sex Determination) comme chez tous les mammifères et oiseaux, et chez beaucoup d'espèces d'amphibiens, de reptiles et poissons ; (2) la détermination environnementale du sexe (ESD, pour Environmental Sex Determination) comme c'est le cas chez certaines espèces de reptiles et de poissons ; (3) ou encore la combinaison des deux systèmes (GSD + ESD) qui est très répandue chez les reptiles et les poissons (Figure 1) (Guiguen et al., 2018; Luckenbach & Yamamoto, 2018; Schartl & Herpin, 2018; Wilhelm & Pask, 2018).

I. La détermination du sexe chez les poissons téléostéens

Parmi les vertébrés, les poissons téléostéens avec près de 35 000 espèces reconnues, sont considérés comme le groupe de vertébrés le plus diversifié aussi bien d'un point de vue physiologique, écologique, morphologique que comportemental (Fricke et al., 2020; Nelson et al., 2016). Par ailleurs, cette étonnante diversité biologique contient également la plus grande variété de stratégies de reproduction avec des espèces : (1) unisexuées (majoritairement des femelles) ; (2) hermaphrodites (synchrones ou séquentielles) ; (3) gonochoriques (deux sexes distincts durant tout le cycle de vie) (Devlin & Nagahama, 2002; Heule et al., 2014). De plus, les poissons téléostéens ont colonisé une multitude d'habitats très contrastés présentant une variabilité des facteurs environnementaux très importante *e.g.* la température, la salinité, le pH, la luminosité, ou encore le taux d'oxygène (Nelson et al., 2016).

Bien que le nombre d'espèces hermaphrodites chez les poissons soit important, la grande majorité des espèces est gonochorique (Herpin & Schartl, 2009). Chez ces espèces gonochoriques, le sexe est déterminé, soit par des facteurs génétiques (GSD) ou environnementaux (ESD), soit par l'interaction entre ces deux composantes (GSD + ESD) (Bachtrog et al., 2014; Baroiller et al., 1999; Devlin & Nagahama, 2002; Heule et al., 2014; Wolff et al., 2007). Ainsi, les téléostéens représentent un modèle particulièrement intéressant pour explorer les mécanismes de détermination du sexe qui se situent à l'interface de la génétique et de l'environnement, afin d'approfondir notre compréhension de l'évolution des mécanismes qui déterminent la formation et le maintien des sexes et plus globalement, la reproduction sexuée.

I.1. La détermination environnementale du sexe

La détermination environnementale du sexe (ESD) est un concept qui est apparu pour la première fois il y a une quarantaine d'années (Charnov & Bull, 1977), et propose que des facteurs environnementaux donnés, appliqués à un stade précis du développement, peuvent influencer la détermination du sexe (Devlin & Nagahama, 2002). Depuis sa découverte, l'ESD a été proposée comme un système alternatif à la GSD chez certaines espèces en raison de l'absence de chromosomes sexuels facilement identifiables (Valenzuela et al., 2003). Le déterminisme environnemental du sexe a été particulièrement étudié chez les reptiles (Janzen & Paukstis, 1991) et certaines espèces de poissons (Devlin & Nagahama, 2002).

Bien que le terme “ESD” soit très utilisé dans la littérature, il convient de souligner que cette terminologie est sujette à débat et entraîne un certain niveau de confusion dû probablement à son utilisation inappropriée dans différentes publications scientifiques (Ospina-Alvarez & Piferrer, 2008; Shen & Wang, 2014; Valenzuela et al., 2003; Yamamoto et al., 2014). Ainsi, chez beaucoup d’espèces, l’existence d’une ESD stricte est remise en question, et de nombreuses publications soutiennent plutôt un scénario d’interaction de l’environnement sur une composante génétique (GSD + ESD) comme c’est le cas pour la température chez les poissons “TE, pour Thermal Effects on GSD” avec un continuum où, à mesure que la force de la GSD diminue, celle de l’ESD augmente (Ospina-Alvarez & Piferrer, 2008).

En tout état de cause, divers facteurs environnementaux de natures différentes peuvent influencer le processus de détermination du sexe chez les téléostéens (Baroiller & D’Cotta, 2001; Baroiller et al., 2009; Devlin & Nagahama, 2002; Ospina-Alvarez & Piferrer, 2008). Parmi ces facteurs, la température est la variable la plus explorée et la plus susceptible d’influencer la détermination du sexe (Baroiller & D’Cotta, 2016). Elle est connue sous l’appellation de “détermination du sexe dépendante de la température” (TSD, pour Temperature-dependent Sex Determination) (Ospina-Alvarez & Piferrer, 2008).

Depuis sa découverte dans les années 80 chez la capucette atlantique *Menidia menidia* (Conover & Kynard, 1981), de nombreux cas de TSD ont été rapportés chez les téléostéens (Ospina-Alvarez & Piferrer, 2008). Cependant, certaines espèces ont été proposées comme ayant une TSD stricte alors qu’elles présentaient une détermination génétique du sexe avec une sensibilité à la température (GSD + TE) (Ospina-Alvarez & Piferrer, 2008). Suite à ces confusions, et sur la base de critères permettant de distinguer un système GSD, de GSD + TE ou encore de la TSD (Ospina-Alvarez & Piferrer, 2008; Valenzuela et al., 2003), ces espèces ont été réévaluées et certaines d’entre elles ont été requalifiées plutôt en tant qu’espèces présentant une GSD + TE et non pas une TSD (Ospina-Alvarez & Piferrer, 2008).

De manière générale, les espèces présentant une détermination du sexe de type TSD (au sens large incluant des définitions plus précises comme celle de GSD + TE) ont été regroupées selon trois modes de réponses à la température : (1) un effet masculinisant des hautes températures (pour 53 à 55 des espèces étudiées) ; (2) un effet masculinisant des faibles températures (pour 2 à 4 des espèces étudiées) ; (3) un effet masculinisant des températures extrêmes hautes et basses (pour 2 espèces) (Ospina-Alvarez & Piferrer, 2008).

Outre le rôle de la température en tant que facteur clé dans la détermination du sexe chez les poissons, d'autres facteurs environnementaux sont connus pour influencer ce processus. Par exemple, l'incubation des œufs à des pH faibles (acides ~5) favorise le sexe mâle, tandis que l'incubation à des pH élevés (basiques > 7) favorise le sexe femelle chez *Xiphophorus helleri*, *Aristogramma caucatoides* et *Aristogramma borelli* (Rubin, 1985). Chez le bar européen *Dicentrarchus labrax*, le transfert d'une faible salinité vers une salinité plus élevée pendant la période de libilité sexuelle peut influencer la détermination du sexe en produisant des sex-ratios biaisés en faveur des mâles (Saillant et al., 2003).

La photopériode peut également influencer la détermination du sexe comme par exemple chez *Leuresthes tenuis* en produisant plus de femelles en longues journées (15 heures de lumière : 9 heures d'obscurité), tandis qu'une photopériode courte (12:12) produit plus de mâles (Brown et al., 2014). Les facteurs sociaux sont aussi susceptibles de jouer un rôle clé dans la détermination du sexe. C'est le cas pour *Macropodus opercularis* chez qui le pourcentage de femelles peut être directement proportionnel à la densité (Francis, 1984). Enfin, les faibles concentrations en oxygène dissous (traitement hypoxique) chez le poisson zèbre *Danio rerio* (Shang et al., 2006) et le médaka *Oryzias latipes* (Cheung et al., 2014) produisent un nombre supérieur de mâles que de femelles.

I.2. La détermination génétique du sexe

La détermination génétique du sexe est déclenchée par des caractères héréditaires transmis lors de la fécondation. Chez les vertébrés, la GSD repose principalement sur deux systèmes monofactoriels simples impliquant la présence d'une paire de "chromosomes sexuels" avec (1) le système à hétérogamétie mâle (XX/XY), où le sexe mâle est de type XY comme chez la quasi-totalité des mammifères (2) le système à hétérogamétie femelle (ZZ/ZW) où le sexe femelle est de type ZW comme chez toutes les espèces d'oiseaux étudiées à ce jour (Capel, 2017; Devlin & Nagahama, 2002).

Toutefois, à l'inverse des mammifères et oiseaux, les systèmes de déterminisme du sexe apparaissent très variables dans les autres groupes de vertébrés comme c'est le cas chez les reptiles et les amphibiens. En plus du système XX/XY chez le reptile *Iguana iguana* et l'amphibien *Rana japonica* (Altmanová et al., 2018; Miura, 2017), d'autres espèces telles que *Varanus komodoensis* et *Xenopus laevis* ont une hétérogamétie de type ZZ/ZW (Pokorná et al.,

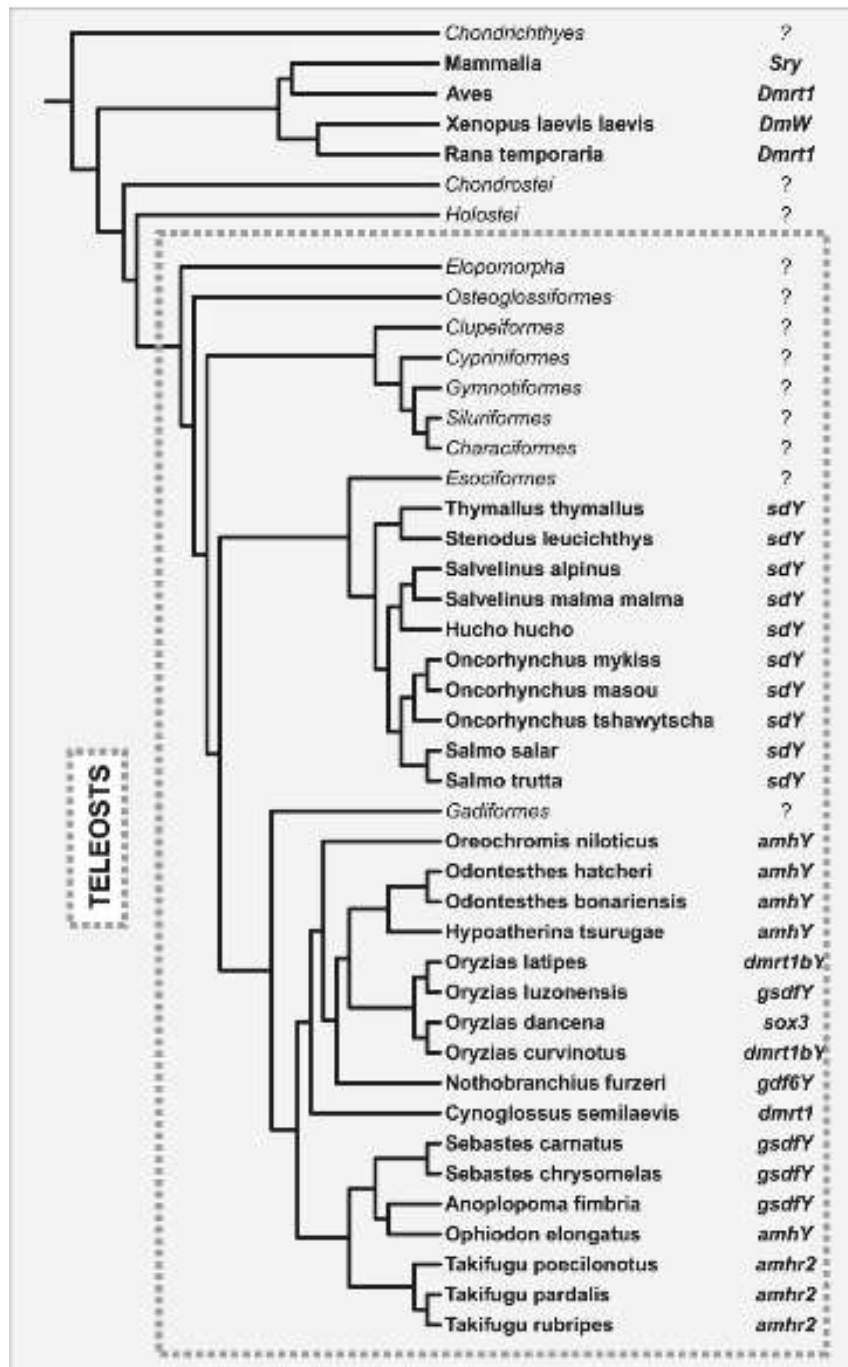


Figure 2. Évolution et diversité des gènes déterminants du sexe chez les vertébrés, avec un focus particulier sur les poissons téléostéens. Les espèces ou groupes d'espèces ayant un gène SD déjà connu ou fortement suspecté sont indiqués par des caractères gras. Les groupes d'espèces dont aucun gène SD n'est connu sont indiqués par des points d'interrogation. Le rectangle en pointillé représente les téléostéens. D'après (Pan et al., 2018).

2016; Yoshimoto et al., 2008). En outre, cette diversité peut même porter sur des espèces qui présentent des populations soit XX/XY soit ZZ/ZW, telle que *Rana rugosa* (Miura, 2007).

Dans un système monofactoriel purement génétique, le sexe est déterminé sous le contrôle d'un gène dit "déterminant majeur du sexe" ou gène SD (Sex Determining gene). Ce dernier déclenche une cascade d'expression génique qui va conduire à la différenciation de la gonade bipotente en ovaire chez les femelles ou en testicule chez les mâles (Mank & Avise, 2009). Ainsi, ce sont les gènes *SRY* (Sex-determining Region Y), porté par le chromosome Y (Capel, 2017; Koopman et al., 1991; Sinclair et al., 1990), *dmrt1* (Doublesex and mab-3 related transcription factor 1) sur le chromosome Z (Smith et al., 2009) et *DM-W* (DM domain binding motif on W) porté par le chromosome W (Yoshimoto et al., 2008) qui vont initier la cascade de différenciation sexuelle de la gonade, respectivement chez les mammifères, les oiseaux et l'amphibien *Xenopus laevis*. Il convient de souligner que *DM-W* n'est pas le déterminant majeur du sexe chez tous les amphibiens.

Les gènes SD agissent selon deux modalités : présence/absence comme c'est le cas de *SRY* chez les mammifères ou *DM-W* chez le xénope, ou dose dépendance comme c'est le cas de *dmrt1* chez le poulet (Capel, 2017). Le gène *SRY* des mammifères présent uniquement sur le chromosome Y va déclencher la cascade de différenciation testiculaire chez les embryons XY (Koopman et al., 1991). Quant à *dmrt1* chez les oiseaux, les individus ZW (femelles) ne possèdent qu'une seule copie de ce gène, tandis que les individus ZZ (mâles) en ont deux copies. Ainsi, c'est le dosage génique de *dmrt1* qui va déterminer le sexe (Smith et al., 2009). Cependant, chez *X. laevis*, *DM-W* est une copie dupliquée du gène autosomal *dmrt1* insérée sur le chromosome W. Ce gène détermine le sexe par une action antagoniste de celle de *dmrt1* autosomal (dominant négatif) conduisant à la formation des ovaires chez les individus ZW, et des testicules chez les individus ZZ (Yoshimoto et al., 2008).

Tout comme les amphibiens et les reptiles, les poissons téléostéens montrent une remarquable diversité des systèmes de détermination du sexe (Bachtrog et al., 2014; Heule et al., 2014). Par ailleurs, au contraire des oiseaux et mammifères qui ont conservé leurs déterminants respectifs sur une longue période évolutive, les déterminants majeurs du sexe chez les poissons sont extrêmement variables (Figure 2) (Pan et al., 2016, 2018).

Sur la base de cette grande diversité des systèmes chromosomiques et des gènes SD, la détermination génétique du sexe chez les poissons gonochoriques peut être divisée principalement en deux types :

- La détermination génétique monofactorielle du sexe impliquant un seul gène SD qui fait office de commutateur principal de la détermination du sexe dans un système à hétérogamétie mâle (XX/XY) ou femelle (ZZ/ZW) (Mank & Avise, 2009).
- La détermination polygénique du sexe (PSD, pour Polygenic Sex Determination) impliquant plusieurs gènes SD (plus de deux allèles) ou sous forme de chromosomes sexuels multiples (Moore & Roberts, 2013).

Chez les espèces de poissons dont le déterminisme est purement génétique, les chromosomes sexuels sont souvent considérés comme peu différenciés (homomorphes) tant d'un point de vue morphologique (*e.g.*, taille) que structurel (*e.g.*, composition en gènes) (Devlin & Nagahama, 2002). Cette notion de chromosomes peu différenciés est souvent associée, pas forcément toujours de façon rigoureuse d'ailleurs, à la notion de chromosomes sexuels "jeunes". Cette dernière va de pair avec une autre caractéristique des poissons qui est la forte variabilité de leurs systèmes de détermination du sexe et donc un fort taux de changement de chromosomes sexuels. En accord avec ce caractère homomorphique de la plupart des chromosomes sexuels chez les poissons, seulement 10 % des espèces étudiées présentent des différences caryotypiques clairement identifiables entre mâles et femelles (Devlin & Nagahama, 2002).

I.2.1. La détermination génétique monofactorielle du sexe

Les systèmes à hétérogaméties mâle (XX/XY) et femelle (ZZ/ZW) ont été identifiés chez de nombreuses espèces de poissons gonochoriques comme c'est le cas chez *Oryzias latipes* avec un système XX/XY et *Cynoglossus semilaevis* avec un système ZZ/ZW (Chen et al., 2014; Matsuda et al., 2002). Par ailleurs, ces systèmes XX/XY et ZZ/ZW sont susceptibles d'évoluer très rapidement et indépendamment avec des espèces très proches présentant des systèmes de détermination génétique opposés comme chez le tilapia du Nil *Oreochromis niloticus* (XX/XY) et le tilapia bleu *Oreochromis aureus* (ZZ/ZW) (Cnaani et al., 2008).

I.2.1.1. Émergence des déterminants majeurs du sexe

Cette évolution rapide des chromosomes sexuels est généralement associée à l'émergence de nouveaux gènes SD portés par ces mêmes chromosomes (Schartl, 2004). Il s'agit de la théorie du “high turnover” qui propose que de nombreux changements de chromosomes sexuels se font via des changements de déterminants majeurs du sexe (Schartl, 2004). Cette labilité à renouveler les chromosomes sexuels et les gènes SD est à l'origine de la diversité des mécanismes de détermination du sexe chez les poissons, ce qui fait de ce groupe des modèles particulièrement intéressants pour comprendre les mécanismes évolutifs à l'origine de cette diversité.

Certains de ces gènes ont été recrutés en tant que déterminants majeurs du sexe de manière récurrente et indépendante entre les espèces. Herpin et collaborateur ont défini ces gènes comme des “coupables présumés” (Usual suspects) (Herpin & Schartl, 2015). Il s'agit principalement des gènes de la famille des protéines à domaine HMG (gènes *SOX*), de la famille des facteurs de transcription *DMRT* (Doublesex and Male-abnormal-3 Related Transcription factors) et de la famille des facteurs de croissance *TGF-β* (Transforming Growth Factor β) qui sont également connus pour jouer un rôle clé dans le développement gonadique chez les vertébrés (Guiguen et al., 2018; Herpin & Schartl, 2015). Deux mécanismes principaux, qui semblent être fréquents, sont à l'origine de l'émergence de ces gènes SD chez les téléostéens : la duplication/insertion de gènes et le phénomène de diversification allélique (Herpin & Schartl, 2015).

La duplication/insertion d'un gène SD concerne la production d'une seconde copie à partir du réseau de gènes impliqués dans la différenciation sexuelle, en particulier les “coupables présumés” (Herpin & Schartl, 2015). La copie dupliquée est ensuite transloquée sur un autre chromosome qui devient le nouveau Y ou W. Prenons l'exemple du *dmrt1bY* (ou *dmy*) chez le medaka *Oryzias latipes* (Matsuda et al., 2002; Nanda et al., 2002) : il est issu de la duplication du gène autosomal *dmrt1* qui a subi par la suite une insertion sur un autre chromosome (Porto-chromosome Y) (Schartl, 2004). Ce dernier a accumulé des éléments transposables et des séquences répétitives entraînant un recâblage transcriptionnel du gène *dmrt1bY* et enfin une néo-fonctionnalisation ou spécialisation dans la voie de gène SD (Herpin & Schartl, 2015).

Toutefois, il est intéressant de souligner qu'une exception à la règle des “coupables présumés” existe. Un gène impliqué dans une fonction autre que le développement gonadique a été recruté comme gène SD chez la truite. Il s'agit de *sdY* (sexually dimorphic on the Y) qui est issu de la

duplication d'un gène lié au système immunitaire *irf9* (*Interferon Regulatory Factor 9*) (Yano et al., 2012). Cette copie a ensuite évolué et acquis une nouvelle fonctionnalité (néofonctionnalisation). Elle est alors devenue le déterminant majeur du sexe chez cette espèce (Bertho et al., 2018). Ainsi, ce gène qui a été qualifié “d’usurpateur” (usurper) (Herpin & Schartl, 2015), est également le gène SD chez la plupart des salmonidés (Yano et al., 2013).

Contrairement aux mécanismes de duplication/insertion, dans le cas de la diversification allélique, le gène déterminant du sexe ne change pas de locus sur le chromosome. Il s’agit d’une variation au niveau d’un locus qui conduit par la suite à ce que l’un des allèles soit en faveur de la détermination mâle ou femelle (Herpin & Schartl, 2015; Schartl & Herpin, 2018). C’est le cas de l’*amhr2* (anti-Mullerian hormone receptor type 2) chez *Takifugu rubripes*. Les deux allèles de l’*amhr2* (*amhr2X* et *amhr2Y*) ne diffèrent que par un seul polymorphisme nucléotidique (SNP, pour Single Nucleotide Polymorphism) qui est hétérozygote chez les mâles (*Amhr2Y*) et homozygote chez les femelles (*Amhr2X*) (Kamiya et al., 2012). Cette variation nucléotidique conduit à une substitution d’un seul acide aminé His (H) / Asp (D) (hétérozygote) dans le domaine kinase de l’*Amhr2Y* et confère une activité réceptrice réduite (mutation hypomorphe) “His (H)/His (H)” (homozygote) à l’allèle du chromosome X (*amhr2X*). C’est ainsi que l’*amhr2Y* détermine le sexe mâle chez cette espèce (Kamiya et al., 2012).

I.2.1.2. Déterminants majeurs du sexe

Au cours des deux dernières décennies, un nombre croissant de déterminants majeurs du sexe ont été identifiés chez les poissons, et ces gènes sont souvent différents y compris chez des espèces très proches phylogénétiquement (Figure 2) (Pan et al., 2016, 2018). Comme déjà mentionné, à l’exception de *sdy* chez les salmonidés qui échappe à la règle puisqu’il n'est lié à aucun gène connu dans les voies de détermination du sexe, tous les autres gènes identifiés chez les poissons gonochoriques sont issus de l'une de ces quatre familles à savoir: (1) des gènes SOX ou les protéines à domaine HMG (High Mobility Group) ; (2) des facteurs de transcription liés à la famille de gènes DMRT ; (3) des facteurs de croissance liés à la famille des TGF-β et leurs voies de signalisation (Guiguen et al., 2018; Herpin & Schartl, 2015; Pan et al., 2018; Schartl & Herpin, 2018) ; (4) et des enzymes impliquées dans la synthèse des hormones stéroïdiennes (Koyama et al., 2019; Purcell et al., 2018).

Les déterminants majeurs du sexe de la famille des gènes SOX

Les protéines de la famille SOX (Sex determining region on Y-bOX), sont des facteurs de transcription qui sont souvent impliqués dans la détermination et la différenciation du sexe et ce, dans l'ensemble du règne animal (Guiguen et al., 2018; Pan et al., 2018). Ils possèdent tous un domaine de liaison à l'ADN appelé domaine HMG (Schepers et al., 2002). Cette famille des gènes SOX contient entre autre, le gène *SRY* qui est le déterminant majeur du sexe conservé chez la très grande majorité des mammifères euthériens (Capel, 2017; Koopman et al., 1991; Sinclair et al., 1990). Ce gène a été proposé comme étant issu de l'évolution du gène *SOX3* qui est toujours présent sur le chromosome X des mammifères (Katoh & Miyata, 1999). Bien que très conservés chez les mammifères euthériens, certaines espèces telles que *Tokudaia osimensis* (Kimura et al., 2014), ou *Mus minutoides* (Veyrunes et al., 2010) ont perdu ce déterminant majeur du sexe.

Le gène *sox3*, localisé sur le chromosome Y chez le médaka *Oryzias dancena* est le déterminant majeur du sexe mâle (Takehana et al., 2014). Chez cette espèce, les deux allèles de *sox3* (allèles X et Y) ont exactement la même séquence codante mais le chromosome Y contient un élément spécifique *cis*-régulateur qui va permettre une expression spécifique de l'allèle *sox3Y* pendant le développement des gonades chez les embryons mâles XY et ainsi initier la différenciation testiculaire (Takehana et al., 2014).

Les déterminants majeurs du sexe de la famille des DMRTs

La famille de gènes DMRT comprend plusieurs gènes qui ont été identifiés comme des acteurs importants dans la détermination, la différenciation et le maintien du sexe mâle aussi bien chez les mammifères, les oiseaux, les reptiles, les amphibiens, les poissons, les mouches, que chez les vers et les coraux (Herpin & Schartl, 2011; Matson & Zarkower, 2012; Wexler et al., 2014). Cette famille est caractérisée par la présence d'un domaine DM qui est très conservé au cours de l'évolution (Matson & Zarkower, 2012). Dix années après la découverte du gène *SRY* chez les mammifères, *dmrt1bY* (ou *dmy*) du médaka *O. latipes* a été le second gène SD connu chez les vertébrés (Matsuda et al., 2002; Nanda et al., 2002). Ce gène *dmrt1bY* est issu d'une duplication/insertion sur le chromosome Y du gène autosomal *dmrt1/dmrt1a* (Herpin & Schartl, 2015).

Bien qu'il ne soit pas le gène SD unique à tous les poissons, *dmrt1bY* a tout de même été identifié comme le déterminant majeur du sexe mâle chez une espèce proche d'*O. latipes*, *O.*

curvinotus (Matsuda et al., 2003), et aussi *dmrt1* chez la sole *Cynoglossus semilaevis* (Chen et al., 2014). Comme chez les oiseaux, la sole *C. semilaevis* possède un système de détermination du sexe à hétérogamétie femelle (ZZ/ZW) dont le chromosome W aurait perdu le gène *dmrt1* (Chen et al., 2014). Ainsi, la détermination du sexe chez *C. semilaevis* dépend de la dose de *dmrt1* : deux copies chez les mâles ZZ et une seule copie chez les femelles ZW.

Les déterminants majeurs du sexe de la famille des facteurs de croissance TGF-β

La superfamille des TGF-β est une grande famille de facteurs de croissance, contenant environ 30 membres chez les mammifères. Certains de ces membres sont très conservés dans divers groupes tels que les vers, les mouches, les grenouilles et les poissons (Huminiecki et al., 2009; Weiss & Attisano, 2013). Cette famille est composée de deux groupes fonctionnels : (1) le groupe des TGF-β-like qui comprend les TGF-β, les Activins, les Nodals, et les GDFs ; (2) et le groupe des BMP-like (Bone Morphogenetic Proteins) composé des protéines BMPs proprement dites, de la plupart des GDFs et de l'*amh* (Weiss & Attisano, 2013). La plupart de ces TGF-β jouent un rôle clé dans les régulations du développement embryonnaire et dans plusieurs processus cellulaires fondamentaux tels que la prolifération, la différenciation, l'organisation du cytosquelette, la migration, et l'homéostasie cellulaire (Ikushima & Miyazono, 2010; Weiss & Attisano, 2013).

La majeure partie des gènes SD identifiés chez les téléostéens qualifiés de “coupables présumés” codent pour les membres de la voie des TGF-β (Guiguen et al., 2018; Pan et al., 2018). Il s’agit notamment du gène codant pour l’hormone anti-müllérienne (*amh*) qui a été identifié sur le chromosome Y (*amhY*) chez le tilapia *Oreochromis niloticus* (Li et al., 2015), le pejerrey *Odontesthes hatcheri* (Hattori et al., 2013), et le brochet Européen *Esox lucius* (Pan et al., 2019) tous issus d’évènements de duplication. Chez le fugu *Takifugu rubripes* et la perche Américaine *Perca flavescens*, c’est le récepteur de type 2 à l’*amh* (*amhr2*) qui est responsable de la détermination du sexe (Feron et al., 2020; Kamiya et al., 2012). Le gène *amhr2bY* (allèle Y) de la perche, issu de la duplication/insertion de la copie autosomale de l’*amhr2* semble être le déterminant majeur du sexe mâle (Feron et al., 2020).

Un autre membre de la famille des TGF-β, le gène *gsdf* (Gonadal soma derived factor), retrouvé seulement chez les poissons (Forconi et al., 2013; Wang et al., 2017), a aussi été identifié comme un acteur essentiel dans le développement testiculaire chez plusieurs espèces (Guiguen et al., 2018). Chez le medaka *Oryzias luzonensis*, une espèce proche d’*O. latipes*, *gsdfY* a remplacé le *dmrt1bY* dans la voie des gènes SD (Myosho et al., 2012). Il a été également

proposé comme un potentiel candidat à la détermination du sexe chez d'autres téléostéens, *Anoplopoma fimbria* (Rondeau et al., 2013), *Sebastes carnatus* et *Sebastes chrysomelasles* (Fowler & Buonaccorsi, 2016).

La voie de signalisation BMP est connue pour être impliquée dans la gamétogenèse et en particulier la spécification des cellules germinales (Itman & Loveland, 2008; Pangas, 2012). Prenons l'exemple des *bmp15* et *gdf9*, ces deux facteurs de croissance jouent un rôle important dans la croissance et la régulation du développement folliculaire et aussi dans la fertilité chez plusieurs espèces (Otsuka et al., 2011; Yan et al., 2001). L'inactivation de *gdf9* chez la souris bloque la folliculogenèse au stade des follicules primaires et provoque une infertilité complète (Dong et al., 1996). Chez le tilapia du Nil *Oreochromis niloticus*, *bmp15*, *gdf9*, et *gdf3* sont exprimés préférentiellement dans les ovaires (Zheng et al., 2018). De plus, *bmp15* et *gdf9* sont très importants au développement ovarien chez le poisson zèbre (Clelland & Kelly, 2011).

Le facteur de croissance et de différenciation (*gdf6*) appartient au groupe des BMPs. Le gène *gdf6aY* a été recruté comme déterminant majeur du sexe par un événement de diversification allélique chez le Killi turquoise *Nothobranchius furzeri* (Reichwald et al., 2015). La comparaison entre les deux allèles (X et Y) de *gdf6a* chez cette espèce, montre une substitution de 15 acides aminés et une délétion de 3 autres acides aminés sur l'allèle Y. À cela s'ajoute une délétion de 241 paires de bases (pb) au niveau de la partie 3'UTR qui comporte potentiellement un site de liaison au microARN (mir-430) (Reichwald et al., 2015). Ce dernier joue un rôle important dans la régulation de l'expression des gènes spécifiques à la lignée germinale (Mishima et al., 2006). En outre, bien qu'aucune fonction gonadique n'ait été signalée auparavant pour *gdfa6*, *gdf6aY* chez *N. furzeri* montre une expression précoce fortement liée au sexe mâle pendant la période de détermination/différenciation testiculaire. Cette expression différentielle pourrait être liée à ces variations alléliques spécifiques affectant probablement l'interaction des protéines au niveau de leur récepteur ou pendant la phase de dimérisation. Ceci pourrait modifier de manière globale la fonction de la protéine Gdf6aY en lui conférant le rôle de déterminant majeur du sexe chez cette espèce (Reichwald et al., 2015).

Les déterminants majeurs du sexe de la famille des enzymes de la stéroïdogenèse

Chez les espèces du genre *Seriola*, le déterminant majeur du sexe est le gène *Hsd17b1* (17 β -hydroxysteroid dehydrogenase b 1) avec des différences notables dans les séquences entre les espèces (Koyama et al., 2019; Purcell et al., 2018). Chez *Seriola dorsalis*, les auteurs ont identifié le locus sexuel de 100 kb sur lequel *Hsd17b1* a été localisé avec six autres gènes. De

plus une délétion de 61 bp a été identifiée en amont de *Hsd17b1* qui est totalement liée au sexe femelle (sur le chromosome W) suggérant ainsi que le déterminisme est de type ZZ/ZW (Purcell et al., 2018). En revanche, chez d'autres espèces du genre *Seriola*, le sexe est déterminé par une mutation faux sens d'un seul nucléotide retrouvé sur le chromosome W et cette mutation n'a pas été retrouvée chez *S. dorsalis* (Koyama et al., 2019).

I.2.2. La détermination polygénique du sexe

Le concept de détermination polygénique du sexe est apparu pour la première fois dans les années 60, décrit par Kosswig (Kosswig, 1964). Chez les poissons, contrairement au système monofactoriel simple faisant intervenir un seul gène SD souvent porté par un des chromosomes sexuels, la détermination polygénique, quant à elle, implique deux configurations différentes avec : (1) des espèces chez qui le sexe est déterminé par l'interaction entre de multiples allèles qui ségrègent de manière indépendante au niveau du locus sexuel ; ou (2) plusieurs gènes répartis sur plusieurs chromosomes (Moore & Roberts, 2013).

Bien que la PSD soit très peu documentée par rapport à la GSD monofactorielle et qu'aucun déterminant n'a été identifié à ce jour dans ce cas de figure, de nombreux cas de PSD ont été rapportés chez les poissons. Il s'agit par exemple de *Xiphophorus maculatus* qui appartient à la famille des poeciliidés, et chez qui la détermination du sexe mâle versus femelle se manifeste par l'interaction de trois allèles sur trois chromosomes homologues (X, Y et W) qui ségrègent au niveau du locus sexuel. Le sexe génétique d'une femelle peut être de type XX, XW ou YW et le sexe mâle est de type YY ou XY (Schultheis et al., 2009; Wolff & Schartl, 2001).

La détermination polygénique du sexe peut se présenter avec une combinaison complexe de nombreux allèles comme c'est le cas chez le bar européen *Dicentrarchus labrax* impliquant au moins 3 QTLs (quantitative trait loci) dans le contrôle de la détermination du sexe (Palaiokostas et al., 2015; Vandepitte et al., 2007). De plus, il a été démontré que *D. labrax* montre une sensibilité à des facteurs environnementaux tels que la salinité (Saillant et al., 2003) et la température (Piferrer et al., 2005; Saillant et al., 2002) durant la période de libilité sexuelle, ce qui vient s'ajouter à la PSD. Les populations de laboratoire du poisson zèbre *Danio rerio* possèdent également un déterminisme polygénique (Anderson et al., 2012; Liew et al., 2012) avec une forte composante environnementale multifactorielle à savoir, la densité, la température et l'hypoxie (Ribas et al., 2017a; Ribas et al., 2017b; Shang et al., 2006). Cependant, les données récentes sur cette espèce ont montré que les populations naturelles ont

un système monofactoriel simple de type ZZ/ZW. De plus, les souches de laboratoires auraient perdu l'allèle W (Wilson et al., 2014).

Les cichlidés Africains présentant une grande diversité d'espèces, possèdent également plusieurs systèmes de détermination du sexe dont la PSD (Roberts et al., 2016). Cette dernière montre une remarquable plasticité dans ce groupe de poissons avec des locus de détermination du sexe qui sont différents d'une espèce à l'autre (Roberts et al., 2009; Ser et al., 2010). C'est le cas chez *Metriaclima pyrsonotus* qui présente un système de chromosomes multiples (multi-locus) avec les deux systèmes à hétérogamétie mâle (XX/XY) et femelle (ZZ/ZW) fonctionnant simultanément. Dans ce cas de figure, l'allèle W est dominant par rapport à celui du Y de façon à ce que les individus ZZ/XX, ZW/XX et ZW/XY soient femelles et uniquement les individus ZZ/XY soient mâles (Moore & Roberts, 2013).

I.2.3. La détermination génétique extra-chromosomique du sexe

Outre la GSD monofactorielle et la PSD qui montrent l'extrême diversité des chromosomes sexuels chez les téléostéens, la détermination du sexe peut être également influencée par des chromosomes surnuméraires connus sous le nom de "chromosomes B" (Camacho et al., 2011). Il s'agit de chromosomes souvent considérés comme des éléments génétiques "égoïstes" n'ayant peu voire pas d'effets sur le phénotype de l'organisme hôte (Camacho et al., 2000). Bien qu'ils soient très peu caractérisés tant d'un point de vue moléculaire que fonctionnel, les données récentes chez de nombreuses espèces d'eucaryotes suggèrent un rôle important de ces chromosomes dans la détermination du sexe (Camacho et al., 2011). Par exemple, il a été démontré que les chromosomes B du cichlidé du lac Victoria *Lithochromis rubripinnis* jouent une fonction clé dans la détermination du sexe femelle (Yoshida et al., 2011).

Dans les sections suivantes, nous présenterons l'état des connaissances actuelles sur l'origine évolutive, la composition moléculaire et les modes de transmission des chromosomes B chez les eucaryotes ainsi que leur implication dans le processus de la détermination du sexe avec un accent particulier sur les téléostéens.

II. Les chromosomes B : une énigme

Les organismes eucaryotes possèdent généralement un nombre spécifique de chromosomes organisés par paires appelés chromosomes A (As), qui constituent le génome de

l'animal. Cependant, au début du siècle dernier et plus exactement en 1907, Wilson a identifié pour la première fois des chromosomes surnuméraires chez les hémiptères (Wilson, 1907). Il aura fallu attendre 21 ans de plus pour que ces chromosomes surnuméraires soient appelés “chromosomes B” (Bs), pour les distinguer des chromosomes A (Randolph, 1928). Depuis cette découverte et en l'espace d'un peu plus d'un siècle, le nombre d'espèces eucaryotes possédant des chromosomes B s'élevait à plus de 2837 espèces en 2019 (Ahmad & Martins, 2019; D'Ambrosio et al., 2017). Dans la littérature, ces chromosomes B sont souvent qualifiés de chromosomes supplémentaires, accessoires, non-essentiels ou encore de parasites génomiques (Camacho, 2005; Camacho et al., 2000; Jones, 1991).

Bien qu'ils soient considérés comme non-essentiels, les chromosomes B ont été une source d'intrigues car ils peuvent être présents chez certains individus d'une population et absents chez d'autres (Houben et al., 2014). De plus, le nombre de copies de ces chromosomes varie d'une espèce à l'autre, avec des espèces ayant une seule copie comme *Cupressus glabra* (Muratova, 2000) ou des espèces pouvant avoir jusqu'à 50 copies ou plus dans la même cellule e.g., *Pachyphytum fittkaui* (Uhl & Moran, 1973).

La diversité numérique existe également entre les individus de la même population, tout comme ils peuvent être présents ou absents et en nombre variable dans des tissus gonadiques ou somatiques du même individu (Burt & Trivers, 2006; Camacho, 2005). Les chromosomes B ne s'apparentent pas et ne recombinent pas avec les chromosomes standards pendant la méiose. De plus, ils sont hérités de façon non mendéienne, faisant de leur mode de transmission un mode irrégulier (Camacho, 2005; Camacho et al., 2000; Jones, 1991).

Pendant des décennies, les questions relatives à leurs origines, leurs structures, leurs compositions moléculaires ainsi que leurs rôles fonctionnels sont restées en suspens. Cependant, la révolution technologique qu'ont connu les domaines de la bioinformatique et de la génomique depuis quelques années contribuent au déchiffrement de ces chromosomes énigmatiques afin d'apporter des éléments de réponse et de compléter le puzzle autour de l'histoire, la régulation, la maintenance et l'évolution des chromosomes B.

II.1. La distribution des chromosomes B chez les eucaryotes

Les chromosomes B pourraient être présents chez environ 15 % des espèces eucaryotes (Camacho, 2005). Ils ont été identifiés majoritairement chez les plantes, avec environ 2087 espèces possédant au moins un chromosome B. Ils ont été également retrouvés dans 520

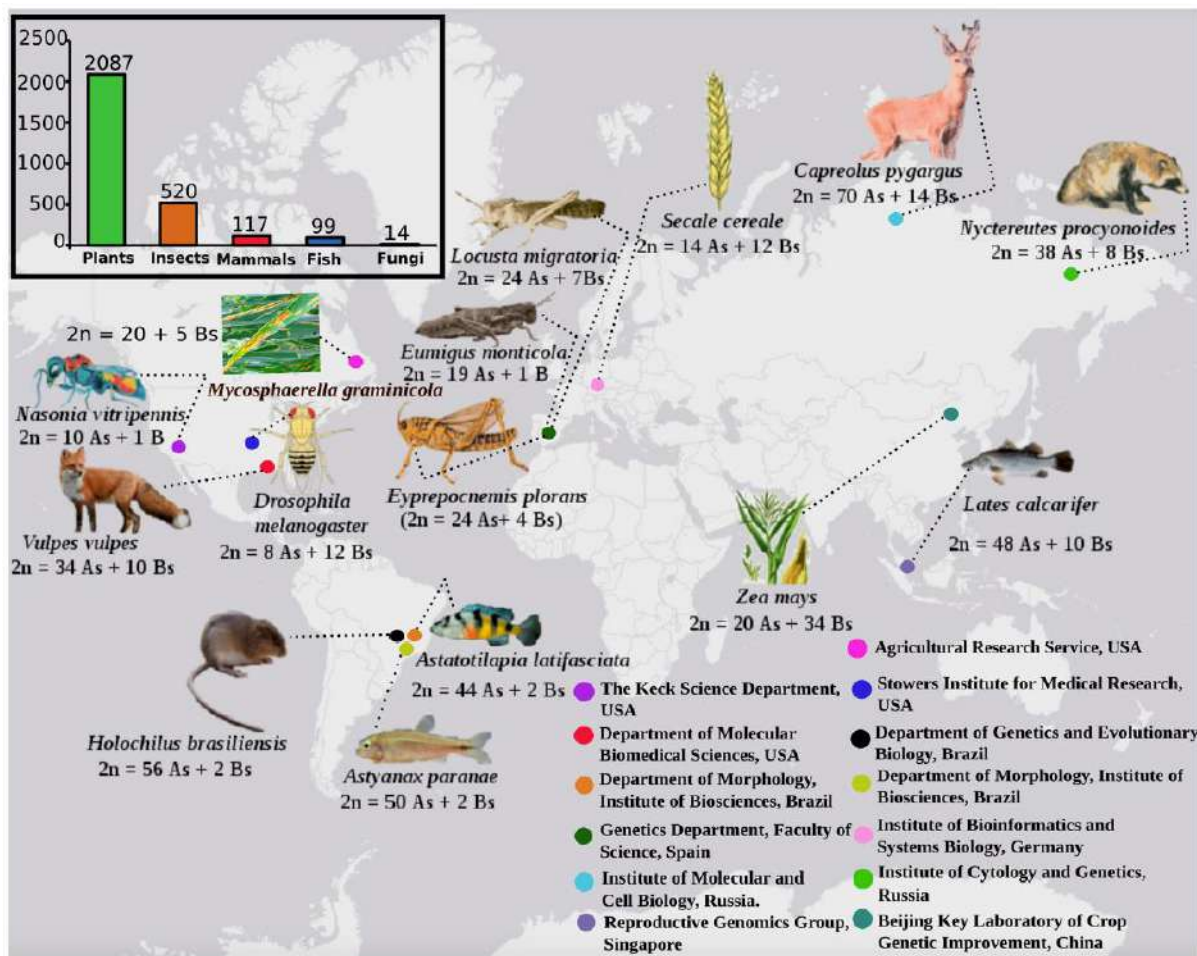


Figure 3. Distribution des chromosomes B dans les principaux groupes d'eucaryotes. Le diagramme en bâtons en haut à gauche montre le nombre d'espèces par groupe possédant le chromosomes B, provenant de la base de données “the B-Chrom database”: <http://www.bchrom.csic.es/> mise à jour en janvier 2019) (Ahmad & Martins, 2019; D’Ambrosio et al., 2017). Les espèces présentées sur la carte correspondent à celles qui sont les plus étudiées par des approches omiques. Le cercle plein en couleur à côté de chaque espèce correspond à la couleur du cercle indiquant les instituts de recherche dans lesquels les études ont été effectuées (en bas à droite) avec l’information géographique. D’après (Ahmad & Martins, 2019).

espèces d'insectes, 117 espèces de mammifères, 99 espèces de poissons, et enfin 14 espèces de champignons (Figure 3) (données extraites à partir de la base de données “the B-Chrom database”: <http://www.bchrom.csic.es/> mise à jour en janvier 2019) (Ahmad & Martins, 2019; D’Ambrosio et al., 2017).

Chez les poissons, les chromosomes B ont été identifiés pour la première fois chez le cyprinidé *Alburnus alburnus* (Hafez et al., 1981), et le characiforme *Prochilodus Scrofa* (Pauls & Bertollo, 1983). Depuis, ces chromosomes ont été rapportés dans plusieurs sous-groupes de poissons et majoritairement dans les familles des cichlidés (ordre des perciformes) et celle des characidés (ordre des characiformes). En effet, environ 23 espèces de cichlidés d’Amérique du Sud et d’Afrique de l’Est, en particulier du lac Victoria présentent un ou plusieurs chromosomes B (D’Ambrosio et al., 2017; Jones, 2017). Chez les characiformes, la famille des characidés comporte à elle seule 24 espèces ayant au moins un chromosome B (D’Ambrosio et al., 2017; Jones, 2017).

La famille des characidés comporte plusieurs genres constitués exclusivement d’espèces d’eau douce très abondantes en Amérique du Sud, mais également en Amérique Centrale (*e.g.*, Mexique). À ce jour, les analyses de caryotypes de cette famille ont révélé la présence de chromosomes B chez 12 des 250 espèces reconnues appartenant au genre *Astyanax* (50 % des espèces de characidés ayant des chromosomes B) (Castro et al., 2019). Parmi ces espèces, les chromosomes B ont été retrouvés chez *Astyanax scabripinnis*, *Astyanax altiparanae*, *Astyanax fasciatus*, ou encore *Astyanax mexicanus* autrement appelé le tétra mexicain (Jones, 2017).

II.2. La structure des chromosomes B

Comme mentionné précédemment, le nombre de chromosomes B peut varier remarquablement entre les espèces, les individus d'une même population, voire même au sein de l'individu *e.g.*, le seigle *Secale cereale*, $2n = 7$ As + 0-8 Bs ; la mouche *Drosophila subsilvestris*, $2n = 6$ As + 0-5 Bs ; le rat *Rattus rattus thai*, $2n = 42$ As + 1-6 Bs (Jones, 2017). Chez la téosinte *Zea mays*, le nombre de chromosomes B peut même excéder celui des chromosomes A, avec $2n = 20$ As + 0-34 Bs (Jones & Rees, 1982).

À ce polymorphisme numérique s’ajoutent des variations morphologiques et structurelles considérables entre les chromosomes B de la même espèce. Par exemple, chez 9 populations Nord-Africaines du criquet *Eyprepocnemis plorans*, 16 variantes du chromosome B ont été identifiées, présentant des polymorphismes très importants dans la structure et la taille (Bakkali

& Camacho, 2004). Cependant, la structure de ces chromosomes peut aussi être identique entre des espèces proches, comme dans le cas des deux espèces de seigle, *Secale cereale* et *Secale segetale* (Houben et al., 2014; Marques et al., 2013; Niwa & Sakamoto, 1995).

Ces polymorphismes numériques, morphologiques et structurels ont été également rapportés chez les poissons : une variabilité numérique importante inter- et intra-espèces existe chez e.g., l'ablette *Alburnus alburnus*, $2n = 50$ As + 0-2 Bs (Schmid et al., 2006) ; le poisson-couteau *Apteronotus albifrons*, $2n = 24$ As + 0-4 Bs (Carvalho et al., 2008); le tétra aux yeux rouges *Moenkhausia sanctaefilomenae*, $2n = 50$ As + 1-8 Bs (Foresti et al., 1989).

Au-delà de ce polymorphisme numérique, les poissons possèdent 3 classes de tailles différentes de chromosomes B qui sont identifiables par comparaison avec la taille des chromosomes standards :

- Les grands chromosomes B : ils peuvent être aussi grands que la grande paire de chromosomes standards. C'est le type de chromosome B le moins fréquent chez les poissons e.g., chez le cichlidé d'Amérique du Sud *Crenicichla reticulata*, $2n = 48$ As + 1-3 Bs (Feldberg et al., 2004).
- Les petits chromosomes B : ils sont généralement de la taille de la petite paire des chromosomes A e.g., chez une espèce très proche de *Crenicichla. reticulata*, *C. lepidota*, $2n = 48$ As + 1-3 Bs (Pires et al., 2015).
- Les microchromosomes B : ils sont très largement répandus chez les poissons e.g., *Prochilodus lineatus*, $2n = 54$ As + 0-7 Bs (Oliveira et al., 1997).

Cette variabilité de taille peut se manifester de manière inter-individuelle comme c'est le cas chez certains cichlidés du Lac Victoria, chez qui les individus de la même espèce contiennent à la fois des microchromosomes et petits chromosomes B, e.g., *Lithocromis rubripinnis* et *Neochromis greenwoodi* (Yoshida et al., 2011). Il convient également de noter que l'ablette *A. alburnus* possède des chromosomes B géants plus grands que les chromosomes A des mêmes individus (Ziegler et al., 2003).

Outre les cichlidés, l'hétérogénéité de taille des chromosomes B a été également observée chez un autre groupe de poissons, l'ordre des characiformes avec des espèces possédant : des grands chromosomes e.g., *Astyanax fasciatus* ; des petits chromosomes e.g., *Astyanax altiparanae* ; des microchromosomes e.g., *Astyanax mexicanus* (Carvalho et al., 2008). De plus, cette

hétérogénéité peut s'étendre à l'échelle des populations d'une même espèce pouvant présenter un ou plusieurs types de chromosomes B de tailles différentes à l'exemple d'*Astyanax scabripinnis* qui possède à la fois des micros, petits et grands chromosomes B (Carvalho et al., 2008).

II.3. Composition moléculaire et fonction des chromosomes B

Initialement, la composition moléculaire des chromosomes B a été explorée par des approches cytogénétiques en se basant sur l'hybridation de sondes spécifiques contenant des séquences répétitives. Ces études ont révélé que les chromosomes B sont partiellement ou totalement hétérochromatiques chez la majeure partie des espèces analysées (Burt & Trivers, 2006; Camacho et al., 2000). Ceci est dû à l'accumulation substantielle de séquences répétitives du génome dont ils proviennent. Parmi ces séquences, on retrouve l'ADN ribosomal, les éléments transposables, ou encore les ADN satellites (Silva et al., 2014).

Grâce aux nouvelles techniques de séquençage de nouvelle génération (NGS, pour Next-Generation Sequencing) et durant cette dernière décennie, des études génomiques ont été réalisées sur un certain nombre d'espèces différentes afin de caractériser les séquences portées par les chromosomes B. Par exemple, chez les mammifères (Becker et al., 2011), les plantes (Huang et al., 2016; Jin et al., 2005; Martis et al., 2012), les insectes (Bauerly et al., 2014; Hanlon et al., 2018), ou encore les poissons (Clark et al., 2017, 2018; Valente et al., 2014).

L'ensemble de ces études ont révélé qu'en plus de l'identification de milliers de séquences répétitives telles que les ADNs satellites, les éléments transposables, les éléments mobiles, ou encore des fragments de gènes (pseudogènes), ces chromosomes B portent également plusieurs gènes intacts (séquence codante entière). C'est le cas chez le criquet *Eyprepocnemis plorans* et deux espèces de souris du genre *Apodemus* (Makunin et al., 2018; Navarro-Domínguez et al., 2017). Chez le cichlidé d'Afrique *Astatotilapia latifasciata*, des milliers de fragments de gènes ont été identifiés mais aussi des gènes entiers qui codent pour des ARN ribosomaux, des gènes impliqués dans la ségrégation chromosomique, ou encore dans la recombinaison (Poletto et al., 2010; Valente et al., 2014).

Parmi ces gènes, certains sont connus pour être exprimés dans l'organisme. Chez *A. latifasciata*, des gènes connus pour jouer un rôle dans la ségrégation chromosomique durant les divisions cellulaires tels que TUBB1 (pour Tubulin B1), KIFF11 (pour kinesin family member 11), ou encore Separin sont exprimés (Valente et al., 2014, 2017). D'autres gènes qui

jouent un rôle dans la régulation du métabolisme, l'olfaction, ou dans la régulation de la transcription sont aussi exprimés chez cette espèce mais aussi chez d'autres espèces (Benetta et al., 2019). Il semblerait, contrairement à ce qui a été supposé depuis des décennies, que les chromosomes B pourraient jouer un rôle dans l'organisme hôte ou du moins dans des processus assurant la transmission même des chromosomes B d'une génération à l'autre.

II.4. Les mécanismes de transmission des chromosomes B

Au cours de la méiose, les chromosomes A homologues (chacun formé de deux chromatides sœurs) s'associent (processus d'appariement) en prophase I pour former un bivalent. C'est à ce moment que les chromatides homologues se croisent entre elles à plusieurs endroits sous forme de tétrade (enjambement) pour échanger du matériel génétique, autrement dit effectuer des "recombinaisons". Les chromosomes homologues vont se séparer en Anaphase I en se dirigeant vers les deux pôles opposés de la cellule, assurant une répartition équitable (50 % dans chaque cellule) du matériel génétique. Ce comportement constitue une des bases de la ségrégation mendélienne.

Contrairement à ces chromosomes standards qui vont par paire, les chromosomes B sont généralement univalents et ne s'apparent pas avec les chromosomes A au cours de la méiose (Camacho et al., 2000). La transmission des chromosomes B est dépendante de mécanismes qui leur sont spécifiques et vont à l'encontre des lois fondamentales de la génétique mendélienne. Ces mécanismes sont capables d'augmenter la fréquence des Bs dans la population de génération en génération pour "assurer leur survie" (Camacho, 2005) et sont connus sous le nom de mécanismes d'accumulation ou de dérive méiotique (meiotic drive) (Camacho, 2005).

En revanche, cette "pression" exercée par les chromosomes B via les mécanismes d'accumulation provoque un conflit génétique avec les chromosomes A. Ces derniers, "agissent" à leur tour pour tenter d'empêcher l'augmentation de leur nombre, particulièrement lorsqu'ils présentent des effets négatifs sur les capacités et la fertilité de l'organisme (Camacho et al., 2003). Un tel mécanisme a été supposé chez le criquet *Eyprepocnemis plorans* qui possède une grande variété de chromosomes B. Ainsi, certains types de ces Bs sont éliminés en faisant intervenir des gènes suppresseurs localisés sur les chromosomes A afin de maintenir une fréquence stable au sein de la population (Camacho et al., 1997; Herrera et al., 1996)

Bien que les mécanismes moléculaires responsables de cette dérive ne soient pas encore décryptés (Burt & Trivers, 2006), les études cytogénétiques chez plusieurs espèces d'animaux et de plantes ont révélé différents types de mécanismes de transmission des chromosomes B, impliquant la non-disjonction chromosomique, ou la ségrégation préférentielle, ou les deux à la fois (Camacho, 2005; Clark et al., 2017) Ces mécanismes peuvent survenir à différents stades du cycle de vie à savoir : dérive pré-méiotique (au cours de la mitose), dérive méiotique (pendant la méiose), ou encore dérive post-méiotique (juste après la méiose qui est plus fréquente chez les plantes) (Camacho et al., 2000).

D'un autre côté, une des nombreuses particularités de ces chromosomes B est leur spécificité tissulaire (présents dans certains tissus et absents dans d'autres). C'est le cas chez *Aegilops speltoides* qui met en route un mécanisme d'élimination programmée de ces Bs de manière spécifique dans les racines, tandis que les autres parties de la plante en contiennent plusieurs copies (Ruban et al., 2020). Ce processus intervient dès les premiers stades de la différenciation des tissus embryonnaires suite à la non-disjonction des chromatides pendant la mitose et à un retard dans l'anaphase, entraînant la micro-nucléation des Bs et leur dégradation par la suite (Ruban et al., 2020). Les hypothèses les plus probables pour expliquer cette élimination spécifique des racines seraient d'éviter l'expression ou la surexpression de gènes spécifiques aux racines pouvant avoir des effets délétères, ou bien la mise en place d'un mécanisme de sélection des Bs permettant leur maintien uniquement dans les autres tissus (Ruban et al., 2020).

II.5. L'origine et l'évolution des chromosomes B

Depuis leur découverte, plusieurs scénarios ont été dressés pour tenter d'expliquer l'origine évolutive des chromosomes B. La comparaison cytogénétique entre les compositions des chromosomes A et B chez plusieurs espèces ont révélé l'existence à la fois de séquences d'ADN qui sont partagées entre les chromosomes A et les chromosomes B, et des séquences spécifiques aux Bs.

II.5.1. L'origine interspécifique

Le premier scénario est fondé sur la présence de séquences spécifiques aux chromosomes B. Ces séquences, étant absentes des chromosomes A de l'organisme hôte sont retrouvées chez d'autres espèces très proches. Un exemple très intéressant est celui du molly

Poecilia formosa, qui se reproduit par gynogenèse et qui a donc besoin du sperme d'une espèce étroitement proche pour initier son développement. Cependant, le matériel génétique paternel transmis par les spermatozoïdes (d'une espèce proche) est éliminé aussitôt après la fécondation mais, dans certains cas des microchromosomes B échappent à cette élimination et persistent dans le génome de l'espèce. Dans le milieu naturel, environ 5 % des individus de cette espèce contiennent ces microchromosomes B. Il s'agit dans ce cas d'une d'origine interspécifique (Schartl et al., 1995).

II.5.2. L'origine intraspécifique

Le second scénario suggère que les chromosomes Bs seraient dérivés d'un ou de plusieurs chromosomes A, et on parle alors d'une origine intraspécifique. Cette origine est souvent soutenue par l'existence de séquences communes entre les chromosomes B et un ou plusieurs chromosomes A de l'organisme hôte. Actuellement, les études réalisées dans ce contexte proposent deux mécanismes possibles :

Hypothèse 1 : les autosomes seraient à l'origine des chromosomes B

Chez la drosophile *Drosophila melanogaster*, l'identification d'une séquence répétitive d'ADN satellite (ou satDNA) connue pour être liée à une histone centromérique présente sur les chromosomes B d'un côté et uniquement sur le chromosome 4 de l'autre côté laisse suggérer que les chromosomes B seraient dérivés d'un seul chromosome, le chromosome 4 (Hanlon et al., 2018). Il a été supposé que la formation du chromosome B serait le résultat d'une mauvaise division centromérique provoquant la séparation des bras longs des petits bras. Les deux petits bras contenant cette séquence répétitive auraient fusionné et formé un isochromosome (Hanlon et al., 2018).

Chez d'autres espèces, les chromosomes B sont constitués d'une quantité substantielle de séquences répétitives, de fragments de gènes ou de gènes entiers qui sont à l'origine retrouvés sur plusieurs autosomes, faisant ainsi du chromosome B une mosaïque multi-chromosomique (Houben et al., 2019). Prenons l'exemple d'*Astatotilapia latifasciata*, un cichlidé originaire d'Afrique, les individus de cette espèce (mâles et femelles) peuvent avoir une ou deux copies identiques de Bs. La formation des chromosomes B aurait pour origine l'apparition d'un chromosome proto-B contenant une région centromérique issu à son tour d'une duplication segmentaire d'un seul autosome. Ce proto-B aurait accumulé des fragments d'ADN correspondant à des séquences dégénérées et des gènes entiers provenant de l'ensemble des

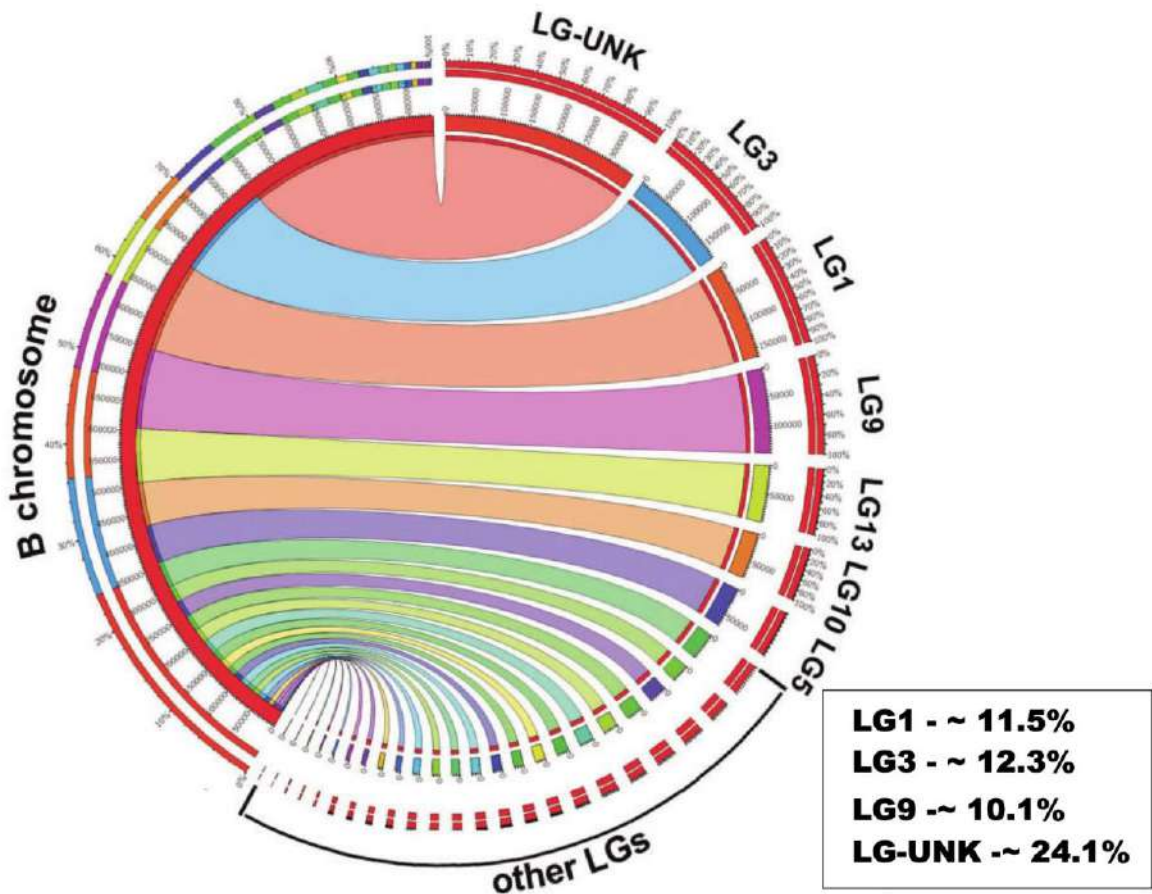


Figure 4. Origine multi-chromosomique du chromosome B chez *Astatotilapia latifasciata*.

Cercle montrant la liaison entre des parties du chromosome B et les groupes de liaison (LG, pour Linkage Group) de *Metriaclima zebra* comme génome de référence. Le chromosome B est représenté à gauche et les LG correspondants à droite. Le pourcentage génomique des principaux LG (1, 3 et 9) est représenté sur le chromosome B et le cadre (à droite) de la figure. D'après (Valente et al., 2014).

autosomes assurant ainsi sa persistance au cours de l'évolution. Ensuite, une amplification intensive de séquences d'ADN en même temps que la formation d'un autre bras du proto-B identique a donné naissance aux chromosomes B (isochromosomes) chez cette espèce qui est donc une mosaïque génomique de l'ensemble des autosomes (Figure 4) (Valente et al., 2014).

Hypothèse 2 : les chromosomes sexuels et les Bs dérivent les uns des autres

Les chromosomes sexuels et les Bs ont également un certain nombre de caractéristiques communes telles que les homologies de séquences, le comportement méiotique ou encore l'accumulation de séquences répétitives suggérant que les uns auraient dérivé des autres (Camacho et al., 2000; Camacho et al., 2011). Chez plusieurs espèces de drosophiles, le chromosome Y qui ne contient pas le déterminant majeur du sexe et qui est très différent de son homologue X, semble ne pas être issu de la dégénérescence du X (Carvalho, 2002; Carvalho et al., 2009; Hackstein et al., 1996). Les auteurs suggèrent plutôt que le Y des espèces du genre *Drosophila* serait dérivé du chromosome B (Carvalho, 2002; Carvalho et al., 2009; Hackstein et al., 1996)

Chez les espèces de la tribu des rongeurs Oryzomyini, le B chromosome proviendrait de l'hétérochromatine péricentrique des chromosomes sexuels (Ventura et al., 2015). Cette hypothèse est également valable pour les chromosomes B de la grenouille *Leiopelma Hochstetter* qui présente une homologie de séquence avec le chromosome sexuel suggérant ainsi que les Bs sont dérivés du chromosome W univalent (Sharbel et al., 1998). Chez les deux espèces du genre *Characidium* (ordre des characiformes) e.g., *Characidium gomesi* et *Characidium pterostictum* possédant un système de détermination du sexe de type ZZ/ZW, les chromosomes B n'ont été identifiés que chez une seule population de chacune d'elles (Pansonato-Alves et al., 2014). L'identification de séquences partagées entre les chromosomes B et les chromosomes sexuels chez ces deux espèces renforce la théorie selon laquelle les Bs proviennent des chromosomes W spécifiques à chacune d'elles (Pansonato-Alves et al., 2014; Serrano-Freitas et al., 2020).

II.6. Les chromosomes B et le déterminisme du sexe

Au-delà de ces aspects génomiques et évolutifs qui suggèrent fortement l'existence d'un lien étroit entre les chromosomes B et les chromosomes sexuels chez de nombreuses espèces, l'implication directe des Bs dans la détermination du sexe a été rapportée chez d'autres espèces à l'instar de la guêpe *Nasonia vitripennis*. Cette dernière possède un chromosome B

appelé PSR (Paternal Sex Ratio) qui est transmis à la progéniture uniquement par le sperme (les mâles) (Reed, 1993). Chez cette espèce, les œufs fécondés produisent des femelles diploïdes alors que les œufs non fécondés (haploïdes) produisent uniquement des mâles (détermination du sexe par ploïdie). Pendant la fécondation, le matériel génétique haploïde du père est transféré à l'ovule et ces derniers devraient se développer en femelles. Cependant, lorsque le spermatozoïde contient un chromosome B, ce dernier provoque la perte complète du matériel génétique paternel (excepté lui-même) suite à un remodelage de sa chromatine, et ce, dès la première division mitotique de l'embryon (Reed & Werren, 1995). De ce fait, l'élimination du matériel génétique spermatique transforme les œufs fécondés diploïdes en mâles haploïdes porteurs du chromosome B, assurant ainsi la transmission du chromosome B et la détermination du sexe mâle.

Le carassin *Carassius gibelio* est une espèce polyplioïde qui présente à la fois une reproduction unisexuée (gynogenèse) et une reproduction sexuée (Gui & Zhou, 2010). La fécondation des œufs par des spermatozoïdes d'une autre espèce produit systématiquement des femelles, tandis qu'une reproduction sexuée nécessite généralement le sperme des mâles de *C. gibelio* (Gui & Zhou, 2010). Des microchromosomes B supplémentaires (au nombre de 3-4) ont été identifiés uniquement chez les mâles de cette espèce (Li et al., 2016). Le croisement entre femelles inversées (mâles génotypiques) suite à un traitement hormonal à l'œstradiol de *C. gibelio* contenant 2 chromosomes B et un mâle de *Cyprinus carpio* donne une descendance à 51,6 % de mâles (avec chromosomes B), tandis que le croisement entre femelles de *C. gibelio* avec 1 seul chromosome B et un mâle de *C. carpio* donne 81,9 % de mâles (avec chromosome B). Ainsi, ces résultats suggèrent que les microchromosomes supplémentaires des mâles de *C. gibelio* jouent un rôle dans la détermination du sexe mâle (Li et al., 2016). En outre, un gène appelé *setdm* (SET domain-containing gene) identifié sur les microchromosomes B, présente une expression spécifique dans les testicules de *C. gibelio*, suggérant que les chromosomes B sont impliqués dans le développement testiculaire et la spermatogenèse chez cette espèce (Li et al., 2017)

Chez les cichlidés d'Afrique de l'Est (du lac Victoria), la présence des chromosomes B est restreinte aux femelles chez *Lithochromis rubripinnis*, et leur nombre peut varier de 0 à 2 en fonction des individus ; cependant, ils sont totalement absents chez les mâles (Yoshida et al., 2011). Les croisements entre mâles et femelles avec 0, 1, ou 2 B chromosomes génèrent des descendances avec des sex-ratios différents. Dans les croisements entre mâles et femelles sans Bs, les descendances présentent des sex-ratios de 50 : 50. Cependant, lorsqu'on croise les mâles

avec des femelles ayant 1 B, les descendances sont constituées de 74 %, 79 %, ou 91 % de femelles. D'un autre côté, les femelles avec 2 chromosomes B donnent naissance à une progéniture 100% femelle. Ces résultats montrent clairement l'existence d'une corrélation positive entre le nombre de chromosomes B chez les femelles et le pourcentage de femelles dans la descendance, suggérant que ces chromosomes B sont impliqués dans la détermination du sexe chez les femelles de *Lithochromis rubripinnis* (Yoshida et al., 2011).

Dans l'ordre des characiformes, les chromosomes B ont été identifiés à la fois chez les mâles et les femelles de plusieurs populations de *Moenkhausia sanctaefilomenae* (Utsunomia et al., 2016). Cependant, il y a une population de cette espèce chez qui, les chromosomes B sont restreints exclusivement aux mâles (Camacho et al., 2011; Portela-Castro et al., 2000). Dans le genre *Astyanax*, *A. scabripinnis* est l'un des modèles chez qui l'origine, l'évolution et le rôle des Bs dans la détermination du sexe ont été le plus explorés (Castro et al., 2019). À ce titre, les travaux de Vicente et collaborateurs, basés sur l'évaluation de la fréquence des chromosomes B chez trois populations d'*A. scabripinnis*, ont révélé que ces Bs sont plus fréquents chez les femelles que chez les mâles avec des nombres pouvant aller de 0 à 2 chromosomes par individu (Vicente et al., 1996). Les auteurs ont également rapporté l'association très forte entre la fréquence des Bs et le sex-ratio dans certaines populations (Vicente et al., 1996). Ces résultats ont été renforcés par ceux de Néo et collaborateurs montrant que les fréquences des chromosomes Bs sont plus importantes chez les femelles que chez les mâles d'*Astyanax scabripinnis* (Néo et al., 2000). Outre les fréquences plus importantes chez les femelles dans certaines populations, les Bs ont été identifiés exclusivement chez les femelles d'autres populations d'*A. scabripinnis* (Mizoguchi & Martins-Santos, 1997).

Au vu de l'accumulation substantielle de données sur le potentiel rôle des chromosomes B dans différents taxons en particulier chez les poissons, il apparaît que l'association forte des chromosomes B aux chromosomes sexuels, au sexe phénotypique et à la détermination du sexe de manière générale n'est pas anodine. D'autre part, l'ensemble de ces données montrent clairement l'intérêt majeur d'étudier la détermination du sexe en lien avec les chromosomes B chez les poissons et plus particulièrement ceux de l'ordre des characiformes en particulier, jusque-là très peu étudiées et chez qui aucun déterminant majeur n'a été identifié à ce jour. Ces derniers s'avèrent être un groupe très intéressant de par la grande diversité d'espèces qu'il contient. Parmi toutes ces espèces, le tétra mexicain *Astyanax mexicanus* est un modèle pertinent pour explorer les mécanismes de détermination du sexe en lien avec la grande diversité populationnelle entre les morphotypes de rivières et ceux des grottes (cavernicoles)

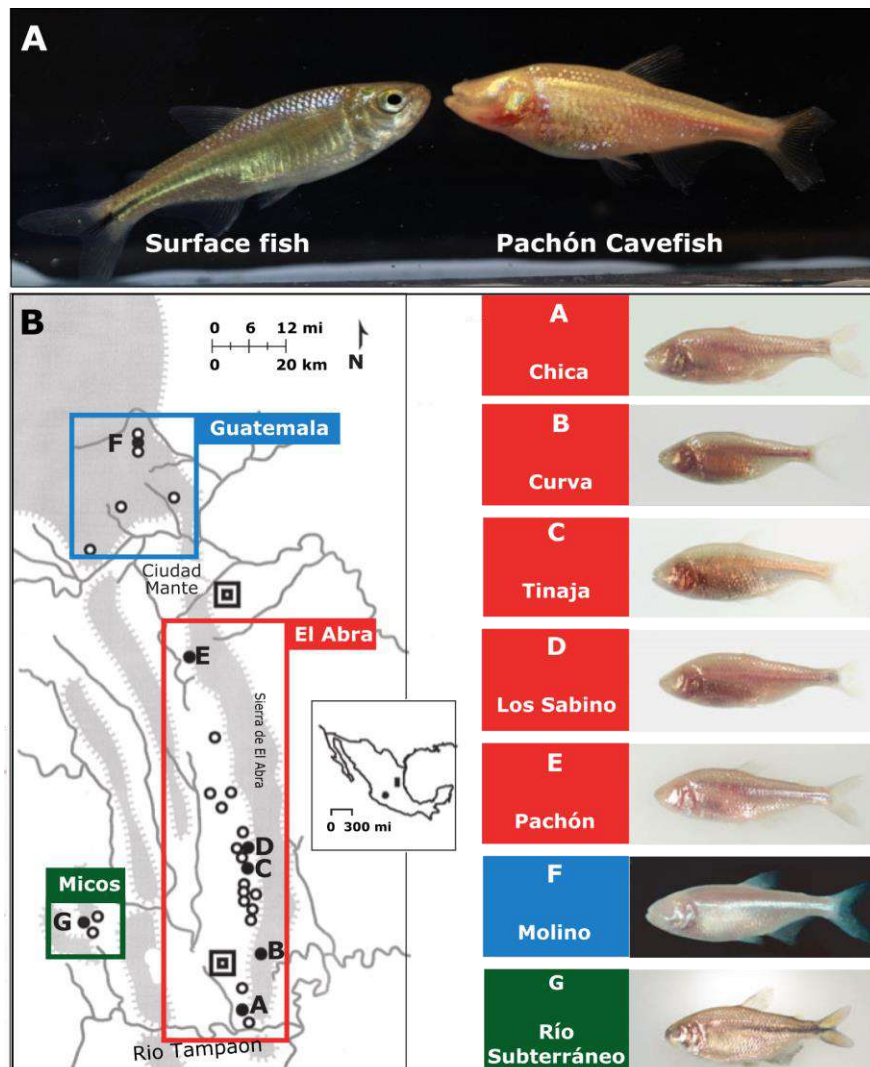


Figure 5. Les différentes formes d'*Astyanax mexicanus* et la distribution géographique des populations cavernicoles. (5A) : Une photographie montrant la forme de surface (à gauche) et la forme cavernicole à (droite) (crédit photo : Alizée Frezel). **(5B) :** La cartographie du Nord-Est du Mexique montrant la distribution géographique de 29 populations de la forme cavernicole (à gauche). L'icône insérée à droite de la carte correspond à la carte géographique du Mexique sur laquelle est indiquée la région du Nord-Est du Mexique (rectangle plein). Les cadres vert, bleu et rouge correspondent respectivement aux populations des régions Micos, Guatemala et de El Abra. Les cercles vides et pleins indiquent la localisation approximative des grottes sur les trois régions. Les lettres (A-G) correspondant aux cercles pleins sur la carte et indiquent la localisation des grottes dont certains individus sont montrés sur la droite avec les noms des grottes correspondant avec le code couleur. Droite : exemples de poissons cavernicoles différents. Adaptée d'après (Jeffery, 2009).

et la présence de chromosomes B. Dans les sections suivantes, nous allons porter un accent particulier sur le modèle *Astyanax mexicanus* et l'intérêt qu'il présente d'un point de vue évolutif.

III. Le modèle *Astyanax mexicanus*

III.1. *Astyanax mexicanus* : une seule espèce, plusieurs populations

La famille des characidés est constituée d'une grande diversité d'espèces vivant exclusivement en eau douce, répartie dans plusieurs régions du Texas, Mexique, Amérique Centrale et Amérique du Sud (Eschemeyer, 2020). Le genre *Astyanax* appartenant à cette famille, est l'un des plus diversifiés du groupe des Characidés. Leur phylogénie est complexe et ils sont supposés être un groupe non monophylétique (Terán et al., 2020). Parmi les espèces de ce genre, on retrouve *Astyanax mexicanus*, appelé communément le tétra mexicain, et ayant la particularité de se présenter en deux morphotypes ou formes très distinctes d'un point de vue morphologique (Mitchell et al., 1977). Il s'agit d'un morphotype de surface très commun, pigmenté et possédant des grands yeux (SF, pour Surface Fish) et d'un autre morphotype cavernicole dépigmenté et totalement aveugle (CF, pour Cave Fish) (Figure 5A).

Alors que le morphotype de surface bénéficie d'une large distribution géographique dans les rivières, les cours d'eau et les lacs de l'Amérique Centrale, s'étendant jusqu'au Texas aux Etats Unis (Miller & Smith, 1986), les formes cavernicoles sont, quant à elles, réparties principalement dans trois chaînes de montagnes karstiques au Nord-Est du Mexique (provinces de San Luis Potosi et Tamaulipas) sur une distance de 200 km de longueur et 60 km de largeur (Elliott, 2016b; Mitchell et al., 1977). Ces régions ont été dénommées par rapport aux chaînes montagneuses qui dominent chacune d'elles à savoir : la Sierra de El Abra (région de El Abra), la Sierra de Guatemala (région de Guatemala) et enfin la région de Micos (Sierra de Colmena), autour de la ville de Ciudad Valles (Figure 5B) (Elliott, 2019; Jeffery, 2009; Mitchell et al., 1977). Actuellement, seulement 30 grottes parmi les centaines de cavités découvertes dans la région sont connues pour abriter des populations d'*Astyanax mexicanus* cavernicoles (Elliott, 2019; Elliott, 2016b; Espinasa et al., 2018; Mitchell et al., 1977).

Initialement lors de la découverte des premiers morphotypes cavernicoles, ces populations ont été identifiées en tant qu'espèces appartenant au genre *Anoptichthys*, à l'instar de la population de la Cueva Chica (*Anoptichthys jordani*), la première découverte à environ 12 km au Sud-Est

de Ciudad Valles, San Luís Potosí (Hubbs & Innes, 1936). Ensuite, la deuxième population décrite correspond à celle de la Cueva de El Pachón en tant que *Anoptichthys antrobius* dans Tamaulipas (Álvarez, 1946), et enfin la population de la Cueva de Los Sabinos dénommée *Anoptichthys hubbsi* (Álvarez, 1947). Cette dernière est située à environ 11 km au Nord-Est de Ciudad Valles, San Luís Potosí (Mitchell et al., 1977). Ces découvertes ont été suivies par 27 autres populations cavernicoles jusqu'en 2018 (Elliott, 2019; Espinasa et al., 2018; Mitchell et al., 1977).

En 1957, des séries de croisements entre ces trois populations et celles de surface ont été réalisées, montrant que les deux formes sont interfertiles et leurs hybrides sont également fertiles et viables (Şadoğlu, 1957). Bien que ces populations des grottes soient initialement définies comme des espèces différentes y compris pour les poissons de surface identifiés auparavant en tant que *Astyanax fasciatus*, aujourd'hui dans la littérature, l'espèce *Astyanax mexicanus* regroupe les 30 formes cavernicoles et celles de surface.

Pour distinguer les populations cavernicoles entre elles, les noms des grottes dans lesquelles elles vivent ont été attribués à chacune des populations correspondantes. La Sierra de El Abra regroupe la majorité des grottes contenant des formes cavernicoles d'*A. mexicanus* avec 21 populations au total délimitées par la Cueva de El Pachón au Nord et les Cuevas de Chica et del Prieto (Los Cuates) au Sud de la région tout près de Ciudad Valles. La Sierra de Guatemala, contient quant à elle, 6 populations et enfin la région Micos comporte 3 populations identifiées à ce jour (Figure 5B) (Elliott, 2019; Espinasa et al., 2018; Gross, 2012; Jeffery, 2009; Mitchell et al., 1977). Parmi toutes ces populations, celles de Molino dans la Sierra de Guatemala et de la Cueva del Río Subterráneo dans la région Micos, ou encore les populations de Sótano de la Tinaja et surtout de la Cueva de El Pachón dans la Sierra de El Abra sont les plus étudiées (Jeffery, 2020).

D'un point de vue d'accessibilité aux grottes, deux terminologies différentes ont été utilisées pour distinguer les grottes entre elles à savoir : la "Cueva" pour les grottes dont l'entrée est horizontale et peut se faire en marchant et la "Sótano" dont l'entrée est verticale. Pour des raisons de simplicité, nous allons regrouper ces deux terminologies dans le terme "grottes". Ainsi, l'accessibilité aux populations cavernicoles peut être facile comme c'est le cas pour la grotte Pachón. Cependant, certaines d'entre elles nécessitent du matériel adapté et des compétences particulières en spéléologie comme c'est le cas pour la grotte Tinaja dans la Sierra de El Abra. Bien que l'exploration humaine des grottes du Nord-Est du Mexique n'ait pas

montré de connexion entre les différentes grottes en raison des difficultés d'accessibilité, Mitchell et collaborateurs ont suggéré que certaines d'entre elles sont probablement en contact ou l'ont été par le passé (Mitchell et al., 1977). Par exemple, le nombre très important de polymorphismes partagés à certains loci entre les individus de Tinaja et Sabinos suggère fortement des migrations ou des contacts souterrains entre ces deux populations (Pierre et al., 2020).

Outre l'accessibilité plus ou moins facile, les grottes sont très différentes les unes des autres. Leurs tailles peuvent aller de 20 mètres (m) de longueur pour la grotte Roca jusqu'à 7 202 m de longueur pour la plus grande, celle de Arroyo (Elliott, 2016b). La profondeur totale des grottes varie également entre 5 m pour celle de Toro jusqu'à la plus profonde, la grotte Soyate avec 234 m (Elliott, 2016b). En fonction de la taille des grottes, lorsque le niveau d'eau est bas en fin de saison sèche, certaines d'entre elles sont constituées uniquement d'une piscine (une sorte de marre plus ou moins grande), tandis que d'autres ont plusieurs piscines qui se reconnectent lorsque le niveau d'eau remonte, comme à Pachón (Elliott, 2016b). Cette dernière est également considérée comme l'une des grottes les plus isolées, située en hauteur dans la montagne (Figure 5B) (Jeffery, 2009). Pendant la saison sèche, l'accessibilité est bonne, le niveau d'eau dans certaines piscines peut aller de quelques dizaines de centimètres jusqu'à 2 ou 3 mètres seulement, et l'accès aux poissons est relativement facile.

III.2. Les formes cavernicoles d'*Astyanax mexicanus* ont-elles une origine unique ou multiple ?

Depuis la découverte des formes cavernicoles d'*Astyanax mexicanus*, les questions sur l'origine évolutive et l'âge des populations cavernicoles ne cessent d'intriguer les scientifiques et ont fait l'objet de nombreuses études. Bien que plusieurs auteurs aient conclu que les CF pourraient avoir des origines multiples suite à plusieurs événements de colonisation des grottes, la datation de l'âge des populations cavernicoles est, quant à elle un sujet de discorde. Actuellement, dans la littérature, la plupart des études réalisées dans ce sens se sont basées principalement sur l'analyse de marqueurs mitochondriaux et de microsatellites. En conséquence, la plupart des publications résultant de ces travaux font référence à l'existence de deux groupes : le groupe le plus ancien, El Abra ("vieux"), et les populations les plus jeunes, Guatemala et Micos ("jeune") (Bradic et al., 2012; Coghill et al., 2014; Dowling et al., 2002; Gross, 2012; Hausdorf et al., 2011; Strecker et al., 2003; Strecker et al., 2004, 2012). Cependant, il est important de noter que les résultats sont très différents d'une étude à l'autre

et montrent des contradictions et des incohérences de par les différences soulignées selon les auteurs, dans la répartition des populations de CF appartenant aux “anciennes” ou aux “nouvelles” lignées (Bradic et al., 2012; Herman et al., 2018; Ornelas-García et al., 2008; Strecker et al., 2004). Par exemple, la population de la grotte Pachón est qualifiée de “vieille” d’après les marqueurs nucléaires, alors que les marqueurs mitochondriaux disent le contraire (“jeune”) (Strecker et al., 2003). Il en va de même pour le temps de divergence des populations cavernicoles et de surface estimé à 10 000 ans (Gross, 2012; Porter et al., 2007), des centaines de milliers d’années (Avise & Selander, 1972; Bradic et al., 2012), ou à quelques millions d’années (Gross, 2012; Ornelas-García et al., 2008; Strecker et al., 2004).

Cependant, ces datations ont été remises en question par les travaux de Fumey et collaborateurs (2018) grâce à l’analyse du polymorphisme nucléotidique entre les populations de surface et celle de Pachón, et la ré-analyse des microsatellites de différentes populations cavernicoles (Fumey et al., 2018). Les résultats, basés sur des modélisations de différentes natures, suggèrent fortement que la période à laquelle les deux formes de surface et de grottes ont divergé est relativement courte et inférieure à 20 000 ans (Fumey et al., 2018). Ces résultats ne sont donc pas en accord avec les données supposant l’existence de deux lignages (vieux et jeunes), d’autant plus que la population de Pachón considérée comme “vieille” semble donc s’être séparée de la lignée de surface très récemment (Fumey et al., 2018). Ces données sont fortement soutenues par l’analyse récente de la “décadence” ou pseudogénisation des gènes “de vision” (gènes liés à la phototransduction et exprimés exclusivement dans les yeux, sur lesquels la pression de sélection est totalement relâchée en absence de lumière). Les auteurs ont identifié une seule mutation perte de fonction parmi les 85 “gènes de vision” analysés dans le génome de Pachón, suggérant ainsi que cette dégénérescence est très récente et ne peut dater de millions d’années (Policarpo et al., 2020).

Les questions sur l’âge des populations cavernicoles ainsi que le nombre de colonisations qui sont à l’origine de la trentaine de populations connues dans une région limitée en termes d’espace sont un débat très controversé et complexe. Néanmoins, il est maintenant largement admis que les populations cavernicoles seraient apparues, il y a quelques dizaines de milliers d’années suite à l’invasion des grottes par une ou plusieurs populations ancestrales de surface, présentant des yeux et une pigmentation (Fumey et al., 2018; Herman et al., 2018; Policarpo et al., 2020). Nous sommes donc en présence d’un phénomène évolutif extrêmement rapide, probablement induit par un changement drastique et soudain d’environnement.



Figure 6. Les formes de surface et cavernicoles d’*Astyanax mexicanus* et leurs environnements respectifs. (A) : Illustration d’un morphotype de surface en provenance de Nacimiento del Rio Choy. Illustration de trois morphotypes des grottes Pachón (B), Chica (C) et Río Subterráneo (D) ainsi que les grottes respectives à chacune des populations. Échelle : 1 cm. D’après (Torres-Paz et al., 2018).

III.3. *Astyanax mexicanus* : une seule espèce, des environnements contrastés

Les formes de surface et de grottes du tétra mexicain vivent dans des environnements très contrastés aussi bien d'un point de vue des paramètres physico-chimiques de l'eau, qu'en terme de disponibilité et d'accessibilité à la nourriture ou encore de la luminosité (Figure 6). La forme de surface tolère une variété d'habitats tels que les eaux stagnantes (mares) ou les eaux courantes (rivière et sources d'eau) en présence de la lumière et où la disponibilité et l'accessibilité à la nourriture sont plus avantageuses (Casane & Rétaux, 2016). Ces environnements sont caractérisés par une végétation importante avec une activité photosynthétique et accueillent une grande diversité d'espèces de poissons de différentes tailles (petits et grands) et de zooplancton (Blin et al., 2020; Casane & Rétaux, 2016).

De ce fait, cet environnement assure une disponibilité permanente des ressources alimentaires aux populations de surface qui se nourrissent généralement du zooplancton, de débris animaux et végétaux, des petits poissons mais également d'insectes et d'algues filamenteuses (Casane & Rétaux, 2016). La taille des populations d'*A. mexicanus* de surface sont beaucoup plus importantes que celles des grottes, pouvant aller jusqu'à des dizaines de milliers d'individus (Bradic et al., 2012; Fumey et al., 2018). Ceci facilite probablement le choix et la recherche du partenaire sexuel pendant les périodes de reproduction (Wilkens & Strecker, 2017).

En revanche, l'environnement des populations de surface peut être aussi contraignant en raison de la présence d'autres espèces telles que les cichlidés et les cyprinidés, ou les oiseaux, qui peuvent être des prédateurs potentiels. De plus, à certaines périodes de l'année, les poissons de surface peuvent être soumis à des pressions environnementales qui peuvent se manifester par des fluctuations de températures quotidiennes (jour/nuit) ou à des hausses périodiques de températures dans les mares isolées pendant la saison de sécheresse modifiant les facteurs abiotiques du milieu.

À l'inverse des morphotypes de surface, la taille des populations cavernicoles semble être réduite, allant de quelques dizaines à quelques centaines d'individus par population, mais certaines grottes présentent des populations plus larges par rapport à d'autres (Bradic et al., 2012; Fumey et al., 2018; Mitchell et al., 1977). Par exemple, des études par capture-recapture dans la grotte Pachón suggéraient une population totale de 1950+/-1926 individus en 2009 (SR pers com, Victor Hugo Reynoso). Par conséquent, la taille de la population peut être une contrainte lors de la recherche et du choix du partenaire sexuel pour se reproduire (Wilkens & Strecker, 2017).

Bien que les températures moyennes soient relativement stables dans les grottes (autour de 23 °C), les formes cavernicoles vivent dans l'obscurité totale de façon permanente, en absence de toute activité photosynthétique et de production primaire (Figure 6) (Elliott, 2016a). En plus de l'absence totale de lumière, il est largement admis que l'environnement cavernicole est très pauvre en nutriments et dépend particulièrement de la présence ou absence de colonies de chauves-souris, ou de l'occurrence des inondations saisonnières pouvant apporter de la matière organique dans les grottes de manière irrégulière (Culver & Pipan, 2009; Mitchell et al., 1977). De ce fait, l'environnement cavernicole est souvent décrit comme très contraignant voire “extrême”.

Dans la grotte Chica, il a été rapporté que les CF se nourrissent principalement de la matière organique (débris) apportée lors des épisodes d'inondations, des mouches, des papillons de nuit, des grenouilles mortes, des criquets ou encore des chauves-souris mortes ou de leurs excréments autrement appelés “le guano” (Figure 6C) (Elliott, 2016b). Outre la population de Chica, les grottes de Los Sabinos et Pachón (Figure 6B) abritent plusieurs colonies de chauves-souris qui constituent un apport de nourriture important et probablement constant (les parasites et invertébrés du guano) durant toute l'année, contrairement aux autres grottes qui abritent très peu de colonies à l'exemple de Tinaja avec 2 colonies ou Río Subterráneo (Figure 6D) avec une seule colonie (Elliott, 2016b).

Très peu d'études se sont intéressées à la caractérisation du régime alimentaire des tétra mexicains dans les grottes hormis celle d'Espinasa et collaborateurs (2017) dans la grotte Pachón. Les analyses des contenus stomacaux et intestinaux des jeunes larves et adultes des *A. mexicanus* de cette grotte ont montré qu'en plus de certains contenus non-identifiables qui pourraient correspondre aux guanos des chauves-souris, les jeunes larves se nourrissent principalement de micro-arthropodes vivants, tandis que les adultes se nourrissent plutôt de guano, d'autres débris et d'insectes morts (Espinasa et al., 2017).

III.4. *Astyanax mexicanus* : l'adaptation convergente à un environnement extrême

Pour s'adapter à l'environnement cavernicole, les 30 populations de grottes d'*Astyanax mexicanus* identifiées à ce jour ont développé un certain nombre de traits régressifs et constructifs troglomorphiques qui ont évolué indépendamment à plusieurs reprises. Certains de ces traits sont largement partagés y compris avec d'autres espèces troglodytes

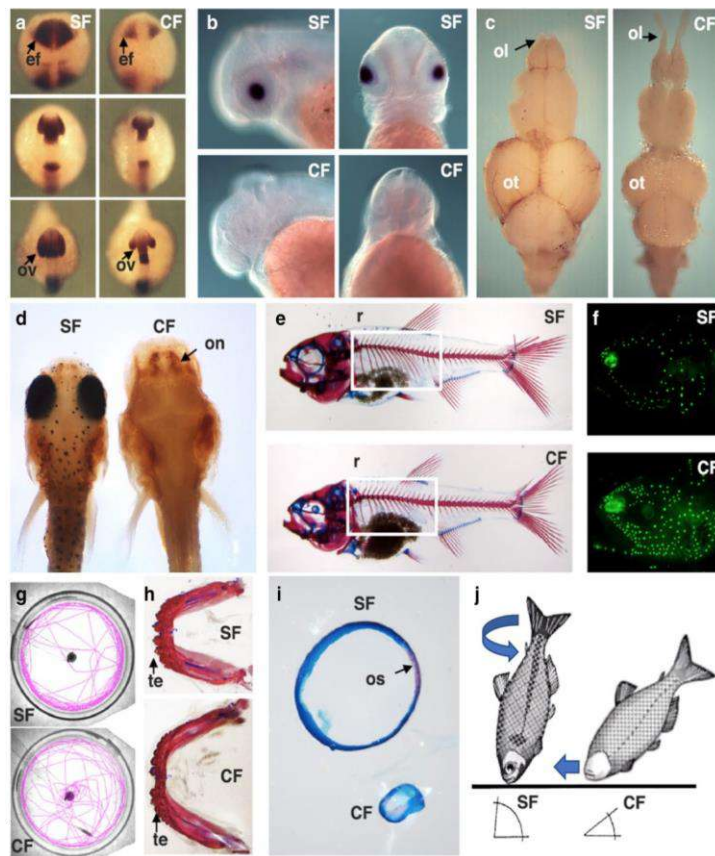


Figure 7. Exemples de différences majeures entre les poissons de surface (SF) et les poissons cavernicoles (CF). (a) : Hybridation in situ montrant des différences d'expression de pax6 à partir du stade de la plaque neurale (en haut) aux stades tardifs de la vésicule optique (en bas). ef : champ oculaire ; ov vésicule optique. (b) : Hybridation in situ montrant les différences d'expression de α A-crystallin dans le cristallin vu des côtés latéral et dorsal à 40 hpf (heures post fécondation). D'après (Ma et al., 2014). (c) : Vue dorsale des différences morphologiques du cerveau adulte vu de face. ot : tectum optique ; ol : lobe olfactif. (d) : Différences morphologiques au niveau de la tête et du marquage anti-tyrosine hydroxylase montrant des différences dans les régions neuronales olfactives (on) chez les larves de 6 jpf (jours post fécondation). (e) : Squelettes larvaires montrant des différences dans le nombre de côtes (r et cadre). (f) : Larves colorées par DASPEI montrant des différences dans la densité des neuromastes crâniens. (g) : Test d'attraction aux vibrations (VAB) en laboratoire montrant des tracés de trajectoires (rose) dans des chambres par rapport à la position d'une tige de verre vibrante (au milieu). (h) : Différences de taille des mâchoires et du nombre de dents chez les adultes. te : dents. (i) Sclère isolée marquée en bleue (le cartilage) et en rouge (l'os) montrant les différences de taille et de formation tige optique (os). (j) : Différences de comportement dans la prise alimentaire par rapport au substrat. (f) et (g) : reproduites à partir de (Yamamoto et al., 2010). D'après (Jeffery, 2020).

phylogénétiquement éloignées tels que l'albinisme et la perte des yeux. À noter que les yeux se développent normalement chez *Astyanax mexicanus* cavernicole durant l'embryogenèse, mais à partir de 40 heures après fécondation le cristallin entre en apoptose (Figure 7b) provoquant la dégénérescence de l'œil (Hinaux et al., 2015; Jeffery, 2020; Yamamoto & Jeffery, 2000).

L'albinisme chez *Astyanax mexicanus* est causé par des mutations perte de fonction dans le gène *Oca2* (oculocutaneous albinism 2), qui intervient lors des premières étapes de la voie de synthèse de la mélanine. Ces mutations sont responsables de la perte de synthèse de la mélanine dans les populations cavernicoles (Bilandžija et al., 2013; Protas et al., 2006). De façon frappante, le même gène (*Oca2*) est responsable de l'albinisme chez Pachón et Molino, mais les mutations (ponctuelles et délétions d'exons) qui sont retrouvées dans ces deux populations d'origine indépendantes sont différentes. Nous sommes donc ici dans un cas d'évolution parallèle.

En plus du gène *Oca2*, le gène *Mc1r* (Melanocortin type 1 receptor) a également été la cible de mutations répétées et indépendantes, qui entraînent une dépigmentation au sein de plusieurs populations cavernicoles d'*Astyanax mexicanus* (Gross et al., 2009).

Outre l'albinisme et la perte des yeux, les poissons cavernicoles ont développé d'autres traits qui les différencient de leurs congénères de surface tels que la réduction de la taille des écailles d'environ de 10 à 13 % par rapport à celle des surfaces (Simon et al., 2017). Les CF ont une vertèbre en moins (Figure 7e), possèdent une grande bouche contenant plus de dents (Figure 7h) et un nombre important de neuromastes crâniaux (Figure 7f) (Dowling et al., 2002; Yamamoto et al., 2003; Jeffery, 2020). Pour trouver de la nourriture dans le noir, les poissons cavernicoles ont développé un odorat très performant (Blin et al., 2018; Hinaux et al., 2016). À cela s'ajoute le nombre important de bourgeons gustatifs (Varatharasan et al., 2009; Yamamoto et al., 2009), accompagné d'un système olfactif plus développé (Figure 7c,d) et d'un nombre supérieur de neuromastes de grande taille sur la ligne latérale par rapport aux populations de surfaces (Bibliowicz et al, 2013; Jeffery, 2020). Les neuromastes constituent un système sensoriel spécifique à la plupart des poissons et amphibiens qui permet de détecter les mouvements et les vibrations de l'eau (Yoshizawa et al., 2010).

D'un point de vue comportemental, dans le noir, les poissons de surface adoptent un angle de 90 °C lors de la recherche de nourriture au fond, tandis que les poissons des grottes s'inclinent de 45 °C seulement leur permettant d'être plus efficaces dans la recherche de la nourriture

(Schemmel, 1980; Yamamoto et al., 2009). De plus, les poissons cavernicoles d'*A. mexicanus* se déplacent de manière individuelle et sont moins agressifs contrairement à leurs congénères de surface qui se déplacent en bancs et adoptent un comportement agressif (Eliot, Hinaux, et al., 2014; Kowalko et al., 2013). Ils ont également développé un comportement d'attraction aux vibrations (VAB, pour Vibration Attraction Behavior) (Figure 7g). Ce comportement semble être une adaptation qui permet une détection plus efficace des aliments qui tombent à la surface de l'eau (Yoshizawa et al., 2010; Yoshizawa, Ashida, et al., 2012).

Le métabolisme des populations cavernicoles a également évolué. En plus de la fécondité réduite chez les *Astyanax* cavernicoles (Simon et al., 2019), leurs œufs sont légèrement plus gros et contiennent plus de réserves que les œufs des poissons de surface (Hüppop & Wilkens, 1991). Par ailleurs, ils ont une meilleure absorption des nutriments particulièrement aux stades larvaires (Riddle, Boesmans, et al., 2018), ont plus de réserves adipeuses (Aspiras et al., 2015; Xiong et al., 2018) et ont développé une insulino-résistance avec une augmentation de leur masse corporelle (Riddle, Aspiras, et al., 2018). Ils ont un taux métabolique standard plus faible que le morphotype de surface (Salin et al., 2010). Ils ont éliminé les rythmes circadiens dans leur métabolisme, ce qui leur confère une capacité d'économie d'énergie d'environ 30 % (Moran et al., 2014), et ils dorment très peu (Keene & Borowsky, 2011; Duboué et al., 2012).

L'ensemble de ces traits adoptés au cours de l'évolution par les populations cavernicoles apparaissent comme des réponses adaptatives dans un environnement pauvre en nourriture, limité en termes d'espace et totalement dépourvu de lumière. Pour survivre dans de telles conditions naturelles, les *Astyanax* ont évolué aussi bien d'un point de vue comportemental, physiologique que morphologique pour économiser de l'énergie (la perte de l'œil et du rythme circadien), augmenter leur efficacité dans la recherche de nutriments (capacités sensorielles très développées), et résister face au manque de nutriments (évolution du métabolisme et augmentation des réserves).

III.5. La diversité génétique et phénotypique dans un contexte d'une évolution répétée chez *Astyanax mexicanus*

L'existence de populations cavernicoles évoluant en parallèle ou par convergence à partir d'un ancêtre de surface est une excellente opportunité pour tenter de comprendre la complexité des relations entre phénotypes et génotypes dans un contexte d'une évolution répétée. Cette complexité est notamment illustrée par la dégénérescence de la "vision" qui fait intervenir

environ une douzaine de gènes qui peuvent être uniques à une population ou en partie partagées (Borowsky, 2008). Le gène *cbsa* (cystathionine β -synthetase a) présente la même mutation dans les populations de Pachón et de Tinaja (groupe de El Abra), tandis que celle de Molino (groupe de Guatemala) présente une mutation différente au même endroit (Ma et al., 2020). D'un autre côté, le gène responsable de l'albinisme, *Oca2*, présente des mutations différentes entre les CF de Molino (groupe de Guatemala) et les CF de Pachón et de Japonès (groupe de EL Abra) (Protas et al., 2006). De même, le gène *mcl1r* présente également des mutations différentes, à savoir une délétion de 2 bp dans la population de Pachón à l'extrémité 5' codante du transcrit et une mutation ponctuelle modifiant l'acide aminé codé d'arginine en cystéine dans les populations de Yerbaniz et Japonès (les trois populations faisant partie du groupe El Abra) (Gross et al., 2009).

Outre l'albinisme et la perte des yeux, les caractéristiques crano-faciales et squelettiques ont également subi des modifications importantes dans les populations cavernicoles par rapport leurs congénères de surface telles que la taille et la forme des os ainsi que la présence de nombreuses asymétries latérales. Ces différences sont aussi observables entre les populations cavernicoles ; cependant les mécanismes génétiques sous-jacents restent encore flous (Gross et al., 2014; Keene et al., 2016).

D'un point de vue comportemental, des différences significatives entre les populations des grottes ont été rapportées pour de nombreux phénotypes cavernicoles. Ces variations phénotypiques pourraient être associées étroitement à la diversité des déterminismes génétiques sous-jacents. C'est le cas de l'agressivité souvent associée aux poissons de surface et qui semble être plus ou moins conservée chez les CF de Molino mais qui est complètement perdue chez les CF de Pachón (Elipot et al., 2012).

D'un point de vue sensoriel, le VAB est supposé aider les poissons des grottes à localiser la nourriture dans l'obscurité totale (Yoshizawa et al., 2010; Yoshizawa, Ashida, et al., 2012). Néanmoins, ce comportement est présent dans certaines populations telles que Pachón, Los Sabinos et Piedras (tous les trois du groupe El Abra) mais absent dans celle de Molino (Yoshizawa, Ashida, et al., 2012). Cette variation peut s'expliquer par les différences observées dans le déterminisme parental de ce comportement entre les populations de Pachón et de Los Sabinos (Yoshizawa, Yamamoto, et al., 2012). De plus, les travaux récents de Blin et collaborateurs (2020, sous presse) réalisés dans le milieu naturel, ont montré des différences de réponse olfactive (absence ou présence) entre différentes populations y compris dans la

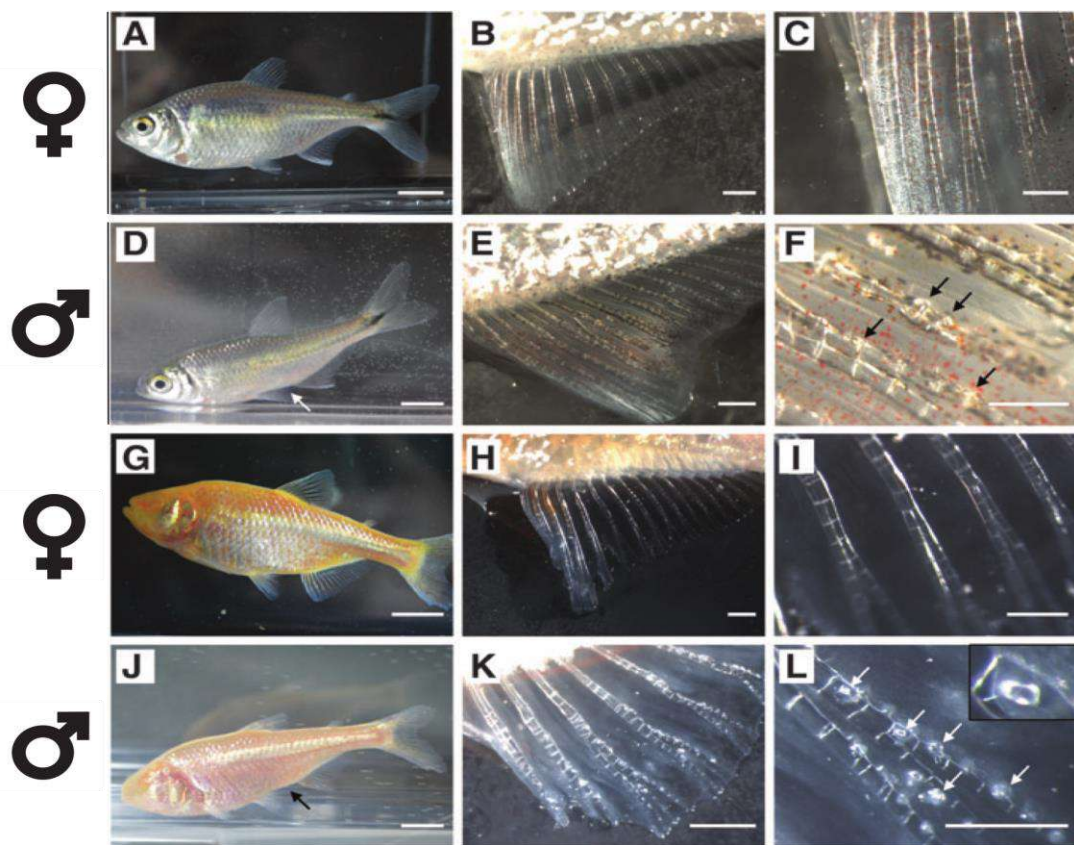


Figure 8. Dimorphisme sexuel chez *Astyanax mexicanus*. (A-L) : Comparaison des poissons de surface femelle (A-C) et mâle (D-F) avec les poissons cavernicoles femelle (G-I) et mâle (J-L), pour la morphologie générale (A, D, G, J), les rayons des nageoires anales (B, E, H, K), et les denticules des nageoires anales (C, F, I, L). Les flèches montrent la forme concave de l'abdomen chez les mâles (D, J) et les denticules (F, L). Barres d'échelles : 1 cm (A, D, G, J), 1 mm (B, E, H, K), et 500 μ m (C, F, I, L). D'après (Elipot, Legendre, et al., 2014).

même région (Pachón, Los Sabino et Tinaja) suite à des stimuli odorants externes (Blin et al., 2020). Bien que les mécanismes génétiques contrôlant ces capacités sensorielles restent inconnus, les auteurs ont suggéré que l'absence de réponse dans les grottes de Sabinos et Tinaja ne serait pas liée à la réduction des capacités sensorielles mais plutôt à l'utilisation équilibrée de leur expression en fonction des conditions environnementales locales (Blin et al., 2020).

Ces données montrent que les mêmes gènes porteurs de différentes mutations peuvent être responsables du phénotype cavernicole dans différentes populations suggérant ainsi une origine complexe et une évolution indépendante des différentes populations cavernicoles. Par conséquent, chaque grotte semble être un cas particulier en termes de phénotype et de combinaisons d'allèles.

III.6. Mais qu'en est-il de la détermination du sexe et de son évolution chez *Astyanax mexicanus* ?

La distinction entre le sexe mâle et le sexe femelle avant l'âge adulte chez le tétra mexicain ne peut se faire que sur des critères histologiques à partir de la différenciation gonadique; ou alors à l'âge adulte (~ 1 an), en se basant sur le dimorphisme sexuel d'un point de vue purement morphologique (Figure 8) (Elipot, Legendre, et al., 2014). À ce stade, la différenciation peut se faire sur la base de la longueur du corps qui est plus importante chez les femelles que chez les mâles. De plus, l'abdomen des mâles présente une forme concave du côté antérieur de l'orifice anal, tandis que les femelles ont une forme convexe à ce niveau-là. Enfin, les mâles possèdent des petits denticules sur la nageoire anale et que l'on peut sentir au toucher, contrairement aux femelles qui ont une nageoire anale lisse (Figure 8) (Elipot, Legendre, et al., 2014).

Le(s) système(s) de détermination du sexe chez le tétra mexicain n'ont jamais été explorés. Cependant, il existe des travaux rapportant des déviations du sex-ratio suite à des croisements de couples de mâles et de femelles dans certaines populations de surface et cavernicoles. Ainsi, dans les travaux d'Elipot et collaborateurs (2014), des séries de croisements entre mâles et femelles des morphotypes cavernicoles et de surface (CF X SF) puis entre populations cavernicoles uniquement (CF X CF) ont été réalisés et le sex-ratio a été analysé à l'âge adulte sur la base des critères morphologiques précédemment mentionnés (> 6 mois) (Tableau 1) (Elipot, Legendre, et al., 2014). Les résultats montrent que les croisements hybrides entre des mâles Pachón ou Molino et des femelles de surface originaires du Texas donnent un sex-ratio

Tableau 1: Sex-ratio dans les différents croisements inter-populations (*, P < 0.05)

Reproduction		Effectif	Nombre de femelles	Nombre de mâles	Ratio		p-Value	Significativité
Male	Femelle				femelles	(%)		
Pachón	Surface (Texas)	7	2	5	28	0.4531	ns	
Molino	Surface (Texas)	7	5	2	71	0.4531	ns	
Surface	Pachón	7	7	0	100	0.01563	*	
Molino	Pachón	7	7	0	100	0.01563	*	

de 50 : 50 dans les deux cas. Inversement, les croisements de femelles Pachón avec des mâles Molino ou de surface donnent des progénitures à 100 % femelles dans les deux cas (Elipot, Legendre, et al., 2014). Ces résultats préliminaires semblent être intéressants mais la taille des échantillons est trop réduite (7 individus par échantillon) pour être concluante.

Par ailleurs, d'autres séries de croisements ont été réalisées entre mâles et femelles (un couple par croisement) entre des populations de surface provenant de plusieurs localités ou de grottes différentes de la Sierra de Guatemala et de El Abra (Wilkens & Strecker, 2017). Les résultats de ces croisements montrent que pour toutes les populations cavernicoles utilisées (Pachón, Micos, Molino, Curva, Piedras et Yerbaniz), le sex-ratio est à chaque fois de 50 : 50 à l'exception de Micos 3, une population qui subit de manière permanente l'introgression des morphotypes de surface et qui présente une déviation du sex-ratio en faveur des mâles (Tableau 2) (Wilkens & Strecker, 2017).

Cependant, pour les populations de surface, le sex-ratio est biaisé, soit en faveur des mâles soit en faveur des femelles indépendamment de l'origine de la population (Tableau 2) (Wilkens & Strecker, 2017). Là encore, les résultats sont intéressants mais restent lacunaires. En effet, aucune précision n'a été apportée quant aux conditions d'élevage (température, oxygène, densité...). En outre, sur la plupart des croisements, les effectifs sur lesquels sont fondées les analyses du sex-ratio sont réduits en particulier pour les populations cavernicoles (de l'ordre de 20 à 40 individus par croisement) (Wilkens & Strecker, 2017). Néanmoins, les auteurs suggèrent l'existence d'une transition d'un système de détermination du sexe polygénique chez les poissons de surface vers un système de détermination du sexe purement génétique de type monofactoriel simple chez les populations des grottes examinées (Wilkens & Strecker, 2017). Ces hypothèses, fondées uniquement sur l'analyse des sex-ratios des différents croisements, nécessitent d'être confirmées ou infirmées par d'autres approches.

III.7. *Astyanax mexicanus* : un modèle pour les études comparatives à une échelle micro-évolutionne

Astyanax mexicanus se distingue des nombreuses espèces cavernicoles identifiées à ce jour du fait qu'elle fait partie des rares espèces pour lesquelles des formes de surface et des formes cavernicoles dérivant de l'ancêtre commun existent encore et sont toujours accessibles. Bien qu'une origine ancienne des CF a été pendant longtemps soutenue dans la littérature, les données récentes suggèrent fortement que l'invasion des grottes du Nord-Est du Mexique par

Tableau 2 : Sex-ratios dans les croisements par couples de poissons de surface et cavernicoles d'*Astyanax mexicanus*

Reproduction	Nombre de femelles	Nombre de mâles	X ²	Significativité
Poissons de surface				
Rio Coy 1	40	81	13.8926	***
Rio Coy 2	177	108	16.7053	***
Rio Coy 3	11	75	47.6279	***
Rio Coy 4	26	70	20.1667	***
Rio Teapao	184	70	51.1654	***
Poissons cavernicoles				
Pachón 1	20	25	0.5556	ns
Pachón 2	17	13	0.5333	ns
Pachón 3	12	14	0.1538	ns
Pachón 4	20	23	0.2093	ns
Piedras 1	66	58	0.5161	ns
Piedras 2	34	33	0.0149	ns
Piedras 3	20	12	2.0000	ns
Curva 1	22	25	0.1915	ns
Curva 2	15	18	0.2727	ns
Yerbaniz	13	13	0.0000	ns
Molino 1	65	64	0.0078	ns
Molino 2	8	13	1.1905	ns
Micos 1	55	72	2.2756	ns
Micos 2	15	16	0.0323	ns
Micos 3	44	72	6.7586	**
Micos 4	17	15	0.1250	ns

les populations ancestrales de surface d'*Astyanax mexicanus* est relativement récente (moins de 20 000 ans) (Fumey et al., 2018; Policarpo et al., 2020).

Ainsi, le tétra mexicain devient une “espèce modèle” qui a été étudiée de manière intensive ces dernières années notamment d’un point de vue évolutif et développemental par des approches de génétique et génotypique comparatives, afin de mieux comprendre le déterminisme des traits biologiques adaptatifs à la vie cavernicole, et ceci au sein de la même espèce (Keene et al., 2016; Wilkens & Strecker, 2017). Les études s’intéressant à la compréhension des traits adaptatifs développés dans un environnement “extrême” sont particulièrement focalisées sur la dégénérescence de l’œil, l’albinisme, et les modifications comportementales.

Plus récemment, les formes cavernicoles d'*Astyanax mexicanus* ont émergé comme un modèle d’étude pour la recherche bio-médicale et les pathologies humaines notamment depuis la découverte des défauts dans la régénération du cœur (Stockdale et al., 2018) ou sa résistance à l’insuline suite à la mutation qui touche le gène du récepteur à l’insuline (*insra*) responsable de l’insulino-résistance chez l’homme (Riddle, Aspiras, et al., 2018). Chez certaines populations de CF, cette mutation provoque une dérégulation de l’homéostasie du glucose sanguin et une hyperglycémie. Cependant, cette insulino-résistance provoquant une augmentation du poids n’affecte aucunement leur longévité puisqu’ils vivent au moins autant que leurs congénères de surface (Riddle, Aspiras, et al., 2018). Enfin, la découverte d’une mutation dans le gène de la *MAO* (Monoamine Oxidase; enzyme de dégradation des monoamines cérébrales, sérotonine et dopamine) qui s’avérerait totalement délétère chez l’homme, affecte “seulement” la réponse au stress chez *Astyanax* cavernicole (Eliot, Hinaux, et al., 2014; Pierre et al., 2020).

Outre la pertinence de ce modèle, de nombreuses ressources génotypiques sont disponibles et en libre accès : génomes, transcriptomes et cartographie génétique. C’est une espèce qui est relativement facile à éliver ou à reproduire en laboratoire (Eliot, Legendre, et al., 2014). De plus, les techniques d’édition de génomes comme le CRISPR/cas9 ont été également développées permettant ainsi de réaliser des études fonctionnelles (Devos et al., 2019; Stahl et al., 2019).

.

PROJET DE THÈSE

Contexte scientifique de la thèse

Compte tenu de la plasticité des mécanismes de détermination du sexe chez les poissons téléostéens, qui représentent environ la moitié des espèces de vertébrés, l'intérêt d'étudier ces mécanismes dans ce groupe est particulièrement évident non seulement d'un point de vue appliqué, notamment pour l'aquaculture, mais aussi d'un point de vue fondamental en biologie évolutive. Cependant et malgré cette diversité des poissons, seulement quelques gènes déterminants majeurs du sexe ont été identifiés à ce jour. Ces derniers ne sont pas ou très peu conservés entre les espèces y compris celles du même genre. Ce renouvellement fréquent et rapide des gènes SD est étroitement associé à l'évolution des chromosomes sexuels qui sont généralement peu différenciés chez les poissons. La découverte de nouveaux systèmes de détermination du sexe et de gènes SD sera donc d'une importance majeure afin d'améliorer notre compréhension des mécanismes évolutifs derrière cette diversité.

Concernant les chromosomes B, bien qu'aucune preuve fonctionnelle n'ait montré leur implication directe dans la détermination du sexe chez les poissons, certaines études suggèrent que les chromosomes B auraient dérivés de chromosomes sexuels ou vice-versa. Chez les poissons téléostéens, la fréquence des Bs chez certaines espèces serait plus élevée dans un sexe que dans un autre, ou encore les Bs seraient exclusivement restreints à un sexe phénotypique. De ce fait, les poissons offrent donc l'opportunité d'explorer le rôle énigmatique que jouent les chromosomes B dans le processus de détermination du sexe pour tenter de répondre aux nombreuses questions relatives à l'évolution des chromosomes B et des chromosomes sexuels qui restent sans réponse.

La question sur l'évolution des systèmes SD chez les poissons a pour l'instant été explorée principalement dans un contexte de macro-évolution, *e.g.*, soit en comparant des espèces très différentes sur des périodes évolutives très longues, soit des espèces très proches et donc sur des périodes évolutives un peu plus courtes. Dans ce contexte, il est plus que nécessaire d'explorer les mécanismes de détermination du sexe chez d'autres groupes ou espèces de poissons afin d'apporter des éléments qui pourraient aider à élucider le rôle des Bs dans ce processus.

À ce titre, le tétra mexicain appartenant au groupe des characiformes dans lequel aucun déterminant n'a été identifié à ce jour, représente un choix quasi-unique pour l'étude des mécanismes de détermination du sexe, l'implication des Bs dans ce processus et les gènes

déterminants du sexe à une échelle micro-évolution. La particularité de cette espèce réside dans l'existence et l'accessibilité des formes de surface et des grottes souvent considérées comme des “mutants naturels”, en plus des populations qui subissent une hybridation introgressive par des populations de surface. Ainsi, ce projet de thèse se propose d'aborder l'évolution à une échelle intra-spécifique ou micro-évolution (< 20 000 ans) de ces mécanismes chez les différentes populations d'*Astyanax mexicanus* qui ont évolué de manière répétée suite à l'adaptation à un environnement contraignant.

Objectifs et stratégie de la thèse

L'objectif principal de ce travail était d'explorer la micro-évolution des mécanismes de détermination du sexe et des gènes SD entre les morphotypes de surface et ceux des grottes chez *Astyanax mexicanus*. Pour ce faire, nous avons fait le choix de réaliser cette étude sur la population de la grotte Pachón et sur une population de surface qui avait été initialement collectée à San Solomon Spring, Balmorhea State Park, Texas. Ces deux populations sont élevées dans le laboratoire de Sylvie Rétaux, ma co-directrice de thèse, depuis 2004 et provenaient du laboratoire de Jeffery de l'université du Maryland, College Park, MD. Ces colonies sont élevées au laboratoire depuis plusieurs générations.

Les données existantes dans la littérature, suggèrent l'existence d'un système monofactoriel simple chez les populations cavernicoles et un système plus complexe chez les poissons de surface (Wilkens & Strecker, 2017). De plus, les données préliminaires obtenues au sein de mes deux laboratoires d'accueils, avant mon arrivée en thèse, corroboraient l'hypothèse d'une micro-évolution des systèmes de détermination du sexe entre les populations de surface et celles des grottes. Afin de répondre à la question de l'existence d'une transition dans les mécanismes de détermination du sexe chez cette espèce, nous avons proposé une stratégie de recherche en trois axes.

Dans la première partie, l'objectif était d'identifier la fenêtre de différenciation gonadique chez la population de la grotte Pachón. Pour ce faire, nous nous sommes intéressés aux “patterns” de migration des cellules germinales primordiales qui sont considérés comme l'une des premières étapes de la formation des gonades, et ce, dès les premiers stades de développement embryonnaire. D'un autre côté et par une approche histologique, nous avons suivi les grandes étapes de la différenciation gonadique à partir de quelques jours après éclosion jusqu'à la différenciation complète en ovaires ou en testicules. Cette différenciation histologique a été

associée à une analyse moléculaire qui avait pour but la caractérisation des profils d'expression des gènes candidats connus pour jouer un rôle clé dans le processus de différenciation sexuelle et de la stéroïdogénèse. Cette étude est publiée (sous presse).

Dans la deuxième partie, nous nous sommes intéressés à la caractérisation du ou des systèmes de détermination du sexe chez *Astyanax mexicanus* de la grotte Pachón. En combinant différentes approches génomiques et cytogénétiques, nous avons identifié la présence prédominante de microchromosomes B chez les mâles. Nous avons démontré que ces microchromosomes B contiennent deux loci dupliqués du gène *gdf6b* (*gdf6b-B*), potentiel candidat dans le rôle du gène déterminant majeur du sexe. Par la suite, la liaison de *gdf6b-B* au sexe mâle a été vérifiée sur un nombre important d'animaux (mâles et femelles). Pour comprendre son rôle dans le processus de la SD, les profils d'expression de *gdf6b* ont été analysés par qPCR pendant le développement gonadique. Enfin, pour vérifier s'il est nécessaire ou non à la détermination du sexe, *gdf6b* a été inactivé par le système CRISPR-Cas9.

Dans la dernière partie, l'objectif était de confirmer ou d'infirmer l'hypothèse de l'existence d'une transition d'un déterminisme complexe chez les SF vers un système monofactoriel simple chez les CF. Suite à l'identification de *gdf6b-B* comme potentiel déterminant majeur du sexe chez les CF de Pachón, nous avons exploré l'implication des chromosomes B et de leurs loci *gdf6b* dans la détermination du sexe chez la population de surface originaire du Texas. Pour cela, différentes approches génomiques et cytogénétique ont été utilisées ici. Nos données montrent un système de détermination du sexe complexe chez les poissons de surface (Texas) avec l'implication partielle des microchromosomes B et de leurs loci *gdf6b* uniquement chez certains mâles. Enfin, cette étude a été étendue aux populations sauvages cavernicoles et de surface du Nord-Est du Mexique.

En annexe (Annexe 1), je présente également un manuscrit publié dans lequel je suis co-auteur, et qui correspond à ma participation à une mission de terrain au Mexique en mars 2019 : “Diversity of olfactory responses and skills in *Astyanax mexicanus* cavefish populations inhabiting different caves”, par Maryline Blin et al. (Blin et al., 2020).

RÉSULTATS

Les résultats de ces travaux de thèse ont donné lieu à une publication acceptée dans un journal international à comité de lecture et deux autres publications en préparation.

PUBLICATION N°1 :

Boudjema Imarazene, Séverine Beille, Elodie Jouanno, Adèle Branthonne, Violette Thermes, Manon Thomas, Amaury Herpin, Sylvie Rétaux, and Yann Guiguen. (2020). Primordial germ cell migration and histological and molecular characterization of gonadal differentiation in Pachón cavefish *Astyanax mexicanus*. (*Accepted in Sexual Development*)

PUBLICATION N°2 :

Boudjema Imarazene, Séverine Beille, Elodie Jouano, Romain Feron, Céline Lopez-Roques, Adrien Castinel, Lisa Gil, Claire Kuchly, Celine Donnadieu, Hugues Parrinello, Laurent Journot, Cédric Cabau, Margot Zham, Christophe Klopp, Alexandr Sember, Tomáš Pavlica, Ahmed Al-Rikabi, Thomas Liehr, Sergey Simanovsky, Joerg Bohlen, Julie Perez, Frédéric Veyrunes, John H. Postlethwait, Manfred Schartl, Amaury Herpin, Sylvie Rétaux, and Yann Guiguen. A supernumerary “B-sex” chromosome controls sex determination in the Pachón cave, *Astyanax mexicanus*. (*en préparation*)

PUBLICATION N°3 :

Boudjema Imarazene, Séverine Beille, Elodie Jouano, Romain Feron, Céline Lopez-Roques, Hugues Parrinello, Laurent Journot, Cédric Cabau, Margot Zham, Christophe Klopp, Julie Perez, Frédéric Veyrunes, John H. Postlethwait, Manfred Schartl, Amaury Herpin, Sylvie Rétaux, and Yann Guiguen. Evolution of sex determination in *Astyanax mexicanus* morphotypes and populations. (*en préparation*)

Ces résultats ont également été présentés dans quatre conférences internationales et deux conférences nationales (le nom du présentateur est souligné dans la liste ci-dessous)

Imarazene Boudjema, Herpin Amaury, Anderson Jennifer, Postlethwait John. H, Schartl Manfred, Rétaux Sylvie, and Guiguen Yann. Micro-evolution of sex determination mechanisms and sex determining genes in the cavefish, *Astyanax mexicanus*. ***1st European Symposium on Sex Determination in Vertebrates***, Mar 01-04. 2017, Dinard (France) - **Oral**

Imarazene Boudjema, Herpin Amaury, Feron Romain, Anderson Jennifer, Postlethwait John. H, Schartl Manfred, Rétaux Sylvie, and Guiguen Yann. Micro-evolution of sex determination mechanisms and sex determining genes in the cavefish, *Astyanax mexicanus*. ***DDiGoV-Réunion transversale “Différenciation des Gonades chez les Vertébrés”*** Mar 12. 2018, Rennes (France) - **Oral**

Imarazene Boudjema, Herpin Amaury, Feron Romain, Anderson Jennifer, Postlethwait John. H, Schartl Manfred, Rétaux Sylvie, and Guiguen Yann. Micro-evolution of sex determination mechanisms and sex determining genes in the cavefish, *Astyanax mexicanus*. ***8th International Symposium on Vertebrate Sex Determination***, Apr 16-20. 2018, Hawaii (USA) - **Oral**

Imarazene Boudjema, Herpin Amaury, Feron Romain, Anderson Jennifer, Postlethwait John. H, Schartl Manfred, Rétaux Sylvie, and Guiguen Yann. Micro-evolution of sex determination mechanisms and sex determining genes in the cavefish, *Astyanax mexicanus*. ***Astyanax International Meeting***, Apr 17-20. 2019, Queretaro (Mexico) - **Oral**

Imarazene Boudjema, Herpin Amaury, Feron Romain, Anderson Jennifer, Postlethwait John. H, Schartl Manfred, Rétaux Sylvie, and Guiguen Yann. Micro-evolution of sex determination mechanisms and sex determining genes in the cavefish, *Astyanax mexicanus*. ***1st Scientific days of EGAAL***, Jul 04-05. 2019, Rennes (France) - **Poster**

Boudjema Imarazene, Séverine Beille, Elodie Jouano, Romain Feron, Céline Lopez-Roques, Hugues Parrinello, Laurent Journot, Christophe Klopp, Julie Perez, Frédéric Veyrunes, John H. Postlethwait, Manfred Schartl, Amaury Herpin, Sylvie Retaux, **Yann Guiguen**. Characterization of the sex determining system(s) of the Mexican tetra, *Astyanax mexicanus*. ***Paradigm shift in sex chromosome evolution***. Sep 20. 2019, Berlin (Germany)

Dans mon manuscrit de thèse, ces résultats seront présentés sous forme de trois parties correspondant aux trois publications.

Publication N° 1 :

Migration des cellules germinales primordiales et caractérisation histologique et moléculaire de la différenciation gonadique chez l'*Astyanax mexicanus* de la grotte Pachón

Objectifs

La différenciation sexuelle est un processus physiologique très important qui conduit le développement des gonades d'un stade indifférencié vers des gonades e.g., testicules et ovaires différenciés. La compréhension de ce processus est une étape clé pour les études des systèmes de détermination du sexe. En absence de données préalables sur ce sujet chez l'*Astyanax mexicanus*, l'objectif principal de cet article était donc d'explorer la différenciation sexuelle aussi bien d'un point de vue cellulaire, morphologique que moléculaire afin de définir les principales étapes de ce processus chez notre modèle d'étude.

Contribution personnelle

Je me suis intéressé dans un premier temps au suivi de la trajectoire migratoire des cellules germinales primordiales pendant le développement embryonnaire grâce à l'injection de la construction (ARNm 3'UTR-*nanos1* couplé à la GFP). Par la suite et sur la base de mes observations personnelles, j'ai élaboré le plan expérimental de cette étude et fait des prélèvements de façon à couvrir les grandes étapes de la différenciation sexuelle d'un point de vue morphologique (histologie). J'ai associé la différenciation morphologique avec les principaux marqueurs connus pour être impliqués dans le processus de différenciation chez d'autres espèces (identification des gènes d'intérêt, analyse des séquences et design de primers). Enfin, j'ai analysé et mis en forme l'ensemble de toutes les données présentées dans cet article. Après analyse des résultats, j'ai rédigé ce manuscrit.

Expérimentations en cours auxquelles j'ai participé

En plus des gènes explorés dans cette publication, j'ai également initié l'analyse des profils d'expression d'autres gènes qui sont impliqués dans la différenciation gonadique (*wnt4a, fsta, fstb, Rspo1, sox3, sox9*).

**Primordial germ cell migration and histological and molecular characterization of
gonadal differentiation in Pachón cavefish *Astyanax mexicanus***

RUNNING HEAD: Gonadal differentiation in cavefish

Boudjema Imarazene^{1,2}, Séverine Beille¹, Elodie Jouanno¹, Adèle Branthonne¹, Violette Thermes¹, Manon Thomas¹, Amaury Herpin¹, Sylvie Rétaux², Yann Guiguen^{1*}

AFFILIATIONS

¹ INRAE, LPGP, 35000, Rennes, France

² Université Paris-Saclay, CNRS, Institut des Neurosciences Paris-Saclay, 91190, Gif-sur-Yvette, France

*Corresponding Author: Yann Guiguen, INRAE, Laboratoire de Physiologie et Génomique des poissons, Campus de Beaulieu, 35042 Rennes cedex, France. Tel: +33 2 99 46 58 09, E-mail: yann.guiguen@inrae.fr

Keywords: gene expression profiling, PGCs, histology, nanos, vasa, ovary, testis

ABSTRACT

Genetic regulatory network governing vertebrate gonadal differentiation appears less conserved than previously thought. Here, we investigated gonadal development of *Astyanax mexicanus* Pachón cavefish, by looking at primordial germ cells (PGCs) migration and proliferation, gonad histology and gene expression patterns. We show that PGCs are first detected at the 80% epiboly stage and then reach the gonadal primordium at one day post-fertilization (dpf). However, in contrast to the generally-described absence of PGCs proliferation during their migration phase, PGCs number in cavefish doubles between early neurula and 8-9 somites stages. Combining both gonadal histology and *vasa* (germ cell marker) expression patterns, we observed that ovarian and testicular differentiation occurs respectively around 65 dpf in females and 90 dpf in males, with an important inter-individual variability. The expression patterns of *dmrt1*, *gsdf*, and *amh* revealed a conserved predominant male expression during cavefish gonadal development. But, none of the ovarian differentiation genes, i.e., *foxl2a*, *cyp19a1a*, and *wnt4b* displayed an early sexually-dimorphic expression and surprisingly all these genes exhibited predominant expression in adult testes. Altogether, our results lay the foundation for further research on sex determination and differentiation in *A. mexicanus* and contribute to the emerging picture that the vertebrate sex differentiation downstream regulatory network is less conserved than previously thought, at least in teleost fishes.

INTRODUCTION

Fishes, with over 35.000 recognized species, constitute the most diverse and abundant group of vertebrates [Fricke et al., 2020]. Besides their remarkable taxonomic diversity and the impressive range of habitats, behaviors, and morphological differences, they exhibit all kinds of reproductive strategies and sex determination (SD) mechanisms [Bachtrog et al., 2014; Devlin, and Nagahama, 2002]. Along with this diversity of SD mechanisms, comparative studies revealed a high turnover of master sex determining (MSD) genes [Pan et al., 2018]. These MSD genes control downstream sex differentiation cascades that include all the physiological, morphological and cellular processes by which the undifferentiated gonad will develop either into a testis or an ovary [Devlin, and Nagahama, 2002]. In contrast to the observed high turnover of both SD systems and MSD genes, the downstream sex differentiation processes are often considered to be relatively stable in fish [Nagahama, 2005; Ijiri et al., 2008]. However, studies on the evolution of the gene regulatory network leading to sex differentiation in the medaka, *Oryzias latipes*, suggest that this downstream regulation is not as conserved as previously thought [Herpin et al., 2013]. Hence, this variability makes teleost fishes interesting and important models for exploring the complexity of the gene network(s) underlying sexual differentiation in vertebrates.

In teleost fish, gonadal differentiation can follow diverse trajectories. It has been explored in several species, from either morphological, cellular or physiological point of views, highlighting a large variety of reproductive strategies, including gonochorism with both differentiated and undifferentiated gonochoristic species, and hermaphroditism [Yamamoto, 1969; Baroiller, and Guiguen, 2001; Devlin, and Nagahama, 2002; Nishimura, and Tanaka, 2014]. In differentiated gonochoristic species, that represent the majority of teleost fish, differentiation proceeds from an undifferentiated gonad into a differentiating testis in males or a differentiating ovary in females and remains stable throughout their complete life span [Yamamoto, 1969]. However, in undifferentiated gonochoristic species, all undifferentiated gonads proceed through ovarian development followed by a later and final differentiation step into either ovaries or testes [Yamamoto, 1969].

During the gonadal differentiation processes, primordial germ cell (PGC) specification, migration, proliferation and colonization of the gonadal anlage constitute the initial steps of early gonadogenesis. Following these early steps of PGC migration and colonization of the sexually undifferentiated embryonic gonad, a sexualization program, leading to a stepwise

differentiation toward a testicular or ovarian fate, will be activated [Guerrero-Estévez, and Moreno-Mendoza, 2010]. This sexually-dichotomic differentiation program will induce morphological and physiological sex-differences that are accompanied by sex-specific changes in the gonadal histology and gene expression patterns. For instance, early signs of female histological differentiation may include, among many criteria that could be variable between species, (i) the ontogenesis of an early ovarian cavity, (ii) an active proliferation of germ cells or (iii) an early meiotic activity and a size increase of female germ cells (auxocytosis) compared to male germ cells [Brusle, and Brusle, 1983]. Concomitantly, many genes involved in the gonadal differentiation process will be expressed in a sexually dimorphic fashion, ensuring the proper development and differentiation of the male and female gonads [Jørgensen et al., 2008; Guerrero-Estévez, and Moreno-Mendoza, 2010; Wang et al., 2019]. For instance, *dmrt1* (doublesex and mab-3 related transcription factor 1), *amh* (anti-Mullerian hormone) and *gsdf* (gonadal somatic cell derived factor) have been described as conserved factors specifically involved in testicular differentiation [Ijiri et al., 2008; Guerrero-Estévez, and Moreno-Mendoza, 2010]. On the other hand, *cyp19a1a* (cytochrome P450, family 19, subfamily A, polypeptide 1a), *foxl2a* (forkhead box L2a), and *wnt4b* (Wnt Family Member 4b) are often documented as classical ovarian differentiation factors [Guiguen et al., 2010; Guerrero-Estévez, and Moreno-Mendoza, 2010; Herpin et al., 2013; Sreenivasan et al., 2014; Bertho et al., 2016]. But as mentioned above, SD and sex differentiation are extremely plastic processes in teleost fish, prompting to new investigations in additional species to be able to better underline conserved and non-conserved sex differentiation pathways.

The Mexican tetra, *A. mexicanus*, belongs to the Characiform group which contains about 2,300 species [Nelson et al., 2016], including a few important aquaculture species like the Tambaqui, *Colossoma macropomum*. It is a native species from Central America rivers where this species comes in two morphotypes inhabiting markedly different environments. Besides the “classical” pigmented and eyed river-dwelling fish, about 30 populations of depigmented and blind cavefish live in the darkness of caves in North-East Mexico [Mitchell et al., 1977; Elliott, 2019]. Many resources, including some genome sequences [Di Palma et al., 2007; Hinaux et al., 2013; McGaugh et al., 2014; Herman et al., 2018], are now available, making this species widely used in evolutionary, developmental and genetic studies for exploring many traits linked to cave adaptation [Keene et al., 2016]. But, despite interesting reports pointing to some odd sex ratio in different *A. mexicanus* populations [Wilkins, and Strecker, 2017], sex differentiation has so far not been explored in this emerging model.

To fill this knowledge gap and provide some essential ground information for further studies on sex determination in that species, we characterized gonadal differentiation in blind and depigmented laboratory raised fish originating from the Pachón cave, located in the North of the sierra de El Abra (Tamaulipas, Mexico), through a combination of PGCs tracking experiments, gonad histology and gonadal gene expression. Our results show that the first signs of gonad histological differentiation occur around 65 day post-fertilization (dpf) in females and 90 dpf in males, but with an important inter-individual variability that is also found in gene expression patterns. Expression of well-known genes involved in testis differentiation in vertebrates revealed a conserved and significant predominant male expression in *A. mexicanus* with an early overexpression of *gsdf* in males. However, none of the classical ovarian differentiation genes that we analyzed, i.e., *foxl2a*, *cyp19a1a*, and *wnt4b* displayed an early sexually-dimorphic expression pattern during gonadal development and these genes were even detected as predominantly expressed during male gametogenesis and adult testis. This revealed major divergences in the classical and rather conserved ovarian differentiation molecular network between *A. mexicanus* and other vertebrates. Altogether, these results lay a solid foundation for further research on sex determination and differentiation in *A. mexicanus*.

MATERIALS AND METHODS

Animal sampling

Animals were treated according to the French and European legislation for handling of animals in research. SR's authorization for use of *Astyanax mexicanus* in research is 91-116. The animal facility of the Institute received authorization 91272105 from the Veterinary Services of Essonne, France, in 2015.

Laboratory stocks of *A. mexicanus* Pachón cave fish were obtained in 2004 from the Jeffery laboratory at the University of Maryland, College Park, MD. Fertilized eggs from an *A. mexicanus* Pachón cave laboratory colony were obtained from the CNRS cavefish experimental facilities (Gif sur Yvette, France). Newly hatched larvae (after 24 hpf) were transferred and reared in the Fish Physiology and Genomics laboratory experimental facilities (LPGP, INRAE, Rennes, France) in a closed recirculating water system with a stable photoperiod regime (12 hr light: 12 hr dark cycle) and at a temperature of $28 \pm 1^{\circ}\text{C}$. In order to avoid any larval cannibalism that might be caused by high densities (based on our previous observations), larvae

were kept in 10 l aquaria with a density of 20 larvae /l from 1 day post fertilization (dpf) to 15 dpf, then fish were transferred into 40 l aquaria from 16 dpf to 30 dpf (density of 5 animals/l) and into 90 l aquaria from 31 dpf to 150 dpf (density: 2 animals/l). Newly hatched larvae were fed twice a day with live artemia (OCEAN NUTRITION) from 6 dpf to 15 dpf, then with commercial dry pellets (BioMar). Forty fish were randomly sampled at 10, 16, 30, 45, 65, 90 and 150 dpf for both histology processing (N=20) and for gene expression studies (N=20). In agreement with the European legislation (directive 2010-63-UE and French decree 2013-118) for laboratory animal protocols, fishes were euthanized by an anesthetic overdose (Tricaine methanesulfonate, MS 222, 400 mg/l supplemented by 150 mg/l of sodium bicarbonate). For histological and gene expression patterns during the sex differentiation period, whole trunks were collected from 10 dpf to 90 dpf as their gonads were too small to be dissected, and gonads were sampled at 150 dpf, when they were large enough to be dissected. For histological processing, tissues were fixed in a solution of glutaraldehyde at 2% (SIGMA G5882-10X), with 4% paraformaldehyde (SIGMA P6148) in a phosphate-buffered saline buffer (pH 7.4; SIGMA P4417-100TAB) for at least 24 hours (h) and up to 48 h for larger samples. For gene expression studies, trunk and gonad samples were first collected at different time points (from 10 to 150 dpf). Then, brain, testis or ovaries, liver, intestine, kidney, swim bladder, gills, bones and skin were dissected from 5 adult males and females for gene expression studies across tissues. Differentiated gonads (testes and ovaries) at different gametogenesis stages were also sampled in 5 to 10 males and females. Based on both macroscopic (size, thickness, color and shape) and histological criteria, we defined five stages from stage 2 to stage 6 for both testes and ovaries. Stage 2 ovaries are translucent and thin fillet-shaped at the macroscopic level and are composed by different sizes of previtellogenic oocytes (PVtg Ooc) and few oogonia clusters. At stage 3, ovaries are slightly opaque and thicker, with a compact structure and an increasing number of PVtg Ooc organized in ovarian lamellae. By stage 4, ovaries appear cream-coloured and the first oocytes are clearly visible to the naked eye corresponding probably to the first vitellogenic oocytes (Vtg Ooc) seen by histology. At stage 5, ovaries at macroscopic level increase in size with oocytes extending over almost the whole surface of the gonads, with larger PVtg Ooc and Vtg Ooc in histology. By stage 6, ovaries become much larger and thicker filling a large part of the peritoneal cavity. Testes of stage 2 look like a fine tube, almost translucent; in histology, this stage is characterized by the presence of clusters of spermatogonia (SpG), spermatocytes (SpC), spermatids (SpT), and spermatozoa (SpZ). At stage 3, testes appear opaque and increase in size macroscopically and are composed in histology by a few clusters of SpG and SpT and a large amount of SpC and SpZ. By stage 4,

gonads are macroscopically entirely white colored and are formed mainly by scarce SpG and large clusters of SpC, SpT, and SpZ. At stage 5, testes appear macroscopically thicker with only sparse SpG, few populations of SpC and SpT, and large amounts of SpZ in histology. By stage 6, gonads are macroscopically much thicker and larger than at stage 5 and histologically mainly contained large amounts of SpZ and few populations of SpC and SpT. All samples were snap frozen in liquid nitrogen and stored at -80°C until RNA extraction. The tails of all animals were preserved in ethanol 100% for DNA extraction and genotyping.

DNA extraction and genotyping

Genomic DNA was extracted from fin clips stored for each individual in 100% ethanol at 4°C. Samples were lysed with 5% Chelex beads supplemented by 10 mg Proteinase K [Gharbi et al., 2006] for 2 hours at 55°C. Samples were then incubated for 10 min at 99°C. They were centrifuged and the supernatant containing the genomic DNA was transferred in clean tubes without beads and stored at -20°C before PCR reaction. Genotypic sex was determined based on the identification of sex specific genomic regions of Pachón cavefish (unpublished data) with a simple PCR genotyping test. Genotyping was performed using HiDi Taq DNA polymerase (myPOLS Biotec, #9201), which is a highly selective polymerase used for allele-specific PCRs (single nucleotide polymorphism detection). PCR reactions were set up with 0.2 μM of each primer (Forward and Reverse), 200 μM of dNTPs, 1X of HiDi buffer (10X), 2.5U/reaction of HiDi DNA polymerase, from 1 to 20 ng/μl of genomic DNA, and finally q.s to 50 μl total volume of nuclease free water. PCR conditions were: 95°C for 2 min + 35 cycles of (95°C for 30 secondes (sec), 60°C for 30 sec and 72°C for 1 min) + 72°C for 5 min using the following primers that are specific of the male allele: 5'-TGGACCTGCGGGACCTCG-3' (forward primer) and 5'-CTTAGACTTCCTACCGTGCCT-3' (reverse primer). Consequently, a single band is amplified only in males, and this PCR protocol has been tested on 200 laboratory Pachón cavefish animals that were reared under similar experimental conditions as the one used in our current experimentation. Among these 200 fishes, we found 102 phenotypic males and 98 phenotypic females. The sex ratio was analyzed by Chi-squared test showing a 1:1 sex ratio ($p < 0.05$) and a complete sex linkage between phenotype and genotype was observed using our genetic marker. In addition, a complete sex-linkage was also observed for all individuals used in the present study and sexed with confidence using histology. Moreover, PCR genotyping on animals used in this study indicated a final balanced sex ratio ($p < 0.05$) with 168 males and 163 females.

Histology and microscopy

Fixed larvae, juveniles and adult gonadal tissues (testes and ovaries) were washed in PBS and then in DEPC water (4 times each). They were dehydrated in increasing ethanol concentration (10%, 30%, 50%, 70% and 100%), and finally stored in ethanol 100% at 4°C. A total of 8 animals (4 males and 4 females) per stage were embedded in historesin (Leica HistoResin) blocks that were sectioned at 4 µm using a Tungsten Carbide D-profile microtome knife (Microm Microtech, Brignais, France), and stained with hematoxylin-eosin-safran (HES) (Microm Microtech, Brignais, France). Slides of all these samples were examined with a Nikon 90i microscope and photographed with a Nikon DS Ri1 camera (Nikon corporation, Melville, NY, USA).

PGCs tracking with a green fluorescent protein nanos1 3'UTR construction (GFP-nos1 3'UTR)

In vivo PGCs labelling was performed by injecting a GFP-*nos1* 3'UTR mRNA construct combined with the mmGFP5 open reading frame (ORF) [Siemering et al., 1996] cloned upstream of the 3'UTR of the zebrafish *nanos1* gene [Köprunner et al., 2001; Herpin et al., 2007]. This construction was injected into the cytoplasm of one-cell stage fertilized eggs of Pachón cavefish, before 1 hour post-fertilization. The number of GFP-*nos1* 3'UTR positive cells was determined as soon as a clear cellular fluorescence was visible from the background signal i.e., around 80% epiboly. Embryos were staged according to previously described developmental staging series [Hinaux et al., 2011]. Observation and imaging was performed from 8 hours post-fertilization (hpf) until 19 dpf, using an Olympus SZX16 stereomicroscope (from 8 hpf to 17 hpf) and a laser microscope (Eclipse C1 laser-scanning, Nikon, Tokyo, Japan) with a 60x Nikon objective (PL APO, 1.4 NA) and the Nikon image software (from 26 hpf to 19 dpf). Confocal images were solely adjusted for contrast and brightness.

Immunostaining, Ethyl Cinnamate (ECi) clearing, and imaging

Larvae displaying GFP-*nos1* 3'UTR positive cells were collected at 20 dpf, fixed overnight in 4% paraformaldehyde (PFA) in phosphate buffer 0.12 M (PBS, pH7.4) at 4°C, and stored for several days in PBS with 0.5% sodium azide (S2002, Sigma-Aldrich) at 4°C. Before staining, specimens were thoroughly washed at room temperature in PBS (overnight), in PBS/0.1% Tween20 (PBSt) (5 min), in PBS/0.2% Triton (PBSTx) (2x30 min) and then at 37°C in PBS/0.2%Triton/20% dimethyl sulfoxide (DMSO) (PBSTxD) (30 min). Permeabilization was

performed for 3h at 37°C in PBSt/0.1% Triton/20% DMSO/0.1% deoxycholate/0.1% NP40/0.05% sodium azide. Specimens were rinsed twice in PBSTx for 15 minutes, preincubated in PBSTx/0.3 M Glycine/0.05% sodium azide for 30 min at 37°C, and placed for 3h at 37°C in a blocking solution containing PBSTxD/6% sheep serum and 0.05% sodium azide. Samples were then incubated for 3 days at 37°C with a chicken anti-GFP antibody (1/500, ref. ab13970, Abcam) in PBSt/5% DMSO/3% sheep serum/10 μ g. μ L⁻¹ heparin and 0.05% sodium azide, and 2 days at 37°C with a goat anti-chicken Alexa Fluor 488-conjugate antibody (1/500, ref. A11039, Life Technologies) in the same solution. Methyl Green (MG, 80 μ g/mL, ref. 323829, Sigma) and 1,1'-Diocadecyl-3,3,3',3'-tetramethylindocarbocyanine perchlorate (DiI, 10 μ M, ref. 145311, Abcam) were added together with the secondary antibody for nuclear staining and cell membrane labeling, respectively. Specimens were then washed overnight in PBS/0.1% Tween 20/0.1% heparin. Before imaging, larvae were optically cleared as described in Klingberg *et al.* [Klingberg et al., 2017] with some modifications. Specimens were dehydrated at room temperature in successive 1 h baths of increasing methanol concentration (20-40-60-80-98%) containing 2% Tween20 under gentle agitation. Specimens were then transferred for 1 h in 100% methanol and overnight in ethyl cinnamate (Eci, ref. 112372, Sigma Aldrich). Imaging was performed in Eci under a Leica TCS SP8 laser scanning confocal microscope equipped with a Leica HC Fluotar L 16x/0.6 IMM CORR VISIR objective. The Alexa Fluor 488, the DiI and the MG were excited by 488, 552 and 638 nm lasers, respectively. Z-stack images (3 μ m steps) were acquired with no laser compensation in depth. No image post-processing was performed and maximal projection was obtained from the z-stack acquisition.

RNA isolation, cDNA synthesis and Real- Time PCR

Total RNA was extracted from trunks, gonads and tissues using Tri-reagent (Molecular Research Center, Cincinnati, OH) according to the supplier's protocol. RNA quantification concentration was measured with a NanoDrop ND 2000 spectrophotometer (Thermo scientific, Wilmington, Delaware). Complementary DNA (cDNA) templates were synthesized by denaturing during 5 minutes at 70°C 2 μ g of RNA supplemented by 5 μ L of 10 mM dNTP. The mixture was then placed on ice for 10 minutes before adding random hexamers and M-MLV reverse transcriptase (Promega, Madison, WI). For each sample, negative controls without reverse transcriptase were included in the analysis. Subsequently, the mixture was incubated at 37°C for 60 minutes and then cooled at 4°C. cDNA samples were diluted 25-fold before Real-

Time PCR. Primers for 7 sex-related genes (Primer and gene names are listed in (Supplementary Tab. 1), and 6 reference housekeeping genes: *actb* (actin b), *rps18* (Ribosomal Protein s18), *gapdh* (glyceraldehyde 3-phosphate dehydrogenase), *eftud2* (Elongation Factor Tu GTP Binding Domain Containing 2), *ubr2* (Ubiquitin Protein Ligase E3 Component N-Recognin 2) and *polr2* (RNA Polymerase II Subunit A) were designed on intron-exon junctions to avoid genomic DNA amplification, except for the *foxl2* gene that is a single exon gene, using the Primer3web software version 4.1.0 [Koressaar, and Remm, 2007; Kõressaar et al., 2018; Untergasser et al., 2012]. Real-time quantitative PCR was performed with SYBR Green reagents kits (Applied Biosystems, Foster City, CA) and amplifications were detected with a LightCycler® 480 Instrument II (Roche). The PCR reaction consisted on 4 µl of diluted cDNA, 1 µl of diluted primers (10 µmol/ml) and 5 µl of SYBR Green master mix, using the following cycling parameters: 95°C for 2 min + (95°C for 15 sec, 60°C for 10 sec and 72°C for 10 sec) for 40 cycles. All samples were analyzed in triplicates. Quantification cycle (Cq) values were normalized by the geometric mean of the 6 reference housekeeping genes and relative expression levels for each target gene were calculated using the following formulae: $2^{-\Delta Cq(\Delta Cq)} = Cq \text{ target gene} - Cq \text{ mean housekeeping gene}$ method.

Statistical analyses

All data are shown as Mean ± Standard Error of the Mean (SEM). Statistical analyses were performed by non-parametric tests since our data did not confirm one or all of the assumptions for parametric test (normal distribution, homogeneity of variances and homoscedasticity) using RStudio (Open Source version) considering the level of significance at $P < 0.05$. Statistical significance of the difference in expression at different time points (multiple comparisons) were tested by Kruskal-Wallis test followed by post hoc Pairwise Wilcoxon Rank Sum Test with Bonferroni corrections for adjustment of critical p -values. For comparisons between two groups, we used Wilcoxon Rank Sum Test.

RESULTS

PGCs visualization and localization

Stages of normal embryonic development in *Astyanax mexicanus* have been described by Hinaux [Hinaux et al., 2011]. At 23°C, hatching of cavefish embryos occurs from 24 hpf onward (+/- 2 hours). For monitoring PGCs formation and migration, a GFP-zebrafish *nos1*-

3'UTR mRNA was injected [Kurokawa et al., 2006; Saito et al., 2006; Herpin et al., 2007; Saito et al., 2010; Saito et al., 2014] during the first hour after fertilization, corresponding to 1 to 4-cell stages in *A. mexicanus*. PGC labelling is based on the fact that *nanos1* (*nos1*) mRNAs are rapidly degraded in somatic cells and only stabilized in PGCs by interacting with several germ plasm components, including microRNA (miR-430), *dnd* (dead end), and *dazl* (Deleted in azoospermia-like) [Köprunner et al., 2001; Giraldez et al., 2006; Mishima et al., 2006; Mishima, 2012].

PGCs were first visualized at 80% epiboly stage (8-9 hpf) (Fig. 1B). They were located above the margin, in a paraxial position on the dorsal side of the embryo. At this early stage, PGC numbers ranged from 1 to 7 per embryo (average=3.37; N=27, see Fig. 2A). Subsequently, PGCs migrated anteriorly on each side of the forming embryonic axis, along the developing somites (Fig. 1C-E). At early neurula stage (~10 hpf), PGCs were scattered and their average number was 4.96 (ranging from 1 to 12 cells, Fig. 1C, Fig. 2A). By the 8-9 somites stages (13-14 hpf), PGCs began to align in raws on both sides of the embryo trunk (Fig. 1D). PGC number doubled between early neurula and 8-9 somites stages (Fig. 2A) and ranged from 1 to 17 at that stage (average= 9.52; N=21), and remained constant up to 20 dpf. Subsequently, PGCs continued to migrate axially until reaching their prospective final position around the mid-trunk region at 16-17 somites stage (17 hpf). At that stage, PGCs were aligned very close to the body axis (Fig. 1E). Finally, in hatching larvae (26 hpf), PGCs moved medially to the gonadal primordia where they formed two lines on both sides of the body axis (Fig. 1F). After hatching and until 20 dpf, PGCs were progressively found at the upper surface of the gut, posteriorly to the swim bladder, where the future gonads will form (Fig. 1G-I). After clearing of the whole larvae at 20 dpf, a two-dimensional view of the area where gonads are localized confirmed that PGCs had already colonized the gonads (Fig. 1J-L). These results also confirmed that the GFP-*nos1* 3'UTR positive cells were bona fide PGCs.

Histological gonadal differentiation

The time-course of differentiation into male or female gonads was then followed by histology. The genotypic sex of larvae, juveniles, and young adult samples was determined based on sex-specific genomic regions of Pachón cavefish with a simple PCR genotyping test (see Methods). In both males and females of *A. mexicanus*, the gonadal primordia appeared as very thin and filiform paired-organs, located dorsally in the peritoneal cavity on both sides of the swim bladder. Between 16 and 30 dpf, although already composed of different types of somatic cells

and a few scarce germ cells, the male and female differentiating gonads did not present any apparent dimorphism (Fig. 3A-C'). At 45 dpf the gonad sizes increased both in males and females, with higher numbers of germ cells detected per section (Fig. 3D-D'), but no clear sign of histological differentiation could be detected, neither in somatic nor in germ cells (Fig. 3D-D'). It is only around 65 dpf that previtellogenic oocytes became clearly visible in some females (in 1 over 4 females examined at 65 dpf) (Fig. 4A'). In contrast to oogonias that were characterized by a rounded shape, a clear cytoplasm and a large nucleus, these previtellogenic oocytes were larger with a dense cytoplasm and a nucleus with multiple peripherally localized nucleoli (Fig. 4A', B', C'). However, at 65 dpf all male gonads remained undifferentiated with regard to germ cell development (Fig. 4A). It is only at 90 dpf that the first signs of germinal differentiation could be seen with the first detection of spermatocytes and spermatids cysts (Fig. 4B). Hence, from 65 dpf onwards in females and 90 dpf onwards in males, gonads were engaged in active gametogenesis. At 150 dpf, this resulted in clear ovarian lamellae with large previtellogenic oocytes in females (Fig. 4C'), and a testicular tissue with all spermatogenesis stages up to large cysts of spermatozoa in males (Fig. 4C). Altogether, these observations suggested that the differentiating gonads of *A. mexicanus* Pachón cavefish remain histologically undifferentiated at least until 45 dpf in females and 65 dpf in males. Thereafter, undifferentiated gonads differentiated directly into ovaries or testes. Comparison of the gonad histology of four males and four females sampled at each stage showed that gonadal development was not synchronous between animals, like for instance in females at 65 dpf for which we observed only one individual displaying some previtellogenic oocytes. Gonadal development variability was even sometimes detected within the same animal, with for instance a marked left/right asymmetry of gonad histology in one 90 dpf female for which the right gonad was large and clearly differentiated, while the left gonad was still at the onset of differentiation (Supplementary Fig. 1).

Expression profiles of sex-related genes in cavefish *A. mexicanus*

In order to better characterize gonadal differentiation molecularly in *A. mexicanus* cavefish, we analyzed the expression profiles of seven genes well-known as markers of germ cells (*vasa*), testicular differentiation (*amh*, *gsdf*, *dmrt1*) and ovarian differentiation (*foxl2a*, *cyp19a1a*, *wnt4b*). Expression of all these marker genes was first checked in various adult tissues including gonads. *dmrt1*, *gsdf*, *amh* and *vasa* genes all displayed a clear predominant gonadal expression, confirming their validity as bona fide gonadal differentiation markers in *A.*

mexicanus. In addition, *foxl2a*, *cyp19a1a*, and *wnt4b* were all expressed at high levels in gonads but also, albeit at a lower extent, in some other tissues (Fig. 5). Surprisingly, apart from *vasa* that was expressed at high levels both in male and female gonads, all these genes were significantly overexpressed in the testis, including classical ovarian markers such as *cyp19a1a*, *foxl2a* and *wnt4b*. Similarly, gonadal specific expression of markers involved in testicular (*amh*, *gsdf*, and *dmrt1*) and ovarian (*foxl2a*, *cyp19a1a*, and *wnt4b*) differentiation at different spermatogenesis and oogenesis stages shows that all these genes were overexpressed predominantly in the testes during gametogenesis (Fig. 6), excepted for *vasa*, which displayed a significantly higher expression levels in the ovaries at stages 3, 4, and 6 compared to testes.

Because of the difficulty of sampling very small differentiating gonads during the early stages of cavefish development, we sampled trunks (whole fish without the head and the tail) between 10 to 90 dpf and we isolated gonads at 150 dpf (Fig. 7). During cavefish early development, all gene expression patterns displayed an important variability, with coefficients of variation ranging from 107,3 to 347,12 % (Supplementary Tab. 2), irrespective of the sex and stage sampled (Fig. 7). Such gene expression variability probably reflected the variability in the timing of gonadal development that we also detected by histology (Supplementary Fig. 1). But, despite this variability, some global trends were clearly observed for germ cell (*vasa*, official symbol *ddx4*) and testicular differentiation gene markers (*amh*, *dmrt1*, *gsdf*). Expression of *vasa* in cavefish showed similar levels between sexes from 10 to 45 dpf (Fig. 2B), followed by a significant increase at 65 dpf in females ($p=0.0257$), and at 90 dpf in males ($p=0.00086$) with a significant ($p<0.001$) difference between sexes at 65 dpf. Male over-expressions were also observed for testicular differentiation gene markers with significant differences between sexes observed at 16, 45, 65 and 90 dpf for *gsdf*, at 90 dpf for *amh* and at 65 and 90 dpf for *dmrt1* (Fig. 7). In contrast, all the female differentiation marker genes did not display any significant differences between sexes (Fig. 7).

DISCUSSION

Despite being an important emerging model species, the morphological and molecular mechanisms underlying *A. mexicanus* cavefish sex differentiation have not been yet investigated. In the present study, we provide evidence that *A. mexicanus* belongs to the differentiated gonochoristic species like most teleost species. Of note, this is in contrast with a

close relative characidae species i.e., the black widow tetra, *Gymnocorymbus ternetzi*, described as an undifferentiated gonochoristic species [Mazzoni et al., 2015]. We also characterized the primordial germ cells (PGCs) migration process and gonadal differentiation steps, using both histological and molecular information in a Pachón cave laboratory population of *A. mexicanus*.

Injections of GFP-zebrafish *nos1 3'UTR* mRNAs at the one-cell stage of *A. mexicanus* enabled a reliable PGC tracking, as described in other teleost species [Kurokawa et al., 2006; Saito et al., 2006; Herpin et al., 2007; Saito et al., 2014]. The visualization of the first PGCs was possible at 80% epiboly in *A. mexicanus*. Comparatively, PGCs were detected in other fish species at different stages ranging from 50% epiboly stage in *Danio rerio* [Saito et al., 2006] to somitogenesis stage in *Prochilodus lineatus* [Coelho et al., 2019]. This variability in the first detection of a clear fluorescence of the GFP-zebrafish *nos1 3'UTR* mRNA reporter is likely due to a weak and variable signal of background noise resulting from the initial GFP expression in both PGCs and somatic cells as described in other fish species [Saito et al., 2006; Saito et al., 2014]. In addition, the number of PGCs in *A. mexicanus* was very low (average 9.5 PGCs at the somitogenesis stage) compared to other species like zebrafish and medaka that have respectively and in average 21.2 and 22.5 PGCs at the same stage [Saito et al., 2006]. It has been reported that PGCs do not proliferate during their migration to the genital crest [Linhartova et al., 2014], but in *A. mexicanus* we detected an almost significant doubling in PGC number between the early neurula and the 8-9 somites stages, followed by an absence of further division until 20 dpf, when the PGCs have already entered the differentiating gonads. In medaka, germ cells undergo two types of division after they reach the differentiating gonads i.e., a first slow intermittent division (type I), where each germ cell divides into two daughter cells, and a synchronous continuous proliferation (type II) [Saito et al., 2007]. The early PGCs proliferation seen in *A. mexicanus* around the late neurula stage looks like the slow type I division of medaka germ cells. These results suggest that the absence of PGC divisions during their migration to the genital crest is not as conserved as previously thought. Comparative studies on PGCs migration have evidenced that this process could be species-specific [Kurokawa et al., 2006; Saito et al., 2006; Coelho et al., 2019], suggesting that the early PGCs proliferation that we detected in the cavefish *Astyanax mexicanus*, could be also a species-specific feature of PGC development, even though the mechanisms underlying PGCs specification and movements seem widely conserved in the animal kingdom [Xu et al., 2010].

The colonization of the genital ridges by PGCs derived from extra-gonadal tissues gives rise to the gonadal primordium [Winkoop et al., 1992; Flores, and Burns, 1993; Braat et al., 1999]. In *A. mexicanus*, the first established germ cells were observed in 16 dpf gonads both in males and females, in two symmetrical differentiating gonads located dorsally in the peritoneal cavity on both sides of the swim bladder. As in most teleost species, these differentiating gonads contained a few germ cells surrounded by a most abundant number of different types of somatic cells [Meijide et al., 2005; Çek, 2006; Mazzoni et al., 2010; Amaral et al., 2020]. As mentioned before, germ cell proliferation during these early differentiation stages can be more active in females compared to males in some species [Nakamura et al., 1998; Saito et al., 2007; Lewis et al., 2008] and this early proliferation has been often associated with the onset of gonadal differentiation. During Pachón *A. mexicanus* early development, i.e., from 16 to 45 dpf, germ cells appeared to be scattered, most often located in the middle of the gonads close to the blood vessels and surrounded by a large number of somatic cells, but no obvious sign of any sex-specific germ cell proliferation was observed by histology. In contrast, a significantly earlier expression (65 dpf) of the well-characterized molecular component of germ cells, *vasa* [Hay et al., 1988; Liang et al., 1994] was observed in cavefish females. Interestingly, *vasa* homologs have been characterized in a wide range of organisms as a germ cell specific marker [Braat et al., 1999; Shinomiya et al., 2000; Toyooka et al., 2000] and such an early female-specific *vasa* overexpression during gonadal differentiation has been also shown in turbot, *Scophthalmus maximus* [Robledo et al., 2015], and the catfish, *Clarias gariepinus* [Raghuvir, and Senthilkumaran, 2010]. In Nile tilapia, *Oreochromis niloticus*, and gibel carp, *Carassius gibelio*, *vasa* is strongly expressed during early oogenesis i.e., in oogonia and previtellogenic oocytes, and during spermatogenesis, i.e., in spermatogonia and to a lesser extent in early spermatocytes [Kobayashi et al., 2000; Xu et al., 2005]. In cavefish, *vasa* expression was clearly biphasic with a sustained basal expression from 10 to 45 dpf in both males and females that could be correlated with an absence of both germ cell proliferation and differentiation, followed by an abrupt increase first in females at 65 dpf then in males at 90 dpf. This second phase of increasing expression can be linked with an earlier germ cell proliferation in females or to a germ cell differentiation process as the first previtellogenic oocytes in females and spermatocytes in males were also detected at 65 and 90 dpf, respectively. The first signs of gonadal differentiation observed in other species are either (i) an early ovarian cavity formation; (ii) or early meiotic activity in females leading to the formation of previtellogenic oocytes and their auxocytosis [Brusle, and Brusle, 1983; Maack, and Segner, 2003; Meijide et al., 2005]. Hence, further histological studies with a particular focus on the period of gonadal

differentiation, i.e., from 45 dpf to 95 dpf would provide a more precise exploration of the first signs and the exact timing of histological gonadal differentiation in *A. mexicanus*.

In *A. mexicanus*, oogenesis begins earlier than spermatogenesis, with the appearance of the first previtellogenic oocytes as early as 65 dpf in some females. In males, the gonads remain quiescent longer than females and testes are histologically clearly identifiable only at 90 dpf with the first sign of an active spermatogenesis and the formation of spermatogonia, spermatocytes and spermatids tubules, followed by spermatozoa tubules at 150 dpf. Similar observations have been reported in other fish species regarding the timing of gonadal development, with oogenesis occurring earlier than spermatogenesis, like for instance in *Oreochromis niloticus*, in which oogenesis and spermatogenesis start 35 or 50–70 days after hatching, respectively [Nakamura, and Nagahama, 1989]. In medaka as well, oogenesis and spermatogenesis start around 20 or 50 days after hatching, respectively [Kurokawa et al., 2007]. However, in *A. mexicanus*, despite early signs of differentiation in females, at 150 dpf the male gonads are close to spermiation, in contrast to female gonads which are still in the previtellogenesis stage, suggesting a delay in sexual maturity in females compared to males. It is also important to note that early gonadal development in *A. mexicanus* is not synchronous within the laboratory population we used. Such results were reported in different species of sturgeons showing asynchronous development during early gonadal differentiation [Wuertz et al., 2018].

Among the three important genes known for their key role during testicular differentiation (*amh*, *gsdf*, *dmrt1*), *dmrt1bY* (a Y-linked duplicated copy) that codes for a transcription factor containing a zinc finger-like DNA binding motif (DM domain) was characterized as a MSD gene in medaka *Oryzias latipes* [Matsuda et al., 2002; Nanda et al., 2002]. Moreover, *dmrt1* expression has been reported to be exclusively or predominantly expressed in the testes of many fish species [Herpin, and Schartl, 2011]. Consistently, cavefish *dmrt1* displays a predominant testicular expression during early development (i.e., from 65 to 90 dpf). Interestingly, a similar *dmrt1* overexpression in male gonads was also observed in two closely-related species in the genus *Astyanax*, i.e., *A. altiparanae* and *A. scabripinnis* [Adolfi et al., 2015; Castro et al., 2019a; Martinez-Bengochea et al., 2020]. The anti-Müllerian hormone is a glycoprotein of the transforming growth factor β superfamily (TGF- β) [Lukas-Croisier et al., 2003]. In teleosts, Y-linked *amh* duplicated copies have been found to act as a master sex determining genes in several species [Hattori et al., 2012; Li et al., 2015; Pan et al., 2019]. In

A. mexicanus, *amh* was detected at roughly equal levels in both male and female undifferentiated gonads and subsequently displayed a testicular overexpression at 90 dpf. Such a dimorphic pattern has been found in many fish species at early differentiating stages [Vizziano et al., 2007; Ijiri et al., 2008; Robledo et al., 2015; Jiang et al., 2020], consistent with *amh* playing an important role in testicular differentiation. In addition, *amh* is expressed highly in adult testes compared to adult ovaries of *Astyanax scabripinnis* and *Astyanax altiparanae* [Castro et al., 2019b; Martinez-Bengochea et al., 2020]. The gonadal soma-derived factor (*gsdf*) is another TGF- β member, that was first identified in rainbow trout *Oncorhynchus mykiss* [Sawatari et al., 2007] and its expression is predominantly detected in Sertoli and granulosa cells in several fish species [Sawatari et al., 2007; Shibata et al., 2010; Gautier et al., 2011a; Gautier et al., 2011b]. Interestingly, Y-chromosome genes or alleles of *gsdf* were characterized or proposed as potential master sex determining genes in the Luzon ricefish *Oryzias luzonensis* [Myosho et al., 2012] and in sablefish *Anoplopoma fimbria* [Rondeau et al., 2013]. In cavefish, *gsdf* displays a clear dimorphic expression with significantly higher levels in males than in females as soon as 16 dpf. Such an early testicular overexpression of *gsdf* was also reported in *O. latipes* [Shibata et al., 2010], *O. niloticus* [Kaneko et al., 2015], *D. rerio* [Yan et al., 2017], and *C. semilaevis* [Zhu et al., 2018].

We have also studied ovarian differentiation genes such as *foxl2b*, *cyp19a1a*, and *wnt4b*, which have been suggested as key sex differentiation players across a wide range of animals [Chassot et al., 2008; Cutting et al., 2013; Herpin et al., 2013; Shen, and Wang, 2014; Herpin, and Schartl, 2015; Fajkowska et al., 2019]. The forkhead box protein L2 (*foxl2*) is a member of the large forkhead box gene family of transcription factors that is expressed predominantly in female gonads of many fish species [Bertho et al., 2016]. For instance, in *Astyanax scabripinnis*, *foxl2a* displays dimorphic expression between adult testes and ovaries with higher expression in females compared to males [Castro et al., 2019b]. Besides *foxl2*, estrogens and *cyp19a1a* have been reported as crucial conserved actors of ovarian differentiation in fish [Guiguen et al., 2010]. But surprisingly, we did not find any female overexpression of *foxl2a* and *cyp19a1a* during early development in *A. mexicanus* cavefish, contrasting with their known implication as classical ovarian differentiation genes [Guiguen et al., 2010; Bertho et al., 2016]. In addition, we also found that these two genes were highly expressed in cavefish testes with only low basal expression levels in ovaries during gametogenesis stages until adult gonads. Such a non-dimorphic expression of these classical ovarian differentiation genes was unexpected. However, it must be noted that *A. mexicanus* is not the only exception to the rule:

similar results have been found for instance in the stellate Sturgeon (*Acipenser stellatus*), in which no significant differences were found for *foxl2* in male and female gonads [Burcea et al., 2018], or in another Characiform, the tambaqui *Colossoma macropomum*, in which no expression of *cyp19a1a* was detected in both males and females [Lobo et al., 2020]. Moreover, in *A. altiparanae*, both *foxl2* and *cyp19a1a* are expressed equally in adult testes and ovaries [Martinez-Bengochea et al., 2020]. In mammalian species, *foxl2* cooperates with *wnt4* in regulating *fst* expression during ovarian development [Garcia-Ortiz et al., 2009] and growing evidence suggests that the Wnt signaling pathway might also play a conserved role in fish sex differentiation [Wu, and Chang, 2009; Chen et al., 2015]. In cavefish, we found that *wnt4b* expression, like *foxl2a* and *cyp19a1a*, did not show any sexually dimorphic expression during early gonadal differentiation. In fact, *wnt4b* is even expressed at higher levels in the testes than in the ovaries during gametogenesis and up to adult gonads.

Although the sex differentiation downstream gene-regulatory network was initially thought to be highly conserved in vertebrates because of the conservation of the genes involved in this process [Cutting et al., 2013], recent results are questioning this hypothesis [Herpin et al., 2013]. In fact, many “important genes” do not exhibit conserved spatiotemporal expression patterns. This is for instance the case in fish for both *dmrt1* and *gsdf* that are dimorphically expressed with a different timing during the early gonadal development of medaka and zebrafish [Kurokawa et al., 2007; Jørgensen et al., 2008] compared to Nile Tilapia [Kaneko et al., 2015]. In cavefish *gsdf* is clearly expressed in a sexually dimorphic fashion much before *dmrt1* and *amh* (from 16 dpf onwards versus 65-90 dpf), supporting the idea that *gsdf* may act as an early switch promoting testis differentiation in cavefish as described in medaka *Oryzias latipes* [Zhang et al., 2016]. In the same vein, although testicular differentiation genes displayed obvious sexually-dimorphic expression patterns, neither *foxl2a* and *cyp19a1a* nor *wnt4b* showed sexually-dimorphic patterns during cavefish gonadal differentiation. Given their well-known implication in fish ovarian differentiation and their tight interaction [Wu, and Chang, 2009; Chen et al., 2015; Guiguen et al., 2010; Bertho et al., 2016; Bertho et al., 2018], these results appear surprising and would probably need additional confirmation. However, estrogen-independent ovarian differentiation has been already suggested in medaka [Kawahara, and Yamashita, 2000; Bertho et al., 2016; Bertho et al., 2018].

In summary, combining both expression patterns of sex-related genes and histological changes in *A. mexicanus* cavefish, we provided a first description of the gonadal differentiation process

in this species. Based on gonadal histology and on the *vasa* germ-cell specific expression we delineated the beginning of sexually dimorphic fates in cavefish between 45 to 65 dpf. This sex-differentiation period is corroborated both by histological features and by the sexually-dimorphic expression patterns of testicular differentiation genes such as *dmrt1*, *amh* and *gsdf*. Altogether, these findings are of prime importance for a better understanding of the sex determination mechanisms in *A. mexicanus*. Our results also revealed major discrepancies with the canonical estrogen action on fish ovarian differentiation [Guiguen et al., 2010], pointing-out to the idea that the control of ovarian development in cavefish would be estrogen-independent and that the downstream regulatory network of sex differentiation is not as conserved in teleost fish as initially thought.

ACKNOWLEDGEMENTS

We are grateful to the Deca team members from CNRS (Institute of Neurosciences Paris-Saclay, Gif-sur-Yvette), particularly Victor Simon for assistance in obtaining eggs and Jorge Torres-Paz for help with injections. We thank A. Patinote and P-L. Sudan from the experimental facility (INRAE UR1037 LPGP, Rennes) for fish maintenance. We want to thank M. Policarpo (CNRS EGCE, Gif-sur-Yvette) and C. Guyomar (INRAE UR1037 LPGP, Rennes) for their support with R software. We also want to thank D. Casane (CNRS EGCE, Gif-sur-Yvette) for statistical advice.

Statement of Ethics

Animal protocols were carried out in accordance with European legislation (directive 2010-63-UE and French decree 2013-118)

Disclosure Statement: The authors have no conflicts of interest to declare.

Funding Sources: This project was supported by funds from the “Agence Nationale de la Recherche” (ANR/DFG, PhyloSex project, 2014-2016) to YG and an « Equipe FRM » grant [DEQ20150331745] from the Fondation pour la Recherche Médicale to SR. The funders had no role in study design, data collection and analysis, decision to publish, or preparation of the manuscript. BI PhD fellowship was supported by the Doctoral School of Ecology, Geosciences, Agronomy, Nutrition of the university of Rennes 1 and INRAE.

Author Contributions

Funding acquisition: Y.G, S.R; Design, planning and discussing the project and experiments: B.I, A.H, S.R and Y.G; Executing experiments: B.I, E.J, A.B, and S.B; Carrying out the immunostaining, clearing and confocal microscopy imaging: B.I, M.T, V.T; Analyzing the data: B.I and Y.G; Writing original draft: B.I; Reviewing and editing final manuscript: B.I, A.H, S.R, Y.G; Supervising the project: A.H, S.R and Y.G.

REFERENCES

- Fricke, R., Eschmeyer, W. N. & R. van der Laan (eds) 2020. Eschmeyer's catalog of fishes: genera, species, references. (<http://researcharchive.calacademy.org/research/ichthyology/catalog/fishcatmain.asp>). Electronic version accessed 15/03/2020.
- Bachtrog D, Mank JE, Peichel CL, Kirkpatrick M, Otto SP, Ashman T-L, et al.: Sex Determination: Why So Many Ways of Doing It? *PLOS Biology* 12:e1001899 (2014).
- Devlin RH, Nagahama Y: Sex determination and sex differentiation in fish: an overview of genetic, physiological, and environmental influences. *Aquaculture* 208:191–364 (2002).
- Pan Q, Guiguen Y, Herpin A: Evolution of Sex Determining Genes in Fish [Internet], in Skinner MK (ed): *Encyclopedia of Reproduction* (Second Edition) (Academic Press, Oxford 2018), pp 168–175.
- Nagahama Y: Molecular mechanisms of sex determination and gonadal sex differentiation in fish. *Fish Physiol Biochem* 31:105–109 (2005).
- Ijiri S, Kaneko H, Kobayashi T, Wang D-S, Sakai F, Paul-Prasanth B, et al.: Sexual Dimorphic Expression of Genes in Gonads During Early Differentiation of a Teleost Fish, the Nile Tilapia *Oreochromis niloticus*. *Biol Reprod* 78:333–341 (2008).
- Herpin A, Adolfi MC, Nicol B, Hinzmann M, Schmidt C, Klughammer J, et al.: Divergent Expression Regulation of Gonad Development Genes in Medaka Shows Incomplete Conservation of the Downstream Regulatory Network of Vertebrate Sex Determination. *Molecular Biology and Evolution* 30:2328–2346 (2013).
- Yamamoto T-O: 3 Sex Differentiation [Internet], in Hoar WS, Randall DJ (eds): *Fish Physiology* (Academic Press, 1969), pp 117–175.
- Baroiller J-F, Guiguen Y: Endocrine and environmental aspects of sex differentiation in gonochoristic fish [Internet], in Scherer G, Schmid M (eds): *Genes and Mechanisms in Vertebrate Sex Determination* (Birkhäuser, Basel 2001), pp 177–201.
- Nishimura T, Tanaka M: Gonadal Development in Fish. *Sex Dev* 8:252–261 (2014).
- Guerrero-Estevez S, Moreno-Mendoza N: Sexual determination and differentiation in teleost fish. *Rev Fish Biol Fisheries* 20:101–121 (2010).
- Brusle J, Brusle S: La gonadogenèse des Poissons. *Reproduction Nutrition Développement* 23:453–491 (1983).
- Jørgensen A, Morthorst JE, Andersen O, Rasmussen LJ, Bjerregaard P: Expression profiles for six zebrafish genes during gonadal sex differentiation. *Reprod Biol Endocrinol* 6:25 (2008).
- Wang W, Zhu H, Dong Y, Dong T, Tian Z, Hu H: Identification and dimorphic expression of sex-related genes during gonadal differentiation in sterlet *Acipenser ruthenus*, a

- primitive fish species. *Aquaculture* 500:178–187 (2019).
- Guiguen Y, Fostier A, Piferrer F, Chang C-F: Ovarian aromatase and estrogens: A pivotal role for gonadal sex differentiation and sex change in fish. *General and Comparative Endocrinology* 165:352–366 (2010).
- Sreenivasan R, Jiang J, Wang X, Bártfai R, Kwan HY, Christoffels A, et al.: Gonad Differentiation in Zebrafish Is Regulated by the Canonical Wnt Signaling Pathway. *Biol Reprod* 90 (2014). DOI: 10.1095/biolreprod.113.110874
- Bertho S, Pasquier J, Pan Q, Trionnaire GL, Bobe J, Postlethwait JH, et al.: Foxl2 and Its Relatives Are Evolutionary Conserved Players in Gonadal Sex Differentiation. *SXD* 10:111–129 (2016).
- Nelson JS, Grande TC, Wilson MVH: Fishes of the World [Internet], in : Fishes of the World (John Wiley & Sons, Ltd, 2016), pp 1–12.
- Mitchell RW, Russell WH, Elliott WR: Mexican eyeless characin fishes, genus *Astyanax*: environment, distribution, and evolution. (Texas Tech Press, Lubbock 1977).
- Elliott WR: The *Astyanax* Caves of Mexico: Cavefishes of Tamaulipas, San Luis Potosí, and Guerrero. *Journal of Fish Biology* 94:205–205 (2019).
- Di Palma F, Kidd C, Borowsky R, Kocher TD: Construction of bacterial artificial chromosome libraries for the Lake Malawi cichlid (*Metriaclima zebra*), and the blind cavefish (*Astyanax mexicanus*). *Zebrafish* 4:41–47 (2007).
- Hinaux H, Poulain J, Da Silva C, Noirot C, Jeffery WR, Casane D, et al.: De novo sequencing of *Astyanax mexicanus* surface fish and Pachón cavefish transcriptomes reveals enrichment of mutations in cavefish putative eye genes. *PLoS ONE* 8 (2013). DOI: 10.1371/journal.pone.0053553
- McGaugh SE, Gross JB, Aken B, Blin M, Borowsky R, Chalopin D, et al.: The cavefish genome reveals candidate genes for eye loss. *Nat Commun* 5:5307 (2014).
- Herman A, Brandvain Y, Weagley J, Jeffery WR, Keene AC, Kono TJY, et al.: The role of gene flow in rapid and repeated evolution of cave-related traits in Mexican tetra, *Astyanax mexicanus*. *Mol Ecol* 27:4397–4416 (2018).
- Keene AC, Yoshizawa M, McGaugh SE: Biology and Evolution of the Mexican Cavefish [Internet]. (Elsevier, 2016). DOI: 10.1016/C2014-0-01426-8
- Wilkens H, Strecker U: Evolution in the Dark: Darwin's Loss Without Selection [Internet]. (Springer-Verlag, Berlin Heidelberg 2017). DOI: 10.1007/978-3-662-54512-6
- Gharbi K, Gautier A, Danzmann RG, Gharbi S, Sakamoto T, Hoyheim B, et al.: A linkage map for brown trout (*Salmo trutta*): Chromosome homeologies and comparative genome organization with other salmonid fish. *Genetics* 172:2405–2419 (2006).
- Siemering KR, Golbik R, Sever R, Haseloff J: Mutations that suppress the thermosensitivity of green fluorescent protein. *Current Biology* 6:1653–1663 (1996).
- Köprunner M, Thisse C, Thisse B, Raz E: A zebrafish nanos-related gene is essential for the development of primordial germ cells. *Genes Dev* 15:2877–2885 (2001).
- Herpin A, Rohr S, Riedel D, Kluever N, Raz E, Schartl M: Specification of primordial germ cells in medaka (*Oryzias latipes*). *BMC Dev Biol* 7:3 (2007).
- Hinaux H, Pottin K, Chalhoub H, Père S, Eliot Y, Legendre L, et al.: A developmental staging table for *Astyanax mexicanus* surface fish and Pachón cavefish. *Zebrafish* 8:155–165 (2011).
- Klingberg A, Hasenberg A, Ludwig-Portugall I, Medyukhina A, Männ L, Brenzel A, et al.: Fully Automated Evaluation of Total Glomerular Number and Capillary Tuft Size in Nephritic Kidneys Using Lightsheet Microscopy. *JASN* 28:452–459 (2017).
- Koressaar T, Remm M: Enhancements and modifications of primer design program Primer3. *Bioinformatics* 23:1289–1291 (2007).
- Koressaar T, Lepamets M, Kaplinski L, Raime K, Andreson R, Remm M: Primer3_masker:

- integrating masking of template sequence with primer design software. *Bioinformatics* 34:1937–1938 (2018).
- Untergasser A, Cutcutache I, Koressaar T, Ye J, Faircloth BC, Remm M, et al.: Primer3—new capabilities and interfaces. *Nucleic Acids Research* 40 (2012). DOI: 10.1093/nar/gks596
- Kurokawa H, Aoki Y, Nakamura S, Ebe Y, Kobayashi D, Tanaka M: Time-lapse analysis reveals different modes of primordial germ cell migration in the medaka *Oryzias latipes*. *Dev Growth Differ* 48:209–221 (2006).
- Saito T, Fujimoto T, Maegawa S, Inoue K, Tanaka M, Arai K, et al.: Visualization of primordial germ cells in vivo using GFP-nos1 3'UTR mRNA. *Int J Dev Biol* 50:691–699 (2006).
- Saito T, Goto-Kazeto R, Fujimoto T, Kawakami Y, Arai K, Yamaha E: Inter-species transplantation and migration of primordial germ cells in cyprinid fish. *Int J Dev Biol* 54:1481–1486 (2010).
- Saito T, Pšenička M, Goto R, Adachi S, Inoue K, Arai K, et al.: The Origin And Migration Of Primordial Germ Cells In Sturgeons. *PLoS ONE* 9:e86861 (2014).
- Giraldez AJ, Mishima Y, Rihel J, Grocock RJ, Dongen SV, Inoue K, et al.: Zebrafish MiR-430 Promotes Deadenylation and Clearance of Maternal mRNAs. *Science* 312:75–79 (2006).
- Mishima Y, Giraldez AJ, Takeda Y, Fujiwara T, Sakamoto H, Schier AF, et al.: Differential regulation of germline mRNAs in soma and germ cells by zebrafish miR-430. *Curr Biol* 16:2135–2142 (2006).
- Mishima Y: Widespread roles of microRNAs during zebrafish development and beyond. *Dev Growth Differ* 54:55–65 (2012).
- Mazzoni TS, Grier HJ, Quaglio-Grassiotto I: The basement membrane and the sex establishment in the juvenile hermaphroditism during gonadal differentiation of the *Gymnophorus ternetzi* (Teleostei: Characiformes: Characidae). *Anat Rec (Hoboken)* 298:1984–2010 (2015).
- Coelho GCZ, Yo IS, Mira-López TM, Monzani PS, Arashiro DR, Fujimoto T, et al.: Preparation of a fish embryo for micromanipulation: staging of development, removal of the chorion and traceability of PGCs in *Prochilodus lineatus*. *Int J Dev Biol* 63:57–65 (2019).
- Linhartova Z, Saito T, Psenicka M: Embryogenesis, visualization and migration of primordial germ cells in tench (*Tinca tinca*). *Journal of Applied Ichthyology* 30:29–39 (2014).
- Saito D, Morinaga C, Aoki Y, Nakamura S, Mitani H, Furutani-Seiki M, et al.: Proliferation of germ cells during gonadal sex differentiation in medaka: Insights from germ cell-depleted mutant zenzai. *Developmental Biology* 310:280–290 (2007).
- Xu H, Li M, Gui J, Hong Y: Fish germ cells. *Sci China Life Sci* 53:435–446 (2010).
- Winkoop A van, Booms GHR, Dulos GJ, Timmermans LPM: Ultrastructural changes in primordial germ cells during early gonadal development of the common carp (*Cyprinus carpio* L., teleostei). *Cell Tissue Res* 267:337–346 (1992).
- Flores JA, Burns JR: Ultrastructural study of embryonic and early adult germ cells, and their support cells, in both sexes of *Xiphophorus* (Teleostei: Poeciliidae). *Cell Tissue Res* 271:263–270 (1993).
- Braat AK, Zandbergen T, van de Water S, Goos HJ, Zivkovic D: Characterization of zebrafish primordial germ cells: morphology and early distribution of vasa RNA. *Dev Dyn* 216:153–167 (1999).
- Meijide FJ, Nistro FLL, Guerrero GA: Gonadal development and sex differentiation in the cichlid fish *Cichlasoma dimerus* (Teleostei, perciformes): A light- and electron-microscopic study. *J Morphol* 264:191–210 (2005).
- Çek Ş: Early gonadal development and sex differentiation in rosy barb (*Puntius conchonius*).

Animal Biol 56:335–350 (2006).

- Mazzoni TS, Grier HJ, Quagio-Grassiotto I: Germline Cysts and the Formation of the Germinal Epithelium During the Female Gonadal Morphogenesis in *Cyprinus carpio* (Teleostei: Ostariophysi: Cypriniformes). *Anat Rec* 293:1581–1606 (2010).
- Amaral A da C, Lima AF, Ganeco-kirschnik LN, Almeida FL de: Morphological characterization of pirarucu Arapaima gigas (Schinz, 1822) gonadal differentiation. *Journal of Morphology* n/a (2020). DOI: 10.1002/jmor.21116
- Nakamura M, Kobayashi T, Chang X-T, Nagahama Y: Gonadal sex differentiation in teleost fish. *Journal of Experimental Zoology* 281:362–372 (1998).
- Lewis ZR, McClellan MC, Postlethwait JH, Cresko WA, Kaplan RH: Female-specific increase in primordial germ cells marks sex differentiation in threespine stickleback (*Gasterosteus aculeatus*). *J Morphol* 269:909–921 (2008).
- Hay B, Jan LY, Jan YN: A protein component of *Drosophila* polar granules is encoded by vasa and has extensive sequence similarity to ATP-dependent helicases. *Cell* 55:577–587 (1988).
- Liang L, Diehl-Jones W, Lasko P: Localization of vasa protein to the *Drosophila* pole plasm is independent of its RNA-binding and helicase activities. *Development* 120:1201–1211 (1994).
- Shinomiya A, Tanaka M, Kobayashi T, Nagahama Y, Hamaguchi S: The vasa-like gene, olvas, identifies the migration path of primordial germ cells during embryonic body formation stage in the medaka, *Oryzias latipes*. *Development, Growth & Differentiation* 42:317–326 (2000).
- Toyooka Y, Tsunekawa N, Takahashi Y, Matsui Y, Satoh M, Noce T: Expression and intracellular localization of mouse Vasa-homologue protein during germ cell development. *Mech Dev* 93:139–149 (2000).
- Robledo D, Ribas L, Cal R, Sánchez L, Piferrer F, Martínez P, et al.: Gene expression analysis at the onset of sex differentiation in turbot (*Scophthalmus maximus*). *BMC Genomics* 16:973 (2015).
- Raghubeer K, Senthilkumaran B: Cloning and differential expression pattern of vasa in the developing and recrudescing gonads of catfish, *Clarias gariepinus*. *Comparative Biochemistry and Physiology Part A: Molecular & Integrative Physiology* 157:79–85 (2010).
- Kobayashi T, Kajiura-Kobayashi H, Nagahama Y: Differential expression of vasa homologue gene in the germ cells during oogenesis and spermatogenesis in a teleost fish, tilapia, *Oreochromis niloticus*. *Mech Dev* 99:139–142 (2000).
- Xu H, Gui J, Hong Y: Differential expression of vasa RNA and protein during spermatogenesis and oogenesis in the gibel carp (*Carassius auratus gibelio*), a bisexual and gynogenetically reproducing vertebrate. *Developmental Dynamics* 233:872–882 (2005).
- Maack G, Segner H: Morphological development of the gonads in zebrafish. *Journal of Fish Biology* 62:895–906 (2003).
- Nakamura M, Nagahama Y: Differentiation and development of Leydig cells, and changes of testosterone levels during testicular differentiation in tilapia *Oreochromis niloticus*. *Fish Physiol Biochem* 7:211–219 (1989).
- Kurokawa H, Saito D, Nakamura S, Katoh-Fukui Y, Ohta K, Baba T, et al.: Germ cells are essential for sexual dimorphism in the medaka gonad. *Proceedings of the National Academy of Sciences* 104:16958–16963 (2007).
- Wuertz S, Güralp H, Pšenička M, Chebanov M: Sex Determination in Sturgeon [Internet], in : Sex Control in Aquaculture (John Wiley & Sons, Ltd, 2018), pp 645–668.
- Matsuda M, Nagahama Y, Shinomiya A, Sato T, Matsuda C, Kobayashi T, et al.: DMY is a Y-

- specific DM-domain gene required for male development in the medaka fish. *Nature* 417:559–563 (2002).
- Nanda I, Kondo M, Hornung U, Asakawa S, Winkler C, Shimizu A, et al.: A duplicated copy of DMRT1 in the sex-determining region of the Y chromosome of the medaka, *Oryzias latipes*. *Proc Natl Acad Sci USA* 99:11778–11783 (2002).
- Herpin A, Schartl M: Dmrt1 genes at the crossroads: a widespread and central class of sexual development factors in fish. *FEBS J* 278:1010–1019 (2011).
- Adolfi MC, Carreira AC, Jesus LW, Bogerd J, Funes RM, Schartl M, et al.: Molecular cloning and expression analysis of dmrt1 and sox9 during gonad development and male reproductive cycle in the lambari fish, *Astyanax altiparanae*. *Reprod Biol Endocrinol* 13:2 (2015).
- Castro JP, Hattori RS, Yoshinaga TT, Silva DMZ de A, Foresti F, Santos MH, et al.: Differential Expression of *dmrt1* in *Astyanax scabripinnis* (Teleostei, Characidae) Is Correlated with B Chromosome Occurrence. *Zebrafish* 16:182–188 (2019a).
- Martinez-Bengochea A, Doretto L, Rosa IF, Oliveira MA, Silva C, Silva DMZA, et al.: Effects of 17 β -estradiol on early gonadal development and expression of genes implicated in sexual differentiation of a South American teleost, *Astyanax altiparanae*. *Comparative Biochemistry and Physiology Part B: Biochemistry and Molecular Biology* 248–249:110467 (2020).
- Lukas-Croisier C, Lasala C, Nicaud J, Bedecarrás P, Kumar TR, Dutertre M, et al.: Follicle-stimulating hormone increases testicular Anti-Müllerian hormone (AMH) production through sertoli cell proliferation and a nonclassical cyclic adenosine 5'-monophosphate-mediated activation of the AMH Gene. *Mol Endocrinol* 17:550–561 (2003).
- Hattori RS, Murai Y, Oura M, Masuda S, Majhi SK, Sakamoto T, et al.: A Y-linked anti-Müllerian hormone duplication takes over a critical role in sex determination. *Proc Natl Acad Sci USA* 109:2955–2959 (2012).
- Li M, Sun Y, Zhao J, Shi H, Zeng S, Ye K, et al.: A Tandem Duplicate of Anti-Müllerian Hormone with a Missense SNP on the Y Chromosome Is Essential for Male Sex Determination in Nile Tilapia, *Oreochromis niloticus*. *PLoS Genet* 11:e1005678 (2015).
- Pan Q, Feron R, Yano A, Guyomard R, Jouanno E, Vigouroux E, et al.: Identification of the master sex determining gene in Northern pike (*Esox lucius*) reveals restricted sex chromosome differentiation. *PLOS Genetics* 15:e1008013 (2019).
- Vizziano D, Randuineau G, Baron D, Cauty C, Guiguen Y: Characterization of early molecular sex differentiation in rainbow trout, *Oncorhynchus mykiss*. *Dev Dyn* 236:2198–2206 (2007).
- Jiang M, Jia S, Chen J, Chen K, Ma W, Wu X, et al.: Timing of gonadal development and dimorphic expression of sex-related genes in gonads during early sex differentiation in the Yellow River carp. *Aquaculture* 518:734825 (2020).
- Castro JP, Hattori RS, Yoshinaga TT, Silva DMZ de A, Ruiz-Ruano FJ, Foresti F, et al.: Differential Expression of Genes Related to Sexual Determination Can Modify the Reproductive Cycle of *Astyanax scabripinnis* (Characiformes: Characidae) in B Chromosome Carrier Individuals. *Genes* 10:909 (2019b).
- Sawatari E, Shikina S, Takeuchi T, Yoshizaki G: A novel transforming growth factor-beta superfamily member expressed in gonadal somatic cells enhances primordial germ cell and spermatogonial proliferation in rainbow trout (*Oncorhynchus mykiss*). *Dev Biol* 301:266–275 (2007).
- Shibata Y, Paul-Prasantha B, Suzuki A, Usami T, Nakamoto M, Matsuda M, et al.: Expression of gonadal soma derived factor (GSDF) is spatially and temporally correlated with early

- testicular differentiation in medaka. *Gene Expression Patterns* 10:283–289 (2010).
- Gautier A, Le Gac F, Lareyre J-J: The gsdf gene locus harbors evolutionary conserved and clustered genes preferentially expressed in fish previtellogenic oocytes. *Gene* 472:7–17 (2011a).
- Gautier A, Sohm F, Joly J-S, Le Gac F, Lareyre J-J: The proximal promoter region of the zebrafish gsdf gene is sufficient to mimic the spatio-temporal expression pattern of the endogenous gene in Sertoli and granulosa cells. *Biol Reprod* 85:1240–1251 (2011b).
- Myoshio T, Otake H, Masuyama H, Matsuda M, Kuroki Y, Fujiyama A, et al.: Tracing the Emergence of a Novel Sex-Determining Gene in Medaka, *Oryzias luzonensis*. *Genetics* 191:163–170 (2012).
- Rondeau EB, Messmer AM, Sanderson DS, Jantzen SG, von Schalburg KR, Minkley DR, et al.: Genomics of sablefish (*Anoplopoma fimbria*): expressed genes, mitochondrial phylogeny, linkage map and identification of a putative sex gene. *BMC Genomics* 14:452 (2013).
- Kaneko H, Ijiri S, Kobayashi T, Izumi H, Kuramochi Y, Wang D-S, et al.: Gonadal soma-derived factor (gsdf), a TGF-beta superfamily gene, induces testis differentiation in the teleost fish *Oreochromis niloticus*. *Mol Cell Endocrinol* 415:87–99 (2015).
- Yan Y-L, Desvignes T, Bremiller R, Wilson C, Dillon D, High S, et al.: Gonadal soma controls ovarian follicle proliferation through Gsdf in zebrafish. *Dev Dyn* 246:925–945 (2017).
- Zhu Y, Meng L, Xu W, Cui Z, Zhang N, Guo H, et al.: The autosomal Gsdf gene plays a role in male gonad development in Chinese tongue sole (*Cynoglossus semilaevis*). *Sci Rep* 8:17716 (2018).
- Chassot AA, Gregoire EP, Magliano M, Lavery R, Chaboissier MC: Genetics of ovarian differentiation: Rspo1, a major player. *Sex Dev* 2:219–227 (2008).
- Cutting A, Chue J, Smith CA: Just how conserved is vertebrate sex determination? *Dev Dyn* 242:380–387 (2013).
- Shen Z-G, Wang H-P: Molecular players involved in temperature-dependent sex determination and sex differentiation in Teleost fish. *Genet Sel Evol* 46:26 (2014).
- Herpin A, Schartl M: Plasticity of gene-regulatory networks controlling sex determination: of masters, slaves, usual suspects, newcomers, and usurpators. *EMBO Rep* 16:1260–1274 (2015).
- Fajkowska M, Ostaszewska T, Rzepkowska M: Review: Molecular mechanisms of sex differentiation in sturgeons. *Rev Aquacult* :raq.12369 (2019).
- Burcea A, Popa G-O, Florescu Gune IE, Maereanu M, Dudu A, Georgescu SE, et al.: Expression Characterization of Six Genes Possibly Involved in Gonad Development for Stellate Sturgeon Individuals (*Acipenser stellatus*, Pallas 1771). *Int J Genomics* 2018:7835637 (2018).
- Lobo IKC, Nascimento ÁR do, Yamagishi MEB, Guiguen Y, Silva GF da, Severac D, et al.: Transcriptome of tambaqui *Colossoma macropomum* during gonad differentiation: Different molecular signals leading to sex identity. *Genomics* 112:2478–2488 (2020).
- Garcia-Ortiz JE, Pelosi E, Omari S, Nedorezov T, Piao Y, Karmazin J, et al.: Foxl2 functions in sex determination and histogenesis throughout mouse ovary development. *BMC Developmental Biology* 9:36 (2009).
- Wu G-C, Chang C-F: wnt4 Is Associated with the Development of Ovarian Tissue in the Protandrous Black Porgy, *Acanthopagrus schlegeli*. *Biol Reprod* 81:1073–1082 (2009).
- Chen H, Li S, Xiao L, Zhang Y, Li G, Liu X, et al.: Wnt4 in protogynous hermaphroditic orange-spotted grouper (*Epinephelus coioides*): identification and expression. *Comp Biochem Physiol B, Biochem Mol Biol* 183:67–74 (2015).
- Zhang X, Guan G, Li M, Zhu F, Liu Q, Naruse K, et al.: Autosomal gsdf acts as a male sex initiator in the fish medaka. *Scientific Reports* 6:1–13 (2016).

Bertho S, Herpin A, Branthonne A, Jouanno E, Yano A, Nicol B, et al.: The unusual rainbow trout sex determination gene hijacked the canonical vertebrate gonadal differentiation pathway. PNAS 115:12781–12786 (2018).

Kawahara T, Yamashita I: Estrogen-Independent Ovary Formation in the Medaka Fish, *Oryzias latipes*. Zool Sci 17:65–68 (2000).

FIGURE LEGENDS

Fig. 1. Migration of *A. mexicanus* Pachón cavefish PGCs during early embryogenesis and larval development, from 50% epiboly (5-6 hpf) to 20 dpf. PGCs were labelled by GFP-zebrafish *nos1 3'UTR* mRNA injections at 1 cell stage. **A.** Lateral view of 50% epiboly stage embryo (No PGCs were clearly observed at this stage). **B.** scattered PGCs appeared at 80% epiboly stage (8-9 hpf). PGCs migration was visualized from that stage until hatching. **C.** At early neurula stage, PGCs were scattered on either side of the body axis (~10 hpf). **D.** By the beginning of somitogenesis, PGCs moved anteriorly to the mid-trunk zone (13-14 hpf). **E.** PGCs reached the mid-trunk zone and roughly aligned in lateral parts of the embryo trunk (17 hpf). **F.** PGCs reached the gonadal ridge at 1 dpf. **G-I.** At 4, 11 and 19 dpf, respectively, PGCs took position at the upper surface of the gut. **J-L.** A 2D view of the abdominal cavity sheltering the gonads at 20 dpf. Blue staining: Methyl Green nuclear staining (MG); red staining: membranes staining with DiI; Green dots: GFP-*nos1 3'UTR* positive cells (PGCs). J = merge (MG + GFP); K = merge (MG + DiI); L = merge (MG + GFP + DiI). At this stage, PGCs had colonized the gonads which appeared as thin threads. Arrowheads in **B-L** point PGCs. Rectangle in **D** shows the areas where PGCs were located. Squares in **J-K** refer to the zoom on the framed area shown in **(L)**. Gu: Gut. Scale bars for panels A-E, & J-L correspond to 100 µm and to 1 mm for panels F-I.

Fig. 2. Changes in germ cell numbers during the embryonic and larval development (**A**), and the expression patterns of *vasa* in male and female trunks from 10 to 90 dpf and differentiated gonads of 150 dpf (**B**) in Pachón cavefish, *Astyanax mexicanus*. The number of GFP- *nos1 3'UTR* positive germ cells are determined in n=21-28 individuals at different stages. The statistical significance of the differences in germ cell numbers are tested by Kruskal-wallis test followed by post hoc Pairwise Wilcoxon Rank Sum Test with Bonferroni correction for adjustment of critical *p*-values. Different letters indicate statistically significant differences between stages, respectively. For *vasa* expression, results are shown as log₁₀ mean ± Standard Errors. Statistical significances between males and females were analyzed by Wilcoxon Rank Sum Test (Wilcoxon-Mann-Whitney Test). The 1 dpf time-point (**A-B**) indicated the hatching stage. Only significant differences between males and females are provided on the figure by red stars (**P < 0.001); All other differences are non-significant (NS, P > 0.05).

Fig. 3. Histology of early male and female gonadal development stages from 16 days post-fertilization (dpf) to 45 dpf in Pachón cavefish *A. mexicanus*. Both undifferentiated testes and ovaries at 16, 23, and 30 dpf (**A-C'**) are formed mainly by elongated somatic cells (Scs) with elongated nucleus, surrounding a few larger circular and isolated germ cells (Gcs) with a large round nucleus (N) containing a prominent nucleolus. At 65 dpf, the undifferentiated male gonads (**D**) are larger due mainly to an increase of Scs, while the undifferentiated female gonads (**D'**) are larger with an increasing number of Gcs. Scale bars for panel A-D' correspond to 10 µm. Bv: Blood vessels; Mu: Muscle.

Fig. 4. Histology of differentiating male and female gonads from 65 dpf to 150 dpf in Pachón cavefish *A. mexicanus*. At 65 dpf (**A**), the undifferentiated testes increase in size but they also display an increasing number of Gcs compared to 45 dpf, while the ovaries (**A'**) are elongated, thin and show previtellogenic oocytes (PVtg Ooc) indicating the onset of the ovarian differentiation. At 90 dpf (**B**) and 150 dpf (**C**), the testes are formed by spermatogonia (SpG), spermatocytes (SpC), spermatids (SpT), and spermatozoa (SpZ). Ovaries of 90 dpf (**B'**) and 150 dpf (**C'**) are characterized by a large number of PVtg Ooc that are clearly organized in ovarian lamellae (Ol) at 150 dpf. Scale bars for panels A-A', B, and C correspond to 10 µm,

20 μm for panel B' and 50 μm for panel C'. Mu: Muscle; N: Nucleus; Nu: Nucleolus; Oog: Oogonia; Rbc: Red blood cells.

Fig. 5. Tissue-specific expression patterns of *gsdf*, *amh*, *dmrt1*, *cyp19a1a*, *foxl2a*, *wnt4b*, and *vasa* in adult male (light grey) and female (dark grey) cavefish quantified by qRT-PCR. Results are presented as boxplots with individual expression values displayed as dots, the expression median as a line and the box displaying the first and third quartiles of expression. Statistical significances for each tissue between males and females were tested with Wilcoxon Rank Test. ** = $P < 0.01$; * = $P < 0.05$. All other differences are non-significant (NS, $P > 0.05$).

Fig. 6. Expression patterns of *gsdf*, *amh*, *dmrt1*, *cyp19a1a*, *foxl2a*, *wnt4b*, and *vasa* in cavefish testes (light grey) and ovaries (dark grey) at different gametogenesis stages. Results are presented as boxplots with individual expression values displayed as dots, the expression median as a line and the box displaying the first and third quartiles of expression. Statistical significances for each stage between testis and ovaries were tested with Wilcoxon Rank Test. *** = $P < 0.01$; ** = $P < 0.01$; * = $P < 0.05$. ns = non-significant, $P > 0.05$.

Fig. 7. Expression patterns of *gsdf*, *amh*, *dmrt1*, *cyp19a1a*, *foxl2a*, and *wnt4b* in male and female trunks from 10 to 90 dpf and testes and ovaries at 150 dpf in cavefish *A. mexicanus* quantified by qRT-PCR (males: dark solid line; females: grey dashed line). Results are presented as \log_{10} mean \pm Standard Errors. Statistical significances between males and females were tested with Wilcoxon Rank Sum Test (Wilcoxon-Mann-Whitney Test). The 1 dpf time-point (**A-B**) indicated the hatching stage. Only significant differences between males and females are provided on this figure (** $P < 0.01$; * $P < 0.05$); All other differences are non-significant (NS, $P > 0.05$). Black and grey dots represent the individual values of relative expression in males and females, respectively.

Supplementary Fig. 1. Variability of the histology during gonadal development in *A. mexicanus*. This variability in gonadal development is observed at early stages i.e., 30 dpf (A-B), with mainly differences in gonad sizes between animals. At 65 dpf (C-D), the variability is more visible since some ovaries are already differentiated (C) with the presence of oogonia (Oog) and previtellogenic oocytes (PVtg Ooc), while others (D) did not show any morphological differentiation signs with gonads mainly containing somatic cells (Sc). At 90 dpf (E-F), we even found differences within the same animal with a left gonad with PVtg Ooc of different sizes (F), whereas the right gonad (E) is formed mainly by few germ cells (Gc) and surrounding Scs. Scale bars for panels A-B correspond to 20 μm and 10 μm for panel C-F. Mu: Muscle; N: Nucleus; Nu: Nucleolus.

Supplementary Table 1: Primers used for RT-qPCR analyses

Primer name: Forward (F) and Reverse (R)	Sequence	Target gene
AsmCF-ActbqPCR-2F	AAGTGTGACGTTGACATCCG	<i>Beta-actin</i>
AsmCF-ActbqPCR-2R	TCAGGAGGAGCAATGATCTTAAT	<i>Beta-actin</i>
AsmCF-rps18qPCR-1F	GTGATCCCCGAGAAGTTCCAG	<i>rps18</i>
AsmCF-rps18qPCR-1R	GGGATTTGTACTGGCGAGGA	<i>rps18</i>
AsmCF-eftud2qPCR-1F	ATCAGGATCTCGGATGGGTT	<i>eftud2</i>
AsmCF-eftud2qPCR-1R	GTGGCGCAGTTGTAGTAAGC	<i>eftud2</i>
AsmCF-ubr2qPCR-1F	TGTGCCAGTGATGAGAGAGTG	<i>ubr2</i>
AsmCF-ubr2qPCR-1R	CTGGGACACACAGTAGCGAAT	<i>ubr2</i>
AsmCF-gapdhqPCR-2F	TAAAGTCGTCAGCAATGCCTCT	<i>gapdh</i>
AsmCF-gapdhqPCR-2R	AGTGCTCATAGGCCTTCAATGA	<i>gapdh</i>
AsmCF-polr2aqPCR-2F	AGAGTTCAGTCGGCATCATCA	<i>polr2</i>
AsmCF-polr2aqPCR-2R	CATGAGACCTCCCAGCTTGG	<i>polr2</i>
AsmCF-ddx4qPCR-2F	TATTGGTCGTGGAAAGGTTGGA	<i>vasa</i>
AsmCF-ddx4qPCR-2R	ATAGGTGGCACTGAACATGAGG	<i>vasa</i>
AsmCF-gsdfqPCR-1F	ACCTTCGTCCTTCATCCGGA	<i>gsdf</i>
AsmCFSF-gsdfbqPCR-1R	GAATCATCCGGGAGCAGAC	<i>gsdf</i>
AsmCF-AmhqPCR-2F	CTACTGACAGCTGACCAGACAA	<i>amh</i>
AsmCF-AmhqPCR-2R	AGTATTGGTCCTGATGTCCCTCT	<i>amh</i>
AsmCF-dmrt1qPCR-2F	CTGTCCTGAGCTCAAAACTGGA	<i>dmrt1</i>
AsmCF-dmrt1qPCR-2R	ATAGGGTTGATGGACATGCAGG	<i>dmrt1</i>
AsmCF-foxl2aqPCR-9F	AGGCGCATGAAGAGACCATTTC	<i>foxl2a</i>
AsmCF-foxl2aqPCR-9R	TGAGCCAGAGACCAGGAGTTAT	<i>foxl2a</i>
AsmCF-cyp19a1aqPCR-12F	GCAGAAATCCAGAGGTAGAGCAG	<i>cyp19a1a</i>
AsmCF-cyp19a1aqPCR-12R	TGAAGCTCTGAGGACACAGA	<i>cyp19a1a</i>
AsmCF-Wnt4bqPCR-3F	CAAAAGGCACATCATCAGGGC	<i>wnt4b</i>
AsmCF-Wnt4bqPCR-3R	GGAGCCTGACACACCATGG	<i>wnt4b</i>

Supplementary Table 2: Coefficients of variation of gene expression

Genes	<i>gsdf</i>	<i>dmrt1</i>	<i>amh</i>	<i>cyp19a1a</i>	<i>foxl2a</i>	<i>Wnt4b</i>	<i>vasa</i>
Coefficients of variation (%)	154,5	347,12	271	235,48	107,3	115,63	242,85

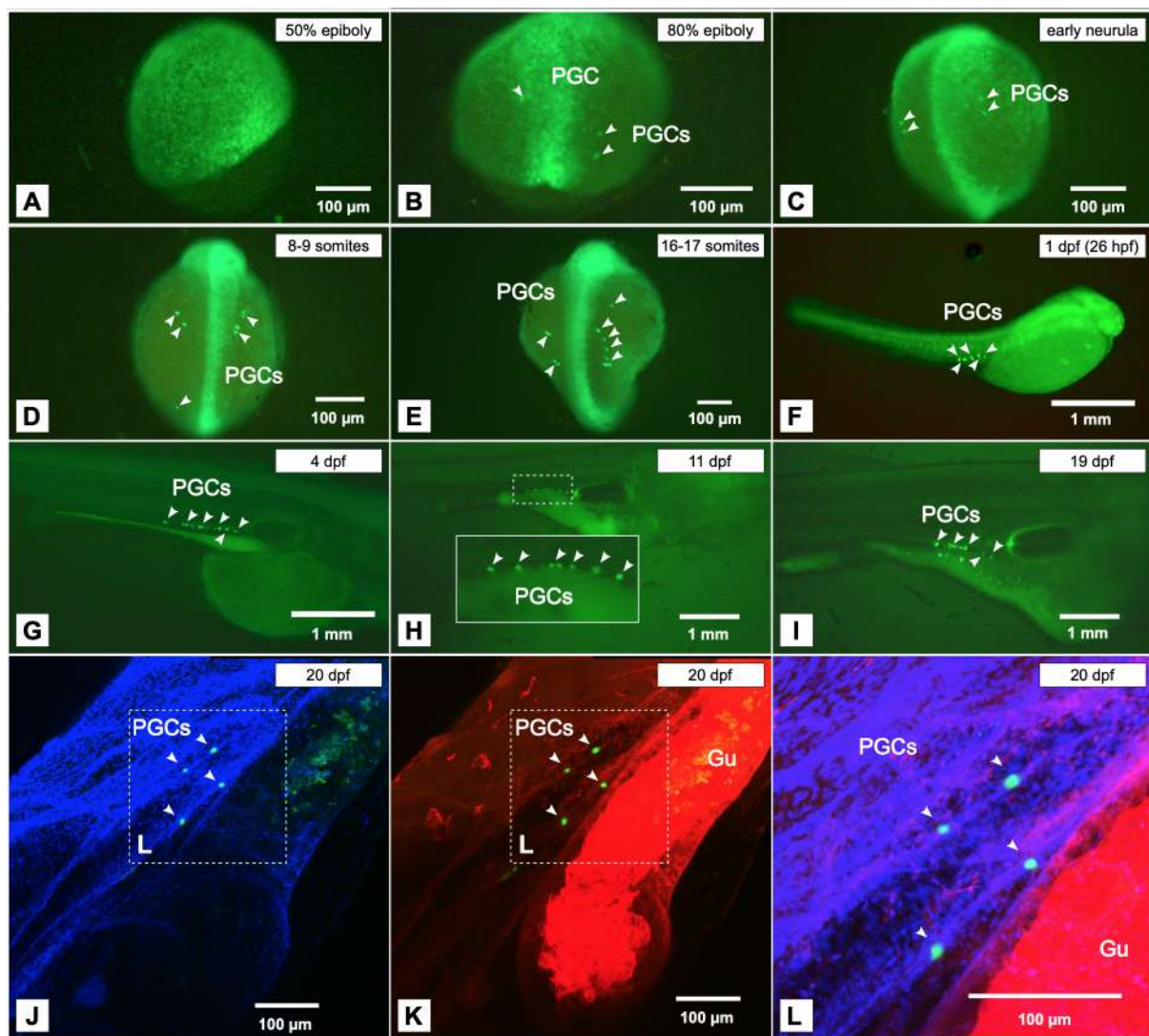


Fig. 1. Migration of *A. mexicanus* Pachón cavefish PGCs during early embryogenesis and larval development, from 50% epiboly (5-6 hpf) to 20 dpf.

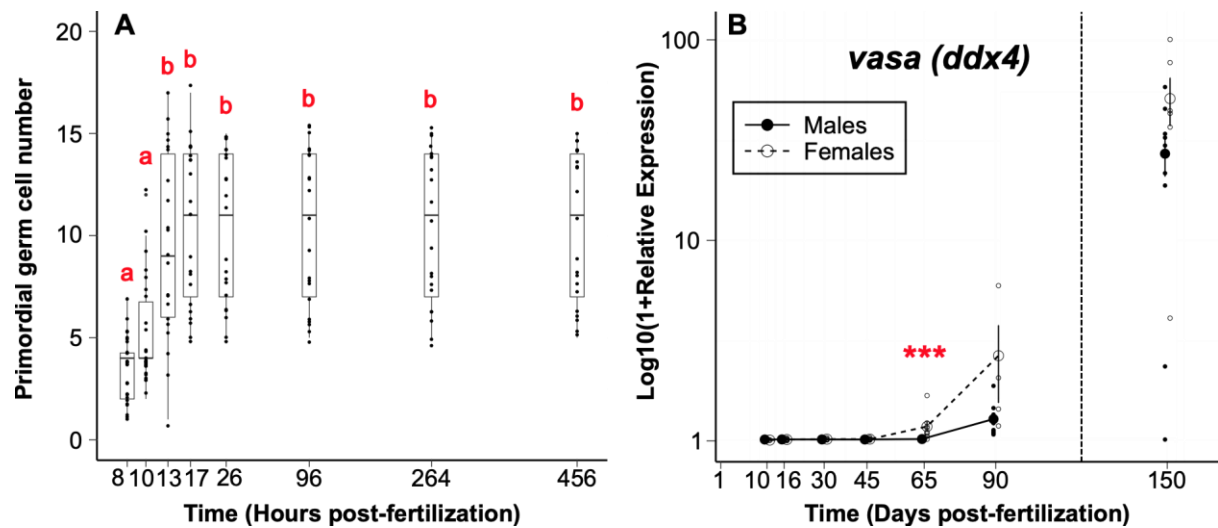


Fig. 2. Changes in germ cell numbers during the embryonic and larval development (A), and the expression patterns of *vasa* in male and female trunks from 10 to 90 dpf and differentiated gonads of 150 dpf (B) in Pachón cavefish, *Astyanax mexicanus*.

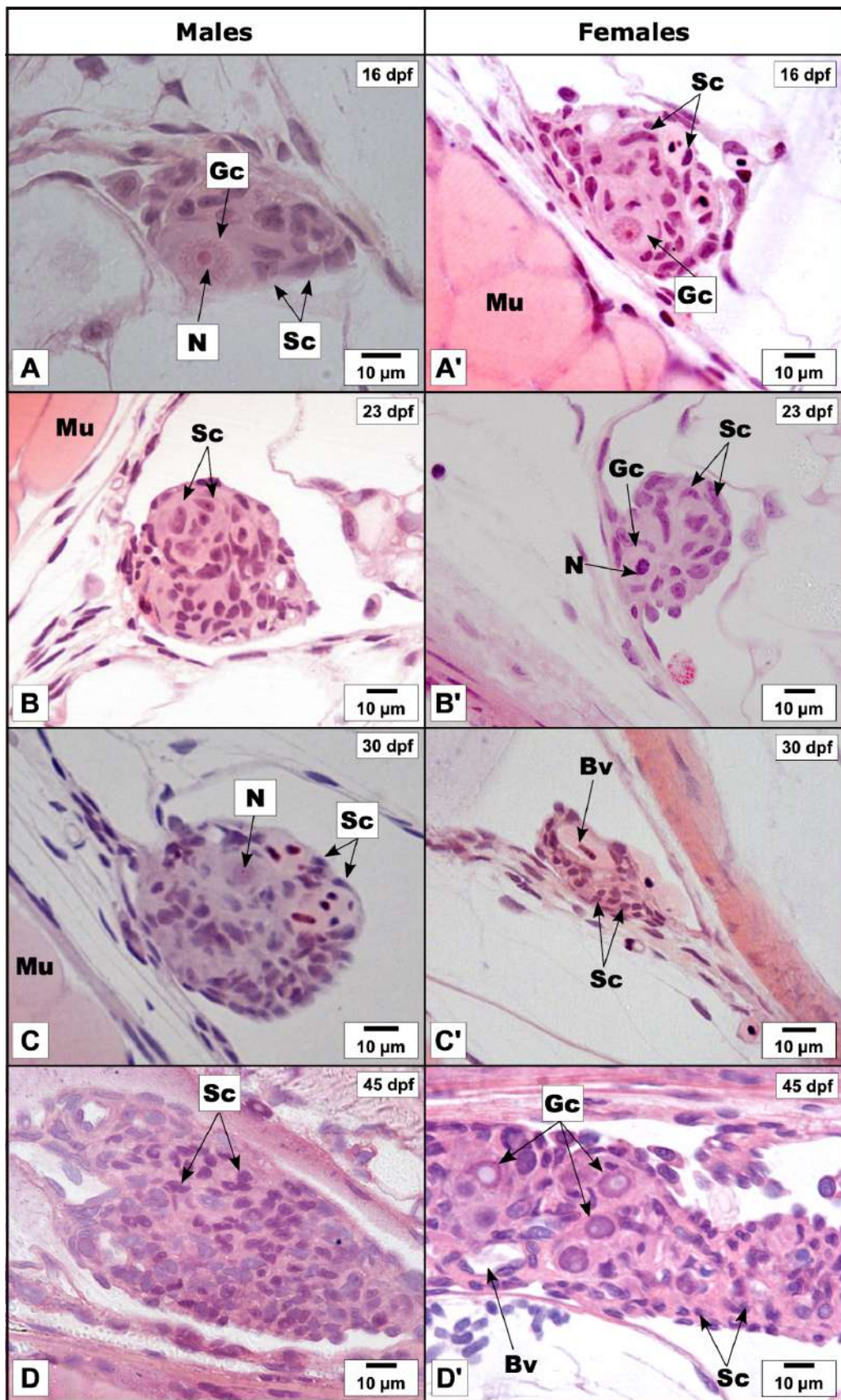


Fig. 3. Histology of early male and female gonadal development stages from 16 days post-fertilization (dpf) to 45 dpf in Pachón cavefish *A. mexicanus*.

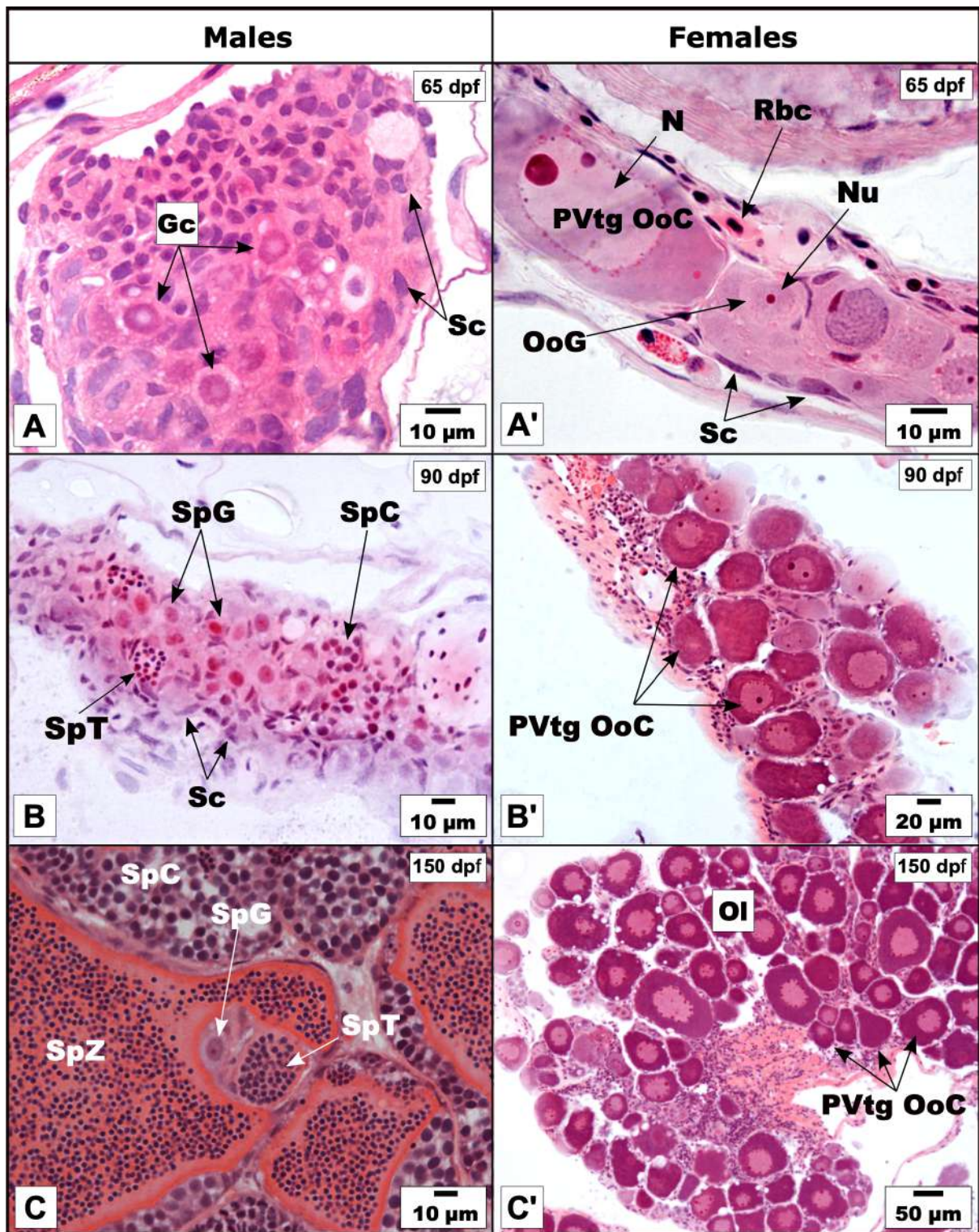


Fig. 4. Histology of differentiating male and female gonads from 65 dpf to 150 dpf in Pachón cavefish *A. mexicanus*.

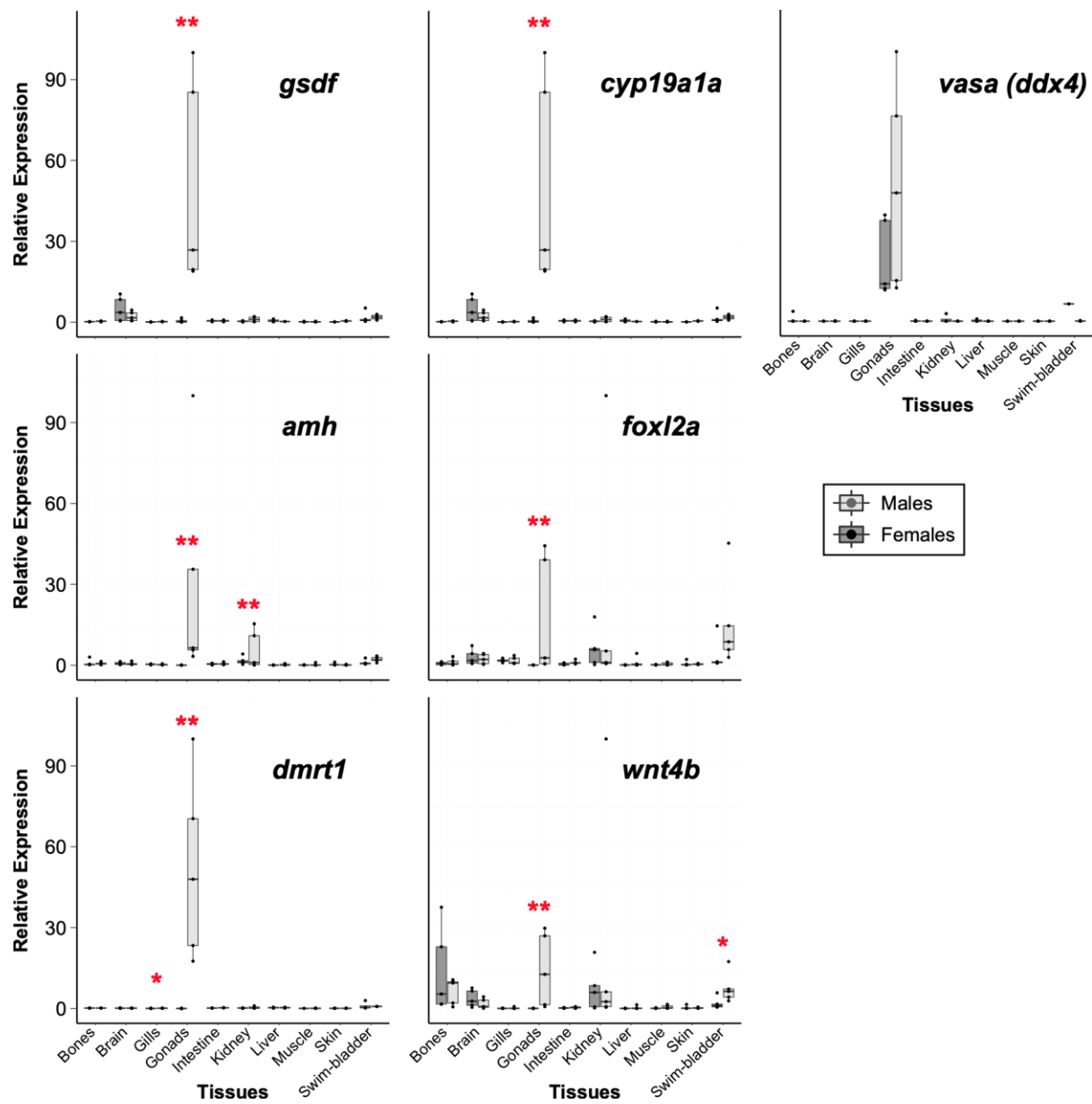


Fig. 5. Tissue-specific expression patterns of *gsdf*, *amh*, *dmrt1*, *cyp19a1a*, *foxl2a*, *wnt4b*, and *vasa* (*ddx4*) in adult male (light grey) and female (dark grey) cavefish quantified by qRT-PCR.

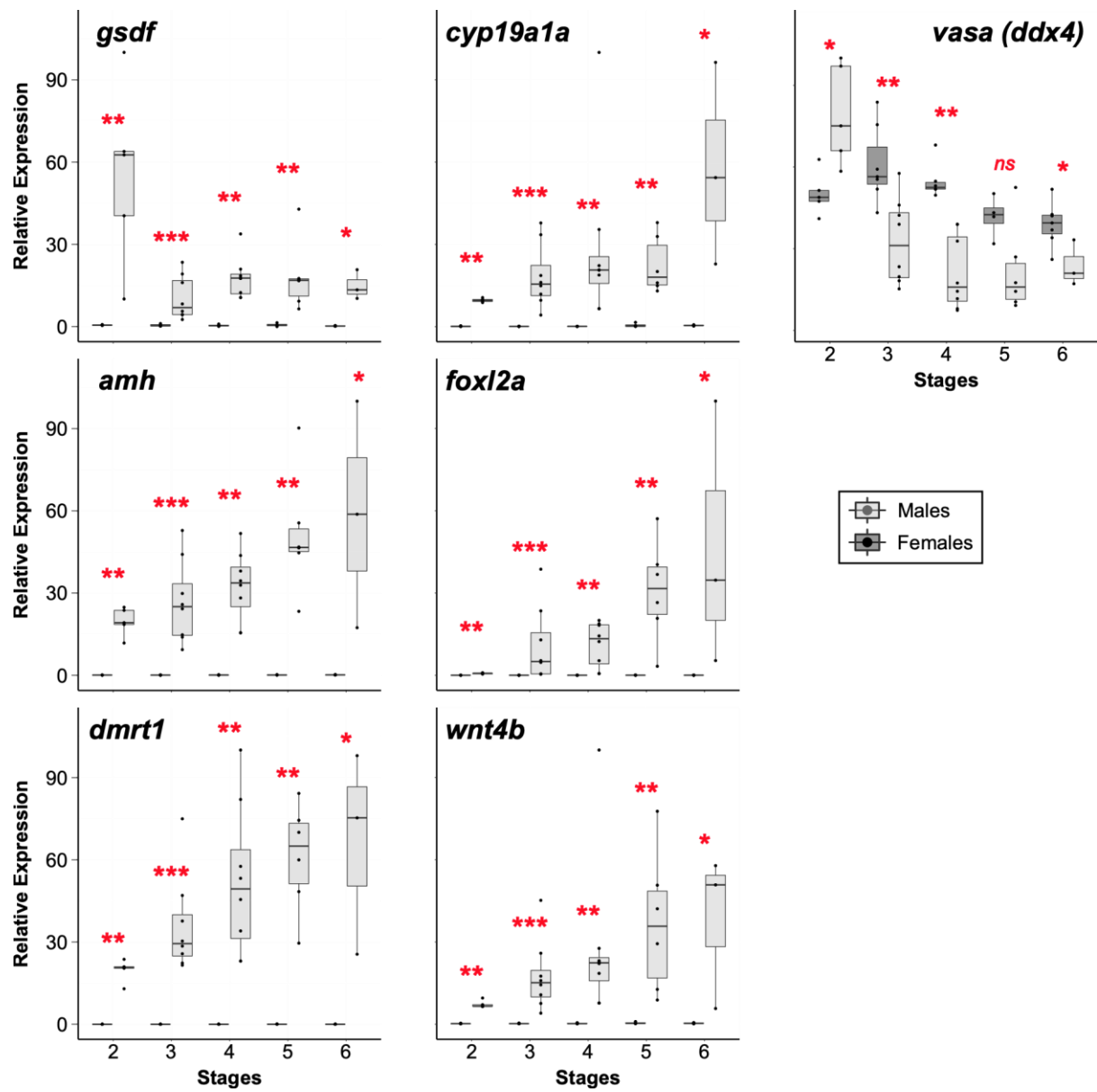


Fig. 6. Expression patterns of *gsdf*, *amh*, *dmrt1*, *cyp19a1a*, *foxl2a*, *wnt4b*, and *vasa* (*ddx4*) in cavefish testes (light grey) and ovaries (dark grey) at different gametogenesis stages.

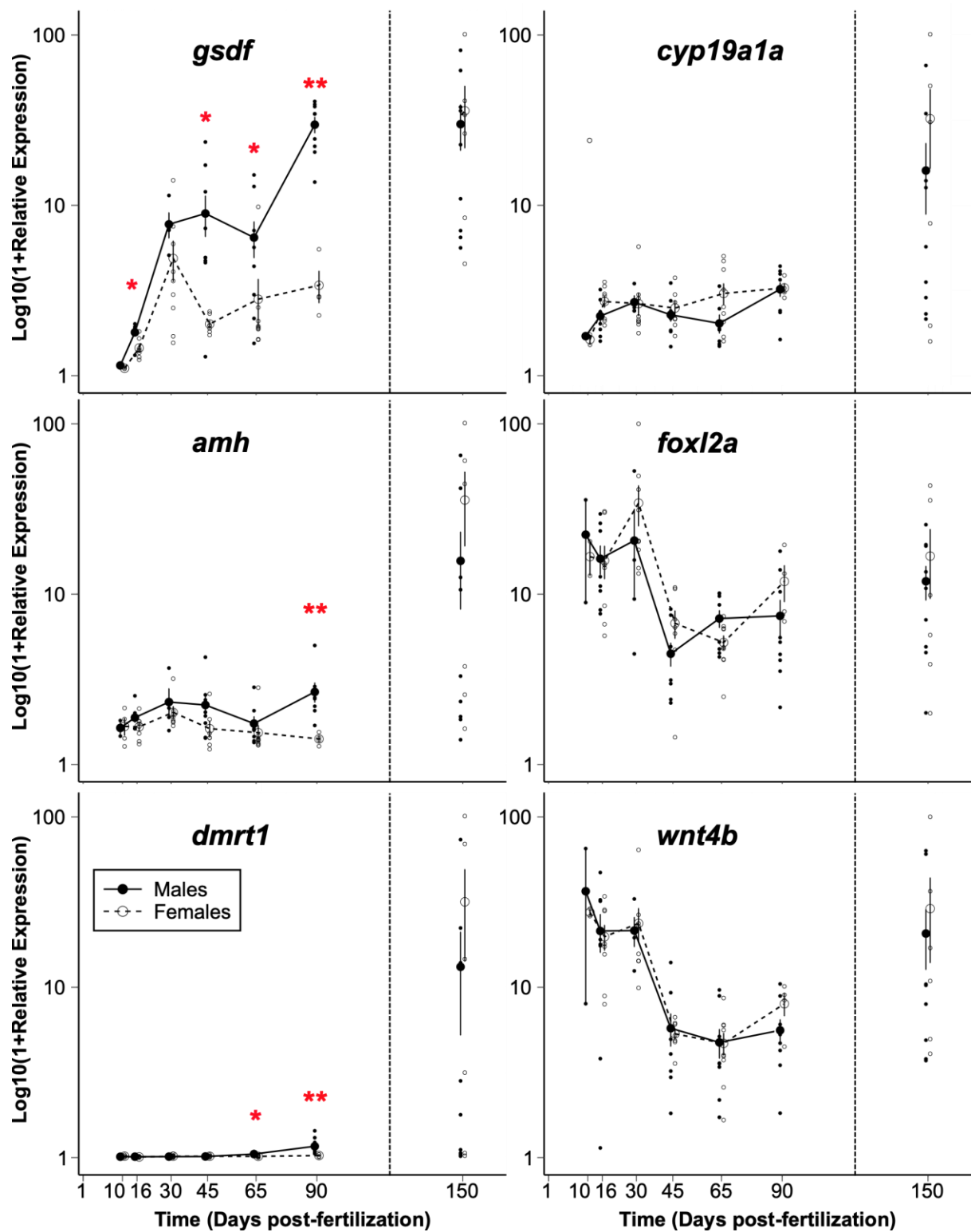
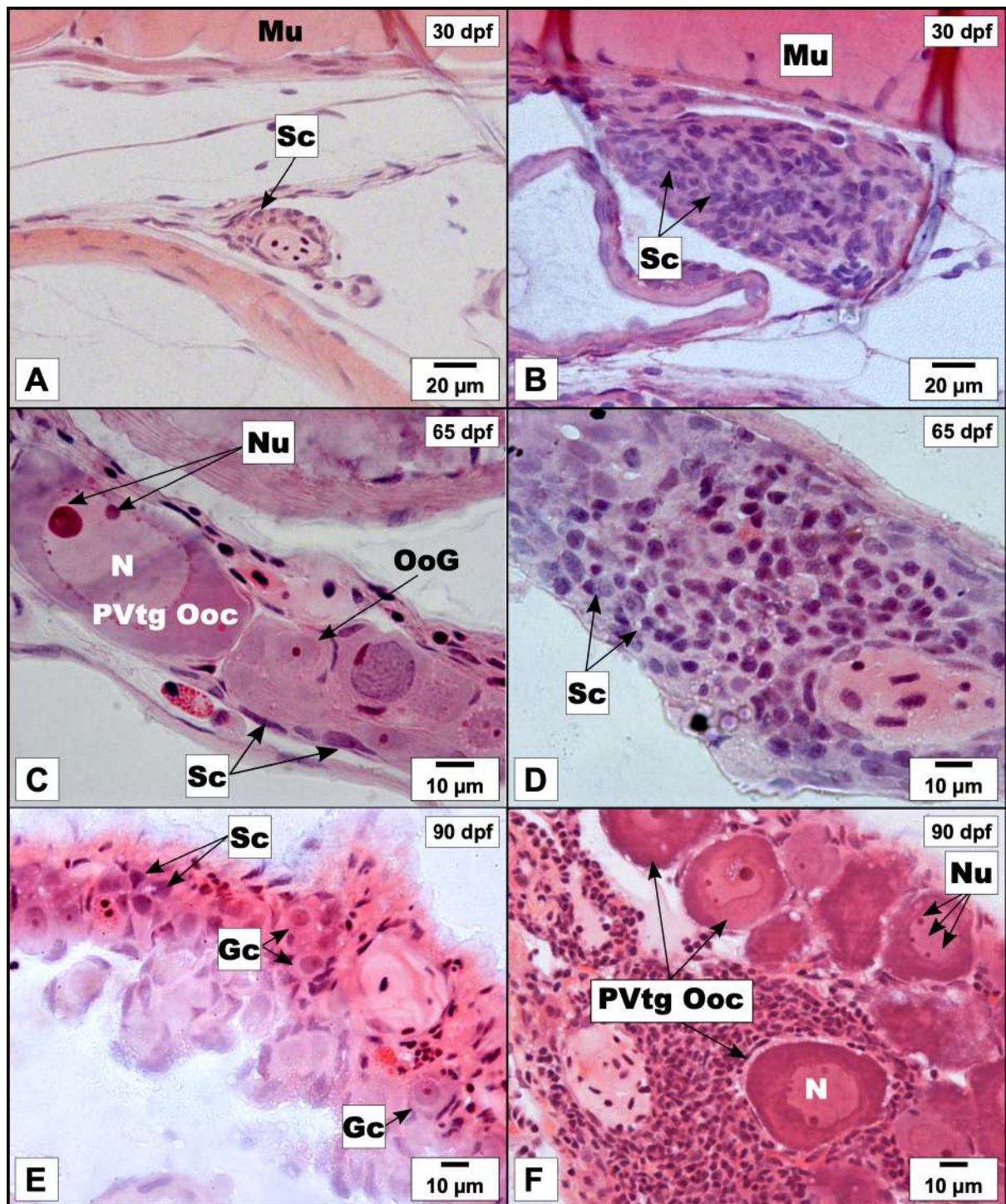


Fig. 7. Expression patterns of *gsdf*, *amh*, *dmrt1*, *cyp19a1a*, *foxl2a*, and *wnt4b* in male and female trunks from 10 to 90 dpf and testes and ovaries at 150 dpf in cavefish *A. mexicanus* quantified by qRT-PCR (males: dark solid line; females: grey dashed line).



Supplementary Fig. 1. Variability of the histology during gonadal development in *A. mexicanus*.

Publication N° 2 :

Un chromosome surnuméraire "B-sexuel" contrôle la détermination du sexe chez l'*Astyanax mexicanus* de la grotte Pachón

Objectifs

Hormis les analyses de sexe-ratios chez certaines populations cavernicoles, aucune autre donnée sur les mécanismes de détermination du sexe n'avait été publiée auparavant chez cette espèce. Cette étude avait donc pour objectif de caractériser le ou les systèmes de détermination du sexe chez la population d'*Astyanax mexicanus* de la grotte Pachón.

Contribution personnelle

J'ai d'abord exploré l'effet de la température sur la détermination du sexe (manipulation de la température). Après l'identification du gène candidat pour la détermination du sexe, j'ai confirmé sa liaison au sexe phénotypique sur tous les animaux utilisés dans cette étude dont le sexe phénotypique était précédemment identifié (histologie, design des amorces, extractions des ADNs génomiques et séquençages). Pour comprendre l'implication *gdf6b* dans la détermination du sexe, j'ai analysé ses profils d'expression durant le développement gonadique (analyse des profils d'expression par qPCR). Pour confirmer les résultats des données génomiques, j'ai réalisé des dosages TaqMan pour déterminer le nombre de copies de *gdf6b-B*. Afin de confirmer sa nécessité pour la différenciation sexuelle mâle, j'ai procédé à l'inactivation de *gdf6b* (*gdf6b-KO*) par le système CRISPR-Cas9 et analysé le phénotype et le génotype des tous les animaux afin d'établir une connexion entre phénotype et génotype. Enfin, j'ai analysé l'ensemble des résultats et rédigé ce manuscrit.

Expérimentations en cours auxquelles j'ai participé

- Génération et analyse d'une F1 de *gdf6b-KO*
- Clonage des cDNA de *gdf6b*, *gdf6a* et *vasa* pour utilisation comme sondes dans des expériences d'hybridation *in situ*
- Préparation de plusieurs constructions promoteur / cDNA surexprimant le gène *gdf6b*
- Génération et analyse des lignées transgéniques
- Analyse des profils d'expressions de *gdf6b-B* et *gdf6b-A* durant le développement par qPCR
- Annotation du chromosome B

**A supernumerary “B-sex” chromosome controls sex determination in the Pachón cave,
*Astyanax mexicanus***

Boudjema Imarazene^{1,2}, Séverine Beille¹, Elodie Jouano¹, Romain Feron¹, Céline Lopez-Roques³, Adrien Castinel³, Lisa Gil³, Claire Kuchly³, Celine Donnadieu³, Hugues Parrinello⁴, Laurent Journot⁴, Cédric Cabau⁵, Margot Zham⁵, Christophe Klopp⁵, Alexandre Sember⁶, Tomáš Pavlica^{6,7}, Ahmed Al-Rikabi⁸, Thomas Liehr⁸, Sergey Simanovsky⁹, Joerg Bohlen⁶, Julie Perez¹⁰, Frédéric Veyrunes¹⁰, John H. Postlethwait¹¹, Manfred Schartl¹², Amaury Herpin¹, Sylvie Rétaux², Yann Guiguen^{1*}

AFFILIATIONS

¹ INRAE, LPGP, 35000 Rennes, France.

² Université Paris-Saclay, CNRS, Institut des Neurosciences Paris-Saclay, 91198 Gif sur Yvette, France.

³ Getplage INRAE, US 1426, GeT-PlaGe, Genotoul, Castanet-Tolosan, France.

⁴ Institut de Génomique Fonctionnelle, IGF, CNRS, INSERM, Univ. Montpellier, F-34094 Montpellier, France.

⁵ SIGENAE, GenPhySE, Université de Toulouse, INRAE, ENVT, Castanet Tolosan, France.

⁶ Laboratory of Fish Genetics, Institute of Animal Physiology and Genetics, Czech Academy of Sciences, Rumburská 89, 277 21 Liběchov, Czech Republic.

⁷ Department of Zoology, Faculty of Science, Charles University, Viničná 7, CZ-12844, Prague, Czech Republic.

⁸ University Clinic Jena, Institute of Human Genetics, 07747 Jena, Germany.

⁹ Severtsov Institute of Ecology and Evolution, Russian Academy of Sciences, Moscow, Russia.

¹⁰ Institut des Sciences de l'Evolution de Montpellier (ISEM), Université de Montpellier, 34095 Montpellier, France.

¹¹ Institute of Neuroscience, University of Oregon, Eugene, USA.

¹² Department of Physiological Chemistry, University of Wuerzburg, Wuerzburg, Germany.

*Corresponding Author: Yann Guiguen, INRAE, Laboratoire de Physiologie et Génomique des poissons, Campus de Beaulieu, 35042 Rennes cedex, France. Tel: +33 2 99 46 58 09, E-mail: yann.guiguen@inrae.fr

Key words: Sex determination, cavefish, B chromosome, sex chromosome, *gdf6b-B*

ABSTRACT

Sex chromosomes are generally thought to be always derived from a pair of classical type A chromosomes, and relatively few alternative models have been proposed up to now. B chromosomes (Bs) are supernumerary and dispensable chromosomes found in many plant and animal species, that have often been considered as selfish genetic elements that behave as genome parasites. Strikingly the observation that in some species these Bs can be restricted or enriched only in one phenotypic sex, raised the hypothesis that they could play a role in sex determination. Here we show that the presence of B microchromosomes is clearly male-dominant in *A. mexicanus* Pachón cave, and that their B microchromosome contains two duplicated loci of the *gdf6b* potential MSD gene candidate. The *gdf6b* gene is overexpressed during gonadal development in males compared to females and its knockout induce male-to-female sex reversal showing that *gdf6b* is necessary for triggering male-sex determination in Pachón cave *A. mexicanus*. Altogether our results bring strong evidences that the *A. mexicanus* Pachón cave B microchromosome could be a “B-sex” chromosome containing duplicated copies of the *gdf6b* gene, that could act as the MSD gene controlling in sex determination in this species.

INTRODUCTION

In nearly all mammals and birds, sex determination (SD) is highly conserved and based on respectively XX/XY or ZZ/ZW monofactorial genetic SD (GSD) systems (Capel, 2017; Smith et al., 2009). These two groups also display a high degree of conservation in their master sex-determining (MSD) genes with *Sry* (sex determining region on the Y-chromosome) in almost all mammals and the Z-linked *dmrt1* (doublesex and mab-3 related transcription factor 1) in all birds explored to date (Capel, 2017; Ioannidis et al., 2020; Sinclair et al., 1990; Smith et al., 2009). In stark contrast, teleost fishes, that comprise about half of all living vertebrate species (Nelson et al., 2016), have an extremely dynamic range of SD mechanisms with monofactorial or polygenic GSD systems to environmental sex determination (ESD) including a mixture of both GSD and ESD (Bachtrog et al., 2014; Heule et al., 2014; Moore & Roberts, 2013).

Several MSD genes have been identified in fish species displaying a monofactorial GSD system and a high MSD turnover is observed, even between species of the same group. This is the case for instance in the *Oryzias*'s genus with *dmrt1bY* (DM-domain gene on the Y-chromosome, also known as *dmy*) in *Oryzias latipes* (Matsuda et al., 2002; Nanda et al., 2002), *gsdfY* (gonadal soma-derived growth factor on the Y-chromosome) in *O. luzonensis* (Myosho et al., 2012), and *sox3Y* (Sry-related high mobility group box transcription factor 3 on the Y-chromosome) in *O. dancena* (Takehana et al., 2014). With the exception of the rainbow trout MSD gene (A. Yano et al., 2012), all the other MSD genes characterized to date belong to four different gene families, namely the Sry-related HMG box (SOX), the doublesex-and mab-3-related transcription factors (DMRT), enzymes involved in steroidogenesis, and the transforming growth factor family (TGF- β) (Guiguen et al., 2018; Herpin & Schartl, 2015; Koyama et al., 2019; Pan et al., 2018; Purcell et al., 2018). This astonishing diversity of MSD genes is linked to a high turnover of sex chromosomes, which have apparently evolved independently and repeatedly (Herpin & Schartl, 2015; Kikuchi & Hamaguchi, 2013; Schartl, 2004; Volff et al., 2007). To expand our knowledge and give an enlarged picture of the evolutionary history of MSD genes and sex chromosomes, it is crucial to investigate these mechanisms in other species.

The *Astyanax* genus is one of the most diverse among the Characid group. Their phylogeny is complex and they are assumed to be a non-monophyletic group (Terán et al., 2020), probably explaining why the *Astyanax* genus presents a remarkable karyotypic and high chromosomal variability (Nishiyama et al., 2016; Oliveira et al., 2009; Salvador & Moreira-Filho, 1992), with diploid numbers ranging from $2n = 36$ to $2n = 50$ (Piscor & Parise-Maltempi, 2016).

Interestingly, many *Astyanax* species also have B supernumerary chromosomes that come in addition to the classical set of A chromosomes (As) (Mestriner et al., 2000; Pazza et al., 2018; Silva et al., 2016; Silva et al., 2017). These B supernumerary chromosomes (Bs) are found in a wide range of taxa from fungi to plants and animals, including fishes (D'Ambrosio et al., 2017; Jones, 2017). They were often considered as selfish genetic elements that behave as parasites of the genomes due to their irregular patterns of inheritance known as “drive” (Camacho et al., 2000; Jones, 1991). However, even though Bs are partially or completely heterochromatic and composed mainly of thousands of non-coding sequences such as transposable elements, ribosomal DNA and satellite DNA, it has been reported that Bs nevertheless carry transcriptionally active genic sequences (Houben et al., 2019). Hence, the occurrence of Bs in *Allium schoenoprasum* has been associated with adaptive advantages in stressful environments (Holmes & Bougourd, 1991; Plowman & Bougourd, 1994). In the *Astyanax* genus, most studies dealing with Bs have been limited to *A. scabripinnis* or *A. altiparanae*, and in *A. scabripinnis*, Bs have been found to be either more frequent (Néo et al., 2000) or exclusive to females depending on the population (Mizoguchi & Martins-Santos, 1997).

The blind cavefish *A. mexicanus*, also called Mexican tetra exists in two morphs, a river-dwelling surface morph and a cave-dwelling morph whose populations are located in the North-East of Mexico (Elliott, 2019; Espinasa et al., 2018; Mitchell et al., 1977). *A. mexicanus* has emerged during the past decade as an important model species for medical, evolutionary, developmental and genetic studies aimed at exploring many traits linked to cave adaptation (Keene et al., 2016). Consequently, many genomic resources have been generated including embryonic and larval stage transcriptomes (Hinaux et al., 2011), and whole genome sequences of different populations (Herman et al., 2018; McGaugh et al., 2014). Moreover, *A. mexicanus* can also be manipulated and raised easily in laboratory conditions and has a relatively short generation time, about 6-8 months. B chromosomes have been also described in *A. mexicanus* (Kavalco & De Almeida-Toledo, 2007; Piscor & Parise-Maltempi, 2016) and a partial association of Bs with phenotypic males has been described recently (Ahmad et al., 2020) making this species an interesting model for investigating the implication of B chromosomes on sex determination mechanisms.

To explore sex determination in *A. mexicanus*, we focused our efforts on the blind and depigmented Pachón cave laboratory population. Using different genomics approaches we demonstrated that the presence of B microchromosomes is clearly male-dominant in *A.*

mexicanus Pachón cave, and that their B microchromosome contains two duplicated loci of the *gdf6b* potential MSD gene candidate. The *gdf6b* gene is overexpressed during gonadal development in males compared to females and its knockout induce male-to-female sex reversal, showing that *gdf6b* is necessary for triggering male-sex determination in Pachón cave *A. mexicanus*. Altogether this brings strong evidences that the *A. mexicanus* Pachón cave B microchromosome is a “B-sex” chromosome containing duplicated copies of the *gdf6b* gene that could act as the MSD gene controlling in sex determination in this species.

RESULTS

Identification of an unusual GSD system in *A. mexicanus* Pachón cave

Based on the fact that some biased sex-ratios have been reported in different populations of *A. mexicanus* (Wilkens & Strecker, 2017), we first characterized the sex-ratio of a large number of fish from our Pachón cave population reared under two different temperature conditions (21°C and 28°C). The resulting sex-ratios were not significantly different from a 1:1 sex-ratio in both temperature conditions (Table 1), suggesting that our Pachón cave population has a rather strict monofactorial GSD system with no influence of temperature on sex determination, at least within the temperature range we screened.

To better characterize this GSD system, we used a pool-sequencing (pool-seq) approach (Gammerdinger et al., 2014) to contrast whole genome sequencing of a gDNA pool of 91 males versus a gDNA pool of 81 females. After remapping the pool-seq reads on the *Astyanax_mexicanus-2.0* female surface fish genome assembly (GCF_000372685.2), male versus female reads coverage differences as well as male- and female-specific SNPs were computed. This analysis identified 37 regions covering a total of 2.1 Mb with a strong male-biased pattern, i.e., “apparent” male-specific indels and heterozygous sites, and a higher reads coverage in males (Figure 1A; Table S2). Surprisingly, these 37 male-biased regions were distributed throughout the genome within twelve different linkage groups (LGs) and fifteen unplaced scaffolds (Figure 1A), conflicting with the classical hypothesis of a single contiguous sex locus on a single sex chromosome (Table S2; Figure S1). Similar results, showing multiple male-biased regions distributed throughout the genome, were also obtained after remapping on the *Astyanax_mexicanus-1.0.2* Pachón female genome assembly (GCA_004802775.1) (Figure S2).

Phenotypic sex in *A. mexicanus* Pachón cave is correlated with the presence of male-dominant B chromosomes

Knowing that acrocentric B microchromosomes have been described in *Astyanax mexicanus* (Kavalco & De Almeida-Toledo, 2007), and that some B chromosomes are made of a complex mosaic of A chromosome segments (Valente et al., 2014), we hypothesized that the multiple male-biased regions that we found to be distributed throughout the *A. mexicanus* female genome assembly could result from the presence of a male-dominant B microchromosome. We then performed cytogenetic analyses in males and females Pachón cavefish that confirmed that *A. mexicanus* has a diploid number ($2n$) of 50 A chromosomes with some supernumerary B microchromosomes as previously described (Kavalco & De Almeida-Toledo, 2007) (Figure 2). Comparison of male and female karyotypes showed that the *A. mexicanus* Pachón cave B microchromosomes are strongly male-dominant, as they were found in all males (17/17) with one (Figure 2a,b) to two B microchromosomes in most analyzed metaphases (Figure 2c,d), and even up to three B microchromosomes in a limited number of metaphases (Figure S3A; Table S4). Only very few male metaphases did not harbor this B microchromosome (Table S4). In contrast, we failed to detect any B microchromosome in most females (7/11), and when B microchromosomes were found in females (4/11), they were detected only in very few metaphases and most often as a unique B copy (Figure 2e-h; Figure S3A; Table S4). C-banding analyses revealed that the *A. mexicanus* B microchromosomes are largely euchromatic (Figure 2b,d,h). The presence of B microchromosomes was confirmed in two male testes in which we observed 25 fully synapsed standard bivalents of A chromosomes and a single unpaired B microchromosome (Figure 3). Altogether these results strongly support the idea that B microchromosomes are mostly male-dominant in Pachón cavefish and are probably composed of a complex mosaic of A chromosome segments. Such a male-dominant B microchromosome would explain our pool-seq results with multiple male-biased regions distributed throughout a female genome assembly that would not contain this B microchromosome sequence.

Identification of *gdf6b* as a potential candidate for SD gene in *A. mexicanus* Pachón cave

To characterize a MSD candidate gene, we next searched for annotated genes in these strongly male-biased regions (LGs and unplaced scaffolds). A total of 63 genes were found, including 25 truncated genes i.e., not completely included within the boundaries of the male-biased regions, and 38 genes completely included within the boundaries of the male-biased regions (Table S3). Within these 38 complete CDS genes, only one gene, encoding for growth differentiation factor 6b (*gdf6b*) on the 54,5 kb scaffold NW_019172904.1, was identified as a

likely candidate MSD gene (Tables S2; Table S3). This *gdf6b* gene is the paralogous copy of the *gdf6a* gene, as a result of the teleost whole genome duplication (Figure S4). The *gdf6a* gene has previously been described to act as the male master sex-determining trigger in the turquoise killifish (Reichwald et al., 2015). In Pachón cavefish, the precise characterization of the male and female genomic differences in this *gdf6b* locus revealed numerous differences both in the *gdf6b* proximal promoter and the *gdf6b* intron 1, including numerous “apparent” male-specific indels and male-specific heterozygous positions (Figure 1D,E). Differences within the *gdf6b* coding sequence (CDS) were limited to three “apparent” male-specific heterozygous sites located within exon 1 (T/G in males versus G/G in females at position 180 bp from the start codon) and exon 2 (C/T in males versus T/T females at 591 bp, and G/A in males versus A/A in females at 679 bp) (Figure 1E; Figure S5). Two of these “apparent” male-specific heterozygous sites were nonsynonymous (180 bp in exon 1 and 679 bp in exon 2). The G to T transversion in exon 1 (180 bp) switches a lysine into a male-specific asparagine (Lys/Asn60) and the A to G transition in exon 2 (679 bp) switches a serine into a male-specific glycine (Ser/Gly227) (Figure 1E; Figure S5). The Lys/Asn change at position 60 of the Gdf6b protein impacts a non conserved amino-acid that is highly variable across many vertebrate Gdf6 proteins (Figure 1; Figure S4; Figure S5). In contrast, the Ser/Gly change at position 227 in the “TGF- β propeptide” domain (Figure S5), impacts a highly conserved glycine that is found in the Gdf6b male-specific protein and in all vertebrate Gdf6 proteins including non-teleosts vertebrate Gdf6 and teleosts Gdf6a and Gdf6b.

Using an allele-specific PCR and primers designed on the exon 2 second “apparent” male-specific heterozygous site (697 bp of the CDS) (Figure 1E; Figure S5), we found a complete association of the G transition (A/A in females and A/G in males) in males (N=700) and a total absence of association in females (N=630) (Figure 1F). This demonstrates that the male-specific A to G transition in *gdf6b* is completely sex-linked (p-value of association with male sex phenotype = 2.2e-16), confirming pool-seq results and providing a first evidence that *gdf6b* gene could be a good candidate as a sex-determining gene in Pachón cave *Astyanax mexicanus*.

Two additional *gdf6b* loci are localized by fluorescence *in situ* hybridization on cavefish B microchromosomes

Fluorescent *in situ* hybridization (FISH) using probes generated from microdissected male B microchromosome from individuals carrying 1B and 2B, strongly painted all B microchromosomes and also revealed weaker signals on different terminal parts of some A chromosomes (Figure 4a-i), suggesting that these male-dominant B microchromosomes of *A.*

mexicanus share a number of sequences with the standard A chromosomes. This also supported the hypothesis that the multiple male-biased regions detected by pool-seq analyses could be explained by a duplication of many different segments of A chromosomes on the B microchromosome. This hypothesis was also validated by FISH using a *gdf6b* locus probe that specifically labelled two different *gdf6b* loci (Figure 4b-i) on all B microchromosomes and one locus on an A chromosome pair (Figure 4c). The copy number variation quantification of the male-specific *gdf6b* locus revealed a significantly higher number of copies in males compared to females (Figure S3B), supporting the idea that B microchromosomes are mostly male-dominant in Pachón cavefish. Altogether this suggests the existence of two *gdf6b* loci on the male-dominant B microchromosomes (*gdf6b-B*), and one *gdf6b* locus on A chromosome in both males and females (*gdf6b-A*).

Chromosome-scale genome sequencing of a male cavefish confirms the presence of two additional *gdf6b* loci on its B microchromosome

Because the two publicly available *Astyanax mexicanus* genome assemblies were made from a female individual, we sequenced a Pachón male cavefish to be able to assemble a B microchromosome. To provide a high-quality genome assembly our initial approach was a combination of Oxford Nanopore Technologies (ONT) long-reads sequencing (50 fold coverage) for genome scaffolding, 10X genomics Illumina short linked reads (160 fold coverage) for ONT assembly error correction, and a chromosome contact map (Hi-C) to generate a chromosome-scale assembly. However, because the *A. mexicanus* B microchromosome contains multiple segments of A chromosomes with only limited differentiation between the A and B duplicated sequences, this approach failed to provide a clean and high continuity B microchromosome sequence. Due to the relatively high error rate of the ONT reads, the ONT assembly had to be corrected by Illumina short reads that were not mapped accurately on their A or B duplicated loci due to their small size (2x150 bp). This ONT-based assembly, despite relatively good whole-genome assembly metrics (Table S5), was locally not accurate with a mix of A and B sequences. To overcome this problem, we produced HiFi PacBio long-reads (33 fold coverage) that were used to build an error-free long-read assembly that was integrated with Hi-C to generate a chromosome-scale assembly. This high-quality assembly (see assembly metrics and comparisons with public assemblies in Table S5) has a cumulated genome size of 1.38 Gb with a total number of 195 scaffolds, a N50 scaffold size of 52 Mb, a L50 contig number of 11 (i.e. half of the assembled genome is included in the 11 longest scaffolds that have a 52 Mb size or higher), and 25 large scaffolds that could

correspond to the 25 A chromosomes previously described in *A. mexicanus* (Kavalco & De Almeida-Toledo, 2007). Using this assembly as a reference we reanalyzed our pool-seq datasets and did not find any sex-biased regions in these 25 putative A chromosomes, with only a very low number of male- and female-specific SNPs (max per 50 kb windows = 24, compared to 340 when remapped onto the female *Astyanax mexicanus*-2.0 assembly) that can be interpreted as background noise all over the genome (Figure S6). Interestingly, only one scaffold (HiC_Scaffold_28) displays a clear sex-biased profile with a higher male reads coverage all over its 2.97 Mb sequence (Figure S7C). This sex-biased male-coverage suggests that this scaffold is the *A. mexicanus* B microchromosome assembled in a single scaffold, as no other unplaced scaffold exhibit a similar sex-biased pattern. Blast analysis of the *gdf6b* CDS on this reference genome returned three significant hits (evalue = 0), one at the beginning of large (64.8 Mb) A chromosome (HiC_scaffold_3:863919-866170) and two hits on the putative B microchromosome (HiC_scaffold_28:1253385-1255976 or *gdf6b-B* locus 1 and HiC_scaffold_28:1892181-1894772 or *gdf6b-B* locus 2) (Figure S7A). All the differences previously detected with the pool-seq analysis, between the CDS of the *gdf6b-A* and the *gdf6b-B* loci were confirmed by this genome assembly sequences, and the CDS of the two B microchromosome *gdf6b* loci are totally identical. Outside this CDS region, the two *gdf6b-B* loci share 99.9% in their overlapping parts (Figure S7B and S7C), and they both share 79.2 % of identity with the *gdf6b-A* locus. Interestingly the *gdf6b-B* locus 2 shares a longest region of identity with the *gdf6b-A* locus than with the *gdf6b-B* locus 1 (Figure S7B and S7C) and the two *gdf6b-B* loci also share a long region of identity that is not present in the *gdf6b-A* locus (Figure S7C). This could be explained by the hypothesis that the *gdf6b-B* locus 2 arose after the duplication / insertion of the *gdf6b-A* locus on the B microchromosome, and that the *gdf6b-B* locus 1 is the result of internal B duplication / insertion of a different portion of the *gdf6b-B* locus 2 (Figure S7D). Altogether this genome information brings additional evidence for the presence of two duplicated *gdf6b-B* loci in the male-dominant B microchromosomes, and shades new light on the complex origin of the mosaic B microchromosome.

The *gdf6b* gene is expressed prior to molecular differentiation in male *A. mexicanus*

During early gonadal development, differential expressions of *gdf6a* and *gdf6b* transcripts were first detected at 10 days post-fertilization (dpf) both in males and females, with *gdf6b* being strongly and significantly over-expressed in males compared to females as early as 16 dpf and from 45 to 90 dpf (Figure 5A,A'). In contrast, *gdf6a* did not show any marked difference between sexes except for a small but significant over-expression in females at 45 dpf (Figure

5A'). In adult fish, *gdf6a* and *gdf6b* were expressed in different tissues with a significantly higher expression in testes compared to ovaries (Figure 5B-C'). Altogether, these results show that *gdf6b* is highly expressed in gonads with a sexually dimorphic expression long before the first sign of histological sex differentiation and at the same time as the gonadal somatic cell derived factor gene (*gsdf*), that has been described as the earliest molecular marker expressed during gonadal sex differentiation in cavefish (Imarazene et al., 2020). This early male-predominant *gdf6b* expression is another evidence that this gene could be acting as a MSD gene in *A. mexicanus*, although we did not succeed in quantifying specifically the *gdf6b-B* and the *gdf6b-A* transcripts due to their too high sequence identities.

***gdf6b* knockout by CRISPR-Cas9 results in male to female sex reversal**

To bring functional evidence that *gdf6b* could be the master sex determining gene in *A. mexicanus*, we next generated *gdf6b* knockout (KO) cavefish by targeting two sgRNA sites on exon 2 that contains the two “apparent” male-specific heterozygous sites detected by pool-seq analysis, using the genome-editing CRISPR-Cas9 system (Figure 6A). Among the 200 first generation (G0) individuals microinjected, eighteen genetic males had a ~470 bp deletion in their *gdf6b* exon 2 (Figure 6B,E; Figure S8) and all these animals were sex reversed into phenotypic females. This large deletion includes most of the TGF- β propeptide region and the beginning of the TGF- β like domain resulting in a truncated, -likely non-functional-, Gdf6b protein (Figure S8). In contrast, all genetic males and females without any mutation, developed normal ovaries and testes (Figure 6C,D). These results show that *gdf6b* is necessary to trigger testicular development in *A. mexicanus* and bring another functional evidence that *gdf6b* could be the MSD gene in Pachón cave *A. mexicanus*.

DISCUSSION

Teleost fishes exhibit a high diversity of genetic sex determination systems and this variability is revealed by frequent changes in MSD genes as well as a high rate of sex chromosome turnovers (Herpin & Schartl, 2015; Kikuchi & Hamaguchi, 2013; Schartl, 2004; Volff et al., 2007). To date, most of the well-described fish GSD systems are monofactorial GSD systems with XX/XY or ZZ/ZW sex chromosomes (Kitano & Peichel, 2012). However, besides these usual “A-type” sex chromosomes, a few reports have suggested that accessory B chromosomes could also be instrumental in establishing the sexual phenotype, like for instance in some cichlid species where a feminizing sex determining gene has been supposed to be on a B “W”

chromosome (Clark & Kocher, 2019; Yoshida et al., 2011). Our study brings new evidences for the existence of such unusual “B-type” sex chromosomes, with the characterization of a male-dominant B-sex chromosome and its MSD in the Pachón cave *Astyanax mexicanus*.

Despite the prevalent view assuming that Bs are non-essential for the host organism, their occurrence has been associated with phenotypic sex in some species (J.P.M. Camacho et al., 2011). For instance, B chromosomes have been found to be restricted or predominantly present in females in two cichlid species, *Lithochromis rubripinnis* and *Metriaclima lombardoi* (Clark et al., 2017; Clark & Kocher, 2019; Yoshida et al., 2011) and in some characiforms species, *Metynnis lippincottianus*, and *Astyanax scabripinnis* (Favarato et al., 2019; Mizoguchi & Martins-Santos, 1997; Néo et al., 2000). B chromosomes with a male dominant pattern have been also reported in one population of *Moenkhausia sanctaefilomenae* (Camacho et al., 2011; Portela-Castro et al., 2000; Utsunomia et al., 2016) and in *A. mexicanus* in which their presence has been described only in males, but not in all males (Ahmad et al., 2020). Contrasting with this last report, our results show a rather complete association of the presence of B microchromosomes with male phenotype in the Pachón cave *A. mexicanus*, with only a few females detected with some rare B microchromosomes in some metaphase spreads. This inconsistency between Ahmad et al (Ahmad et al., 2020) and our results could be potentially explained by a different origin of the cave populations used. The exact origin of the cavefish is not described Ahmad et al (Ahmad et al., 2020) and could be subject to caution as they were obtained in local pet shops. Population differences of the frequency and sex-linkage of B chromosomes have been reported in many species (Camacho, 2005; Camacho et al., 2000; Houben, 2017; Jones, 2017). More than 30 cave-dwelling *A. mexicanus* populations have been described in northeastern Mexico (Elliott, 2019; Espinasa et al., 2018; Mitchell et al., 1977). The existence of these many, partly independently-evolved cave populations and the lack of precise information on the origin of the Ahmad and al. samples support the idea that the differences in B chromosome sex-linkage may be due to population differences in *A. mexicanus*. Of note, our laboratory population of Pachón cavefish derives from founders sampled in the Pachón cave, which have since then been bred without outcrossing of any kind, and which are indistinguishable from the wild Pachón cavefish with regards to the *Gdf6b* genotype (Imarazene et al., paper3 in preparation).

B chromosomes are thought to arise from A chromosomes (Hanlon et al., 2018; Martis et al., 2012; Ruban et al., 2020; Valente et al., 2014) and their relation with sex chromosomes has often been suspected and discussed. Different hypothesis stating either that they might be

derived from sex chromosomes or on the contrary, that they may have evolved as sex chromosomes have been put forward (Camacho et al., 2011; Pansonato-Alves et al., 2014; Serrano-Freitas et al., 2020; Vujošević et al., 2018; Zhou et al., 2012). Our FISH with B microdissected probes and whole genome analyses of the B microchromosome of *A. mexicanus* clearly revealed that Bs are composed of a complex mosaic of many A chromosome regions, as already described in other species (Ahmad et al., 2020; Martis et al., 2012; Ruban et al., 2020; Valente et al., 2014). These successive duplications / insertions events have shaped the current structure of the *A. mexicanus* B microchromosome, which contains genes with complete CDS as well as many truncated CDS that could reflect the random process of these duplications / insertions. Interestingly, we observed that some B regions can also stem from internal Bs duplications / insertions, showing in this way that their structure is probably more complex than initially thought, and that they were constructed stepwise. For the sex-linked *gdf6b-B* locus, we propose a specific scenario which includes both types of events (Figure S7D). This contribution of many A chromosome regions to the structure of *A. mexicanus* B microchromosome is in line with results from Ahmad et al that also found a large amount of transposable elements (TEs) on the *A. mexicanus* Bs (Ahmad et al., 2020). However, the 2,350 genes identified on *A. mexicanus* B chromosome in their study far exceeds the 63 genes that we identified based on our pool-seq analyses. This discrepancy could be explained by the fact that they inferred these numbers based on the whole genome sequencing of a limited number of individuals (two B+ versus two B-). As individual genome variations could be quite important this simple comparison probably provided some real B-specific sequences but also many polymorphic individual sequences that are not related to the B sequences. The large number of males and females in our pooled strategy would have erased this individual polymorphism that is not linked to sex, allowing us to better calling potential genes on the *A. mexicanus* B chromosome.

Sex chromosomes are generally thought to be derived from a pair of autosomes (Kitano et al., 2009; Ross et al., 2009), in which a single initial allele or a duplication / insertion of a potential sex determining gene will be fixed as a heterozygous variation. In general, following its “birth”, the sex chromosome region around this sex determining gene will start accumulating specific alleles, including potential sexually antagonistic alleles and also repetitive sequences (Bull, 1983; Charlesworth, 1991; Marshall Graves, 2008). However, this A-type chromosomal origin has been challenged in some species like for instance in oreochromine cichlids in which the sex megachromosome is supposed to be the result of a fusion of an autosome with a B

chromosome (Conte et al., 2020). However, up to now, no functional proof, including the characterization of a potential MSD gene, has been brought to support the idea that some B chromosomes could be considered as real sex chromosomes. Here we provide clear evidence, in the *A. mexicanus* Pachón cavefish, that the *A. mexicanus* B microchromosome is male-dominant, together with expression and knockout functional evidence supporting that the duplicated *gdf6b* genes on this B microchromosome could be a potential MSD gene. The fact that the *gdf6b*-knockout resulted in a complete gonadal sex reversal of male mutants, constitutes a strong evidence that *gdf6b* is necessary for triggering testicular differentiation in *A. mexicanus*. However, because of the high similarity of the B loci with the A locus we have not been able to specifically knockout the B copies of *gdf6b*. Further studies would then be needed to bring more functional proofs supporting the role of the *gdf6b-B* genes in Pachón cavefish *A. mexicanus* sex determination, including the specific *gdf6b-B* knockout and the overexpression of *gdf6b* by transgenesis in genetic females.

The *gdf6b* gene stemmed with its paralogous copy *gdf6a* from the teleost specific whole genome duplication (TGD) (Christoffels et al., 2004; Vandepoele et al., 2004) of an ancestral single copy *gdf6* gene. Quite interestingly, a Y-chromosome specific allele of *gdf6a* (*gdf6aY*), has been characterized as a potential MSD gene in the African turquoise killifish *Nothobranchius furzeri* (Reichwald et al., 2015). *gdf6* belongs to the BMP group of the TGF- β superfamily within which many sex determining genes have been found like the *amhY* (anti-Müllerian hormone on the Y-chromosome) in *Oreochromis niloticus* (M. Li et al., 2015), *Odontesthes hatcheri* (Hattori et al., 2012), and *Esox lucius* (Pan et al., 2019), *amhr2Y* (anti-Mullerian Hormone Receptor Type 2 on the Y-chromosome) in *Takifugu rubripes* and *Perca flavescens* (Feron et al., 2020; Kamiya et al., 2012), *bmpr1bbY* (BMP type I receptor bb on the Y chromosome) in *Clupea harengus* (Rafati et al., 2020), and *gdf6aY* (growth differentiation factor 6a on the Y-chromosome) in *N. furzeri* (Reichwald et al., 2015). This diversity of MSD TGF- β family genes highlights the key and conserved function of this pathway.

In *N. furzeri* the comparison between the X and Y alleles of *gdf6a* (*gdf6aY* and *gdf6aX*) revealed 15 amino acids substitution, and the deletion of three additional amino acids in the CDS of the Y allele. Moreover, these two alleles also differ in their 3'UTR region with a Y-specific deletion of 241 bp which potentially includes a microRNA binding site (mir-430) (Reichwald et al., 2015). In *A. mexicanus*, the B microchromosome *gdf6b* (*gdf6b-B*) and its A chromosome paralog, *gdf6b-A*, differ by only 2 amino acids substitutions in their CDS. In addition, many differences were detected in their respective promoters and intron 1 sequences,

possibly implying regulatory changes between these two paralogs. Whether these two amino acids changes could be responsible for a different function of the B chromosome Gdf6b remains to be explored. But in *Takifugu rubripes* and *Oreochromis niloticus*, point mutations in respectively *amhr2Y* and *amhY*, were described to be directly responsible for male sex determination (Kamiya et al., 2012; M. Li et al., 2015). Interestingly in the Pachón cave *A. mexicanus* one of the two nonsynonymous substitutions that we found between the two A and B chromosome genes impacts a serine in the Gdf6b-A protein that is changed into a glycine in the Gdf6b-B protein. Surprisingly the glycine of the B chromosome copy is conserved in all vertebrate Gdf6 proteins, while the serine is an unique feature of the Gdf6b-A protein, potentially suggesting that the Gdf6b-A protein could be an hypoactive protein. Additional functional explanations could be due to specific-promoter sequence variations between *gdf6b-A* and *gdf6b-B* that could result in a the lower *gdf6b* expression profile that we observed during female sex differentiation compared to males. Such a dimorphic expression was also reported in *N. furzeri* with a significantly higher expression of *gdf6aY* in male trunks at 3 days post-hatching (dph) and 7 dph during the sex differentiation period (Reichwald et al., 2015). Finally, a potential function of *gdf6b* as a potential sex determining gene maybe triggered by a sex-specific dosage, as male have an extra load of *gdf6b* genes. This *gdf6b* dosage hypothesis is interesting in the context of the *A. mexicanus* B microchromosome as our genomic and FISH analyses revealed the presence of two *gdf6b* copies on these Bs. This dosage difference would be even increased in many males in which we found multiple Bs.

Despite being male-dominant, the Pachón cave *A. mexicanus* B microchromosome is also found in some females albeit often as a single copy and only in very few metaphases. B chromosomes frequency has been described as being highly variable between species, sexes, and even in individuals of the same population and in different cells in a single individual (Camacho, 2005; Camacho et al., 2000; Houben, 2017; Jones, 2017). This is assumed to be the result of a mitotic instability of B chromosomes that can be present only in some tissues and absent from others (Bernardino et al., 2017; Schmid et al., 2002; Stevens & Bougourd, 1994). One of the species in which this instability has been well characterized is a plant from the family Poaceae, *Aegilops speltoides*. In this species, a programmed elimination mechanism of the Bs has been found specifically in the roots, while Bs are stables in all other organs' cells (Ruban et al., 2020). This programmed elimination mechanism occurs at early stages of the proto-root embryonic tissue differentiation, and results from the B chromatid nondisjunction during the anaphase, leading to the micronucleation of Bs and their subsequent degradation

(Ruban et al., 2020). The hypotheses proposed to explain this root-specific elimination are that this mechanism would prevent the expression or overexpression of root-specific genes that could have deleterious effects, or the establishment of a selection mechanism for Bs that would allow their maintenance only in other tissues (Ruban et al., 2020). Although we have no evidence supporting such a mechanism in *A. mexicanus*, we cannot exclude that the low numbers of female B chromosomes could be restricted to somatic tissues and completely eliminated from the female germline. Hence, further studies would be required for understanding such patterns.

FISH analysis with a *gdf6b* probe clearly showed that the rare female Bs also contain the *gdf6b* loci, contrasting somehow with all our PCR genotyping results that never detected any *gdf6b-B* fragment in hundreds of phenotypic females. To explain this discrepancy a hypothesis would be that these female Bs would only have truncated and non functional copies of *gdf6b*. Our results on copy number variation of *gdf6b-B* in males and females support this potential hypothesis as the average *gdf6b-B/gdf6b-A* ratio is just below 0.5 in females. This hypothesis awaits the characterization of the female B-chromosome sequence for confirmation.

Using different genomics approaches we demonstrated that the presence of B microchromosomes is clearly male-dominant in *A. mexicanus* Pachón cave, and that their B microchromosome contains two duplicated loci of the *gdf6b* potential MSD gene candidate. The *gdf6b* gene is overexpressed during gonadal development in males compared to females and its knockout induces male-to-female sex reversal, showing that *gdf6b* is necessary for triggering male-sex determination in Pachón cave *A. mexicanus*. Altogether our work brings strong evidences that the *A. mexicanus* Pachón cave B microchromosome is a “B-sex” chromosome containing duplicated copies of the *gdf6b* gene, the MSD gene candidate for controlling sex determination in this species.

MATERIAL AND METHODS

Statement of Ethics

All animal protocols were carried out in strict accordance with the French and European legislations (French decree 2013-118 and directive 2010-63-UE) applied for ethical use and care of laboratory animals used for scientific purposes. SR's and CNRS authorizations for maintaining and handling of *A. mexicanus* in experimental procedures were 91-116 and 91272105, respectively. For Karyotypic analysis, all handling of fish individuals followed

European standards in agreement with §17 of the Act No. 246/1992 coll to prevent fish suffering. The procedures involving fish were supervised by the Institutional Animal Care and Use Committee of the Institute of Animal Physiology and Genetics CAS, v.v.i., the supervisor's permit number CZ 02361 certified and issued by the Ministry of Agriculture of the Czech Republic.

Cavefish breeding and sampling

Laboratory stocks of *A. mexicanus* Pachón cave fish were obtained in 2004 from the Jeffery laboratory at the University of Maryland, College Park, MD. Fish were raised as previously described (Imarazene et al., 2020). Fertilized eggs were provided by CNRS cavefish experimental facilities (Gif sur Yvette, France) and maintained at 24°C until the hatching stage occurring around 24 ± 2 hours post-fertilization (hpf) (Hinaux et al., 2011). Subsequently, larvae were transferred and raised in the Fish Physiology and Genomics laboratory experimental facilities (LPGP, INRAE, Rennes, France) under standard photoperiod (12 h light / 12 h dark) and at two different temperatures: 21 ± 1 °C and 28 ± 1 °C. Animals were fed twice a day, firstly with live artemia (OCEAN NUTRITION) until 15 dpf, then with commercial diet (BioMar) until adult stage. For animal dissections and organ sampling, fish were euthanized with a lethal dose of tricaine methanesulfonate (MS 222, 400 mg/l), supplemented by 150 mg/l of sodium bicarbonate. Phenotypic sex of individuals was determined at 4 months and more, either by macroscopical examination of the gonads when they were enough differentiated, or by histology when gonads were not totally differentiated (Imarazene et al., 2020). Caudal fin clips were collected from all individuals and stored in ethanol 90% at 4°C before genomic DNA (gDNA) extraction. For the chromosome contact map (Hi-C), 80 µl of blood was sampled from three males using a syringe rinsed with EDTA 2%. The fresh blood was slowly freezed in a Freezing Container (Mr. Frosty, Nalgene®) after addition of 15% of dimethyl sulfoxide (DMSO). Karyotypic analyses were carried out in 17 males and 11 females of Pachón cave *Astyanax mexicanus*. Tissue samples (a narrow stripe of the tail fin) were taken from the live specimens under the effect of the anaesthetic MS-222 (Merck KGaA, Darmstadt, Germany). In case of direct preparation, fishes were euthanized using 2-phenoxyethanol (Sigma-Aldrich, St. Louis, MO, USA) before being dissected.

DNA extraction

For fish genotyping, gDNA was extracted from fin clips stored in ethanol 90%, after lysis in 5% chelex and 10 mg Proteinase K at 55°C for 2 h, followed by 10 min at 99°C (Gharbi et al.,

2006). Following extraction, samples were centrifuged and the supernatant containing the gDNA was transferred in clean tubes and stored at -20°C. For pool-sequencing and TaqMan assay, gDNA was extracted using NucleoSpin Kits for Tissue (Macherey-Nagel, Duren, Germany) according to the supplier's recommendations. For long read male genome sequencing, high molecular weight (HMW) gDNA was extracted from a mature testis grounded in liquid nitrogen and lysed in TNES-Urea buffer (TNES-Urea: 4M urea; 10 mM Tris-HCl, pH 7.5; 120 mM NaCl; 10 mM EDTA; 5% SDS) for two weeks at room temperature. For HMW gDNA extraction the TNES-Urea solution was supplemented with Proteinase K at a final concentration of 150 µg / ml and incubated at 37 °C overnight. HMW gDNA was extracted with a modified phenol-chloroform protocol as previously described (Pan et al., 2019). The gDNA concentrations for both pool-seq and genome sequencing were quantified with Qubit3 fluorometer (Invitrogen, Carlsbad, CA) and HMW gDNA quality and purity was assessed using spectrophotometry, fluorometry and capillary electrophoresis.

Primer and probe designing

All primers used in this study including PCR genotyping, qPCR gene expression, TaqMan assays, and cDNA cloning were designed using Primer3web software version 4.1.0 (Kõressaar et al., 2018) and are listed in (Table S1).

Genotyping sex-specific marker

Genetic sex of individuals was determined by a PCR test using primers designed to amplify specifically the male *gdf6b* allele based on the male-specific heterozygous site on exon 2 located at position 679 bp. The HiDi Taq DNA polymerase (myPOLS Biotec, #9201) was used for detecting a single nucleotide polymorphism. PCRs were then performed in a total volume of 50 µl containing 0.2 µM of each primer, a final concentration of 20 ng/µl gDNA, 200 µM dNTPs mixture, 1X of HiDi buffer (10X), and 2.5U/reaction of HiDi DNA polymerase. Cycling conditions were as follows: 95°C for 2 min, then 35 cycles of (95°C for 30 seconds (sec) + 60°C for 30 sec + 72°C for 1 min), and 72°C for 5 min.

10× Genomics sequencing

10X Chromium Library was prepared according to 10X Genomics protocols using the Genome Reagent Kits v2. Optimal performance has been characterized on input gDNA with a mean length greater than 50 kb (~144Kb). GEM reactions were performed on 0,625 ng of genomic DNA, and DNA molecules were partitioned and amplified into droplets to introduce a 16-bp

partition barcodes. GEM reactions were thermally cycled (30°C for 3h and 65°C for 10 min; held at 4°C) and after amplification the droplets were fractured. P5 and P7 primers, Read 2, and Sample Index were added during library construction. The library was amplified using 10 cycles of PCR and the DNA was subsequently size selected to 450 pb by performing a double purification on AMPure Xp beads. Library quality was assessed using a Fragment Analyzer and quantified by qPCR using the Kapa Library Quantification Kit. Sequencing has been performed on an Illumina HiSeq3000 using a paired-end read length of 2x150 bp with the Illumina HiSeq3000 sequencing kits.

Oxford nanopore genome sequencing

HMW gDNA purification steps were performed using AMPure XP beads (Beckman Coulter). Library preparation and sequencing was performed using Oxford Nanopore Ligation Sequencing Kit SQK-LSK109 according to manufacturer's instructions "1D gDNA selecting for long reads (SQK-LSK109)". Five µg of DNA was purified then sheared at 20 kb using the megaruptor1 system (diagenode). A one step DNA damage repair + END-repair + dA tail of double stranded DNA fragments was performed on 2µg of sample. Then adapters were ligated to the library. Library was loaded onto 1 R9.4.1 flowcell and sequenced on a PromethION instrument at 0.02 pM within 72H.

PacBio Hifi genome sequencing

Library preparation and sequencing were performed according to the manufacturer's instructions "Procedure & Checklist Preparing HiFi SMRTbell Libraries using SMRTbell Express Template Prep Kit 2.0". Fifteen µg of DNA was purified then sheared at 15 kb using the Megaruptor3 system (Diagenode). Using SMRTbell Express Template prep kit 2.0, a Single strand overhangs removal then a DNA and END damage repair step were performed on 10 µg of sample. Then blunt hairpin adapters were ligated to the library. The library was treated with an exonuclease cocktail to digest unligated DNA fragments. A size selection step using a 12 kb cutoff was performed on the BluePippin Size Selection system (Sage Science) with "0.75% DF Marker S1 3-10 kb Improved Recovery" protocol. Using Binding kit 2.0 kit and sequencing kit 2.0, the primer V2 annealed and polymerase 2.0 bounded library was sequenced by diffusion loading onto 2 SMRTcells on Sequel2 instrument at 50 pM with a 2 hours pre-extension and a 30 hours movie.

Hi-C sequencing

Hi-C data was generated using the Arima-HiC kit (Ref. 510008), according to the manufacturers protocols using 10µl of blood as starting material, the Truseq DNA PCR-Free kit and Truseq DNA UD Indexes (Illumina, ref. 20015962, ref. 20020590) and the KAPA library Amplification kit (Roche, ref. KK2620). Hi-C library was sequenced in paired end 2*150nt mode on Novaseq6000 (Illumina), using half a lane of a SP flow cell (ref. 20027464). Image analyses and base calling were performed using the Illumina NovaSeq Control Software and Real-Time Analysis component (v3.4.4). Demultiplexing was performed using Illumina's conversion software (bcl2fastq v2.20). The quality of the raw data was assessed using FastQC (v0.11.8) from the Babraham Institute and the Illumina software SAV (Sequencing Analysis Viewer). Potential contaminants were investigated with the FastQ Screen (v0.14.0) software from the Babraham Institute (Wingett & Andrews, 2018).

Genome assembly

Pacbio HiFi reads were assembled with hifiasm version 0.9 using standard parameters. The genome assembly fasta file was extracted from the principal gfa assembly graph file using an awk command line. This assembly was then scaffolded using Hi-C and 10X as a source of linking information. 10X reads were aligned using Long Ranger v2.1.1 (10x Genomics). Hi-C reads were aligned to the draft genome using Juicer (Durand, Shamim, et al., 2016) with default parameters. A candidate assembly was then generated with 3D de novo assembly (3D-DNA) pipeline (Dudchenko et al., 2017) with the -r 0 and --polisher-input-size 100000 parameters. Finally, the candidate assembly was manually reviewed using the Juicebox Assembl (Durand, Robinson, et al., 2016). Due to the specific structure of the B microchromosome, both Hi-C and 10X signals show some uncertainties in the order and orientation of the contigs. To improve the quality of the B microchromosome assembly, ONT reads were aligned to the final version of the genome using minimap2 (Li, 2018). Both reads spanning contig junctions and reads showing supplementary alignments linking contigs belonging to the B microchromosome were analyzed to resolve these ambiguities.

Male and female Pool-sequencing

DNA was collected from 91 phenotypic males and 81 phenotypic females and was pooled as male and female pools separately. Before pooling, the DNA concentration was normalized in order to obtain an equal amount of each individual genome in the final pool. Pool-sequencing libraries were prepared using the Illumina TruSeq Nano DNA HT Library Prep Kit (Illumina,

San Diego, CA) according to the manufacturer's protocol. After the fragmentation of each gDNA pool (200 ng/pool) by sonication using an M220 Focused-ultrasonicator (COVARIS), the size selection was performed using SPB beads retaining fragments of 550 bp. Following the 3' ends of blunt fragments mono-adenylation and the ligation to specific paired-end adaptors, the amplification of the construction was performed using Illumina-specific primers. Library quality was verified with a Fragment Analyzer (Advanced Analytical Technologies) and then quantified by qPCR using the Kapa Library Quantification Kit (Roche Diagnostics Corp, Indianapolis, IN). The enriched male and female pool libraries were then sequenced using a paired-end multiplexed sequencing mode on a NovaSeq S4 lane (Illumina, San Diego, CA), combining the two pools on the same lane and producing 2 × 150 nt with Illumina NovaSeq Reagent Kits according to the manufacturer's instructions. Sequencing produced 288 million paired reads and 267 million paired reads for the male and female pool libraries, respectively.

Pool-sequencing analysis

Characterization of genomic regions enriched for sex-biased signals between males and females, consisting of coverage and Single Nucleotide Polymorphism (SNP) differences was performed as described previously (Feron et al., 2020; Pan et al., 2019). *A. mexicanus* paired-end reads from male and female pool-seq pools were mapped onto publicly available or our own genome assemblies of *Astyanax mexicanus* using BWA mem version 0.7.17 (Li, 2013). The resulting BAM files were sorted and the duplicate reads due to PCR amplification during library preparation were then removed using Picard tools version 2.18.2 (<http://broadinstitute.github.io/picard>) with default parameters. Then, for each pool and each genomic position, a file containing the nucleotide composition was generated using samtools mpileup version 1.8 (Li, 2013), and popoolation2 mpileup2sync version 1201 (Kofler et al., 2011). This file was then analysed with custom software (PSASS version 2.0.0: https://zenodo.org/recor d/26159 36#.XTyIS 3s6_AI) to compute: (a) the position and density of sex-specific SNPs, defined as SNPs heterozygous in one sex but homozygous in the other, and (b) the average read depths for male and female pools along the genome to look for regions present in one sex but absent in the other (i.e., sex-specific insertions). All PSASS analyses were run with default parameters except for the range of frequency for a sex-linked SNP in the homogametic sex, --range-hom, that was set to 0.01 instead of 0.05, and the size of the sliding window, --window-size, that was set at 50,000 instead of 100,000.

Chromosome Preparation and Conventional Cytogenetics

Mitotic or meiotic chromosome spreads were obtained either from regenerating caudal fin tissue as described by (Völker & Ráb, 2015), with slight modifications (Sember et al., 2015) and altered time of fin regeneration (one week), or by direct preparation from the cephalic kidney and gonads (Ráb and Roth 1988). In the latter, the quality of chromosomal spreading was enhanced by a previously described dropping method (Bertollo et al., 2015). Chromosomes were stained with 5% Giemsa solution (pH 6.8) (Merck, Darmstadt, Germany) for conventional cytogenetic analyses, or left unstained for other methods. For fluorescence *in situ* hybridization (FISH), slides were dehydrated in an ethanol series (70%, 80% and 96%, 3 min each) and stored at -20 °C before analysis. Constitutive heterochromatin was visualized by C-banding according to (Haaf & Schmid, 1984), with chromosomes being counterstained by 4',6-diamidino-2-phenolindole (DAPI), 1.5 µg/mL in antifade (Cambio, Cambridge, United Kingdom).

gdf6b isolation and probe synthesis for FISH painting

gDNA was extracted using NucleoSpin Kits for Tissue (Macherey-Nagel, Duren, Germany) as described above. A *gdf6b* fragment comprising the two exons, the intron and 2,260 bp of the proximal promoter (with a total size of 4,368 bp) was amplified by PCR in a total volume of 50 µl. The mixture contained 0.5 µM of each primer, a final concentration of 20 ng/µl gDNA, 1X of 10X AccuPrime™ PCR Buffer II, 1U/reaction of AccuPrime™ Taq DNA Polymerase, High Fidelity (Thermofisher), was adjusted to 50 µl with autoclaved and distilled water. Cycling conditions were as follows: 94°C for 45 sec, then 35 cycles of (94°C for 15 sec + 64°C for 30 sec + 68°C for 5 min and 30 sec), and 68°C for 5 min. The resulting PCR product was cloned into TOPO TA cloning Kit XL (Thermofisher) and after sequence verification was purified using NucleoSpin plasmid DNA purification kit (Machery-Nagel, Düren, Germany) according to the supplier's indications. This *gdf6b* cloned DNA fragment was labeled by nick translation with Cy3-dUTP using Cy3 NT Labeling Kit (Jena Bioscience, Jena, Germany). The optimal fragment size of the probe (approx. 200–500 bp) was achieved after 30 min of incubation at 15 °C.

Chromosome microdissection, painting probe preparation, and labeling

Twelve copies of B chromosome from *A. mexicanum* male individual AM10 and twelve copies encompassing two B chromosomes (per cell) from a male individual AM9 (hereafter designated as AM10-1B and AM9-2B, respectively) were manually microdissected as

previously described (Al-Rikabi et al., 2020) under an inverted microscope (Zeiss Axiovert 135) using a sterile glass needle attached to a mechanical micromanipulator (Zeiss). The chromosomes were subsequently amplified by degenerate oligonucleotide primed-PCR (DOP-PCR) following (Yang et al., 2009). One μ L of the resulting amplification product was used as a template DNA for a labeling DOP-PCR reaction, with Spectrum Orange-dUTP and Spectrum Green-dUTP, for AM9-2B and AM10-1B, respectively (both Vysis, Downers Grove, USA). The amplification was done in 30 cycles, following (Yang & Graphodatsky, 2009). Depending on the experimental scheme, the final probe mixture contained i) both painting probes (200 ng each) or ii) a single painting probe (200 ng) and a labeled 4368 bp long fragment containing *gdf6b* gene and its promoter (300 ng; see below). To block the shared repetitive sequences, the probe also contained 4-5 μ g of unlabelled competitive DNA prepared from female gDNA (on male preparations) or male gDNA (on female preparations). Male and female genomic DNAs (gDNAs) were isolated from liver and spleen using MagAttract HMW DNA kit (Qiagen) and C₀t-1 DNA (i.e., fraction of gDNA enriched with highly and moderately repetitive sequences) was then generated from them according to (Zwick et al., 1997). The complete B probe mixture was dissolved in the final volume 20 μ L (in case of two painting probes) or 14 μ L (in case of one painting probe and a *gdf6b* gene probe) of hybridization mixture (50% formamide and 10% dextran sulfate in 2 \times SSC).

FISH used for WCP and combined WCP/*gdf6*-mapping experiments

The FISH experiments were done using a combination of two previously published protocols (Sember et al., 2015; C. F. Yano et al., 2017), with slight modifications. Briefly, the aging of slides took place overnight at 37 °C and then 60 min at 60 °C, followed by treatments with RNase A (200 μ g/mL in 2 \times SSC, 60–90 min, 37 °C) (Sigma-Aldrich) and then pepsin (50 μ g/mL in 10 mM HCl, 3 min, 37 °C). Subsequently, the slides were incubated in 1% formaldehyde in PBS (10 min) to stabilize the chromatin structure. Denaturation of chromosomes was done in 75% formamide in 2 \times SSC (pH 7.0) (Sigma-Aldrich) at 72 °C, for 3 min. The hybridization mixture was denatured for 8 min (86 °C) and then pre-hybridized at 37 °C for 45 min to outcompete the repetitive fraction. After application of the probe cocktail on the slide, the hybridization took place in a moist chamber at 37 °C for 72 h. Subsequently, non-specific hybridization was removed by post-hybridization washes: two times in 1 \times SSC (pH 7.0) (65 °C, 5 min each) and once in 4 \times SSC in 0,01% Tween 20 (42°C, 5 min). Slides were then washed in PBS (1 min), passed through an ethanol series and mounted in antifade containing 1.5 μ g/mL DAPI (Cambio, Cambridge, United Kingdom).

Synaptonemal complex analysis by immunostaining

Pachytene chromosome spreads from two *A. mexicanum* males (Ame 2 and Ame 4) were prepared from testes following the protocol for *Danio rerio* (Kochakpour & Moens, 2008; Kochakpour, 2009; Moens, 2006) with some modifications. Briefly, dissected testes were suspended in 200 – 600 µL (based on the cell density) of cold PBS. Cell suspensions were applied onto poly-l-lysine slides (Superfrost, with 1:30 (v/v) dilution in hypotonic solution (PBS: H₂O, 1:2 v/v). After 20 min (RT), slides were fixed with cold 2% formaldehyde (pH 8.0 – 8.5) for 3 min at RT. Slides were then washed three times in 0,1% Tween-20 (pH 8.0 – 8.5), 1 min each. Afterwards, immunofluorescence analysis of synaptonemal complexes took place, using antibodies against the proteins SYCP3 (lateral elements of synaptonemal complexes) and MLH1 (mismatch repair protein; marker for visualization recombination sites). The primary antibodies – rabbit anti-SYCP3 (1:300; Abcam, Cambridge, UK) and mouse anti-MLH1 (1:50, Abcam) – were diluted (v/v) in 3% BSA (bovine serum albumin) in 0.05% Triton X-100/ PBS. After application onto the slides, the incubation was carried out overnight in a humid chamber at 37°C. Next day, secondary antibodies, diluted (v/v) in 3% BSA (bovine serum albumin) in 0.05% Triton X-100/ PBS, were applied. Specifically, we used goat anti-rabbit Alexa 488 (1:300; Abcam) and goat anti-mouse Alexa555 (1:100; Abcam) and the slides were incubated for 3 h at 37 °C. Then, after brief washing in 0,01% Tween-20 in distilled H₂O, slides were mounted in antifade containing DAPI, as described above.

Microscopy and image analysis

At least 50 metaphase spreads per individual were analyzed to confirm the diploid chromosome number (2n), karyotype structure, and FISH results. Giemsa-stained preparations were analyzed under Axio Imager Z2 microscope (Zeiss, Oberkochen, Germany), equipped with automatic Metafer-MSearch scanning platform. Photographs of the chromosomes were captured under 100× objective using CoolCube 1 b/w digital camera (MetaSystems, Altlussheim, Germany). The karyotypes were arranged using Ikaros software (MetaSystems, Altlussheim, Germany). Chromosomes were classified according to their centromere positions according to (Levan et al., 1964), but modified as metacentric (m), submetacentric (sm), subtelocentric (st), or acrocentric (a).

FISH preparations were inspected using an Provis AX 70 epifluorescence microscope (Olympus, Tokyo, Japan), equipped with appropriate fluorescence filter set. Black-and-white images were captured under 100× objective for each fluorescent dye with a cooled DP30BW CCD camera (Olympus) using Olympus Acquisition Software. The digital images were then pseudocoloured (blue for DAPI, red for Cy3, green for FITC) and merged in DP Manager (Olympus). Composed images were then optimized and arranged using Adobe Photoshop CS6.

Expression analysis by Real- Time PCR

For gene expression studies, mRNA transcripts levels were quantified during gonadal development from 10 dpf to 150 dpf, male and female gametogenesis stages and finally in 10 adult tissues including gonads as described previously (Imarazene et al., 2020). All samples were frozen in liquid nitrogen and stored at -80°C until RNA extraction. Total RNA extraction from gonads, trunks, and adult tissues, followed by cDNA synthesis, and expression analysis by RT-PCR were carried out as previously described (Imarazene et al., 2020). Specific primers were designed for *gdf6a* and *gdf6b* in the most divergent sequence regions between the two paralogous genes.

Generation of Pachón A. mexicanus gdf6b knockout mutants

Pachón cave *A. mexicanus* inactivated for *gdf6b* were generated using the CRISPR/Cas9 method. Guide RNAs (sgRNAs) targeting two sites located in exon 2 of *gdf6b* were designed using ZiFiT software (<http://zifit.partners.org/ZiFiT/Disclaimer.aspx>). DR274 vector (Addgene #42250) containing the guide RNA universal sequence was first linearized with Bsa1, electrophoresed in a 2% agarose gel and purified. PCR amplifications were then performed using linearized DR274 as a template and two primers for each sgRNA. Forward primers containing sgRNAs target sequences (#site 1 and #site 2) (bolded and underlined) between the T7 promoter sequence in the 5' end and the conserved tracrRNA domain sequence were as follows. Forward primer (#site 1): 5'-
GAAATTAAATACGACTCACTATAGGAGTCTGAAACCGGTTCTGGTTAGAGCTA
GAAATAGCAAG-3'. Forward primer (#site 2): 5'-
GAAATTAAATACGACTCACTATAGGGAGCTGGGCTGGGACGACGTTTAGAGCT
AGAAATAGCAAG-3'. Universal Reverse primer: 5'-
AAAAGCACCGACTCGGTGCCACT-3'. Subsequently, residual plasmid was digested with Dpn1 (renewed once) at 37°C for 3 hours. The final product was purified and used as a DNA template for transcription. The sgRNAs were transcribed using the MAXIscript™ T7

Transcription Kit (Ambion) according to the manufacturer's instructions. The sgRNAs were precipitated in 200 µl of isopropanol solution at -20°C, centrifuged and the supernatant was removed. The precipitated sgRNAs were resuspended in RNase-free water. The sgRNAs were co-injected with Cas9 protein. Synthesized RNAs were then injected into 1-cell stage *A. mexicanus* Pachón cave embryos at the following concentrations: 72 ng/µL for each sgRNA and 216 ng/µL for the Cas9 protein. Genotyping was performed on gDNA from caudal fin-clips of adult fishes. CRISPR-positive fish were screened for mutations by amplifying the region surrounding the sgRNAs target sites. The genetic sex of the mutants was determined by specific primers of the *gdf6b* promoter polymorphism between male and female alleles amplifying specifically two bands in males and a single band in females (Figure 5B).

TaqMan probe assay

TaqMan probe-based qPCR was used to determine specifically the quantity of *gdf6b-B* and *gdf6b-A* using *dmrt1* as an autosomal reference gene. The specific primers and probes were listed in the (Table S1). qPCRs were carried out in a total volume of 10 µl containing 4 µl of 20 ng/µl gDNA, 10 µM of each forward and reverse primer, 10 µM of each TaqMan probe, and 5µl of 2X TaqMan® Fast Advanced Master Mix (Applied Biosystem, carlsbad, USA). We used 40 cycles of amplification on a StepOne machine (Applied Biosystem, carlsbad, USA) following cycling conditions: a first denaturation step at 50 °C for 2 min, polymerase activation at 95 °C for 2 min, 40 cycles of denaturation (95 °C for 1 sec) and annealing/extension (60 °C for 20 sec). Copy number variation was defined as *gdf6b-B/gdf6b-A* ratios after normalization with *dmrt1*.

Histology

Gonads were fixed in Bouin's fixative solution for 48 h and then dehydrated serially in aqueous 70% and 95% ethanol, ethanol/butanol (5:95), and butanol. Tissues were embedded in paraffin blocks that were cutted serially into 5 µm sections, and were stained with hematoxylin-eosin-safran (HES) (Microm Microtech, Brignais, France).

Statistical analyses

For the sex genotyping marker based on the heterozygous and specific site of the B chromosome on the exon 2 (position 679 bp of the *gdf6b-B* CDS), the correlation between this polymorphism and the male phenotypic sex is verified by the Pearson's Chi-squared test with Yates' continuity correction. For gene expression, normality of data residuals, homogeneity of variances and homoscedasticity were verified before performing parametric or non-parametric

tests. Consequently, statistical analyses were carried out only with non-parametric tests using RStudio (Open Source version) considering the level of significance at $p<0.05$. For comparisons between two groups, we used Wilcoxon signed rank test. All data are shown as Mean \pm Standard Error of the Mean (SEM).

REFERENCES

- Ahmad, S. F., Jehangir, M., Cardoso, A. L., Wolf, I. R., Margarido, V. P., Cabral-de-Mello, D. C., O'Neill, R., Valente, G. T., & Martins, C. (2020). B chromosomes of multiple species have intense evolutionary dynamics and accumulated genes related to important biological processes. *BMC Genomics*, 21(1), 656. <https://doi.org/10.1186/s12864-020-07072-1>
- Al-Rikabi, A., Leon, B. L., & Thomas, L. (2020). Glass needle-based chromosome microdissection—How to set up probes for molecular cytogenetics? *Video Journal of Clinical Research*, 2(2), 1. <https://doi.org/10.5348/100004VAM08AR2020TR>
- Bachtrog, D., Mank, J. E., Peichel, C. L., Kirkpatrick, M., Otto, S. P., Ashman, T.-L., Hahn, M. W., Kitano, J., Mayrose, I., Ming, R., Perrin, N., Ross, L., Valenzuela, N., Vamosi, J. C., & Consortium, T. T. of S. (2014). Sex Determination: Why So Many Ways of Doing It? *PLOS Biology*, 12(7), e1001899. <https://doi.org/10.1371/journal.pbio.1001899>
- Bernardino, A. C. S., Cabral-de-Mello, D. C., Machado, C. B., Palacios-Gimenez, O. M., Santos, N., & Loreto, V. (2017). B Chromosome Variants of the Grasshopper *Xyleus discoideus angulatus* Are Potentially Derived from Pericentromeric DNA. *Cytogenetic and Genome Research*, 152(4), 213-221. <https://doi.org/10.1159/000480036>
- Bertollo, L., Cioffi, M., & Moreira-Filho, O. (2015). Direct Chromosome Preparation from Freshwater Teleost Fishes (p. 21-26). <https://doi.org/10.1201/b18534-4>
- Bull, J. J. (1983). Evolution of Sex Determining Mechanisms. Benjamin/Cummings Publishing Company, Advanced Book Program.
- Camacho, J.P.M., Schmid, M., & Cabrero, J. (2011). B Chromosomes and Sex in Animals. *Sexual Development*, 5(3), 155-166. <https://doi.org/10.1159/000324930>
- Camacho, JUAN PEDRO M. (2005). CHAPTER 4—B Chromosomes. In T. R. Gregory (Ed.), *The Evolution of the Genome* (p. 223-286). Academic Press. <https://doi.org/10.1016/B978-012301463-4/50006-1>
- Camacho, Juan Pedro M., Sharbel, T. F., & Beukeboom, L. W. (2000). B-chromosome evolution. *Philosophical Transactions of the Royal Society of London. Series B: Biological Sciences*, 355(1394), 163-178. <https://doi.org/10.1098/rstb.2000.0556>
- Capel, B. (2017). Vertebrate sex determination: Evolutionary plasticity of a fundamental switch. *Nature Reviews Genetics*, 18(11), 675-689. <https://doi.org/10.1038/nrg.2017.60>
- Charlesworth, B. (1991). The evolution of sex chromosomes. *Science* (New York, N.Y.), 251(4997), 1030-1033. <https://doi.org/10.1126/science.1998119>
- Christoffels, A., Koh, E. G. L., Chia, J.-M., Brenner, S., Aparicio, S., & Venkatesh, B. (2004). Fugu genome analysis provides evidence for a whole-genome duplication early during the evolution of ray-finned fishes. *Molecular Biology and Evolution*, 21(6), 1146-1151. <https://doi.org/10.1093/molbev/msh114>
- Clark, F. E., Conte, M. A., Ferreira-Bravo, I. A., Poletto, A. B., Martins, C., & Kocher, T. D. (2017). Dynamic Sequence Evolution of a Sex-Associated B Chromosome in Lake

- Malawi Cichlid Fish. Journal of Heredity, 108(1), 53-62. <https://doi.org/10.1093/jhered/esw059>
- Clark, F. E., & Kocher, T. D. (2019). Changing sex for selfish gain: B chromosomes of Lake Malawi cichlid fish. *Scientific Reports*, 9(1), 20213. <https://doi.org/10.1038/s41598-019-55774-8>
- Conte, M., Clark, F., Roberts, R., Xu, L., Tao, W., Zhou, Q., Wang, D., & Kocher, T. (2020). Evolution of a sex megachromosome. <https://doi.org/10.1101/2020.07.02.182808>
- D'Ambrosio, U., Alonso-Lifante, M. P., Barros, K., Kovařík, A., Mas de Xaxars, G., & Garcia, S. (2017). B-chrom : A database on B-chromosomes of plants, animals and fungi. *New Phytologist*, 216(3), 635-642. <https://doi.org/10.1111/nph.14723>
- Dudchenko, O., Batra, S. S., Omer, A. D., Nyquist, S. K., Hoeger, M., Durand, N. C., Shamim, M. S., Machol, I., Lander, E. S., Aiden, A. P., & Aiden, E. L. (2017). De novo assembly of the *Aedes aegypti* genome using Hi-C yields chromosome-length scaffolds. *Science* (New York, N.Y.), 356(6333), 92-95. <https://doi.org/10.1126/science.aal3327>
- Durand, N. C., Robinson, J. T., Shamim, M. S., Machol, I., Mesirov, J. P., Lander, E. S., & Aiden, E. L. (2016). Juicebox Provides a Visualization System for Hi-C Contact Maps with Unlimited Zoom. *Cell Systems*, 3(1), 99-101. <https://doi.org/10.1016/j.cels.2015.07.012>
- Durand, N. C., Shamim, M. S., Machol, I., Rao, S. S. P., Huntley, M. H., Lander, E. S., & Aiden, E. L. (2016). Juicer Provides a One-Click System for Analyzing Loop-Resolution Hi-C Experiments. *Cell Systems*, 3(1), 95-98. <https://doi.org/10.1016/j.cels.2016.07.002>
- El-Gebali, S., Mistry, J., Bateman, A., Eddy, S. R., Luciani, A., Potter, S. C., Qureshi, M., Richardson, L. J., Salazar, G. A., Smart, A., Sonnhammer, E. L. L., Hirsh, L., Paladin, L., Piovesan, D., Tosatto, S. C. E., & Finn, R. D. (2019). The Pfam protein families database in 2019. *Nucleic Acids Research*, 47(D1), D427-D432. <https://doi.org/10.1093/nar/gky995>
- Elliott, W. R. (2019). The *Astyanax* Caves of Mexico: Cavefishes of Tamaulipas, San Luis Potosí, and Guerrero. *Journal of Fish Biology*, 94(1), 205-205. <https://doi.org/10.1111/jfb.13889>
- Espinasa, L., Legendre, L., Fumey, J., Blin, M., Rétaux, S., & Espinasa, M. (2018). A new cave locality for *Astyanax* cavefish in Sierra de El Abra, Mexico. *Subterranean Biology*, 26, 39-53. <https://doi.org/10.3897/subtbiol.26.26643>
- Favarato, R. M., Braga Ribeiro, L., Ota, R. P., Nakayama, C. M., & Feldberg, E. (2019). Cytogenetic Characterization of Two *Metynnis* Species (Characiformes, Serrasalmidae) Reveals B Chromosomes Restricted to the Females. *Cytogenetic and Genome Research*, 158(1), 38-45. <https://doi.org/10.1159/000499954>
- Feron, R., Zahm, M., Cabau, C., Klopp, C., Roques, C., Bouchez, O., Eché, C., Valière, S., Donnadieu, C., Haffray, P., Bestin, A., Morvezen, R., Acloque, H., Euclide, P. T., Wen, M., Jouano, E., Schartl, M., Postlethwait, J. H., Schraadt, C., ... Guiguen, Y. (2020). Characterization of a Y-specific duplication/insertion of the anti-Mullerian hormone type II receptor gene based on a chromosome-scale genome assembly of yellow perch, *Perca flavescens*. *Molecular Ecology Resources*, 20(2), 531-543. <https://doi.org/10.1111/1755-0998.13133>
- Frazer, K. A., Pachter, L., Poliakov, A., Rubin, E. M., & Dubchak, I. (2004). VISTA: Computational tools for comparative genomics. *Nucleic Acids Research*, 32(suppl_2), W273-W279. <https://doi.org/10.1093/nar/gkh458>
- Gammerdinger, W. J., Conte, M. A., Acquah, E. A., Roberts, R. B., & Kocher, T. D. (2014). Structure and decay of a proto-Y region in Tilapia, *Oreochromis niloticus*. *BMC*

- Genomics, 15(1), 975. <https://doi.org/10.1186/1471-2164-15-975>
- Gharbi, K., Gautier, A., Danzmann, R. G., Gharbi, S., Sakamoto, T., Hoyheim, B., Taggart, J. B., Cairney, M., Powell, R., Krieg, F., Okamoto, N., Ferguson, M. M., Holm, L. E., & Guyomard, R. (2006). A linkage map for brown trout (*Salmo trutta*): Chromosome homeologies and comparative genome organization with other salmonid fish. *Genetics*, 172, 2405-2419. <https://doi.org/10.1186/1471-2164-15-975> (doi:10.1186/1471-2164-15-975)
- Guiguen, Y., Fostier, A., & Herpin, A. (2018). Sex Determination and Differentiation in Fish. In *Sex Control in Aquaculture* (p. 35-63). John Wiley & Sons, Ltd. <https://doi.org/10.1002/9781119127291.ch2>
- Haaf, T., & Schmid, M. (1984). An early stage of ZW/ZZ sex chromosome differentiation in *Poecilia sphenops* var. *Melanistica* (Poeciliidae, Cyprinodontiformes). *Chromosoma*, 89(1), 37-41. <https://doi.org/10.1007/BF00302348>
- Hanlon, S. L., Miller, D. E., Eche, S., & Hawley, R. S. (2018). Origin, Composition, and Structure of the Supernumerary B Chromosome of *Drosophila melanogaster*. *Genetics*, 210(4), 1197-1212. <https://doi.org/10.1101/283304>
- Hattori, R. S., Murai, Y., Oura, M., Masuda, S., Majhi, S. K., Sakamoto, T., Fernandino, J. I., Somoza, G. M., Yokota, M., & Strüssmann, C. A. (2012). A Y-linked anti-Müllerian hormone duplication takes over a critical role in sex determination. *Proceedings of the National Academy of Sciences*, 109(8), 2955-2959. <https://doi.org/10.1073/pnas.1018392109>
- Herman, A., Brandvain, Y., Weagley, J., Jeffery, W. R., Keene, A. C., Kono, T. J. Y., Bilandžija, H., Borowsky, R., Espinasa, L., O'Quin, K., Ornelas-García, C. P., Yoshizawa, M., Carlson, B., Maldonado, E., Gross, J. B., Cartwright, R. A., Rohner, N., Warren, W. C., & McGaugh, S. E. (2018). The role of gene flow in rapid and repeated evolution of cave-related traits in Mexican tetra, *Astyanax mexicanus*. *Molecular Ecology*, 27(22), 4397-4416. <https://doi.org/10.1111/mec.14877>
- Herpin, A., & Schartl, M. (2015). Plasticity of gene-regulatory networks controlling sex determination: Of masters, slaves, usual suspects, newcomers, and usurpators. *EMBO Reports*, 16(10), 1260-1274. <https://doi.org/10.15252/embr.201540667>
- Heule, C., Salzburger, W., & Böhne, A. (2014). Genetics of Sexual Development: An Evolutionary Playground for Fish. *Genetics*, 196(3), 579-591. <https://doi.org/10.1101/283304>
- Hinaux, H., Pottin, K., Chalhoub, H., Père, S., Elipot, Y., Legendre, L., & Rétaux, S. (2011). A developmental staging table for *Astyanax mexicanus* surface fish and Pachón cavefish. *Zebrafish*, 8(4), 155-165. <https://doi.org/10.1089/zeb.2011.0713>
- Holmes, D. S., & Bougourd, S. M. (1991). B-chromosome selection in *Allium schoenoprasum* II. Experimental populations. *Heredity*, 67(1), 117-122. <https://doi.org/10.1038/hdy.1991.70>
- Houben, A. (2017). B Chromosomes – A Matter of Chromosome Drive. *Frontiers in Plant Science*, 08. <https://doi.org/10.3389/fpls.2017.00210>
- Houben, A., Jones, N., Martins, C., & Trifonov, V. (2019). Evolution, Composition and Regulation of Supernumerary B Chromosomes. *Genes*, 10(2). <https://doi.org/10.3390/genes10020161>
- Imarazene, B., Beille, S., Jouanno, E., Branthonne, A., Thermes, V., Thomas, M., Herpin, A., Rétaux, S., & Guiguen, Y. (2020). Primordial germ cell migration and histological and

molecular characterization of gonadal differentiation in Pachón cavefish *Astyanax mexicanus*. (Accepted in Sexual Development)

- Ioannidis, J., Taylor, G., Zhao, D., Liu, L., Idoko-Akoh, A., Gong, D., Lovell-Badge, R., Guioli, S., McGrew, M., & Clinton, M. (2020). Primary sex determination in chickens depends on DMRT1 dosage, but gonadal sex does not determine secondary sexual characteristics in adult birds. *BioRxiv*, 2020.09.18.303040. <https://doi.org/10.1101/2020.09.18.303040>
- Jones, N. (2017). New species with B chromosomes discovered since 1980. *The Nucleus*, 60(3), 263-281. <https://doi.org/10.1007/s13237-017-0215-6>
- Jones, R. N. (1991). B-Chromosome Drive. *The American Naturalist*, 137(3), 430-442. <https://doi.org/10.1086/285175>
- Kamiya, T., Kai, W., Tasumi, S., Oka, A., Matsunaga, T., Mizuno, N., Fujita, M., Suetake, H., Suzuki, S., Hosoya, S., Tohari, S., Brenner, S., Miyadai, T., Venkatesh, B., Suzuki, Y., & Kikuchi, K. (2012). A Trans-Species Missense SNP in Amhr2 Is Associated with Sex Determination in the Tiger Pufferfish, *Takifugu rubripes* (Fugu). *PLOS Genetics*, 8(7), e1002798. <https://doi.org/10.1371/journal.pgen.1002798>
- Kavalco, K. F., & De Almeida-Toledo, L. F. (2007). Molecular Cytogenetics of Blind Mexican Tetra and Comments on the Karyotypic Characteristics of Genus *Astyanax* (Teleostei, Characidae). *Zebrafish*, 4(2), 103-111. <https://doi.org/10.1089/zeb.2007.0504>
- Keene, A. C., Yoshizawa, M., & McGaugh, S. E. (2016). Biology and Evolution of the Mexican Cavefish. Elsevier. <https://doi.org/10.1016/C2014-0-01426-8>
- Kikuchi, K., & Hamaguchi, S. (2013). Novel sex-determining genes in fish and sex chromosome evolution. *Developmental Dynamics: An Official Publication of the American Association of Anatomists*, 242(4), 339-353. <https://doi.org/10.1002/dvdy.23927>
- Kitano, J., & Peichel, C. L. (2012). Turnover of sex chromosomes and speciation in fishes. *Environmental Biology of Fishes*, 94(3), 549-558. <https://doi.org/10.1007/s10641-011-9853-8>
- Kitano, J., Ross, J. A., Mori, S., Kume, M., Jones, F. C., Chan, Y. F., Absher, D. M., Grimwood, J., Schmutz, J., Myers, R. M., Kingsley, D. M., & Peichel, C. L. (2009). A role for a neo-sex chromosome in stickleback speciation. *Nature*, 461(7267), 1079-1083. <https://doi.org/10.1038/nature08441>
- Kochakpour, N., & Moens, P. B. (2008). Sex-specific crossover patterns in Zebrafish (*Danio rerio*). *Heredity*, 100(5), 489-495. <https://doi.org/10.1038/sj.hdy.6801091>
- Kochakpour, Nazafarin. (2009). Immunofluorescent Microscopic Study of Meiosis in Zebrafish. In S. Keeney (Ed.), *Meiosis: Volume 2, Cytological Methods* (p. 251-260). Humana Press. https://doi.org/10.1007/978-1-60761-103-5_15
- Kofler, R., Pandey, R. V., & Schlötterer, C. (2011). PoPoolation2: Identifying differentiation between populations using sequencing of pooled DNA samples (Pool-Seq). *Bioinformatics*, 27(24), 3435-3436. <https://doi.org/10.1093/bioinformatics/btr589>
- Kõressaar, T., Lepamets, M., Kaplinski, L., Raime, K., Andreson, R., & Remm, M. (2018). Primer3_masker: Integrating masking of template sequence with primer design software. *Bioinformatics*, 34(11), 1937-1938. <https://doi.org/10.1093/bioinformatics/bty036>
- Koyama, T., Nakamoto, M., Morishima, K., Yamashita, R., Yamashita, T., Sasaki, K., Kuruma, Y., Mizuno, N., Suzuki, M., Okada, Y., Ieda, R., Uchino, T., Tasumi, S., Hosoya, S., Uno, S., Koyama, J., Toyoda, A., Kikuchi, K., & Sakamoto, T. (2019). A SNP in a Steroidogenic Enzyme Is Associated with Phenotypic Sex in Seriola Fishes. *Current Biology*, 29(11), 1901-1909.e8. <https://doi.org/10.1016/j.cub.2019.04.069>

- Levan, A., Fredga, K., & Sandberg, A. A. (1964). Nomenclature for Centromeric Position on Chromosomes. *Hereditas*, 52(2), 201-220. <https://doi.org/10.1111/j.1601-5223.1964.tb01953.x>
- Li, H. (2013). Aligning sequence reads, clone sequences and assembly contigs with BWA-MEM. *ArXiv*, 1303.
- Li, H. (2018). Minimap2: Pairwise alignment for nucleotide sequences. *Bioinformatics* (Oxford, England), 34(18), 3094-3100. <https://doi.org/10.1093/bioinformatics/bty191>
- Li, M., Sun, Y., Zhao, J., Shi, H., Zeng, S., Ye, K., Jiang, D., Zhou, L., Sun, L., Tao, W., Nagahama, Y., Kocher, T. D., & Wang, D. (2015). A Tandem Duplicate of Anti-Müllerian Hormone with a Missense SNP on the Y Chromosome Is Essential for Male Sex Determination in Nile Tilapia, *Oreochromis niloticus*. *PLOS Genetics*, 11(11), e1005678. <https://doi.org/10.1371/journal.pgen.1005678>
- Louis, A., Muffato, M., & Roest Crolius, H. (2013). Genomicus: Five genome browsers for comparative genomics in eukaryota. *Nucleic Acids Research*, 41(D1), D700-D705. <https://doi.org/10.1093/nar/gks1156>
- Marshall Graves, J. A. (2008). Weird animal genomes and the evolution of vertebrate sex and sex chromosomes. *Annual Review of Genetics*, 42, 565-586. <https://doi.org/10.1146/annurev.genet.42.110807.091714>
- Martis, M. M., Klemme, S., Banaei-Moghaddam, A. M., Blattner, F. R., Macas, J., Schmutz, T., Scholz, U., Gundlach, H., Wicker, T., Šimková, H., Novák, P., Neumann, P., Kubaláková, M., Bauer, E., Haseneyer, G., Fuchs, J., Doležel, J., Stein, N., Mayer, K. F. X., & Houben, A. (2012). Selfish supernumerary chromosome reveals its origin as a mosaic of host genome and organellar sequences. *Proceedings of the National Academy of Sciences of the United States of America*, 109(33), 13343-13346. <https://doi.org/10.1073/pnas.1204237109>
- Matsuda, M., Nagahama, Y., Shinomiya, A., Sato, T., Matsuda, C., Kobayashi, T., Morrey, C. E., Shibata, N., Asakawa, S., Shimizu, N., Hori, H., Hamaguchi, S., & Sakaizumi, M. (2002). DMY is a Y-specific DM-domain gene required for male development in the medaka fish. *Nature*, 417(6888), 559-563. <https://doi.org/10.1038/nature751>
- McGaugh, S. E., Gross, J. B., Aken, B., Blin, M., Borowsky, R., Chalopin, D., Hinaux, H., Jeffery, W. R., Keene, A., Ma, L., Minx, P., Murphy, D., O'Quin, K. E., Rétaux, S., Rohner, N., Searle, S. M. J., Stahl, B. A., Tabin, C., Volff, J.-N., ... Warren, W. C. (2014). The cavefish genome reveals candidate genes for eye loss. *Nature Communications*, 5(1), 5307. <https://doi.org/10.1038/ncomms6307>
- Mestriner, C. A., Galetti, P. M., Valentini, S. R., Ruiz, I. R. G., Abel, L. D. S., Moreira-Filho, O., & Camacho, J. P. M. (2000). Structural and functional evidence that a B chromosome in the characid fish *Astyanax scabripinnis* is an isochromosome. *Heredity*, 85(1), 1-9. <https://doi.org/10.1046/j.1365-2540.2000.00702.x>
- Mitchell, R. W., Russell, W. H., & Elliott, W. R. (1977). Mexican eyeless characin fishes, genus *Astyanax*: Environment, distribution, and evolution. Texas Tech Press.
- Mizoguchi, S. M. H. N., & Martins-Santos, I. C. (1997). Macro- and Microchromosomes B in Females of *Astyanax scabripinnis* (Pisces, Characidae). *Hereditas*, 127(3), 249-253. <https://doi.org/10.1111/j.1601-5223.1997.00249.x>
- Moens, P. B. (2006). Zebrafish: Chiasmata and interference. *Genome*, 49(3), 205-208. <https://doi.org/10.1139/g06-021>
- Moore, E. C., & Roberts, R. B. (2013). Polygenic sex determination. *Current Biology*, 23(12), R510-R512. <https://doi.org/10.1016/j.cub.2013.04.004>
- Myoshio, T., Otake, H., Masuyama, H., Matsuda, M., Kuroki, Y., Fujiyama, A., Naruse, K., Hamaguchi, S., & Sakaizumi, M. (2012). Tracing the Emergence of a Novel Sex-

- Determining Gene in Medaka, *Oryzias luzonensis*. *Genetics*, 191(1), 163-170. <https://doi.org/10.1534/genetics.111.137497>
- Nanda, I., Kondo, M., Hornung, U., Asakawa, S., Winkler, C., Shimizu, A., Shan, Z., Haaf, T., Shimizu, N., Shima, A., Schmid, M., & Schartl, M. (2002). A duplicated copy of DMRT1 in the sex-determining region of the Y chromosome of the medaka, *Oryzias latipes*. *Proceedings of the National Academy of Sciences of the United States of America*, 99(18), 11778-11783. <https://doi.org/10.1073/pnas.182314699>
- Nelson, J. S., Grande, T. C., & Wilson, M. V. H. (2016). Phylum Chordata. In *Fishes of the World* (p. 13-526). John Wiley & Sons, Ltd. <https://doi.org/10.1002/9781119174844.ch2>
- Néo, D. M., Bertollo, L. A. C., & Filho, O. M. (2000). Morphological Differentiation and Possible Origin of B Chromosomes in Natural Brazilian Population of *Astyanax Scabripinnis* (PISCES, CHARACIDAE). *Genetica*, 108(3), 211-215. <https://doi.org/10.1023/A:1004157901097>
- Nishiyama, P. B., Vieira, M. M. R., Porto, F. E., Borin, L. A., Portela-Castro, A. L. B., & Santos, I. C. M. (2016). Karyotypic diversity among three species of the genus *Astyanax* (Characiformes: Characidae). *Brazilian Journal of Biology*, 76(2), 360-366. <https://doi.org/10.1590/1519-6984.15414>
- Oliveira, C., Foresti, F., & Hilsdorf, A. W. S. (2009). Genetics of neotropical fish: From chromosomes to populations. *Fish Physiology and Biochemistry*, 35(1), 81-100. <https://doi.org/10.1007/s10695-008-9250-1>
- Pan, Q., Feron, R., Yano, A., Guyomard, R., Jouanno, E., Vigouroux, E., Wen, M., Busnel, J.-M., Bobe, J., Concorde, J.-P., Parrinello, H., Journot, L., Klopp, C., Lluch, J., Roques, C., Postlethwait, J., Schartl, M., Herpin, A., & Guiguen, Y. (2019). Identification of the master sex determining gene in Northern pike (*Esox lucius*) reveals restricted sex chromosome differentiation. *PLOS Genetics*, 15(8), e1008013. <https://doi.org/10.1371/journal.pgen.1008013>
- Pan, Q., Guiguen, Y., & Herpin, A. (2018). Evolution of Sex Determining Genes in Fish. In M. K. Skinner (Ed.), *Encyclopedia of Reproduction* (Second Edition) (p. 168-175). Academic Press. <https://doi.org/10.1016/B978-0-12-809633-8.20552-9>
- Pansonato-Alves, J. C., Serrano, É. A., Utsunomia, R., Camacho, J. P. M., Costa Silva, G. J. da, Vicari, M. R., Artoni, R. F., Oliveira, C., & Foresti, F. (2014). Single Origin of Sex Chromosomes and Multiple Origins of B Chromosomes in Fish Genus Characidium. *PLoS ONE*, 9(9), e107169. <https://doi.org/10.1371/journal.pone.0107169>
- Parey, E., Louis, A., Cabau, C., Guiguen, Y., Crolius, H., & Berthelot, C. (2020). Synteny-Guided Resolution of Gene Trees Clarifies the Functional Impact of Whole-Genome Duplications. *Molecular biology and evolution*. <https://doi.org/10.1093/molbev/msaa149>
- Parey, E., Louis, A., Cabau, C., Guiguen, Y., Roest Crolius, H., & Berthelot, C. (s. d.). Synteny-Guided Resolution of Gene Trees Clarifies the Functional Impact of Whole-Genome Duplications. *Molecular Biology and Evolution*. <https://doi.org/10.1093/molbev/msaa149>
- Pazza, R., Dergam, J. A., & Kavalco, K. F. (2018). Trends in Karyotype Evolution in *Astyanax* (Teleostei, Characiformes, Characidae): Insights From Molecular Data. *Frontiers in Genetics*, 9, 131. <https://doi.org/10.3389/fgene.2018.00131>
- Piscor, D., & Parise-Maltempi, P. P. (2016). Chromosomal mapping of H3 histone and 5S rRNA genes in eight species of *Astyanax* (Pisces, Characiformes) with different diploid numbers: Syntenic conservation of repetitive genes. *Genome*, 59(3), 167-172. <https://doi.org/10.1139/gen-2015-0112>
- Plowman, A. B., & Bougourd, S. M. (1994). Selectively advantageous effects of B

- chromosomes on germination behaviour in *Allium schoenoprasum* L. *Heredity*, 72(6), 587-593. <https://doi.org/10.1038/hdy.1994.81>
- Portela-Castro, A. L. de B., Júnior, H. F. J., & Nishiyama, P. B. (2000). New occurrence of microchromosomes B in *Moenkhausia sanctaefilomenae* (Pisces, Characidae) from the Paraná River of Brazil: Analysis of the synaptonemal complex. *Genetica*, 110(3), 277-283. <https://doi.org/10.1023/A:1012742717240>
- Purcell, C. M., Seetharam, A. S., Snodgrass, O., Ortega-García, S., Hyde, J. R., & Severin, A. J. (2018). Insights into teleost sex determination from the *Seriola dorsalis* genome assembly. *BMC Genomics*, 19(1), 31. <https://doi.org/10.1186/s12864-017-4403-1>
- Ráb P, Roth P. (1988) Cold-blooded vertebrates. In: Balíček P, Forejt J, Rubeš J. (Eds) *Methods of Chromosome Analysis*. Czechoslovak Biological Society Publishers, Brno, 115–124.
- Rafati, N., Chen, J., Herpin, A., Pettersson, M. E., Han, F., Feng, C., Wallerman, O., Rubin, C.-J., Péron, S., Cocco, A., Larsson, M., Trötschel, C., Poetsch, A., Korschning, K., Bönigk, W., Körschen, H. G., Berg, F., Folkvord, A., Kaupp, U. B., ... Andersson, L. (2020). Reconstruction of the birth of a male sex chromosome present in Atlantic herring. *Proceedings of the National Academy of Sciences of the United States of America*, 117(39), 24359-24368. <https://doi.org/10.1073/pnas.2009925117>
- Reichwald, K., Petzold, A., Koch, P., Downie, B. R., Hartmann, N., Pietsch, S., Baumgart, M., Chalopin, D., Felder, M., Bens, M., Sahm, A., Szafranski, K., Taudien, S., Groth, M., Arisi, I., Weise, A., Bhatt, S. S., Sharma, V., Kraus, J. M., ... Platzer, M. (2015). Insights into Sex Chromosome Evolution and Aging from the Genome of a Short-Lived Fish. *Cell*, 163(6), 1527-1538. <https://doi.org/10.1016/j.cell.2015.10.071>
- Ross, J. A., Urton, J. R., Boland, J., Shapiro, M. D., & Peichel, C. L. (2009). Turnover of Sex Chromosomes in the Stickleback Fishes (Gasterosteidae). *PLoS Genetics*, 5(2). <https://doi.org/10.1371/journal.pgen.1000391>
- Ruban, A., Schmutzter, T., Wu, D. D., Fuchs, J., Boudichevskaia, A., Rubtsova, M., Pistrick, K., Melzer, M., Himmelbach, A., Schubert, V., Scholz, U., & Houben, A. (2020). Supernumerary B chromosomes of *Aegilops speltoides* undergo precise elimination in roots early in embryo development. *Nature Communications*, 11(1), 2764. <https://doi.org/10.1038/s41467-020-16594-x>
- Salvador, L. B., & Moreira-Filho, O. (1992). B chromosomes in *Astyanax scabripinnis* (Pisces, Characidae). *Heredity*, 69(1), 50-56. <https://doi.org/10.1038/hdy.1992.93>
- Schartl, M. (2004). Sex chromosome evolution in non-mammalian vertebrates. *Current Opinion in Genetics & Development*, 14(6), 634-641. <https://doi.org/10.1016/j.gde.2004.09.005>
- Schmid, M., Ziegler, C. G., Steinlein, C., Nanda, I., & Haaf, T. (2002). Chromosome banding in Amphibia. XXIV. The B chromosomes of *Gastrotheca espeletia* (Anura, Hylidae). *Cytogenetic and Genome Research*, 97(3-4), 205-218. <https://doi.org/10.1159/000066615>
- Sember, A., Bohlen, J., Šlechtová, V., Altmanová, M., Symonová, R., & Ráb, P. (2015). Karyotype differentiation in 19 species of river loach fishes (Nemacheilidae, Teleostei): Extensive variability associated with rDNA and heterochromatin distribution and its phylogenetic and ecological interpretation. *BMC Evolutionary Biology*, 15(1), 251. <https://doi.org/10.1186/s12862-015-0532-9>
- Serrano-Freitas, É. A., Silva, D. M. Z. A., Ruiz-Ruano, F. J., Utsunomia, R., Araya-Jaime, C., Oliveira, C., Camacho, J. P. M., & Foresti, F. (2020). Satellite DNA content of B chromosomes in the characid fish *Characidium gomesi* supports their origin from sex chromosomes. *Molecular Genetics and Genomics*, 295(1), 195-207. <https://doi.org/10.1007/s00438-019-01615-2>
- Silva, D. M. Z. A., Daniel, S. N., Camacho, J. P. M., Utsunomia, R., Ruiz-Ruano, F. J.,

- Penitente, M., Pansonato-Alves, J. C., Hashimoto, D. T., Oliveira, C., Porto-Foresti, F., & Foresti, F. (2016). Origin of B chromosomes in the genus *Astyanax* (Characiformes, Characidae) and the limits of chromosome painting. *Molecular Genetics and Genomics: MGG*, 291(3), 1407-1418. <https://doi.org/10.1007/s00438-016-1195-y>
- Silva, D. M. Z. de A., Utsunomia, R., Ruiz-Ruano, F. J., Daniel, S. N., Porto-Foresti, F., Hashimoto, D. T., Oliveira, C., Camacho, J. P. M., & Foresti, F. (2017). High-throughput analysis unveils a highly shared satellite DNA library among three species of fish genus *Astyanax*. *Scientific Reports*, 7(1), 12726. <https://doi.org/10.1038/s41598-017-12939-7>
- Sinclair, A. H., Berta, P., Palmer, M. S., Hawkins, J. R., Griffiths, B. L., Smith, M. J., Foster, J. W., Frischauf, A. M., Lovell-Badge, R., & Goodfellow, P. N. (1990). A gene from the human sex-determining region encodes a protein with homology to a conserved DNA-binding motif. *Nature*, 346(6281), 240-244. <https://doi.org/10.1038/346240a0>
- Smith, C. A., Roeszler, K. N., Ohnesorg, T., Cummins, D. M., Farlie, P. G., Doran, T. J., & Sinclair, A. H. (2009). The avian Z-linked gene DMRT1 is required for male sex determination in the chicken. *Nature*, 461(7261), 267-271. <https://doi.org/10.1038/nature08298>
- Stevens, J. P., & Bougourd, S. M. (1994). Unstable B-chromosomes in a European population of *Allium schoenoprasum* L. (Liliaceae). *Biological Journal of the Linnean Society*, 52(4), 357-363. <https://doi.org/10.1006/bijl.1994.1056>
- Takehana, Y., Matsuda, M., Myoshio, T., Suster, M. L., Kawakami, K., Shin-I, T., Kohara, Y., Kuroki, Y., Toyoda, A., Fujiyama, A., Hamaguchi, S., Sakaizumi, M., & Naruse, K. (2014). Co-option of Sox3 as the male-determining factor on the Y chromosome in the fish *Oryzias dancena*. *Nature Communications*, 5(1), 4157. <https://doi.org/10.1038/ncomms5157>
- Terán, G., Benítez, M., & Mirande, juan marcos. (2020). Opening the Trojan horse: Phylogeny of *Astyanax*, two new genera and resurrection of *Psalidodon* (Teleostei: Characidae). *Zoological Journal of the Linnean Society*, 1-18. <https://doi.org/10.1093/zoolinnean/zlaa019/5819054>
- Utsunomia, R., Silva, D. M. Z. de A., Ruiz-Ruano, F. J., Araya-Jaime, C., Pansonato-Alves, J. C., Scacchetti, P. C., Hashimoto, D. T., Oliveira, C., Trifonov, V. A., Porto-Foresti, F., Camacho, J. P. M., & Foresti, F. (2016). Uncovering the Ancestry of B Chromosomes in *Moenkhausia sanctaefilomenae* (Teleostei, Characidae). *PLoS One*, 11(3), e0150573. <https://doi.org/10.1371/journal.pone.0150573>
- Valente, G. T., Conte, M. A., Fantinatti, B. E. A., Cabral-de-Mello, D. C., Carvalho, R. F., Vicari, M. R., Kocher, T. D., & Martins, C. (2014). Origin and Evolution of B Chromosomes in the Cichlid Fish *Astatotilapia latifasciata* Based on Integrated Genomic Analyses. *Molecular Biology and Evolution*, 31(8), 2061-2072. <https://doi.org/10.1093/molbev/msu148>
- Vandepoele, K., De Vos, W., Taylor, J. S., Meyer, A., & Van de Peer, Y. (2004). Major events in the genome evolution of vertebrates: Paramecium age and size differ considerably between ray-finned fishes and land vertebrates. *Proceedings of the National Academy of Sciences of the United States of America*, 101(6), 1638-1643. <https://doi.org/10.1073/pnas.0307968100>
- Volff, J.-N., Nanda, I., Schmid, M., & Schartl, M. (2007). Governing Sex Determination in Fish: Regulatory Putsches and Ephemeral Dictators. *Sexual Development*, 1(2), 85-99. <https://doi.org/10.1159/000100030>
- Völker, M., & Ráb, P. (2015). Direct Chromosome Preparations from Embryos and Larvae (p. 42-48). <https://doi.org/10.1201/b18534-8>
- Vujošević, M., Rajčić, M., & Blagojević, J. (2018). B Chromosomes in Populations of

- Mammals Revisited. *Genes*, 9(10), 487. <https://doi.org/10.3390/genes9100487>
- Wilkens, H., & Strecker, U. (2017). Evolution in the Dark: Darwin's Loss Without Selection. Springer-Verlag. <https://doi.org/10.1007/978-3-662-54512-6>
- Wingett, S. W., & Andrews, S. (2018). FastQ Screen: A tool for multi-genome mapping and quality control. *F1000Research*, 7. <https://doi.org/10.12688/f1000research.15931.2>
- Yang, F., & Graphodatsky, A. S. (2009). Animal Probes and ZOO-FISH. In T. Liehr (Ed.), *Fluorescence In Situ Hybridization (FISH)—Application Guide* (p. 323-346). Springer. https://doi.org/10.1007/978-3-540-70581-9_29
- Yang, F., Trifonov, V., Ng, B. L., Kosyakova, N., & Carter, N. P. (2009). Generation of Paint Probes by Flow-Sorted and Microdissected Chromosomes. In T. Liehr (Ed.), *Fluorescence In Situ Hybridization (FISH)—Application Guide* (p. 35-52). Springer. https://doi.org/10.1007/978-3-540-70581-9_3
- Yano, A., Guyomard, R., Nicol, B., Jouanno, E., Quillet, E., Klopp, C., Cabau, C., Bouchez, O., Fostier, A., & Guiguen, Y. (2012). An immune-related gene evolved into the master sex-determining gene in rainbow trout, *Oncorhynchus mykiss*. *Current Biology: CB*, 22(15), 1423-1428. <https://doi.org/10.1016/j.cub.2012.05.045>
- Yano, C. F., Bertollo, L. a. C., Ezaz, T., Trifonov, V., Sember, A., Liehr, T., & Cioffi, M. B. (2017). Highly conserved Z and molecularly diverged W chromosomes in the fish genus *Triportheus* (Characiformes, Triportheidae). *Heredity*, 118(3), 276-283. <https://doi.org/10.1038/hdy.2016.83>
- Yoshida, K., Terai, Y., Mizoiri, S., Aibara, M., Nishihara, H., Watanabe, M., Kuroiwa, A., Hirai, H., Hirai, Y., Matsuda, Y., & Okada, N. (2011). B Chromosomes Have a Functional Effect on Female Sex Determination in Lake Victoria Cichlid Fishes. *PLoS Genetics*, 7(8), e1002203. <https://doi.org/10.1371/journal.pgen.1002203>
- Zhou, Q., Zhu, H., Huang, Q., Xuan, Z., Zhang, G., Zhao, L., Ding, Y., Roy, S., Vicoso, B., Ruan, J., Zhang, Y., Zhao, R., Mu, B., Min, J., Zhang, Q., Li, J., Luo, Y., Liang, Z., Ye, C., ... Bachtrog, D. (2012). Deciphering neo-sex and B chromosome evolution by the draft genome of *Drosophila albomicans*. *BMC Genomics*, 13(1), 109. <https://doi.org/10.1186/1471-2164-13-109>
- Zwick, M. S., Hanson, R. E., Islam-Faridi, M. N., Stelly, D. M., Wing, R. A., Price, H. J., & McKnight, T. D. (1997). A rapid procedure for the isolation of C0t-1 DNA from plants. *Genome*, 40(1), 138-142. <https://doi.org/10.1139/g97-020>

FIGURE LEGENDS

Figure 1. Genomic analysis of sex determination in Pachón cave *Astyanax mexicanus*. **(A)** Circular plot representation of the pool-seq analysis on the Astyanax_mexicanus-2.0 female genome assembly (GCF_000372685.2), showing multiple sex-biased regions (black arrows) in different linkage groups (LGs) and unplaced scaffolds. Differences between males and females, i.e., “apparent” indels and heterozygous sites, and read coverage differences were counted in a 50 kb sliding window with an output point every 500 bp. The number of each LG is indicated and all unplaced scaffolds are fused together. Outer to inner tracks show respectively: the number of “apparent” male-specific SNPs (blue), the number of “apparent” female-specific SNPs (red), and the read coverage ratio (log2 of the male versus female read depth). **(B-B' and C-C')** Zoomed views of the LG05 and LG09 with combined “apparent” female- (in red) and male- (in blue) specific SNPs and the coverage ratio between males and females. **(D)** Integrative genomics viewer (IGV) visualization of the male and female pooled-reads around the *gdf6b* locus (3,800 bp), showing a much higher coverage in the male pool compared to the female pool and many “apparent” male-specific heterozygous sites (Het) and male-specific indels (MsI). **(E)** Schematic representation of the structure of the *gdf6b* gene containing 2,108 bp downstream from the first ATG on exon1 to the codon stop on exon 2 and 2,388 bp of the upstream proximal promoter. Blue and red boxes respectively indicated male-specific gaps and indels (MsI) on the proximal *gdf6b* promoter with their corresponding sizes. Dark lines indicated the “apparent” male-specific heterozygous sites on the *gdf6b* coding region (CDS) and its proximal promoter. Male-specific nonsynonymous and synonymous “apparent” heterozygous sites are shown respectively by green and black triangles on the *gdf6b* CDS. Each of the three “apparent” heterozygous sites in the *gdf6b* CDS is magnified to show their representative chromatogram sequences in males and females and the corresponding amino acid changes. **(F)** Representative examples of the Pachón cave *A. mexicanus* sex genotyping test, that is based on an allele-specific PCR at the “apparent” heterozygous (Het) site highlighted by red star on panel C. Males (N=7) display a 200 bp *gdf6b* PCR amplification with no PCR amplification in females (N=7). **(G)** This sex genotyping test has been used on 1,330 Pachón cave individuals demonstrating a complete sex-linkage in males.

Figure 2. Karyotypes and C-banded mitotic metaphases of Pachón cave *Astyanax mexicanus*, with different male and female B microchromosome constitution. Representative male and

female Pachón cave karyotypes arranged from Giemsa-stained mitotic chromosomes (**a, c, e, g**) and their corresponding C-banding patterns (**b, d, f, h**). B chromosome (B) numbers were found to be variable among individuals (from 0 to 2 Bs on these examples) with all males having a single (**a, b**) or multiple Bs (**c, d**) in most of their metaphases, most females having no B (**e, f**), and only a few females having rare B positive metaphases (**g, h**). Notice also the lack of C-bands on B chromosome(s). Scale bar = 10 μm .

Figure 3. Synaptonemal complex analysis reveals that Pachón cave B microchromosomes do not pair with A chromosomes. Synaptonemal complex (SC) analyses reveal 25 fully synapsed standard bivalents of A chromosomes and a single unpaired B microchromosome (arrow). SC were visualized by anti-SYCP3 antibody (green) and the recombination sites were identified by anti-MLH1 antibody (red). Chromosomes were counterstained by DAPI (blue). (**a,b**) male individual AME 2; (**c,d**) male individual AME 4. Merged image (**a,c**) and SYCP3 (**b,d**) visualization only. Scale bar = 10 μm .

Figure 4. Male and female Pachón cave *Astyanax mexicanus* mitotic metaphases after fluorescent in situ hybridization (FISH) with *gdf6b*- and B chromosome-derived probes. (**a**) FISH of mitotic metaphases labelled with a B microchromosome (B) probe microdissected from a 1B male (AM10 probe in green) and a 2Bs male (AM9 probe in red). (**b-i**) FISH co-labelling of mitotic metaphases with the AM10-1B probe (green) and a *gdf6b*-specific probe (red; arrowheads). B chromosomes are indicated by arrows. (**b-c**) Male AME 10; B chromosome from yet another metaphase is framed (**b**), merged signals on the left and individual channels on the right. Either one (**b**) or the two (**c**) pairs of A chromosome sister chromatids are labelled by the *gdf6b* probe and that two *gdf6b* loci are detected on the B microchromosome. (**d-g**) Female AME 8 with either none (**d**), one (**e**) or even two (**f,g**) B microchromosomes. (**f,g**) right inset - B microchromosome with two *gdf6b* signals; left inset – B chromosome lacking *gdf6b* signals. Chromosomes were counterstained by DAPI (blue). Scale bar = 10 μm .

Figure 5. Expression patterns of *gdf6b* and *gdf6a* in Pachón cave *Astyanax mexicanus*. (**A,A'**) Expression profiles of *gdf6b* and *gdf6a* in male and female trunks during early development from 10 to 90 dpf and in testes and ovaries at 150 dpf (males: black solid line; females: grey dashed line). Results are presented as \log_{10} mean \pm standard errors; black and grey dots represent the individual values of relative expression in males and females, respectively. (**B,B'**)

Expression profiles of *gdf6b* and *gdf6a* in different adult tissues in males (light grey) and females (dark grey). (**C,C'**) Expression profiles of *gdf6b* and *gdf6a* during male (light grey) and female (dark grey) gametogenesis. Stages 2 to 6 of gametogenesis are according to Imarazene et al., 2020. Results are presented as boxplots with individual expression values displayed as dots, the expression median as a line and the box displaying the first and third quartiles of expression. Statistical significance between males and females were tested with the Wilcoxon Rank Sum Test (Wilcoxon-Mann-Whitney Test) and only significant differences are shown (** = P < 0.01; * = P < 0.05).

Figure 6. *gdf6b* gene knockout in Pachón cave *A. mexicanus* results in male to female sex reversal. (**A**) Gene knockout (KO) was performed by genome editing using the CRISPR-cas9 method. (**A**) The position of the two guide RNAs target sites (sgRNA) designed in order to target *gdf6b* exon 2 (E2) are shown (#target sites) on a simplified *gdf6b* gene structure scheme. Genotypic sex was characterized based on primers flanking large male-specific indels (blue boxes) observed in the *gdf6b-B* loci, resulting in an additional PCR fragment in genetic males compared to a single PCR fragment in genetic females. Knockout individuals were genotyped using primers flanking the 2 target sites that induced a 470 bp deletion in *gdf6b* mutant individuals (Mut) compared to the wild type (WT) *gdf6b* sequence. (**B**) Representative examples of the *gdf6b* sequence in some mutant individuals aligned with the wild type *gdf6b-B* and *gdf6b-A* sequences (the sequence framed in red corresponds to the deleted fragment in mutants). (**C-E**) Mutant genetic males with a *gdf6b* deletion developed ovaries with previtellogenic oocytes (PVtg Ooc) and vitellogenic oocytes (Vtg Ooc) (E), indistinguishable from the ovary of a WT female (D) and contrasting with the testis histology of a WT male. Ol: Ovarian lamellae. SpC: Spermatocytes; SpG: Spermatogonia; SpT: Spermatids; SpZ: Spermatozoa. Scale bars: 100 µm.

TABLES

Table 1. Percentage of males and females Pachón cave *A. mexicanus* obtained after rearing at two different temperatures

Temperature	Number of females	Number of males	X-squared	p-value	Significance
28 °C	124	150	2.4672	0.1162	ns
21 °C	112	130	1.3388	0.2472	ns

FIGURES

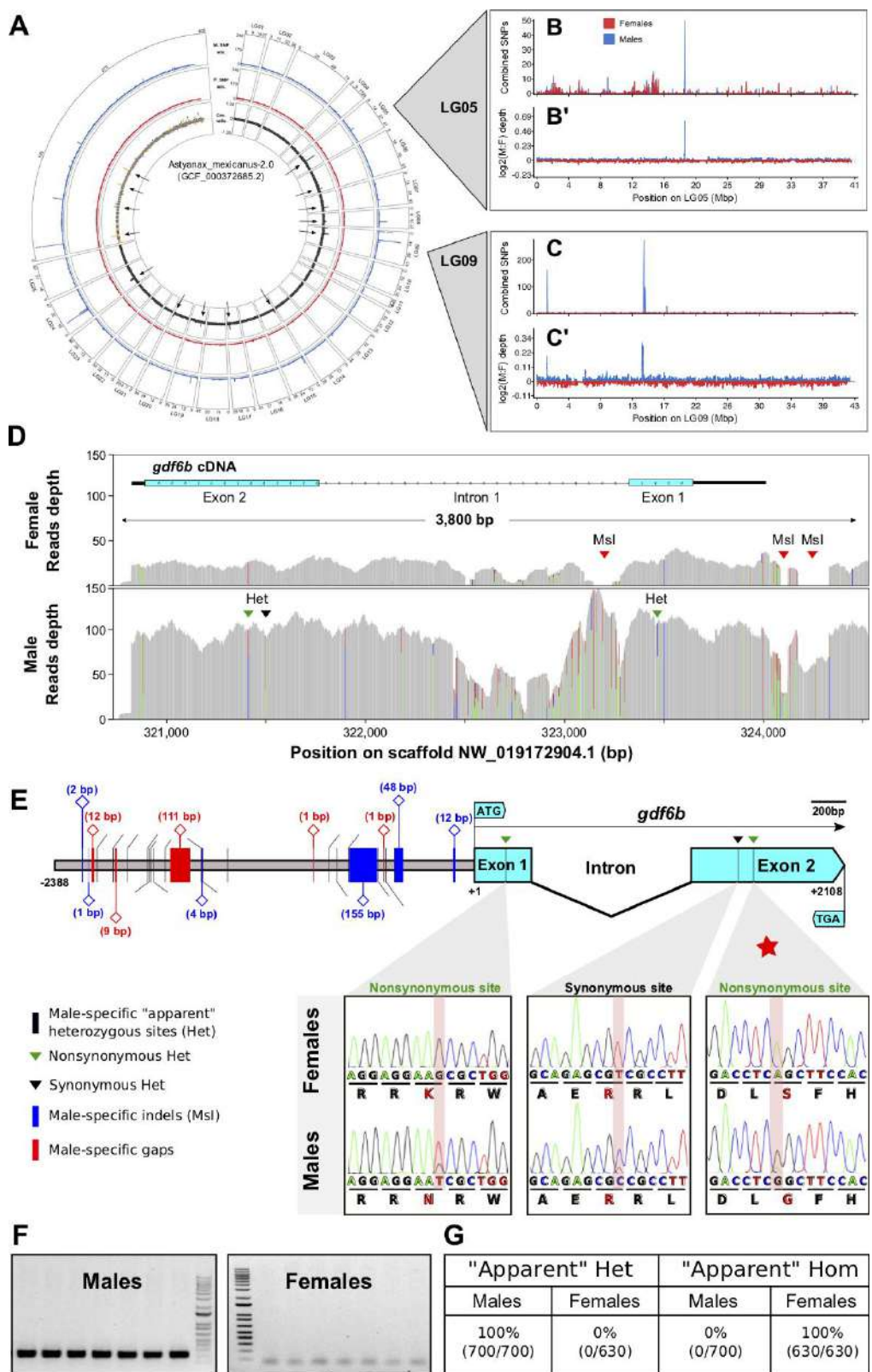


Figure 1. Genomic analysis of sex determination in Pachón cave *Astyanax mexicanus*.

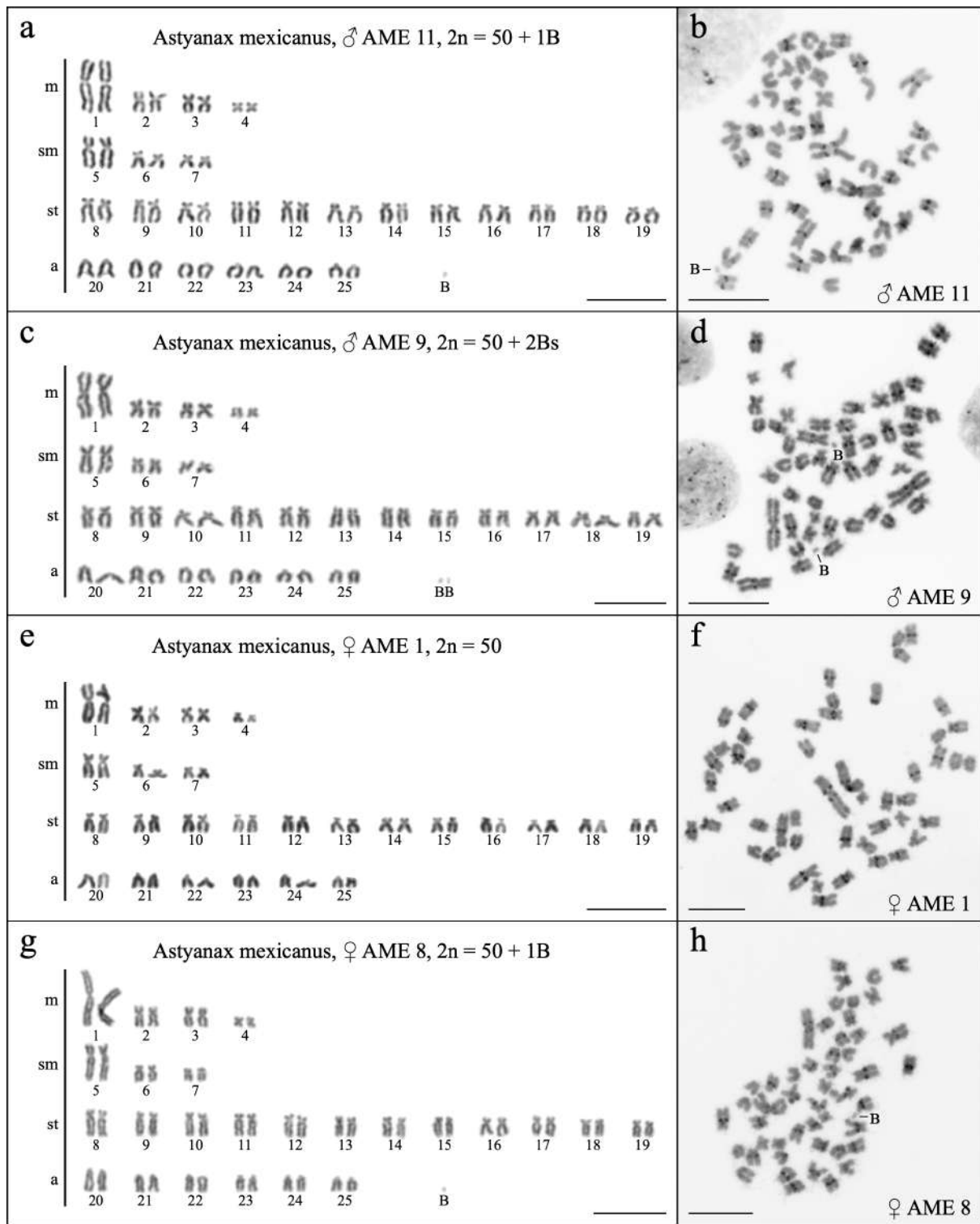


Figure 2. Karyotypes and C-banded mitotic metaphases of Pachón cave *Astyanax mexicanus*, with different male and female B microchromosome constitution.

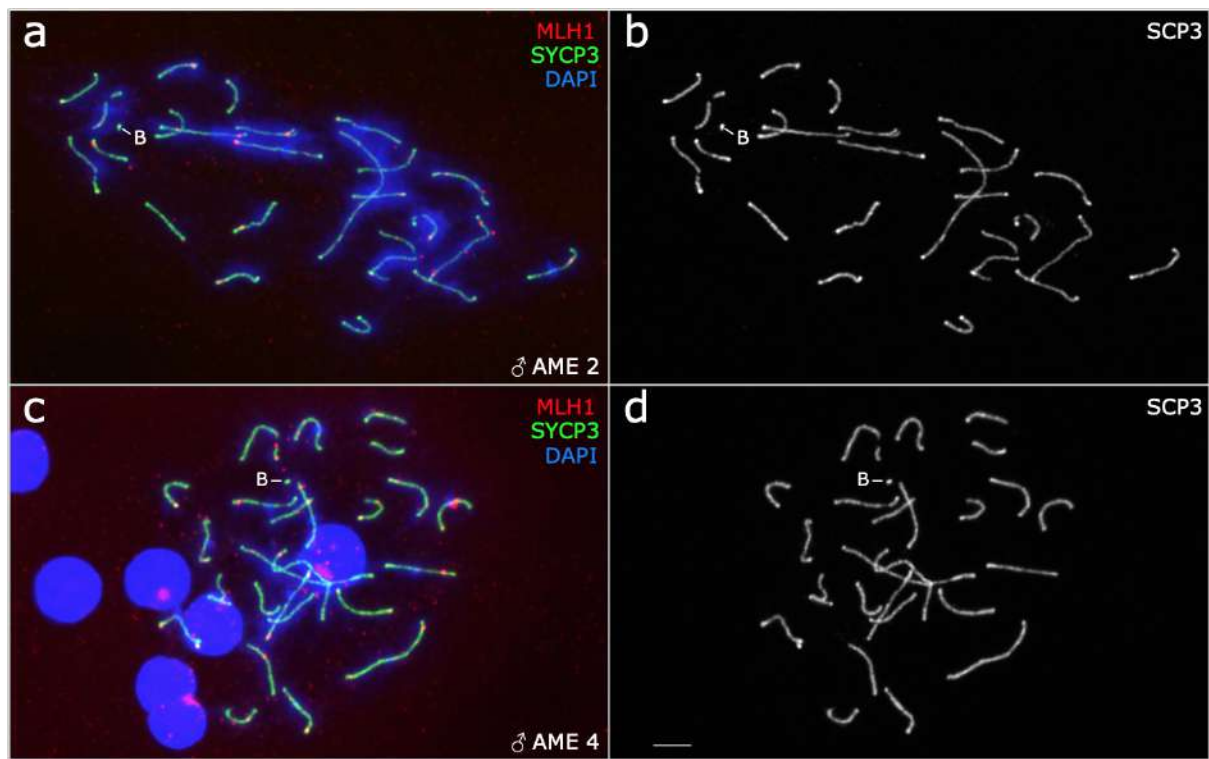


Figure 3. Synaptonemal complex analysis reveals that Pachón cave B microchromosomes do not pair with A chromosomes.

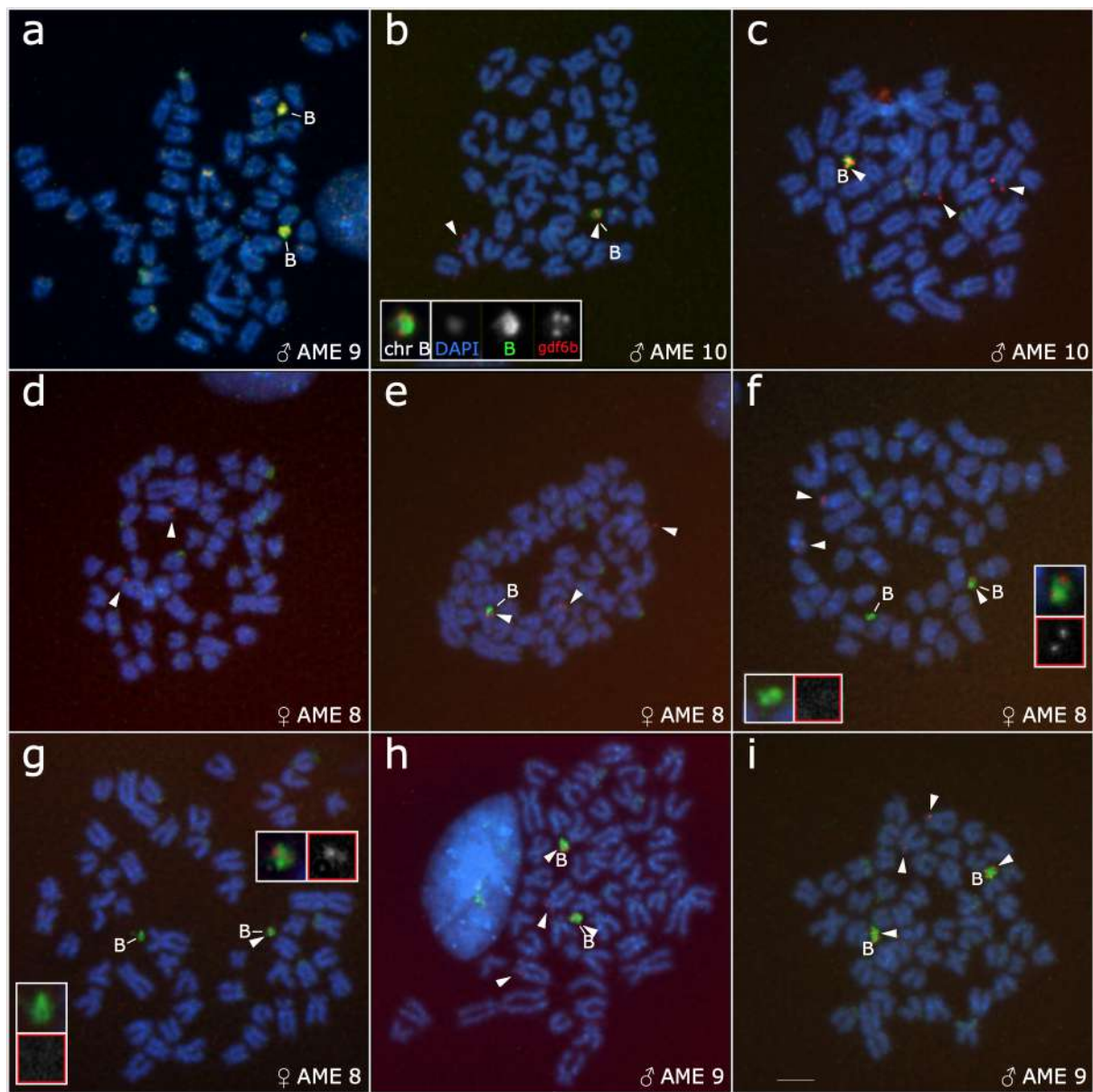


Figure 4. Male and female Pachón cave *Astyanax mexicanus* mitotic metaphases after fluorescent in situ hybridization (FISH) with *gdf6b*- and B chromosome-derived probes.

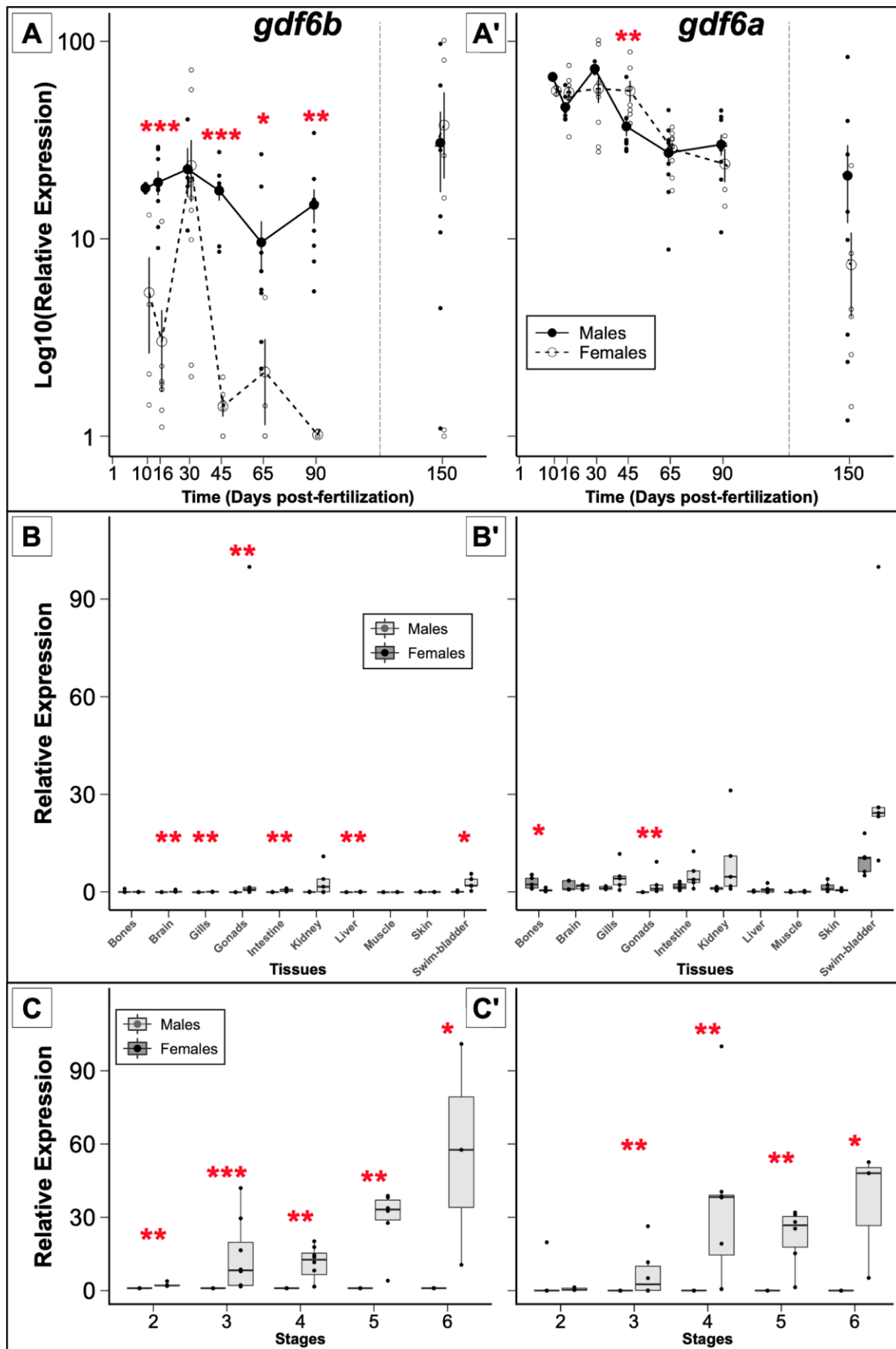


Figure 5. Expression patterns of *gdf6b* and *gdf6a* in Pachón cave *Astyanax mexicanus*.

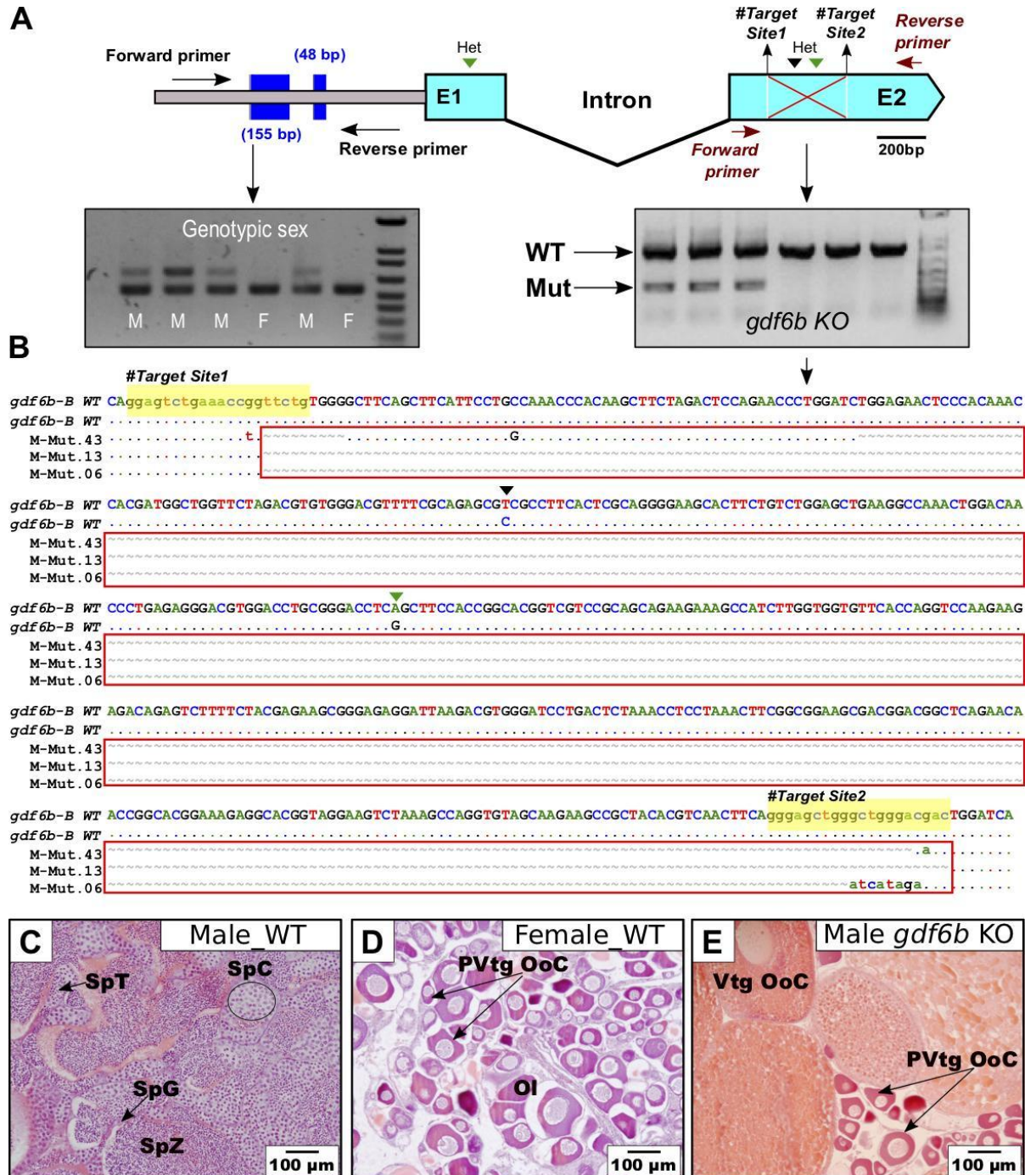


Figure 6. *gdf6b* gene knockout in Pachón cave *A. mexicanus* results in male to female sex reversal.

SUPPLEMENTARY DATA

Table S1. Primer names, sequences, target genes, and their corresponding experiments

Primer names: Forward (Fw) and Reverse (Rv) and TaqMan probes	Sequences	Target genes	Experiments
Gdf6b_SNP_Fw	TGGACCTGCGGGACCTCG	<i>Gdf6b-B</i>	Sex genotyping marker (WT fish)
Gdf6b_SNP_Rv	CTTTAGACTTCCTACCGTGCCT	<i>Gdf6b-B</i>	
Gdf6b-FISH_Probe_Fw	CACAGCAACCACCTCTATACCGG	<i>Gdf6b</i>	<i>gdf6b</i> FISH Probe synthesis
Gdf6b-FISH_Probe_Rv	TCACCTGCACCCACACGACTC	<i>Gdf6b</i>	
Gdf6b_EX2_Fw	CGTTTGATGTGCTACGCTCT	<i>Gdf6b</i>	CRISPR-Cas9 <i>gdf6b</i> -KO screening
Gdf6b_EX2_Rv	GACTCCACCACCATGTCCTCGTA	<i>Gdf6b</i>	
Gdf6b_cDNA_Fw	CTCCTCAGCTCTCTCCTCCT	<i>Gdf6b</i>	<i>gdf6b</i> cDNA cloning for ISH
Gdf6b_cDNA_Rv	GGTTGTCCAGTTGGCCTTC	<i>Gdf6b</i>	
dmrt1_TaqMan_Fw	AGGCCAACTCTGATTCTGGA	<i>dmrt1</i>	TaqMan assay (autosomal reference gene)
dmrt1_TaqMan_Probe	GGATTCCATCATAGAGGGAGCGGC C	<i>dmrt1</i>	
dmrt1_TaqMan_Rv	TGGCTCTCAGATACTGTCACT	<i>dmrt1</i>	
gdf6b_TaqMan_A&B_Primer_Fw	CGTTTGATGTGCTACGCTCTGA	<i>Gdf6b-B</i>	TaqMan assay (<i>gdf6b</i> B chromosome specific allele)
gdf6b_TaqMan_Probe_B_chromosome	GCAGAGCGCCGCCTCACTC	<i>Gdf6b-B</i>	
gdf6b_TaqMan_B_Specific_Primer_Rv	GAGGGAGGGTATTTCAGCAGGT	<i>Gdf6b-B</i>	
gdf6b_TaqMan_A&B_Primer_Fw	ACAGAGGTATTGTTGATGTGTCT	<i>Gdf6b</i>	TaqMan assay (<i>gdf6b</i> Autosomal allele)
gdf6b_TaqMan_Probe_Autosomal	GCAGAGCGTCGCCCTCACTC	<i>Gdf6b</i>	
gdf6b_TaqMan_A_Specific_Primer_Rv	CGCTCAGGTGTGTTCTGGAGAG	<i>Gdf6b</i>	
gdf6b_KO_Promoter_M&F_Primer_Fw	TTTCTGACTGTTGCCACCA	<i>Gdf6b</i>	Sex genotyping marker (<i>gdf6b</i> Mutant fishes)
gdf6b_KO_Promoter_M&F_Primer_Rv	CACCTCACAGAACGACCTCC	<i>Gdf6b</i>	
gdf6a_qPCR_Fw	AGAGGGAAAGATGATCTCGTGC	<i>Gdf6a</i>	Gene expression
gdf6a_qPCR_Rv	TGTAGAGGCCCGAGTCAGG	<i>Gdf6a</i>	
gdf6b_qPCR_Fw	GCTGGTTCTAGACGTGTGGG	<i>Gdf6b</i>	Gene expression
gdf6b_qPCR_Rv	CTTTCTTCTGCTGCGGACGA	<i>Gdf6b</i>	

Table S2. Male-biased regions detected in Pachón cave *A. mexicanus*, by contrasting female and male pool-seq reads. Only one region of 2.5 kb (Scaffold NW_019171027.1) displayed a female bias with reads M/F coverage below 0.75 and 37 regions covering a total of 2.1 Mb were biased in males. Sliding windows with at least an average of 10 reads at each position in males or in females were parsed to retains contiguous regions (more than two consecutive windows with a maximum gap of 5000 bp) of 500 bp windows with either more than 18 male specific-SNPs (female maximum value) or a depth ratio (M/F) superior of 1.25 or inferior of 0.75.

LG number	LG or Contig ID	LG or Contig size	Start position	End position	Region size (bp)
LG05	NC_035901.1	40584741	19056000	19125500	69500
LG06	NC_035902.1	52532229	44437500	44439500	2000
LG07	NC_035903.1	40813162	31147000	31278500	131500
LG08	NC_035904.1	27092187	18590500	18691000	100500
LG09	NC_035905.1	42966623	1342500	1423000	80500
LG09	NC_035905.1	42966623	14444500	14681500	237000
LG09	NC_035905.1	42966623	17531500	17581000	49500
LG13	NC_035909.1	44161018	36875500	36914000	38500
LG15	NC_035911.1	35718434	1085500	1191000	105500
LG15	NC_035911.1	35718434	1232500	1377000	144500
LG17	NC_035913.1	28317440	22838500	22855000	16500
LG17	NC_035913.1	28317440	22891500	22900000	8500
LG17	NC_035913.1	28317440	22996000	23040500	44500
LG17	NC_035913.1	28317440	23098500	23144500	46000
LG17	NC_035913.1	28317440	23169000	23215500	46500
LG19	NC_035915.1	35429340	9301500	9363000	61500
LG20	NC_035916.1	36262418	35754000	35792500	38500
LG23	NC_035919.1	38085671	18964000	18998500	34500
LG24	NC_035920.1	47266144	12786500	12853500	67000
LG24	NC_035920.1	47266144	13400500	13491500	91000
LG24	NC_035920.1	47266144	15263000	15324500	61500
LG24	NC_035920.1	47266144	15340000	15442500	102500
Scaffold	NW_019170697.1	42250	500	1500	1000
Scaffold	NW_019170910.1	68752	500	19000	18500
Scaffold	NW_019171067.1	59165	500	8500	8000
Scaffold	NW_019171252.1	36603	7000	8500	1500
Scaffold	NW_019171322.1	36357	0	11000	11000
Scaffold	NW_019171463.1	55246	1500	24000	22500
Scaffold	NW_019171721.1	76365	6000	17500	11500
Scaffold	NW_019172542.1	52023	22500	25500	3000
Scaffold	NW_019172624.1	138424	61000	137500	76500
Scaffold	NW_019172760.1	107226	0	1000	1000
Scaffold	NW_019172868.1	3184142	657500	723000	65500
Scaffold	NW_019172881.1	1059932	558000	611500	53500
Scaffold	NW_019172881.1	1059932	792000	877500	85500
Scaffold	NW_019172890.1	7215798	2022000	2142000	120000
Scaffold	NW_019172904.1	1535826	302000	356500	54500
Total =					2111000

Table S3. Genes found in the male-biased regions including LGs and unplaced scaffolds.

LG (scaffolds)	CDS	Start	End	Name	Product	M_snps	F_snps	M/F
LG05	truncated CDS	18998628	19165059	dennd1b	DENN domain-containing protein 1B	59	0	1,4
LG06	truncated CDS	44435858	44446503	LOC111192736	uncharacterized protein LOC111192736	0	1	1,1
LG07	truncated CDS	31093730	31181389	phtf2	putative homeodomain transcription factor 2	23	0	1,2
LG07	complete CDS	31178555	31239388	prf5	proline-rich protein 5 isoform X2	24	0	1,3
LG07	complete CDS	31259633	31263291	LOC103061510	protein SC2 homolog%2C mitochondrial	3	0	1,4
LG07	complete CDS	31263968	31278884	ncaph2	condensin-2 complex subunit H2	6	0	1,4
LG08	truncated CDS	18577789	18615121	LOC103026996	laminin subunit beta-1	15	0	1,0
LG08	complete CDS	18619136	18625195	dld	dihydrodipoyl dehydrogenase%2C mitochondrial	17	0	1,4
LG08	complete CDS	18632303	18634947	LOC103027288	EF-hand calcium-binding domain-containing protein 10-like	0	0	1,0
LG08	complete CDS	18637244	18644079	LOC10302021	zinc finger protein 800-like	0	0	1,0
LG08	complete CDS	18653276	18668450	LOC103032349	zinc finger protein 800-like	58	0	1,4
LG08	truncated CDS	18672401	18838757	LOC103033497	metabotropic glutamate receptor 8	0	0	1,0
LG09	truncated CDS	1329338	132943117	RAS guanyl-releasing protein 1-like	0	0	1,0	
LG09	complete CDS	1348948	1355774	LOC103039408	zinc finger protein DPY3-like	7	0	1,0
LG09	truncated CDS	1368097	1431244	LOC103042803	signal-induced proliferation-associated 1-like protein 1	132	0	1,2
LG09	complete CDS	14451121	14478899	LOC103027082	coiled-coil domain-containing protein 6	137	0	1,4
LG09	complete CDS	14495258	1511030	LOC103027375	monocarboxylate transporter 9-like	47	0	1,3
LG09	complete CDS	14513410	14534923	LOC103028846	protein FAM13A-like	30	0	1,3
LG09	complete CDS	14537252	14566205	LOC103028326	phytanoyl-CoA hydroxylase-interacting protein-like	17	0	1,2
LG09	complete CDS	14574548	14635052	LOC103029905	protein bicaudal Chomolog 1-B-like	47	0	1,4
LG09	complete CDS	14637735	14646363	LOC103029158	ubiquitin-conjugating enzyme E2 D4-like	23	0	1,4
LG09	complete CDS	14654221	14659392	LOC103029061	visual system homeobox 1	10	0	1,5
LG09	truncated CDS	17522678	17633629	LOC103043425	kinase D-interacting substrate of 220 kDa	29	3	1,0
LG13	truncated CDS	36876648	36882405	LOC103040875	keratin%2C type II cytoskeletal 8-like	0	0	1,0
LG13	complete CDS	36882810	36892152	LOC103041181	uncharacterized protein LOC103041181	16	0	1,0
LG13	complete CDS	36895859	36902148	LOC103040574	ankyrin repeat domain-containing protein 33-like	10	0	0,9
LG13	truncated CDS	36904618	36919543	LOC103040047	rho guanine nucleotide exchange factor 25	1	0	1,0
LG15	truncated CDS	1081632	1160587	LOC103028753	fibulin-2	88	0	1,3
LG15	truncated CDS	1175424	1253640	LOC103029069	nuclear pore membrane glycoprotein 210	11	0	1,1
LG15	truncated CDS	1270292	1596944	LOC103026485	IQ motif and SEC7 domain-containing protein 1-like	91	0	1,1
LG17	complete CDS	22891702	22893127	LOC111194623	uncharacterized protein LOC111194623	0	0	0,9
LG17	truncated CDS	23067926	23103690	LOC103043232	NTPase KAP family P-loop domain-containing protein 1	0	0	1,1
LG17	complete CDS	23116871	2319814	LOC111194578	uncharacterized protein LOC111194578	7	0	3,1
LG17	complete CDS	23191844	23121956	LOC111194579	vegetative cell wall protein gp1-like	1	0	1,3
LG17	truncated CDS	23170006	23170900	LOC111194627	uncharacterized protein LOC111194627	0	0	1,0
LG17	complete CDS	23190946	23195245	LOC111194580	uncharacterized protein LOC111194580	6	1	2,4
LG17	complete CDS	23196054	23197229	LOC111194628	N-lysine methyltransferase KMT5A-A-like	0	0	MS
LG17	complete CDS	23196880	23205291	LOC111194629	uncharacterized protein LOC111194629	0	0	1,6
LG17	complete CDS	23207519	23209926	LOC111194630	uncharacterized protein LOC111194630	0	0	0,9
LG19	complete CDS	9323336	9331783	LOC103025110	gap junction gamma-1 protein-like	48	0	1,9
LG19	truncated CDS	9334276	9365222	lct	lactase-phlorizin hydrolase	21	0	1,2
LG23	truncated CDS	18927454	18949652	necab1	N-terminal EF-hand calcium-binding protein 1	18	0	1,0
LG24	truncated CDS	12768917	12796871	canx	calnexin isoform X2	0	0	1,0
LG24	complete CDS	12805853	12825007	mamll1	mastermind-like protein 1	78	0	1,8
LG24	complete CDS	12823164	12837913	ltds	leukotriene C4 synthase	0	0	1,0
LG24	truncated CDS	13382812	13438173	LOC103037758	janus kinase and microtubule-interacting protein 1	83	0	1,2
LG24	complete CDS	13449216	13452337	LOC111195720	zinc finger MYM-type protein 1-like isoform X1	0	0	1,0
LG24	complete CDS	13457721	13473736	LOC103038069	wolframin	101	0	1,3
LG24	truncated CDS	15410176	15567635	pcdh19	protocadherin-19 isoform X1	30	9	1,1
LG29	truncated CDS	35736965	35789237	LOC103024448	pleckstrin homology-like domain family B member 2	23	0	1,3
NW_019170910_1	complete CDS	1871	7488	LOC111196700	cationic amino acid transporter 2-like	0	0	1,4
NW_019172624_1	complete CDS	84698	88102	LOC111190568	HLA class I histocompatibility antigen%2C Cw-5 alpha chain-like	29	0	1,8
NW_019172624_1	complete CDS	88231	96269	LOC103047423	H-2 class I histocompatibility antigen%2C D-K alpha chain-like	5	0	1,0
NW_019172624_1	complete CDS	128554	134207	LOC111190570	0	0	1,0	
NW_019172904_1	complete CDS	320824	324012	LOC103035745	growth/differentiation factor 6-B	2	0	4,1
NW_019172904_1	truncated CDS	325014	392647	plhd1l	fibrocystin-L	24	0	1,2
NW_019172868_1	truncated CDS	680358	707514	LOC103023958	putative bifunctional UDP-N-acetylglucosamine transferase and deubiquitinase ALG13	117	0	1,5
NW_019172868_1	truncated CDS	708917	733199	LOC103023630	RING finger protein 145-like	0	0	1,1
NW_019172881_1	complete CDS	807810	809794	foxe1	forkhead box protein E1	0	0	1,4
NW_019172881_1	complete CDS	815382	846511	spag5	sperm-associated antigen 5	19	0	1,5
NW_019172881_1	complete CDS	863206	867509	LOC111191550	ankyrin repeat domain-containing protein 34C-like	2	0	1,3
NW_019172881_1	truncated CDS	871293	878535	trmo	tRNA (adenine(37)-N6)-methyltransferase	0	0	1,1
NW_019172890_1	complete CDS	2023538	2047401	LOC111191619	0	0	1,1	

Table S4. The number of metaphases (NM) containing B chromosomes (Bs) in males and females of Pachón cave *A. mexicanus*. % M = percentage of metaphases.

Individual Sex	Total NM	Total NM 0 Bs	Total NM 1 Bs	Total NM 2 Bs	Total NM 3 Bs	Total NM with Bs	% M with Bs
Male1	10	0	7	3	0	10	100
Male2	15	6	9	0	0	9	60
Male3	14	11	1	2	0	3	21,4
Male4	5	1	4	0	0	4	80
Male5	17	2	15	0	0	15	88,2
Male6	16	1	15	0	0	15	93,7
Male7	30	0	5	25	0	30	100
Male8	26	0	4	22	0	26	100
Male9	29	0	22	7	0	29	100
Male10	58	10	48	0	0	48	82,7
Male11	109	8	95	6	0	101	92,6
Male12	144	8	135	1	0	136	94,4
Male13	147	4	20	121	2	143	97,2
Male14	194	6	183	3	0	186	95,8
Male15	44	1	43	0	0	43	97,7
Male16	113	9	102	2	0	104	92
Male17	57	2	53	2	0	55	96,4
Female1	9	9	0	0	0	0	0
Female2	13	13	0	0	0	0	0
Female3	32	29	2	1	0	3	9,3
Female4	59	57	2	0	0	2	3,3
Female5	31	31	0	0	0	0	0
Female6	23	22	1	0	0	1	4,3
Female7	55	51	4	0	0	4	7,2
Female8	82	82	0	0	0	0	0
Female9	53	39	0	0	0	0	0
Female10	148	118	28	2	0	30	20,2
Female11	77	77	0	0	0	0	0

Table S5. Pachón cave *A. mexicanus* male assemblies' statistics.

Assembly metrics	Astyanax_mexicanus-1.0.2	Astyanax_mexicanus-2.0	ONT	Hifi PacBio
Number of scaffolds	12,1345	2,415	1,543	195
Total size of the assembly	964,248,202	1,335,239,194	1,284,380,570	1,378,679,465
Longest scaffold	179,788	74,127,438	126,506,226	133,971,750
Shortest scaffold	241	1,866	1000	1000
Mean scaffold size	7,946	552,894	832,392	7,071,002
Median scaffold size	4,258	47,283	10,114	37,544
N50 scaffold length	14,739	35,377,769	48,372,107	52,029,803
L50 scaffold count	16,919	16	11	11
Assembly completeness	Astyanax_mexicanus-1.0.2	Astyanax_mexicanus-2.0	ONT	Hifi PacBio
Complete BUSCOs	2,263 (62.2%)	3,482 (95.7%)	3,496 (96 %)	3,530 (97%)
Complete and single-copy BUSCOS	2,246 (61.7%)	3,438 (94.5%)	3,452 (94.8%)	3,479 (95.6%)
Complete and duplicated BUSCOS	17 (0.5%)	44 (1.2%)	44 (1.2%)	51 (1.4%)
Fragmented BUSCOs	475 (13%)	28 (0.8%)	19 (0.5%)	17 (0.5%)
Missing BUSCOs	902 (24.8%)	130 (3.5%)	125 (3.5%)	93 (2.5%)
Total BUSCO groups searched	3,640	3,640	3,640	3,640
Chromosome-scale metrics	Astyanax_mexicanus-1.0.2	Astyanax_mexicanus-2.0	ONT	Hifi PacBio
Number of A chromosomes	unknown	25	25	25
Number of B chromosome fragments	Not relevant	Not relevant	unknown	1
Cumulated B chromosome size	Not relevant	Not relevant	unknown	2,975,147
% of assembly in A chromosomes	0%	78.3%*	97.56%	97.98%
% of assembly in unanchored scaffolds	100%	21.7%*	2.44%	2.12%

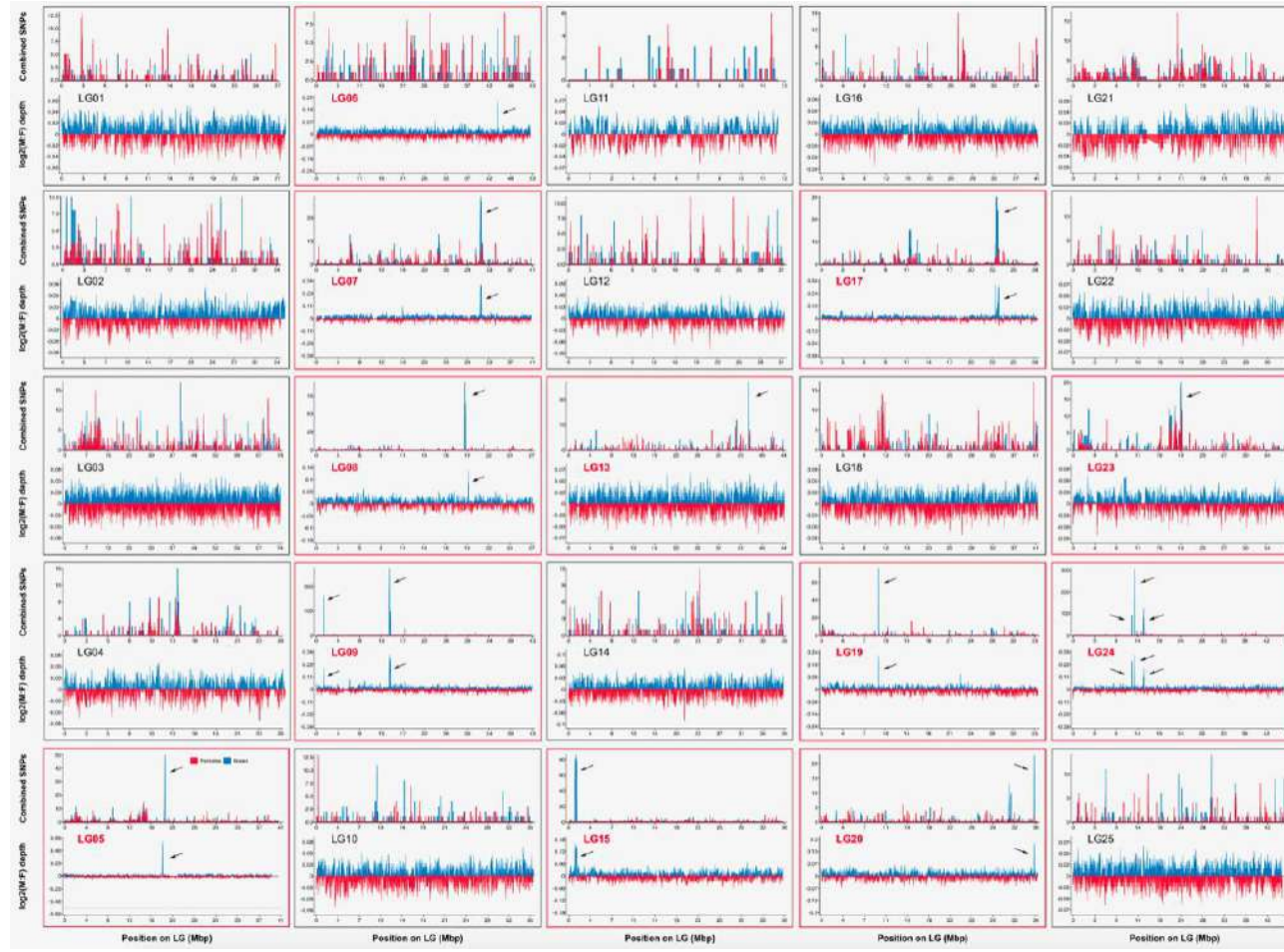


Figure S1. Pool-seq data illustrating the “apparent” male (blue) and female (red) SNPs and the \log_2 M/F depth ratio across the different LGs (from LG01 to LG25). Details of the pool-seq analysis of sex determination in Pachón cave *Astyanax mexicanus* for each linkage groups of the *Astyanax mexicanus*-2.0 female genome assembly (GCF_000372685.2). Differences between males and females, i.e., “apparent” indels and heterozygous sites, and read coverage differences were counted in a 50 kb sliding window with an output point every 500 bp. Read coverage ratio was calculated as the \log_2 of the male versus female read depth and sex-biased SNPs is shown as combined “apparent” female- (in red) and male- (in blue) specific SNPs.

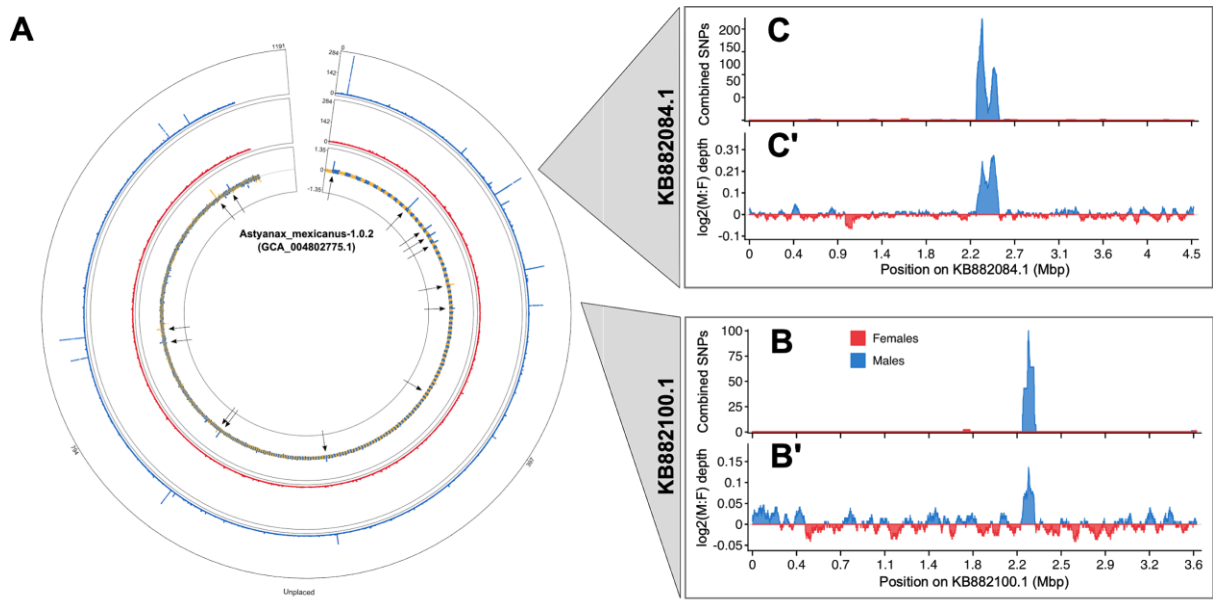


Figure S2. Circular plot of the remapped pool-seq reads onto the Pachón cave female reference genome (assembly accession: GCA_004802775.1) showing the male and female biased regions highlighted by dark arrows. Differences between males and females, i.e., “apparent” indels and heterozygous sites, and read coverage differences were counted in a 50 kb sliding window with an output point every 500 bp. Outer to inner tracks show respectively: the “apparent” male-specific SNPs (blue), the “apparent” female-specific SNPs (red), and the read coverage ratio between males and females. (**B-B'** and **C-C'**) Zoomed views of scaffolds KB882100.1 and KB882084.1.

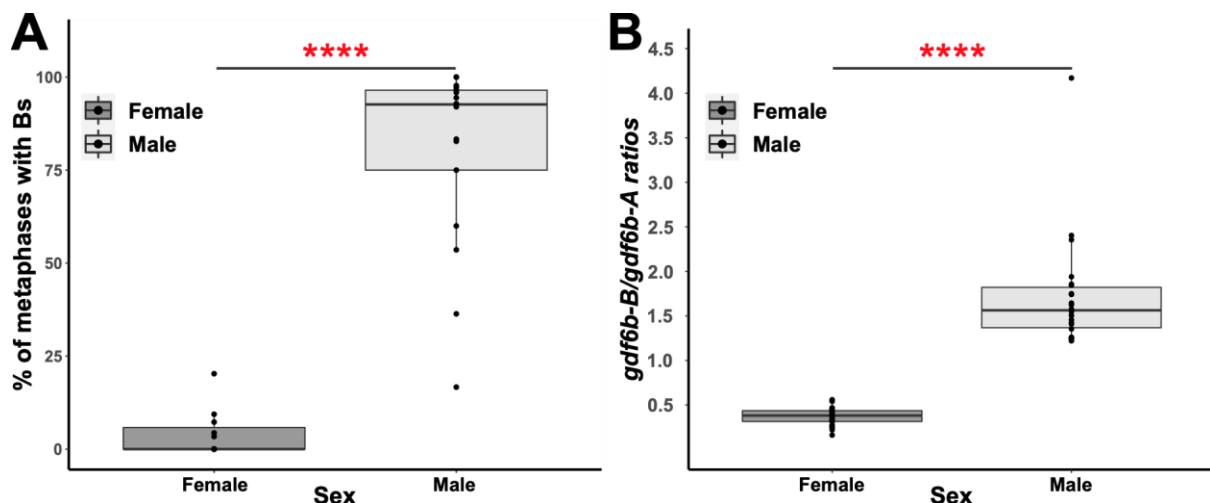


Figure S3. Percentage of metaphases with B microchromosomes (A) and copy number variation of the *gdf6b* B microchromosome gene (*gdf6b-B*) in males and females. (A). percentage (%) of metaphases with a B microchromosome in males and females (graphical representation of the last column of Table S4). (B). Copy number variation of the *gdf6b* B microchromosome gene (*gdf6b-B*) was quantified using specific TaqMan PCR assays for both *gdf6b-B* and *gdf6b-A* genes normalized using the single copy gene *dmrt1*. Results are presented as boxplots of the ratio of *gdf6b-B* over *gdf6b-A* in males (light grey) and females (dark grey), with individual copy number values displayed as dots, the copy number median as a line and the box displaying the first and third quartiles of copy number variation. Statistical significance between males and females were tested with the Wilcoxon Rank Test (**** = P < 0.001).

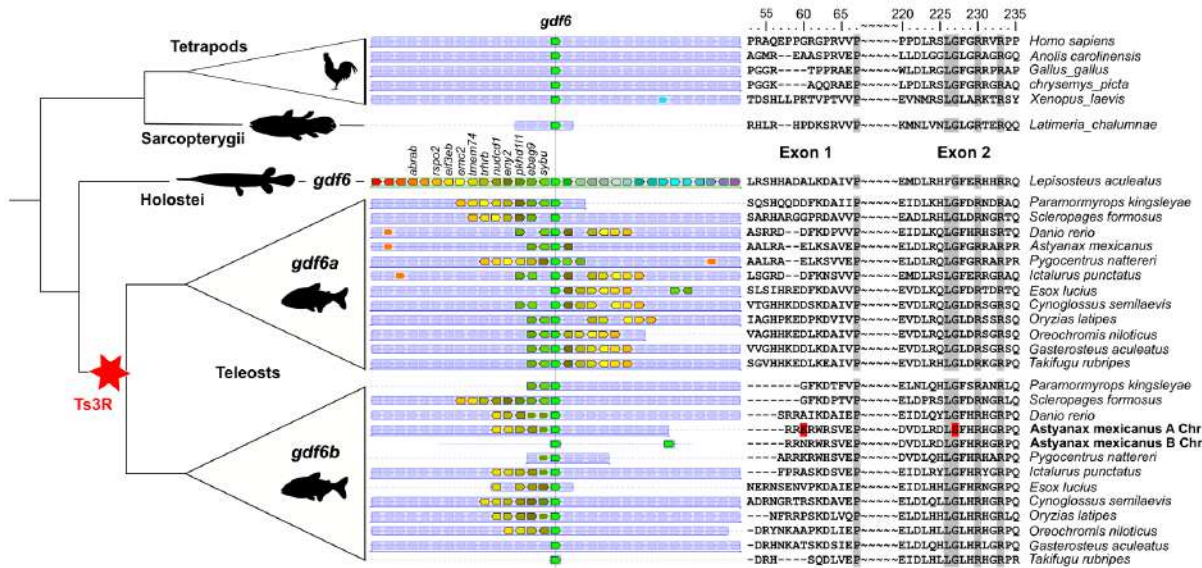


Figure S4. The *gdf6b* and *gdf6b* genes are duplicated paralogues stemming from the teleost whole genome duplication (Ts3R). Phylogeny (left panel) and synteny (middle panel) relationships were inferred from a private genomic instance (Louis et al., 2013) in which synteny and phylogeny have been reconciled with the Scorpions pipeline (Parey et al., 2020). Species names including 4 tetrapod species, one sarcopterygii species, one holostei species and 13 teleosts are given on the right with the additional duplications of the *gdf6b-B* loci in *Astyanax mexicanus*. The right panel is a multiple Gdf6 protein coding sequence alignment around the two amino-acids (AA) encoded by the two nonsynonymous “apparent” male-specific heterozygous sites found between the *gdf6b-A* (AA in red) and *gdf6b-B* loci.

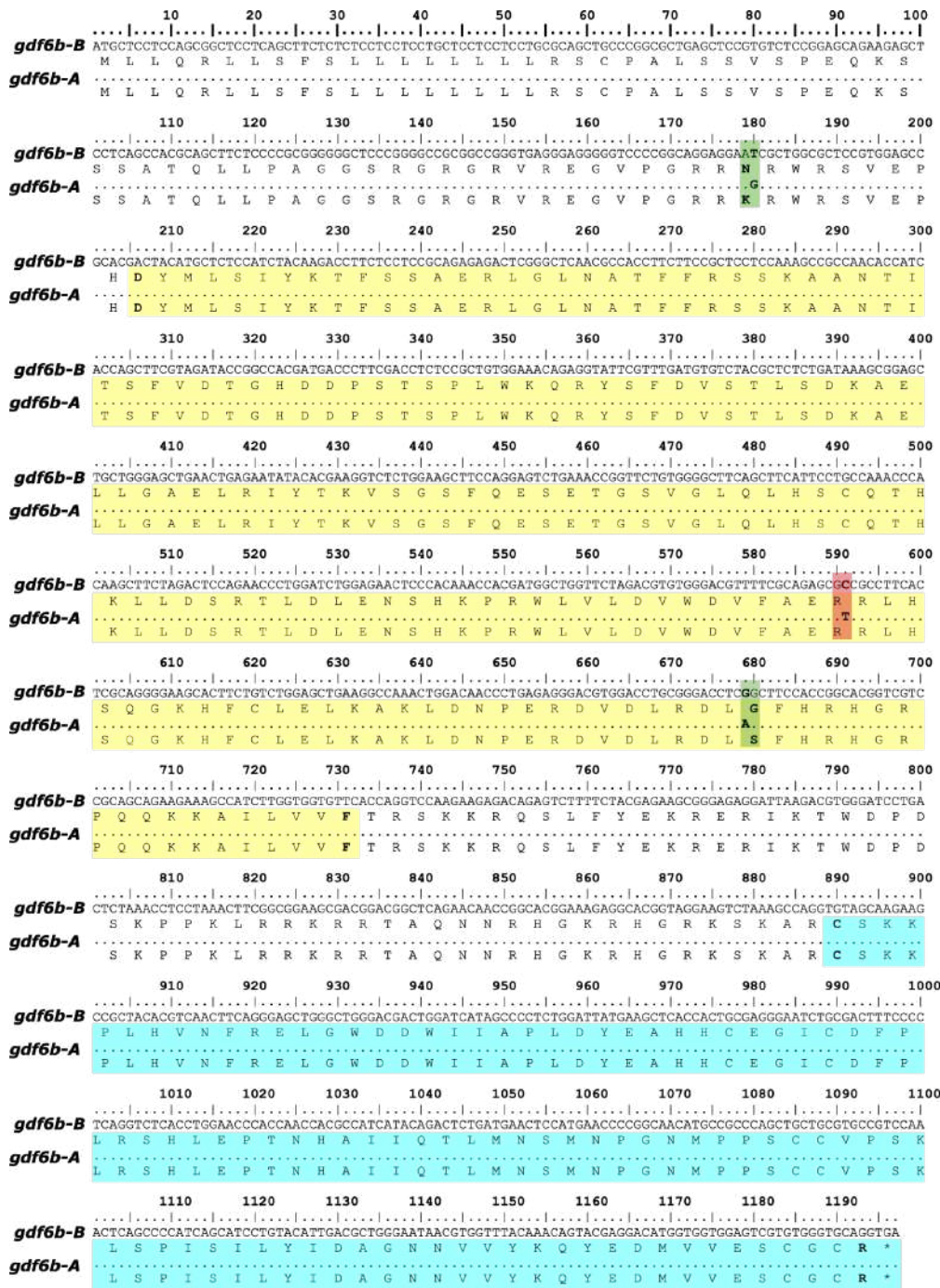


Figure S5. Alignment of nucleotide and protein sequences of the *gdf6b-A* and *gdf6b-B* genes. Sequences were aligned with BioEdit 7.2. The three “apparent” male-specific heterozygous sites are boxed (green for nonsynonymous sites and red for synonymous sites) at position 180 bp, 591 bp and 679 bp positions of the CDS. Regions highlighted in yellow and blue indicated the Pfam “TGF-β propeptide” and “TGF-β-like” domains (El-Gebali et al., 2019). “.”: Identical nucleotides; “*”: stop codon.

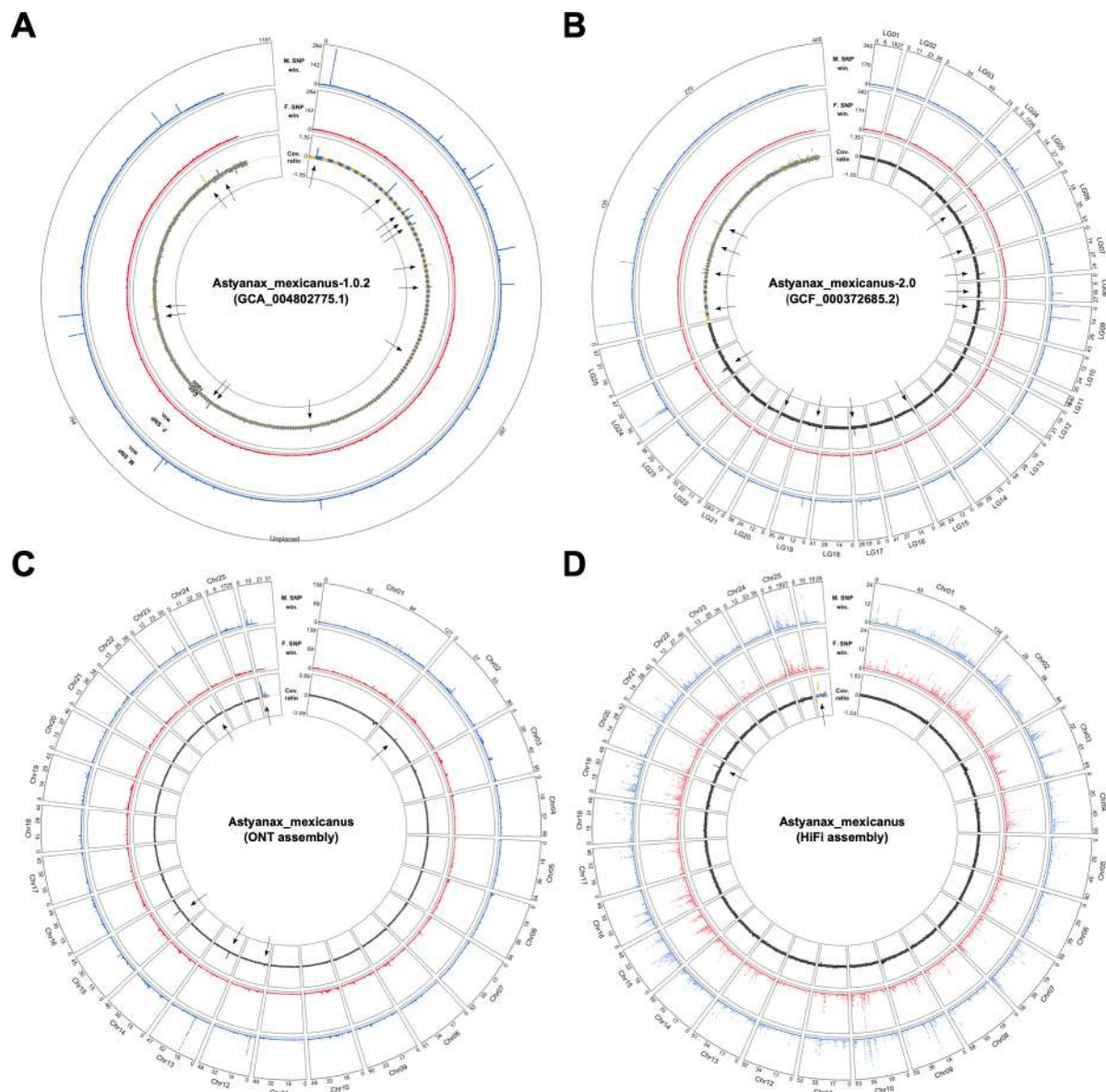


Figure S6. Pool-seq analysis with different public and private *A. mexicanus* genome assemblies. (A) *A. mexicanus* (cavefish population) female reference genome (assembly accession: GCA_004802775.1). (B) *A. mexicanus* (surface fish population) female reference genome (assembly accession: GCA_000372685.2). (C) *A. mexicanus* (Pachón cavefish population) male reference genome (male ONT genome assembly). (D) *A. mexicanus* (Pachón cavefish population) male reference genome (male HiFi genome assembly). The main sex-biased regions are highlighted by black arrows. Linkage groups (LGs) or chromosomes (longest scaffolds) are given outside the circular plots. Differences between males and females, i.e., “apparent” indels and heterozygous sites, and read coverage differences were counted in a 50 kb sliding window with an output point every 500 bp. Outer to inner tracks show respectively: the “apparent” male-specific SNPs (blue), the “apparent” female-specific SNPs (red), and the read coverage ratio between males and females.

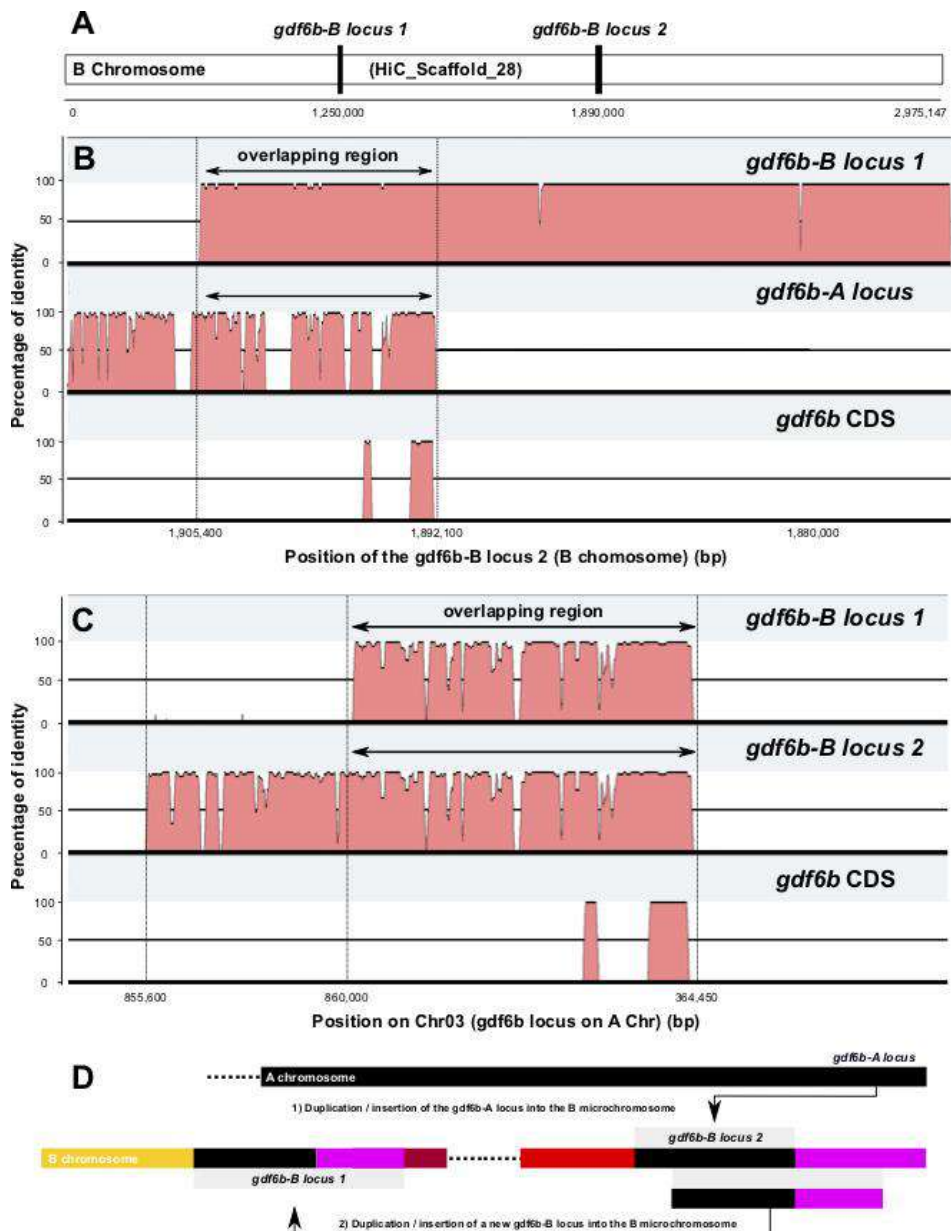


Figure S7. The duplicated *gdf6b* loci on the Pachón cave *A. mexicanus* B microchromosome stemmed from two successive A and B duplications. **(A).** Schematic representation of the location of the two *gdf6b* loci on the *A. mexicanus* B microchromosome (HiC_scaffold_28). **(B).** Vista alignments (Frazer et al., 2004) of the *gdf6b-A* locus, the *gdf6b-B* locus 1 and the *gdf6b* CDS on the *gdf6b-B* locus 2 genome sequence showing a common overlapping sequence between all loci (double sided arrows), a left region only shared by the *gdf6b-B* locus 2 and the *gdf6b-A* locus and a right region shared by the *gdf6b-B* loci. **(C).** Similar vista genome sequence alignments with the *gdf6b-A* used as a reference. **(D).** A two-steps duplication hypothesis scheme suggesting that the *gdf6b-B* locus 2 was originated from an initial duplication of the *gdf6b-A* locus and that the *gdf6b-B* locus 1 was duplicated in a second step from the duplication of the *gdf6b-B* locus 2.

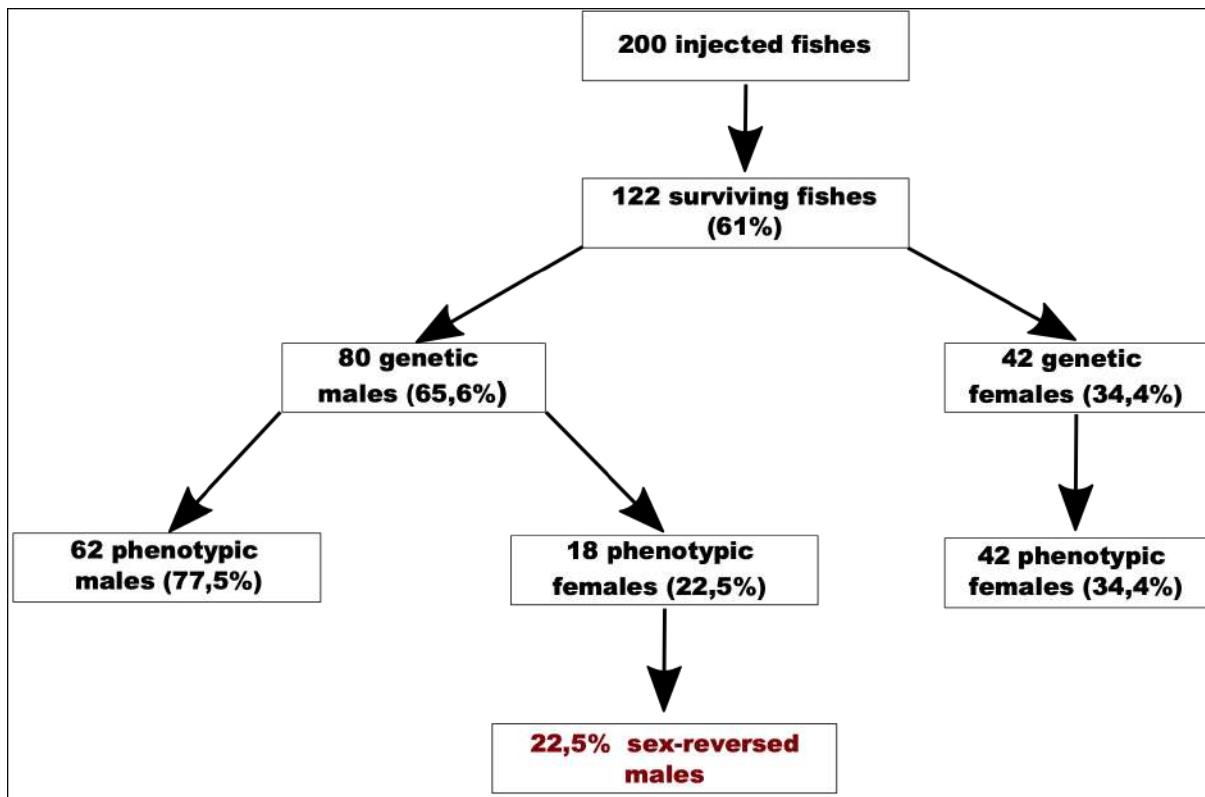


Figure S8: Numbers of *gdf6b* knockout generated by CRISPR-Cas9 method including the number of fish injected, and the number and percentage of sex-reversed males obtained. Out of the 200 micro-injected eggs (at 1 cell stage), 122 adult fishes were obtained including 80 genetic males and 42 genetic females. Among the 80 genetic males, we found 62 phenotypic males (77,5%), and 18 phenotypic females (22,5%) displaying a 470 bp deletion on the exon 2 of *gdf6b* gene.

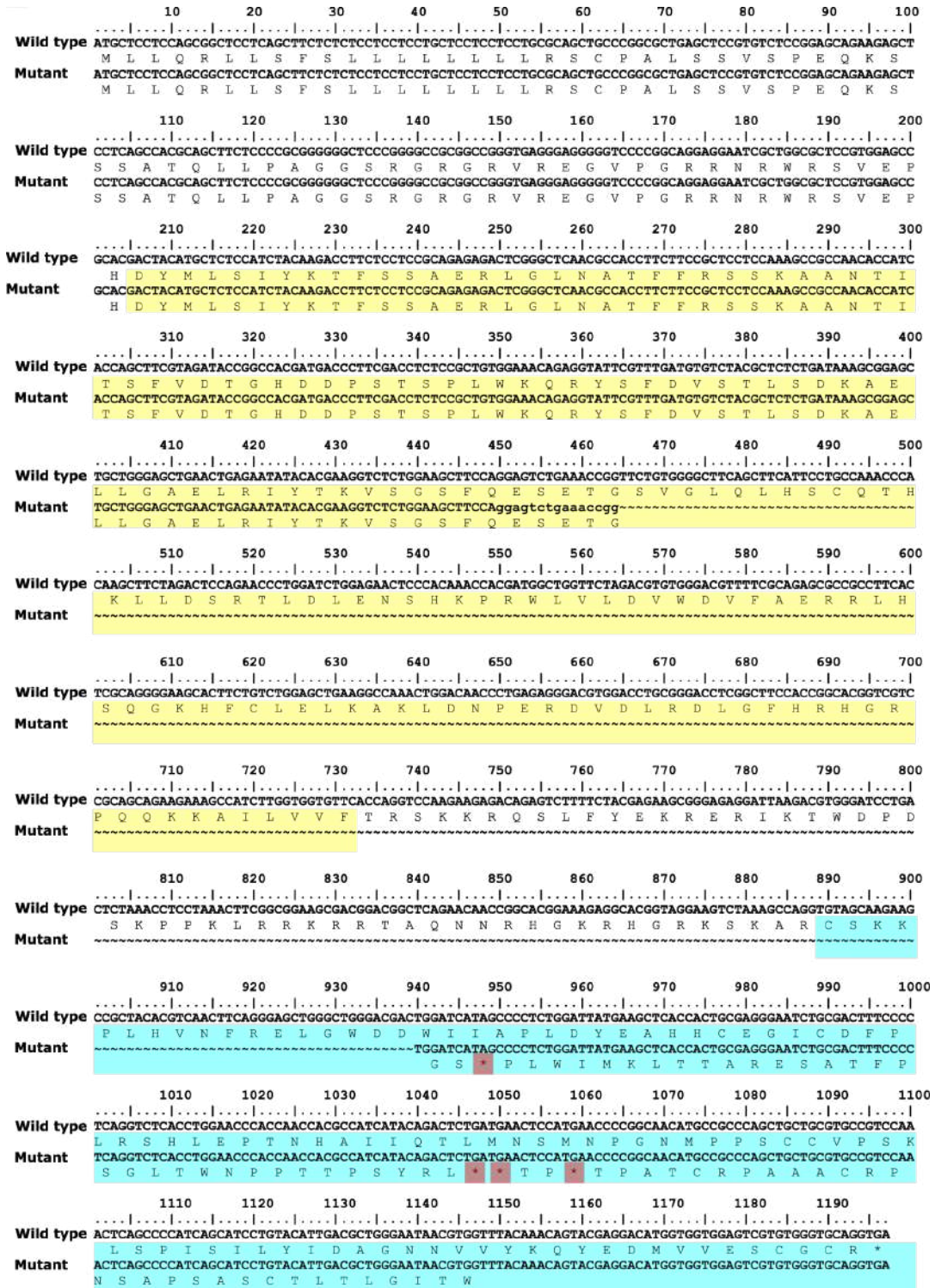


Figure S9. Alignment of nucleotide (*gdf6b-B*) and translated protein sequences (Gdf6-B) in wild type and mutant males showing the deletion of the 470 bp region in F0 fish in the exon 2 encoding for the Pfam “TGF- β propeptide” (yellow) and the “TGF- β -like” (blue) domains. The resulting fish displayed a frame-shifted and truncated Gdf6b-B protein with premature stop codon (red).

Publication N° 3 :

Évolution de la détermination du sexe chez les morphotypes et les populations d'*Astyanax mexicanus*

Objectifs

Suite à la caractérisation du système de détermination du sexe chez la population de la grotte Pachón, nous avons étendu notre analyse sur d'autres morphotypes et populations de laboratoire et sauvages d'*A. mexicanus* afin de comprendre, si le système de détermination du sexe de type "B-sexuel" était conservé chez les autres morphotypes et populations.

Contribution personnelle

J'ai d'abord exploré l'effet de la température sur la détermination du sexe chez la population du Texas (manipulation de la température). Suite à l'identification de *gdf6b-B* comme déterminant majeur du sexe chez la population de la grotte Pachón, j'ai analysé sa liaison au sexe phénotypique sur tous les animaux utilisés dans cette étude, dont le sexe phénotypique était précédemment identifié (histologie, design des amorces, extractions des ADNs génomiques et séquençages). Pour confirmer les résultats des données génomiques, j'ai quantifié le nombre de copies de *gdf6b* chez les mâles et les femelles (dosages TaqMan). Par la suite, j'ai vérifié la liaison de *gdf6b-B* au sexe mâle dans les populations sauvages cavernicoles et de surface (contribution à une campagne d'échantillonnage dans les grottes mexicaines, extractions des ADNs génomiques, génotypages, analyses de séquence). Enfin, j'ai analysé l'ensemble des résultats présentés dans cette étude et rédigé le manuscrit.

Expérimentations en cours auxquelles j'ai participées

- Contribution aux prélèvements, traitement et préparation des échantillons prévus pour l'analyse histologique et moléculaire de la différenciation gonadique chez la population Texane
- Séquençages de génomes d'animaux sauvages appartenant à différentes populations (Pachón, Molino, Texas)

Evolution of sex determination in *Astyanax mexicanus* morphotypes and populations

Boudjema Imarazene^{1,2}, Séverine Beille¹, Elodie Jouano¹, Romain Feron¹, Céline Lopez-Roques³, Hugues Parrinello⁴, Laurent Journot⁴, Cédric Cabau⁵, Margot Zham⁵, Christophe Klopp⁵, Julie Perez⁶, Frédéric Veyrunes⁶, John H. Postlethwait⁷, Manfred Schartl⁸, Amaury Herpin¹, Sylvie Rétaux^{2*}, Yann Guiguen^{1*}

AFFILIATIONS

¹ INRAE, Fish Physiology and Genomics Laboratory, 35042 Rennes, France.

² Université Paris-Saclay, CNRS, Institut des Neurosciences Paris-Saclay, 91198 Gif sur Yvette, France.

³ Getplage INRAE, US 1426, GeT-PlaGe, Genotoul, Castanet-Tolosan, France.

⁴ Institut de Génomique Fonctionnelle, IGF, CNRS, INSERM, Univ. Montpellier, F-34094 Montpellier, France.

⁵ SIGENAE, GenPhySE, Université de Toulouse, INRAE, ENVT, Castanet Tolosan, France.

⁶ Institut des Sciences de l'Evolution de Montpellier (ISEM), Université de Montpellier, 34095 Montpellier, France.

⁷ Institute of Neuroscience, University of Oregon, Eugene, USA.

⁸ Department of Physiological Chemistry, University of Wuerzburg, Wuerzburg, Germany.

*Corresponding Authors: Yann Guiguen, INRAE, Laboratoire de Physiologie et Génomique des poissons, Campus de Beaulieu, 35042 Rennes cedex, France. Tel: +33 2 99 46 58 09, E-mail: yann.guiguen@inrae.fr ; Sylvie Retaux, Université Paris-Saclay, CNRS, Institut des Neurosciences Paris-Saclay, 91198 Gif sur Yvette, France. E-mail: sylvie.retaux@cnrs.fr

Key words: microevolution, Sex determination, mexican tetra, B-sex chromosome, *gdf6b-B*

ABSTRACT

Teleost fishes employ a high diversity of sex determination (SD) mechanisms ranging from strict chromosomal control to environmental factors over this process. Comparative studies on master SD genes and sex chromosomes evolution within distantly or closely related species revealed that MSD genes and their associated sex chromosomes could display either a high degree of conservation or a rapid evolution depending on the species groups. Following the discovery of the “unusual” B-sex chromosome system and its gdf6b-B loci in *A. mexicanus* inhabiting the Pachón cave, the main aim of this study is to explore whether this B-sex chromosome and gdf6b-B are conserved in the different populations and morphotypes of this species. Here we report the potential conservation of gdf6b-B located on its B microchromosome (gdf6b-B) in wild cavefish and Mexican surface fish populations of the El Abra region. Moreover, we show that this MSD gene is either totally absent in the cavefish populations of the Guatemala region or partially sex-linked in the laboratory surface fish stocks. Altogether our results give a first insight to a novel case of an intra-population turnover of SD systems suggesting transitions from a fixed and dominant B-sex chromosomal system to a potential polygenic system relying only partially on male-dominant B-sex chromosome.

INTRODUCTION

Among vertebrates, Teleosts species exhibit the most amazing variability in their sex determination (SD) mechanisms. In gonochoristic fish species, sex is controlled either by genetic factors (GSD), environmental factors (ESD) or a combination of both (Bachtrog et al., 2014; Devlin & Nagahama, 2002; Heule et al., 2014). Most of the documented species have a monofactorial GSD system either with XX/XY or ZZ/ZW sex chromosomes (Herpin & Schartl, 2015; Pan et al., 2018). In addition to simple monofactorial systems in which a unique master sex-determining (MSD) gene is found in the heterogametic sex-chromosome, examples of polygenic sex determination systems with several alleles on the same sex locus or multiple alleles on several sex chromosomes have been also described in fish (Kikuchi & Hamaguchi, 2013; Mank & Avise, 2009; Moore & Roberts, 2013; Roberts et al., 2016).

Although all MSD genes characterized so far are located on classical sex chromosomes known as "A chromosomes", several reports have argued for a role of B chromosomes in sex determination (Camacho et al., 2011; Clark & Kocher, 2019; Reed, 1993; Yoshida et al., 2011). The first experimental and functional evidence for such a role comes from the case of the *Astyanax mexicanus* Pachón blind cavefish, in which the MSD gene *gdf6b-B* (*growth differentiation factor 6b* on B chromosomes) is harbored by the male-dominant B-sex chromosomes, hence revealing an unusual sex chromosome system (Imarazene et al., *in prep*). These findings highlight an additional dimension to the extraordinary complexity and diversity of sex chromosomes in fish.

To date, most of the comparative studies carried out on MSD genes and sex chromosomes evolution have focused on distantly or closely related species at a rather macro-evolutionary scale, such as the Esociformes, medaka, salmonid, and cichlid groups (Gammerdinger & Kocher, 2018; Myosho et al., 2015; Pan et al., 2020; Yano et al., 2013). However, studies on sex chromosomes and MSD gene turnovers within a single species would provide a more detailed picture of their potential rapid evolution. In this regard, the Mexican tetra, *Astyanax mexicanus* is an attractive model species for micro-evolutionary studies and has become popular for understanding adaptation to life underground. The species comprises fully-eyed surface-dwelling morphs inhabiting the rivers of the southern United States and Central America, as well as about 30 blind and depigmented cave-dwelling populations distributed in northeastern Mexico (Elliott, 2019; Espinasa et al., 2018; Mitchell et al., 1977). The cave-adapted populations are endemic to the caves of the Sierra de El Abra, Sierra de Guatemala

and Sierra de Colmena located in the states of San Luis Potosi and Tamaulipas (Elliott, 2019; Espinasa et al., 2018; Mitchell et al., 1977). Despite displaying morphological and behavioural differences, surface and cave morphs can breed together giving rise to viable and fertile offspring (Casane & Rétaux, 2016; Şadoğlu, 1957). In fact, recent studies have suggested that cave populations derived from surface-like ancestors colonized caves very recently, about 20,000 years ago (Fumey et al., 2018; Policarpo et al., 2020). Today, some cave populations are still undergoing an introgression of the surface forms living in the nearby rivers. Furthermore, the migration of cavefish between different caves using underground flows has also been suggested. Moreover, some cave-dwelling populations have adapted to life underground in a partly convergent manner, as their striking depigmented and blind phenotypes are controlled by different gene sets or even different mutations fixed on the same genes (Borowsky, 2008; Protas et al., 2006). Interestingly, it has been shown that crosses between cavefish populations originating from geographically distant caves give rise to eyed-progeny, suggesting their independent evolution in the subterranean environment (Borowsky, 2008).

All together, these data make *Astyanax mexicanus* an essential model for exploring the evolutionary history of a B-sex chromosome from a micro-evolutionary point of view. In fact, some reports have revealed some odd sex-ratios in different *A. mexicanus* populations (Elipot et al., 2014; Wilkens & Strecker, 2017) suggesting possible evolutionary variations in their SD mechanisms.

Following the identification of a B-sex chromosome and its *gdf6-B* duplicated gene in the Pachón cavefish population inhabiting the sierra de El Abra, we sought to assess the dynamics of B-sex chromosome and MSD gene at a micro-evolutionary scale in that species. Taking advantage of the accessibility of various *A. mexicanus* populations, we expanded our comparative analyses of SD to other wild and lab-raised surface fish and cavefish stocks. Our results show the conservation of *gdf6b* located on its B microchromosome (*gdf6b-B*) in wild cavefish populations of the El Abra region as well as in Mexican surface fish populations. Conversely, this MSD gene seemed absent in the cavefish populations of the Guatemala region. Furthermore, we provide evidence for a potentially polygenic SD system in the Texas surface fish population, with the male-dominant B-sex chromosome and its *gdf6b-B* locus operating as the sex determination system in some males, and another sex determinism acting in the other males and females. This study highlights a novel case of an intra-population turnover of SD systems suggesting transitions from a fixed and dominant B-sex chromosomal system to a polygenic system relying only partially on male-dominant B-sex chromosome.

RESULTS

Identification of a partial sex-linkage of *gdf6b-B* with male phenotype

We have recently characterized a monofactorial GSD system with *gdf6b-B* (*growth differentiation factor 6b* on the B chromosome) as the potential master sex determining gene in *Astyanax mexicanus* Pachón cavefish (Imarazene et al., *in prep*). Here, we investigated the sex determination system(s) in a surface population of the species originating from San Solomon spring (Texas, USA), raised in the laboratory since 2004. Deviated sex-ratios had been reported in laboratory breedings of different populations of surface-dwelling *A. mexicanus* (Wilkens & Strecker, 2017), suggesting the co-existence of different SD systems and / or environmental effects on SD.

Based on that possibility, we first investigated a potential effect of temperature, i.e., environmental influence on SD. We carried out two independent experiments in order to determine the sex-ratios of Texas surface fish reared under two different temperature conditions (21 °C and 28 °C). Sex-ratios were found to be not different from a 1:1 sex-ratio at 21 °C in both experiments (Table 1). At 28 °C, sex-ratios were either not different from a 1:1 sex-ratio (first experiment), or significantly biased towards females (second experiment; Table 1). These findings confirmed that the SD system in surface fish seemed different from the strictly monofactorial GSD system of the Pachón cave population.

We next explored sex-linkage of the *gdf6b-B* loci in this Texas surface fish population, as these loci was found to be completely sex-linked in Pachón cavefish (Imarazene et al., *in prep*). To do so, we amplified the exon 1 and exon 2 as well as the intron 1 of this gene, both in males and females. We found an incomplete sex-linkage of *gdf6b-B* with the male phenotype. In fact, all phenotypic females (n=615) presented a single PCR fragment (~1.1 kb) along with 45.8% of the phenotypic males (n=231 over 504). All the other males (54.2%, n=273) displayed two bands, including the ~1.1 kb band plus another one of ~600 bp. Males with a female PCR genotype were named males- and the males with two bands were referred to as male⁺ (Figure 1B). To clarify these genotypes, we sequenced these *gdf6b* genomic fragments and we assembled the sequences to generate a consensus gene sequence in both sexes. Alignments with Pachón cavefish sequences showed that the 1.1 kb band corresponds to the A chromosome copy of the *gdf6b* gene (*gdf6b-A*), while the ~600 bp band amplified in 45% of the males corresponds to its B chromosome gene copies (*gdf6b-B*) (Figure 1C). Of note, the surface fish male-specific *gdf6b-B* gene and the previously characterized Pachón cavefish *gdf6b-B* gene

shared some polymorphism in their coding sequence (CDS), i.e., at position 591 bp of the CDS, further reinforcing its annotation as a potential *gdf6b-B* gene (Figure 1B). However, in the surface fish *gdf6b-B* copy, an additional deletion of approximately 500 bp in the intron and several other variations in the CDS were found. This included 2 synonymous variations (at positions 120 and 591 of the CDS), 3 nonsynonymous variations changing the amino acids of the Gdf6b-B protein (at positions 233 bp in exon 1, and 868 and 1115 bp in exon 2), and a 18 bp deletion causing a deletion of 6 amino acids in the Gdf6b-B protein (Figures 1C). Altogether, these results suggested a partial association of putative surface fish *gdf6b-B* gene and the male phenotype, consistent with the hypothesis that the sex determination system in Texas surface fish is different from a simple monofactorial GSD system driven by a B-sex chromosome that we previously characterized in Pachón cavefish.

The presence of B microchromosomes correlates with *gdf6b-B* in Texas surface fish

To determine the relationship between the presence of B microchromosomes (Bs) and the putative *gdf6b-B* copy, and to test whether these Bs could be only present in certain phenotypic males in Texas surface fish, we performed cytogenetic analyses in females, males⁺ and males-. Like Pachón cavefish, Texas surface fish have a diploid number (2n) of 50 A chromosomes, plus some additional B microchromosomes (Figure 2; Table 2) in agreement with previous results (Kavalco & De Almeida-Toledo, 2007). Interestingly, B microchromosomes were found in all males⁺ (n=4/4), with all their metaphases (100%) carrying either one or two Bs (Table 2). Conversely, B microchromosomes were found only in one female (n=1/6) and one male- (n=1/2), in which they were detected only in a small proportion of metaphases (5% or 16%; Table 2). Altogether, these findings revealed a male⁺-dominant B microchromosome, suggesting that when present in males this B microchromosome could also be a B-sex chromosome in the Texas surface fish population. However, the fact that a large proportion of phenotypic males do not have this B-sex chromosome also suggest the existence of an additional sex determination mechanism.

Searching for additional sex-linked markers and sex-determining regions in *Astyanax mexicanus* surface fish

Our results above strongly could suggest the existence of a multifactorial sex determination system with a partial involvement of *gdf6b-B* triggering the sex in the Texas surface fish. We then performed genome-wide association analysis using RAD-Seq data in surface fish contrasting 30 females, 14 males⁺ and 12 males-. We identified a total of 67 polymorphic

markers that were found in all males⁺ and that were completely absent in the males- and in all phenotypic females (Figure 3). These 67 marker sequences were then blasted against the *Astyanax mexicanus*-2.0 female surface fish genome assembly (GCF_000372685.2) and one of them returned an annotated gene corresponding to the *gdf6b* locus. Conversely to the 47 markers identified in males⁺, none of the RAD-seq markers from this analysis showed significant association with the females nor the males-. These findings further support the partial albeit very strong association of *gdf6b-B* with the sex determination in some Texas surface fish males.

To decipher the SD system and potentially identify an additional sex locus with higher resolution in our Texas surface fish population, we adopted a pool-seq strategy using three gDNA pools from 66 females, 66 males⁺ and 66 males- allowing whole genome comparison in a pair-wise manner (Gammerdinger et al., 2014). The pool-seq reads were remapped on the *Astyanax mexicanus*-2.0 female surface fish genome assembly (GCF_000372685.2) and pool-specific SNPs were computed in the different linkage groups (LGs) and unplaced scaffolds. Results from these analyses showed a strong male⁺-biased pattern with a high number of “apparent” male⁺-specific indels and heterozygous sites distributed throughout 4 different LGs (LG3, LG7, LG9, and LG14) (Figure 4A) and several unplaced scaffolds (Figure 4B). Such multiple signals were previously reported in the Pachón cavefish population (Imarazene et al., *in prep*), and were interpreted as a false “apparent” remapping of the male-dominant B microchromosome reads on the A chromosome segments of a female genome that does not contain a B chromosome sequence. Therefore, the present results obtained for the Texas surface population also suggested that these patterns could represent duplicated A segments specifically on the B microchromosomes of the males⁺. Having localized *gdf6b-B* on scaffold NW_019172904.1 in the Pachón cave population, we analyzed the genomic sequence of the *gdf6b* locus by remapping the pool-seq data of the 3 groups i.e., Texas surface fish females, males-, and males⁺ on this scaffold (Figure 5A). The coverage comparison of the pool-seq reads between these three groups clearly showed a high coverage in the *gdf6b* locus in males⁺. Such a high coverage was also observed in Pachón cavefish where *gdf6b-B* is duplicated in two copies on the B chromosomes of males (Imarazene et al. *in prep*). This suggests that the *gdf6b-B* of Texas surface fish is also likely duplicated on the specific B microchromosomes of males⁺. This was further supported by TaqMan assays showing a significantly higher copy number of *gdf6b* in males⁺ compared to males- and females (Figure 5B). Besides these strong male⁺-specific signals, no clear sex-biased signal has been found between the female- and male- pools

suggesting that if a secondary sex locus is present in the Texas surface population, this sex locus is too small to be detected by RAD-seq or pool-seq approaches.

***Gdf6b-B* in wild cavefish and surface fish populations**

Finally, to investigate whether sex-linkage is a general feature of *gdf6b-B* and B microchromosomes in other *A. mexicanus* populations, we extended our study to wild cavefish and surface fish populations. For that purpose, we analyzed tail fin clip samples from wild-caught individuals covering the different regions in northeastern Mexico where the *A. mexicanus* surface fish and cavefish populations are localized, and collected over the past 10 years. This included the cavefish populations of the El Abra group (Pachón, Los Sabinos, Tinaja, Curva, Toro and Chica), the Micos group (Subterraneo), and the Guatemala group (Molino, Jineo and Escondido) (Figure 6A). In addition, two different Mexican wild surface fish locations were sampled in 2016, including the Arroyo Tampe mole near the village of El Barranco (Rio Guayalejo drainage) (and the Rio Gallinas near Rascon (Rio Tampaon drainage) (Figure 6A). To screen for the presence of *gdf6b-B* and the B-sex chromosome in these populations, we designed primers to amplify almost the entire exon 2 of *gdf6b-B* and its 3' region that are B chromosome-specific. These specific primers were first tested and validated in our laboratory Pachón cavefish population where all males (n=30) displayed a single band, while all females (n=30) displayed no band, indicating the specificity of this genotyping test and confirming the *gdf6b-B* locus as male sex-specific in our Pachón laboratory stock.

For wild-caught cavefish samples, dissection and histological analysis to determine phenotypic sex was not available as these specimens were fin-clipped and returned alive to their natural habitat. Hence, morphologically unidentifiable individuals (based on presence/absence of anal fin denticles; abdomen shape; eggs sometimes visible) were referred to as “undetermined” (Figure 6B). A significant sex-linkage, with *gdf6b-B* present in 100% of males and 0% of the females was found in the cave-dwelling and blind *A. mexicanus* populations sampled in the Pachón, Los Sabinos, Tinaja, and Curva caves. This was also true in the Toro natural hybrid cave population which undergoes introgression with surface fish living in the nearby rivers (Espinasa et al., 2020), and possibly in Chica, also a natural hybrid population, even though in this case the phenotypic sex of individuals was unknown (Figure 6B). This indicates that sex could be also determined by the B-sex chromosome harboring the *gdf6b-B* locus as a MSD gene in these natural *A. mexicanus* populations, all localized in the El Abra region -the group from which our laboratory Pachón cavefish is derived (Figure 6). In *A. mexicanus* native to the

Subterraneo cave localized in the Micos region, which also contains natural hybrid fishes due to frequent introgression events, the *gdf6b-B* gene was found in only 1 out of 16 “undetermined” individuals. Finally, in the Molino, Jineo, and Escondido blind cavefish populations belonging to the Guatemala group, the *gdf6b-B* locus was not found, possibly because of the conjunction of the small sampling sizes and unknown phenotypic sex (Figure 6). On the other hand, a complete sex-linkage with *gdf6b-B* was detected in 100% of male samples and 0% of female samples in the wild surface river-dwelling populations native to the Rio Gallinas in Rascon (N males = 26; N females = 10) and the Arroyo Tampemole (N males = 9; N females = 29) rivers (Figure 6B). These findings strongly suggest that these wild Mexican populations have a simple monofactorial GSD system ruled by a B-sex chromosome and *gdf6b-B* as a master sex determining gene, conversely to what we found in our laboratory surface fish strain native to the San Solomon Spring (Texas). Taken together, these results show that the B-sex chromosome and its *gdf6b-B* locus are conserved features of SD system in wild populations of *A. mexicanus*, at least in the cavefish populations from the El Abra (and possibly Micos) region and in the wild Mexican surface fish investigated in this study.

DISCUSSION

Our previous work on the laboratory Pachón cavefish *A. mexicanus* revealed a monofactorial GSD system, in which the sex of individuals is governed by an unusual sex chromosome i.e., a male-dominant B-sex chromosome harboring the *gdf6b-B* MSD gene (Imarazene et al., *in prep*). Here, we extend this finding to wild *A. mexicanus* populations in Mexico including several cave populations from the El Abra group i.e., Pachón, Los Sabinos, Tinaja, Curva, Toro and Chica. In these populations, we found evidences for a conserved monofactorial GSD system in agreement with the unbiased, 1:1 sex-ratios previously observed in the Pachón cave laboratory-raised population originating from this region (Wilkens & Strecker, 2017).

However, this B-sex chromosome system and their *gdf6b-B* MSD genes may not be conserved in all *Astyanax* cavefish populations. Indeed, we failed to detect *gdf6b-B* in cavefish populations belonging to the Guatemala group. We cannot exclude that all sampled individuals were females or that our primers failed to amplify the *gdf6b-B* locus in Molino, Jineo, and Escondido, maybe, because of some population-specific sequence variations preventing a specific PCR amplification with primers designed on other population-specific sequences. In fact, the unbiased sex-ratios that have been reported in laboratory stock of the Molino cavefish

population suggests a monofactorial GSD system (Wilkens & Strecker, 2017). The possibility that this Molino population does not have a B-sex chromosome and the *gdf6-B* genes is also attested by preliminary results (data not shown) of the remapping of some publicly available whole genome Molinos datasets that did not show any signature of a potential conserved B-sex chromosome in this population. Indeed, here also sex phenotypes were not recorded and we cannot exclude that all these sequenced individuals were all females or eventually B minus males. Of note, an incomplete association of the B microchromosome with the male phenotype has been also reported in a commercial pet shop cavefish stock (Ahmad et al., 2020). Further, in-depth investigations in the Guatemala group using fish with known phenotypic sex and additional sequencing data of sex phenotyped individuals will be required to elucidate this hypothesis of a rapid sex chromosome turnover at the population level.

For Mexican surface fish, our results also showed a complete association of the *gdf6b-B* with the male phenotype in two wild surface fish populations originating from the Rio Gallinas and the Arroyo Tampemole, SLP, Mexico. This is in line with our findings in Pachón laboratory-raised cavefish (Imarazene et al., *in prep*) and in wild cavefish El Abra populations (current study), hence suggesting that *gdf6b* genes on the B microchromosome could also operate as MSD genes in these Mexican surface fish populations. In our laboratory stock of Texas surface fish, however, the duplicated *gdf6b-B* displayed an incomplete sex-linkage with the male phenotype. This could suggest a non-monofactorial SD system with the partial involvement of a B-sex chromosome and its *gdf6b-B* genes that would act as a dominant male determining factor in all Bs-carrying males. Again, these results are similar to what has been reported in a commercial pet shop cavefish, in which B chromosomes were found in some males and totally absent from others as well as in all the females (Ahmad et al., 2020). However, the lack of information about the precise origin of the samples obtained in this study makes it difficult to draw a clear scenario. Nevertheless, it appears obvious that the B microchromosomes were totally absent in some males and all females in our laboratory Texas surface fish population and that of Ahmad et al (Ahmad et al., 2020), demonstrating a more complex SD system in some populations of *A. mexicanus*.

Biased sex-ratios towards females or males were also observed in different laboratory stocks of surface fish populations, independently from their origin (Wilkens & Strecker, 2017), supporting our hypothesis of population differences in sex determination in *A. mexicanus*. To date, it is widely shown that environmental cues (i.e., temperature, pH, or density) can modulate the monofactorial GSD system in a number of fish species (Baroiller et al., 2009; Devlin &

Nagahama, 2002), and even in species with a strong GSD like for instance in medaka (Cheung et al., 2014; Sato et al., 2005). Temperature is likely the most described environmental factor that is able to override the GSD system in some fish species (Baroiller & D'Cotta, 2016; Ospina-Alvarez & Piferrer, 2008). In such cases, the effect of temperature occurs quite early, during larval and post-larval stages (Baroiller et al., 1999; Devlin & Nagahama, 2002). In the present study, we detected a biased sex-ratio towards females after raising Texas surface fish at 28°C (but not at 21°C). However, we do not interpret it as a temperature effect since all produced females had a genuine female genotype (all *gdf6b-B* negative). Other complex, unknown mechanisms may have occurred to explain this result.

An interesting possibility would be that sex determination in our surface fish Texas laboratory stocks relies on a polygenic SD: *gdf6b-B* would act as a male sex determinant on the B microchromosome, together with another sex-determining gene harbored by another sex-chromosome. However, we currently failed to detect any other sex-biased markers between Texan surface females and B negative males using both RAD-seq and pool-seq approaches. This suggests that if a secondary sex locus is present in this surface population it is too small to be detected using these whole genome strategies. Re-analyses using for instance our new Pachón cave genome assembly, could provide more precise results as this new genome assembly is less fragmented. The question then remains unanswered whether a secondary and potentially polygenic GSD system is present in this laboratory Texas surface fish population, and potentially also in other populations (Ahmad et al., 2020; Wilkens & Strecker, 2017). Such polygenic SD systems have been described in a few fish species (Kallman, 1984; Moore & Roberts, 2013; Roberts et al., 2016). In zebrafish, wild strains have ZZ/ZW sex determination, but laboratory strains lost their W chromosome after a few decades of breeding (Wilson et al., 2014), and their SD system has evolved towards an unknown polygenic system (Liew et al., 2012; Liew & Orbán, 2014) which is subject to environmental effects (Ribas et al., 2017; Santos et al., 2017). A similar hypothesis could be also proposed in the Texas laboratory surface population as we cannot completely rule out the idea that the B-sex chromosomes may have been introgressed from a B-sex carrying population during the early domestication phases of what may have been an initial B-minus Texas surface laboratory population. In line with this hypothesis many early genetic experiments in cavefish have used cross-populations breeding strategies and the introgression of a B chromosome is probably a likely event. The exploration of wild Texan populations of *A. mexicanus* would be needed to confirm or infirm this hypothesis. But the relatively high divergence between the *gdf6b-B* locus sequence of Pachón

cave and its homologous region in Texas surface laboratory population tends to contradict this hypothesis of a recent introgression of the Pachón cave B-sex chromosome in the laboratory Texan surface population.

Sex chromosome turnover is thought to be caused by the emergence of a new MSD gene by genetic drift (Bull & Charnov, 1977; Saunders et al., 2018), its linkage to sexually antagonistic alleles (Doorn & Kirkpatrick, 2007; Doorn & Kirkpatrick, 2010), or deleterious mutational load (Blaser et al., 2013). Sex chromosome turnovers could lead to the change of heterogamety (Bull & Charnov, 1977). A scenario of the emergence of a new SD system with a new sex chromosome and its interaction with environmental cues after a few years and generations of rearing might be considered for laboratory *A. mexicanus* Texas surface fish. However, further studies are needed to better characterize the complex sex determination system in laboratory surface fish.

In terms of geography, it is interesting to note that the distant Texas surface fish population (and maybe the northernmost Guatemala cave populations, to be confirmed) are different from all other populations of Mexican surface fish and cavefish we have studied and in which *gdf6b-B* is strongly or completely sex-linked. If any, the difference between Guatemala and El Abra caves can be attributed to the independent origins of *A. mexicanus* populations in these two groups (Borowsky, 2008; Bradic et al., 2012). Now regarding the established Mexico/Texas difference, the sequence comparison between the Pachón cavefish and the surface fish (Texas) *gdf6b-B* showed substantial differences in the non-coding region (e.g., intron) as well as the coding sequence. In fact, the *gdf6b-B* CDS of surface fish accumulated several amino acid changing nucleotide variations and a 6 amino acids deletion in the propeptide TGF- β domain (Figure S1), but this gene is still sex-linked in at least 50% of males in this population. It would therefore be interesting to investigate whether these mutations have a role in the rapid transition of the SD system in this species.

In conclusion, our study provides a first insight to the quick evolutionary transition of SD systems in *A. mexicanus* populations, between what could be a complex and eventually polygenic sex determination system in the laboratory Texas surface fish population and a monofactorial GSD system in almost all the Mexican populations.

MATERIAL AND METHODS

Statement of Ethics

All animal protocols were carried out in strict accordance with the French and European legislations (French decree 2013-118 and directive 2010-63-UE) applied for ethical use and care of laboratory animals used for scientific purposes. SR's and CNRS authorizations for maintaining and handling of *A. mexicanus* in experimental procedures were 91-116 and 91272105, respectively.

Laboratory Astyanax mexicanus surface fish breeding and sampling

Laboratory stocks of *A. mexicanus* surface fish endemic to Texas (USA) rivers were obtained in 2004 from the Jeffery laboratory at the University of Maryland, College Park, MD, USA and were since then reared in our experimental facilities (Gif sur Yvette, France). Fish husbandry and tail fin clip sampling protocols were performed as described in (Imarazene et al., 2020; *in prep*).

Animal sampling for karyotypic analysis

Six females, 4 genetic males⁺ and 2 phenotypic males- of laboratory Texas surface fish, *Astyanax mexicanus* were prepared for karyotypic analysis. For preparation, fish were first anaesthetized in a Eugenol bath (60 µl/L) during ~ 3 minutes. Animals were then injected with yeast solution (20 µl/1g of weight) below the dorsal fin and kept individually in an oxygenated water for 24 hours (h) at 28 °C or 48 h at 26 °C in the dark. The fish were anaesthetized a second time with the same concentration of Eugenol and subsequently injected with 0.25% colchicine (20 µl/1g of weight). Finally, male and female individuals were kept in their tanks for one hour before being euthanized by a lethal dose of Eugenol (1.5 ml/L).

Wild cavefish and surface fish sampling

Several sampling campaigns were carried out in the field between 2013 and 2019 resulting in a collection of tail fin clips of several cavefish and surface fish populations. In the field, the phenotypic sex of animals was determined by checking the presence or absence of denticles on the anal fins as described previously in (Elipot et al., 2014). The presence/absence of denticles was verified independently by 3 researchers. In addition, pictures of each individual sampled

were taken to confirm the phenotypic sex in the laboratory based on the morphological criteria described previously (Elipot et al., 2014). The permits for field sampling (02241/13, 02438/16, 05389/17 and 1893/19) were delivered by the Mexican authorities (Mexican Secretaría del Medio Ambiente y Recursos Naturales) to Sylvie Rétaux and Patricia Ornelas-Garcia.

DNA extraction

For fish genotyping, gDNA was obtained from tail fin clips stored in ethanol 90%, after lysis in 5% chelex and 10 mg Proteinase K at 55°C for 2 h, followed by 10 min at 99°C (Gharbi et al., 2006). Following extraction, samples were centrifuged and the supernatant containing the gDNA was transferred in clean tubes and stored at -20°C. For pool-sequencing (pool-seq) and RAD-sequencing (RAD-seq), gDNA was extracted using NucleoSpin Kits for Tissue (Macherey-Nagel, Duren, Germany) according to the supplier's recommendations. The DNA concentrations for both pool-seq and RAD-seq were quantified with Qubit3 fluorometer (Invitrogen, Carlsbad, CA).

Primer and probe designing

All primers used in this study including PCR genotyping and TaqMan assays were designed using Primer3web software version 4.1.0 (Kõressaar et al., 2018) and are listed in Table S1.

Sex-specific genotyping PCR test

For laboratory surface fish, the genetic sex of individuals was determined by a PCR test using primers designed to amplify specifically the *gdf6b* intron 1 using the Jumpstart™ Taq DNA Polymerase (Sigma-Aldrich). PCRs were performed in a total volume of 50 µl containing 0.5 µM of each primer, a final concentration of 20 ng/µl gDNA, 10 µM dNTPs mixture, 1X of Jumpstart™ buffer (10X), and 2.5U/reaction of Jumpstart™ Taq DNA polymerase. Cycling conditions were as follows: 95°C for 2 min, then 35 cycles of (95°C for 30 seconds (sec) + 60°C for 30 sec + 72°C for 1 min and 30 seconds (sec)), and 72°C for 5 min. For wild surface fish and cavefish populations, specific primers (Table S1) were designed to amplify only the *gdf6b-B* copy based on the sequence of *gdf6b* on the B microchromosome of Pachón cavefish *A. mexicanus*. PCRs were carried out in a total volume of 50 µl containing 0.5 µM of each primer, a final concentration of 20 ng/µl gDNA, 10 µM dNTPs mixture, 1X of Jumpstart™ buffer (10X), and 2.5U/reaction of Jumpstart™ Taq DNA polymerase. Cycling conditions were

as follows: 95°C for 2 min, then 35 cycles of (95°C for 30 seconds (sec) + 60°C for 30 sec + 72°C for 2 min), and 72°C for 5 min.

Chromosome preparation and conventional cytogenetics

Mitotic or meiotic chromosome spreads were obtained by direct preparation from the cephalic kidney. The quality of chromosomal spreading was enhanced by a dropping method described by (Bertollo et al., 2015). Chromosomes were stained with 5% Giemsa solution (pH 6.8) (Merck, Darmstadt, Germany) for a conventional cytogenetic analysis, or left unstained for other methods. Constitutive heterochromatin was visualized by C-banding according to (Haaf & Schmid, 1984), with chromosomes being counterstained by 4',6-diamidino-2-phenolindole (DAPI) at 1.5 µg/mL in antifading medium (Cambio, Cambridge, United Kingdom).

Microscopy and image analysis

At least 50 metaphase spreads per individual were analyzed to confirm the diploid chromosome number ($2n$) karyotype structure. Giemsa-stained preparations were analyzed under Axio Imager Z2 microscope (Zeiss, Oberkochen, Germany), equipped with automatic Metafer-MSearch scanning platform. Photographs of the chromosomes were captured under $100\times$ objective using CoolCube 1 b/w digital camera (MetaSystems, Altlussheim, Germany). The karyotypes were arranged using Ikaros software (MetaSystems, Altlussheim, Germany). Chromosomes were classified according to their centromere positions according to (Levan et al., 1964), but modified as metacentric (m), submetacentric (sm), subtelocentric (st), or acrocentric (a).

Restriction-site association sequencing (RAD-seq) and male-marker discovery

RAD-seq library was constructed from Genomic DNA of 30 phenotypic females and 26 phenotypic males according to the standard protocols (Amores et al., 2011; Baird et al., 2008). Briefly, for each sample, 1 µg of DNA was digested with the restriction enzyme *SbfI* and then purified using AMPure PX magnetic beads (Beckman Coulters). Subsequently, each sample was ligated to one indexed P1 adapter using concentrated T4 DNA ligase (NEB) followed by a second purification step using AMPure XP magnetic beads. Before pooling in equal amounts, samples were quantified using microfluorimetry (Qubit dsDNA HS assay kit, Thermofisher). Following this step, the pool was fragmented on a Biorputor (Diagenode) and purified using a

Minelute column (Qiagen). Sonicated DNA was size selected on an 1,5% agarose cassette aiming for an insert size of 300 bp to 500 bp, extracted from the gel using the Qiaquick gel extraction kit (Qiagen), repaired using the End-It DNA-end repair kit (Tebu Bio) and finally adenylated on its 3' ends using Klenow (exo-) (Tebu-Bio). P2 adapter was ligated using concentrated T4 DNA ligase (NEB) and 50 ng of the ligated product was engaged in a 12 cycles PCR followed by AMPure XP beads purification. The library was checked on a Bioanalyzer (Agilent) using the DNA 1000 kit and quantified by qPCR using the KAPA Library quantification kit (Roche, ref. KK4824). The library was sequenced on one lane of Hiseq2500 in single read 100 nt mode using the clustering and SBS v3 kit following the manufacturer's instructions. The RAD-seq reads were analyzed using the RADSex pipeline (Feron et al., 2020).

Pool-sequencing libraries preparation and data analysis

DNA was collected from 66 males⁺, 66 males-, and 66 phenotypic females (laboratory Texas surface fish) and was pooled as male⁺, males-, and female pools separately. Before pooling, the DNA concentration was normalized in order to obtain an equal amount of each individual genome representation in the final pool. Pool-sequencing libraries were prepared with the same protocol as the one used for the Pachón cavefish *A. mexicanus* (Imarazene et al., *in prep*). Sequencing produced 116 839 236 of read pairs for the males⁺, 84 099 466 of read pairs for the males-, and 129 639 149 of read pairs for the females' pool libraries. The pool-seq reads obtained from the three groups were mapped onto the *Astyanax mexicanus*-2.0 female surface fish genome assembly (GCF_000372685.2) and the analyses were processed as described for the Pachón cavefish *A. mexicanus* (Imarazene et al., *in prep*).

TaqMan probe assay

TaqMan probe-based qPCR was used to determine the quantity of *gdf6b* in both sexes using *dmrt1* as an autosomal reference gene. The specific primers and probes are listed in Table S1. qPCRs were carried out in a total volume of 10 µl containing 4 µl of 20 ng/µl gDNA, 10 µM of each forward and reverse primer, 10 µM of each TaqMan probe, and 5µl of 2X TaqMan® Fast Advanced Master Mix (Applied Biosystem, carlsbad, USA). We used 40 cycles of amplification on a StepOne machine (Applied Biosystem, carlsbad, USA) following cycling conditions: a first denaturation step at 50 °C for 2 min, polymerase activation at 95 °C for 2 min, 40 cycles of denaturation (95 °C for 1 sec) and annealing/extension (60 °C for 20 sec).

Copy number variation was defined as *gdf6b/dmrt1* ratios of the mean quantity of three technical replicates for each sample.

REFERENCES

- Ahmad, S. F., Jehangir, M., Cardoso, A. L., Wolf, I. R., Margarido, V. P., Cabral-de-Mello, D. C., O'Neill, R., Valente, G. T., & Martins, C. (2020). B chromosomes of multiple species have intense evolutionary dynamics and accumulated genes related to important biological processes. *BMC Genomics*, 21(1), 656. <https://doi.org/10.1186/s12864-020-07072-1>
- Amores, A., Catchen, J., Ferrara, A., Fontenot, Q., & Postlethwait, J. H. (2011). Genome Evolution and Meiotic Maps by Massively Parallel DNA Sequencing: Spotted Gar, an Outgroup for the Teleost Genome Duplication. *Genetics*, 188(4), 799-808. <https://doi.org/10.1534/genetics.111.127324>
- Bachtrog, D., Mank, J. E., Peichel, C. L., Kirkpatrick, M., Otto, S. P., Ashman, T.-L., Hahn, M. W., Kitano, J., Mayrose, I., Ming, R., Perrin, N., Ross, L., Valenzuela, N., Vamosi, J. C., & Consortium, T. T. of S. (2014). Sex Determination: Why So Many Ways of Doing It? *PLOS Biology*, 12(7), e1001899. <https://doi.org/10.1371/journal.pbio.1001899>
- Baird, N. A., Etter, P. D., Atwood, T. S., Currey, M. C., Shiver, A. L., Lewis, Z. A., Selker, E. U., Cresko, W. A., & Johnson, E. A. (2008). Rapid SNP Discovery and Genetic Mapping Using Sequenced RAD Markers. *PLOS ONE*, 3(10), e3376. <https://doi.org/10.1371/journal.pone.0003376>
- Baroiller, Jean., D'Cotta, & E. S. (2009). Environmental effects on fish sex determination and differentiation. *Sexual Development: Genetics, Molecular Biology, Evolution, Endocrinology, Embryology, and Pathology of Sex Determination and Differentiation; Sex Dev*. <https://doi.org/10.1159/000223077>
- Baroiller, Jean-François, & D'Cotta, H. (2016). The Reversible Sex of Gonochoristic Fish: Insights and Consequences. *Sexual Development*, 10(5-6), 242-266. <https://doi.org/10.1159/000452362>
- Baroiller, J.-F., Guiguen, Y., & Fostier, A. (1999). Endocrine and environmental aspects of sex differentiation in fish. *Cellular and Molecular Life Sciences CMLS*, 55(6), 910-931. <https://doi.org/10.1007/s000180050344>
- Bertollo, L., Cioffi, M., & Moreira-Filho, O. (2015). Direct Chromosome Preparation from Freshwater Teleost Fishes (p. 21-26). <https://doi.org/10.1201/b18534-4>
- Blaser, O., Grossen, C., Neuenschwander, S., & Perrin, N. (2013). Sex-Chromosome Turnovers Induced by Deleterious Mutation Load. *Evolution*, 67(3), 635-645. <https://doi.org/10.1111/j.1558-5646.2012.01810.x>
- Borowsky, R. (2008). Restoring sight in blind cavefish. *Current Biology*, 18(1), R23-R24. <https://doi.org/10.1016/j.cub.2007.11.023>
- Bradic, M., Beerli, P., García-de León, F. J., Esquivel-Bobadilla, S., & Borowsky, R. L. (2012). Gene flow and population structure in the Mexican blind cavefish complex (*Astyanax mexicanus*). *BMC Evolutionary Biology*, 12, 9. <https://doi.org/10.1186/1471-2148-12-9>
- Bull, J. J., & Charnov, E. L. (1977). Changes in the heterogametic mechanism of sex determination. *Heredity*, 39(1), 1-14. <https://doi.org/10.1038/hdy.1977.38>
- Camacho, J. P. M., Schmid, M., & Cabrero, J. (2011). B Chromosomes and Sex in Animals. *Sexual Development*, 5(3), 155-166. <https://doi.org/10.1159/000324930>

- Casane, D., & Rétaux, S. (2016). Evolutionary Genetics of the Cavefish *Astyanax mexicanus*. *Advances in Genetics*, 95, 117-159. <https://doi.org/10.1016/bs.adgen.2016.03.001>
- Cheung, C. H. Y., Chiu, J. M. Y., & Wu, R. S. S. (2014). Hypoxia turns genotypic female medaka fish into phenotypic males. *Ecotoxicology*, 23(7), 1260-1269. <https://doi.org/10.1007/s10646-014-1269-8>
- Clark, F. E., & Kocher, T. D. (2019). Changing sex for selfish gain: B chromosomes of Lake Malawi cichlid fish. *Scientific Reports*, 9(1), 20213. <https://doi.org/10.1038/s41598-019-55774-8>
- Devlin, R. H., & Nagahama, Y. (2002). Sex determination and sex differentiation in fish: An overview of genetic, physiological, and environmental influences. *Aquaculture*, 208(3), 191-364. [https://doi.org/10.1016/S0044-8486\(02\)00057-1](https://doi.org/10.1016/S0044-8486(02)00057-1)
- El-Gebali, S., Mistry, J., Bateman, A., Eddy, S. R., Luciani, A., Potter, S. C., Qureshi, M., Richardson, L. J., Salazar, G. A., Smart, A., Sonnhammer, E. L. L., Hirsh, L., Paladin, L., Piovesan, D., Tosatto, S. C. E., & Finn, R. D. (2019). The Pfam protein families database in 2019. *Nucleic Acids Research*, 47(D1), D427-D432. <https://doi.org/10.1093/nar/gky995>
- Eliot, Y., Legendre, L., Père, S., Sohm, F., & Rétaux, S. (2014). *Astyanax* transgenesis and husbandry: How cavefish enters the laboratory. *Zebrafish*, 11(4), 291-299. <https://doi.org/10.1089/zeb.2014.1005>
- Elliott, W. R. (2019). The *Astyanax* Caves of Mexico: Cavefishes of Tamaulipas, San Luis Potosí, and Guerrero. *Journal of Fish Biology*, 94(1), 205-205. <https://doi.org/10.1111/jfb.13889>
- Espinasa, L., Legendre, L., Fumey, J., Blin, M., Rétaux, S., & Espinasa, M. (2018). A new cave locality for *Astyanax* cavefish in Sierra de El Abra, Mexico. *Subterranean Biology*, 26, 39-53. <https://doi.org/10.3897/subtbiol.26.26643>
- Espinasa, L., Ornelas-García, C. P., Legendre, L., Rétaux, S., Best, A., Gamboa-Miranda, R., Espinosa-Pérez, H., & Sprouse, P. (2020). Discovery of Two New *Astyanax* Cavefish Localities Leads to Further Understanding of the Species Biogeography. *Diversity*, 12(10), 368. <https://doi.org/10.3390/d12100368>
- Feron, R., Pan, Q., Wen, M., Imarazene, B., Jouanno, E., Anderson, J., Herpin, A., Journot, L., Parrinello, H., Klopp, C., Kottler, V., Roco, A., Du, K., Kneitz, S., Adolfi, M., Wilson, C., McCluskey, B., Amores, A., Desvignes, T., ... Guiguen, Y. (2020). RADSex : A computational workflow to study sex determination using Restriction Site-Associated DNA Sequencing data. <https://doi.org/10.1101/2020.04.22.054866>
- Fumey, J., Hinaux, H., Noirot, C., Thermes, C., Rétaux, S., & Casane, D. (2018). Evidence for late Pleistocene origin of *Astyanax mexicanus* cavefish. *BMC Evolutionary Biology*, 18(1), 43. <https://doi.org/10.1186/s12862-018-1156-7>
- Gammerdinger, W. J., Conte, M. A., Acquah, E. A., Roberts, R. B., & Kocher, T. D. (2014). Structure and decay of a proto-Y region in Tilapia, *Oreochromis niloticus*. *BMC Genomics*, 15(1), 975. <https://doi.org/10.1186/1471-2164-15-975>
- Gammerdinger, W. J., & Kocher, T. D. (2018). Unusual Diversity of Sex Chromosomes in African Cichlid Fishes. *Genes*, 9(10), 480. <https://doi.org/10.3390/genes9100480>
- Gharbi, K., Gautier, A., Danzmann, R. G., Gharbi, S., Sakamoto, T., Hoyheim, B., Taggart, J. B., Cairney, M., Powell, R., Krieg, F., Okamoto, N., Ferguson, M. M., Holm, L. E., & Guyomard, R. (2006). A linkage map for brown trout (*Salmo trutta*): Chromosome homeologies and comparative genome organization with other salmonid fish. *Genetics*, 172, 2405-2419. <https://doi.org/>
- Haaf, T., & Schmid, M. (1984). An early stage of ZW/ZZ sex chromosome differentiation in *Poecilia sphenops* var. *Melanistica* (Poeciliidae, Cyprinodontiformes). *Chromosoma*, 89(1), 37-41. <https://doi.org/10.1007/BF00302348>

- Herpin, A., & Schartl, M. (2015). Plasticity of gene-regulatory networks controlling sex determination: Of masters, slaves, usual suspects, newcomers, and usurpators. *EMBO Reports*, 16(10), 1260-1274. <https://doi.org/10.15252/embr.201540667>
- Heule, C., Salzburger, W., & Böhne, A. (2014). Genetics of Sexual Development: An Evolutionary Playground for Fish. *Genetics*, 196(3), 579-591. <https://doi.org/10.1534/genetics.114.161158>
- Kallman, K. D. (1984). A New Look at Sex Determination in Poeciliid Fishes. In B. J. Turner (Ed.), *Evolutionary Genetics of Fishes* (p. 95-171). Springer US. https://doi.org/10.1007/978-1-4684-4652-4_3
- Kavalco, K. F., & De Almeida-Toledo, L. F. (2007). Molecular Cytogenetics of Blind Mexican Tetra and Comments on the Karyotypic Characteristics of Genus *Astyanax* (Teleostei, Characidae). *Zebrafish*, 4(2), 103-111. <https://doi.org/10.1089/zeb.2007.0504>
- Kikuchi, K., & Hamaguchi, S. (2013). Novel sex-determining genes in fish and sex chromosome evolution. *Developmental Dynamics: An Official Publication of the American Association of Anatomists*, 242(4), 339-353. <https://doi.org/10.1002/dvdy.23927>
- Kõressaar, T., Lepamets, M., Kaplinski, L., Raime, K., Andreson, R., & Remm, M. (2018). Primer3_masker: Integrating masking of template sequence with primer design software. *Bioinformatics*, 34(11), 1937-1938. <https://doi.org/10.1093/bioinformatics/bty036>
- Levan, A., Fredga, K., & Sandberg, A. A. (1964). Nomenclature for Centromeric Position on Chromosomes. *Hereditas*, 52(2), 201-220. <https://doi.org/10.1111/j.1601-5223.1964.tb01953.x>
- Liew, W. C., Bartfai, R., Lim, Z., Sreenivasan, R., Siegfried, K. R., & Orban, L. (2012). Polygenic Sex Determination System in Zebrafish. *PLOS ONE*, 7(4), e34397. <https://doi.org/10.1371/journal.pone.0034397>
- Liew, W. C., & Orbán, L. (2014). Zebrafish sex: A complicated affair. *Briefings in Functional Genomics*, 13(2), 172-187. <https://doi.org/10.1093/bfgp/elt041>
- Mank, J. E., & Avise, J. C. (2009). Evolutionary diversity and turn-over of sex determination in teleost fishes. *Sexual Development: Genetics, Molecular Biology, Evolution, Endocrinology, Embryology, and Pathology of Sex Determination and Differentiation*, 3(2-3), 60-67. <https://doi.org/10.1159/000223071>
- Mitchell, R. W., Russell, W. H., & Elliott, W. R. (1977). Mexican eyeless characin fishes, genus *Astyanax*: Environment, distribution, and evolution. Texas Tech Press.
- Moore, E. C., & Roberts, R. B. (2013). Polygenic sex determination. *Current Biology*, 23(12), R510-R512. <https://doi.org/10.1016/j.cub.2013.04.004>
- Myosho, T., Takehana, Y., Hamaguchi, S., & Sakaizumi, M. (2015). Turnover of Sex Chromosomes in Celebensis Group Medaka Fishes. *G3: Genes, Genomes, Genetics*, 5(12), 2685-2691. <https://doi.org/10.1534/g3.115.021543>
- Ospina-Alvarez, N., & Piferrer, F. (2008). Temperature-dependent sex determination in fish revisited: Prevalence, a single sex ratio response pattern, and possible effects of climate change. *PloS One*, 3(7), e2837. <https://doi.org/10.1371/journal.pone.0002837>
- Pan, M., Feron, R., Jouanno, E., Darras, H., Herpin, A., Koop, B., Rondeau, E., Goetz, F., Larson, W., Bernatchez, L., Tringali, M., Curran, S., Saillant, E., Denys, G., von Hippel, F., Chen, S., López, J., Verreycken, H., Ocalewicz, K., & Guiguen, Y. (2020). The rise and fall of the ancient northern pike master sex determining gene. <https://doi.org/10.1101/2020.05.31.125336>
- Pan, Q., Guiguen, Y., & Herpin, A. (2018). Evolution of Sex Determining Genes in Fish. In M. K. Skinner (Ed.), *Encyclopedia of Reproduction* (Second Edition) (p. 168-175).

- Academic Press. <https://doi.org/10.1016/B978-0-12-809633-8.20552-9>
- Policarpo, M., Fumey, J., Lafargeas, P., Naquin, D., Thermes, C., Naville, M., Dechaud, C., Volff, J.-N., Cabau, C., Klopp, C., Moller, P., Bernatchez, L., García-Machado, E., Rétaux, S., & Casane, D. (2020). Contrasting gene decay in subterranean vertebrates: Insights from cavefishes and fossorial mammals. *Molecular biology and evolution*. <https://doi.org/10.1093/molbev/msaa249>
- Protas, M. E., Hersey, C., Kochanek, D., Zhou, Y., Wilkens, H., Jeffery, W. R., Zon, L. I., Borowsky, R., & Tabin, C. J. (2006). Genetic analysis of cavefish reveals molecular convergence in the evolution of albinism. *Nature Genetics*, 38(1), 107-111. <https://doi.org/10.1038/ng1700>
- Reed, K. M. (1993). Cytogenetic analysis of the paternal sex ratio chromosome of *Nasonia vitripennis*. *Genome*, 36(1), 157-161. <https://doi.org/10.1139/g93-020>
- Ribas, L., Liew, W. C., Díaz, N., Sreenivasan, R., Orbán, L., & Piferrer, F. (2017). Heat-induced masculinization in domesticated zebrafish is family-specific and yields a set of different gonadal transcriptomes. *Proceedings of the National Academy of Sciences of the United States of America*, 114(6), E941-E950. <https://doi.org/10.1073/pnas.1609411114>
- Roberts, N. B., Juntti, S. A., Coyle, K. P., Dumont, B. L., Stanley, M. K., Ryan, A. Q., Fernald, R. D., & Roberts, R. B. (2016). Polygenic sex determination in the cichlid fish *Astatotilapia burtoni*. *BMC Genomics*, 17(1), 835. <https://doi.org/10.1186/s12864-016-3177-1>
- Şadoğlu, P. (1957). A mendelian gene for albinism in natural cave fish. *Experientia*, 13(10), 394-394. <https://doi.org/10.1007/BF02161111>
- Santos, D., Luzio, A., & Coimbra, A. M. (2017). Zebrafish sex differentiation and gonad development: A review on the impact of environmental factors. *Aquatic Toxicology*, 191, 141-163. <https://doi.org/10.1016/j.aquatox.2017.08.005>
- Sato, T., Endo, T., Yamahira, K., Hamaguchi, S., & Sakaizumi, M. (2005). Induction of female-to-male sex reversal by high temperature treatment in Medaka, *Oryzias latipes*. *Zoological Science*, 22(9), 985-988. <https://doi.org/10.2108/zsj.22.985>
- Saunders, P. A., Neuenschwander, S., & Perrin, N. (2018). Sex chromosome turnovers and genetic drift: A simulation study. *Journal of Evolutionary Biology*, 31(9), 1413-1419. <https://doi.org/10.1111/jeb.13336>
- van Doorn, G. S., & Kirkpatrick, M. (2007). Turnover of sex chromosomes induced by sexual conflict. *Nature*, 449(7164), 909-912. <https://doi.org/10.1038/nature06178>
- van Doorn, G. Sander, & Kirkpatrick, M. (2010). Transitions Between Male and Female Heterogamety Caused by Sex-Antagonistic Selection. *Genetics*, 186(2), 629-645. <https://doi.org/10.1534/genetics.110.118596>
- Wilkens, H., & Strecker, U. (2017). Evolution in the Dark: Darwin's Loss Without Selection. Springer-Verlag. <https://doi.org/10.1007/978-3-662-54512-6>
- Wilson, C. A., High, S. K., McCluskey, B. M., Amores, A., Yan, Y., Titus, T. A., Anderson, J., Batzel, P., Carvan III, M. J., Schartl, M., & Postlethwait, J. H. (2014). Wild sex in Zebrafish: Loss of the natural sex determinant in domesticated strains. *Genetics*, 198(3), 1291-1308. <https://doi.org/10.1534/genetics.114.169284>
- Yano, A., Nicol, B., Jouanno, E., Quillet, E., Fostier, A., Guyomard, R., & Guiguen, Y. (2013). The sexually dimorphic on the Y-chromosome gene (sdY) is a conserved male-specific Y-chromosome sequence in many salmonids. *Evolutionary Applications*, 6(3), 486-496. <https://doi.org/10.1111/eva.12032>
- Yoshida, K., Terai, Y., Mizoiri, S., Aibara, M., Nishihara, H., Watanabe, M., Kuroiwa, A., Hirai, H., Hirai, Y., Matsuda, Y., & Okada, N. (2011). B Chromosomes Have a

Functional Effect on Female Sex Determination in Lake Victoria Cichlid Fishes. PLoS Genetics, 7(8), e1002203. <https://doi.org/10.1371/journal.pgen.1002203>

FIGURE LEGENDS

Figure 1. The incomplete sex-linkage of *gdf6b-B* with the male phenotype in *A. mexicanus* Texas surface fish. **(A)** PCR amplifications of the *gdf6* intron. A ~1.1 kb band is detected in all individuals, while an additional ~600 bp band is amplified in about half of phenotypic males. **(B)** *gdf6b-B* genotyping in males and females Texas surface fish. **(C)** Schematic representation of the variations between the Texas surface fish and Pachón cavefish *gdf6b* copies, i.e., *gdf6b-A* and *gdf6b-B* (total 2,108 bp from the first ATG on exon1 to the stop codon in exon 2, including intron 1 in its version with the 500 bp deletion). The dark blue box and line indicate specific *gdf6b-B* indels on the exon 1 and intron 1 in surface fish, respectively. Dark vertical lines indicate variable positions. The specific variations in *gdf6b-B* in surface fish males⁺ (dark triangle; highlighted in yellow) and cavefish males (red triangles; highlighted in blue) or shared variation (green triangle; highlighted in green) are indicated on alignments. Each variable site for surface fish and cavefish is magnified to show the nucleotide sequence and the corresponding amino acids changes in both *gdf6b-A* and *gdf6b-B*.

Figure 2. Karyotypes and C-banded mitotic metaphases of *Astyanax mexicanus* Texas surface fish. **(A,B,C)** karyotypes arranged for mitotic chromosomes (from cephalic kidney). **(A',B',C')** C-banding patterns; B chromosomes are indicated by arrows. Note the lack of C-bands on B chromosome(s). Scale bar = 10 μm.

Figure 3. RAD-seq haplotypes distribution and male⁺-specific markers in *A. mexicanus* Texas surface fish. **(A)** Heatmap showing the distribution of haplotypes between males (n=26) and females (n=30). Each square in the heatmap indicates the number of haplotypes presented in N1 phenotypic males (horizontal axis) and N2 phenotypic females (vertical axis). Haplotypes found in about 13-15 males⁺ and absent from all females and males⁻ are highlighted by a red box. **(B)** Heatmap showing individual depth for the sex-polymorphic RAD-seq markers (vertical axis) present only in 14 males⁺ and totally absent from all females and males⁻ (horizontal axis). Each line represents one sex-polymorphic marker, and each column represents an individual.

Figure 4. Pool-seq data mapped onto a female genome surface fish assembly (GCF_000372685.2) illustrating the “apparent” male⁺-specific SNPs (blue) across the different LGs and unplaced scaffolds. SNPs were counted using a 50 kb sliding window with an output point every 500 bp. Female- and male⁺- specific SNPs as well as male⁻- specific SNPs are indicated by red, blue and yellow color, respectively. **(A)** The “apparent” male⁺-specific SNPs

on different LGs (LG03, LG07, LG09, LG14). **(B)** The “apparent” male⁺-specific SNPs on unplaced scaffolds NW_019171094.1, NW_019171635.1, NW_019172868.1, NW_019172881.1, NW_019172890.1, and NW_019172904.1. The regions corresponding to the high density of “apparent” male⁺-specific SNPs obtained by contrasting the pool-seq data in pairs are indicated by arrows on the different LGs and unplaced scaffolds.

Figure 5. The specific duplication of *gdf6b* in male⁺ compared to males⁻ and females. **(A)** Integrative genomics viewer (IGV) visualization of the male⁺, male⁻ and female pooled-reads around the *gdf6b* locus (2,857 bp), showing a much higher coverage in the male⁺ pool compared to the male⁻ and female pools and many “apparent” male-specific heterozygous sites (Het) and male-specific indels (MsI). **(B)** Copy number variation of the *gdf6b* was quantified using specific TaqMan PCR assays normalized using the single copy autosomal gene *dmrt1*. Results are presented as boxplots of the ratio of *gdf6b* over *dmrt1* in males⁺ (White) and males⁻ (light grey), and females (dark grey), with individual copy number values displayed as dots, the copy number median as a line and the box displaying the first and third quartiles of copy number variation. Statistical significance between males and females were tested with the Wilcoxon Rank Test (**** = P < 0.001).

Figure 6. *gdf6b-B* sex-linkage in wild cavefish and surface fish populations. **(A)** Localization of the *A. mexicanus* caves and surface populations from the North-East of Mexico (San Luis Potosi) to the south of USA (Texas). Boxes in red, brown and green show locations of *Astyanax* caves (Internal colored circles) in the Sierra de El Abra, de Guatemala, and Micos, respectively. **(B)** Table showing the *gdf6b-B* sex-linkage in the wild. The caves belonging to the different groups are indicated with the same color code as on the map. “*”: significant sex-linkage

TABLES

Table 1: Sex-ratios in Surface fish *A. mexicanus* (Texas) at different rearing temperatures

Experiment	Temperature	Number of males	Number of females	X-squared	p-value	Significance
ID						
1	28 °C	143	131	0.52555	0.4685	ns
	21 °C	207	204	0.021898	0.8824	ns
2	28 °C	44	182	86.817	< 2.2e-16	****
	21 °C	95	98	0.046632	0.829	ns

Table 2: The number of metaphases containing B chromosomes in Surface fish *A. mexicanus* (Texas) males and females

Individual Sex	Total NM	Total NM 0 B	Total NM 1 B	Total NM 2 Bs	Total NM with Bs	% M with Bs
Male ⁺ 1	6	0	0	6	6	100
Male ⁺ 2	8	0	8	0	8	100
Male ⁺ 3	8	0	8	0	8	100
Male ⁺ 4	5	0	5	0	5	100
Male ⁻ 1	12	10	2	0	2	16,66
Male ⁻ 2	21	21	0	0	0	0
Female 1	53	50	3	0	3	5,66
Female 2	23	23	0	0	0	0
Female 3	10	10	0	0	0	0
Female 4	4	4	0	0	0	0
Female 5	45	45	0	0	0	0
Female 6	21	21	0	0	0	0

FIGURES

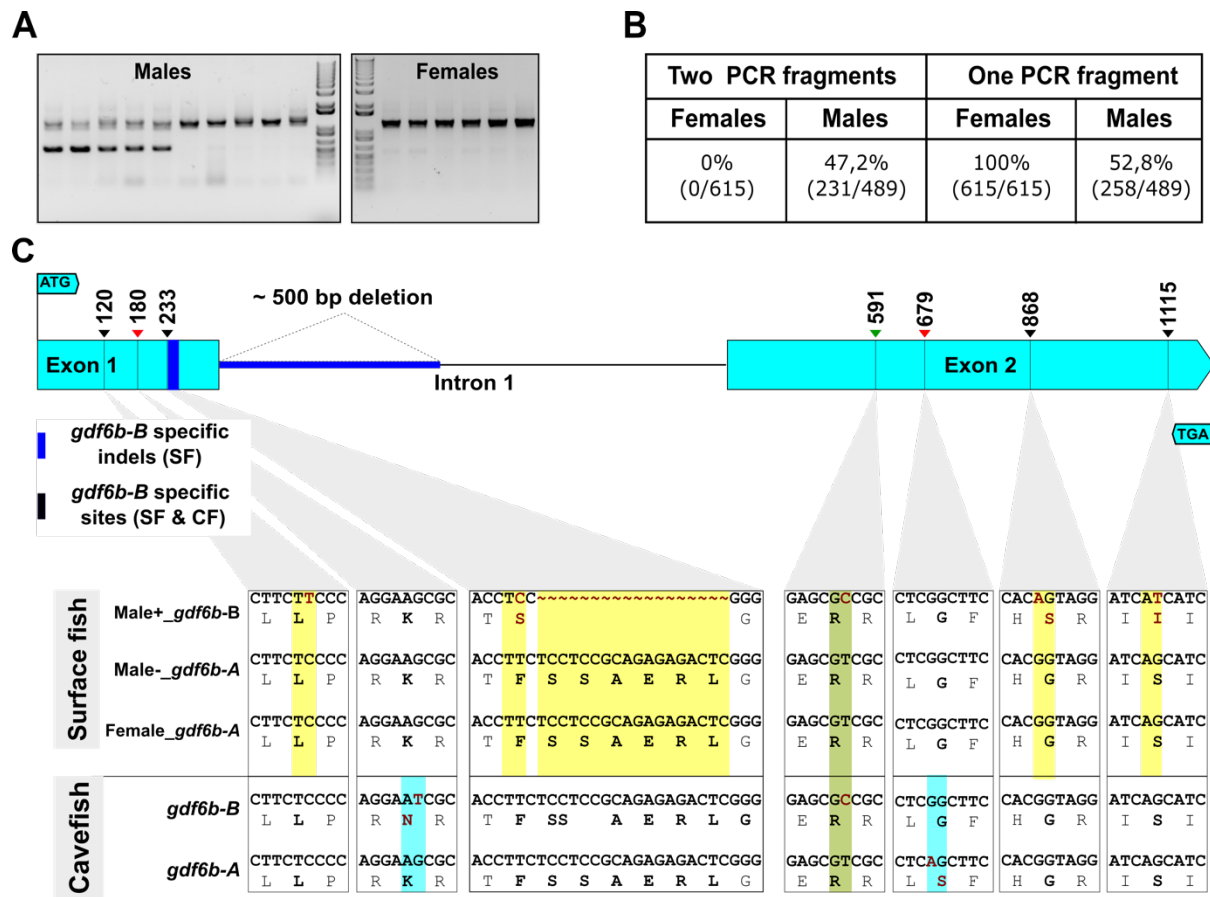


Figure 1. The incomplete sex-linkage of *gdf6b-B* with the male phenotype in *A. mexicanus* Texas surface fish.

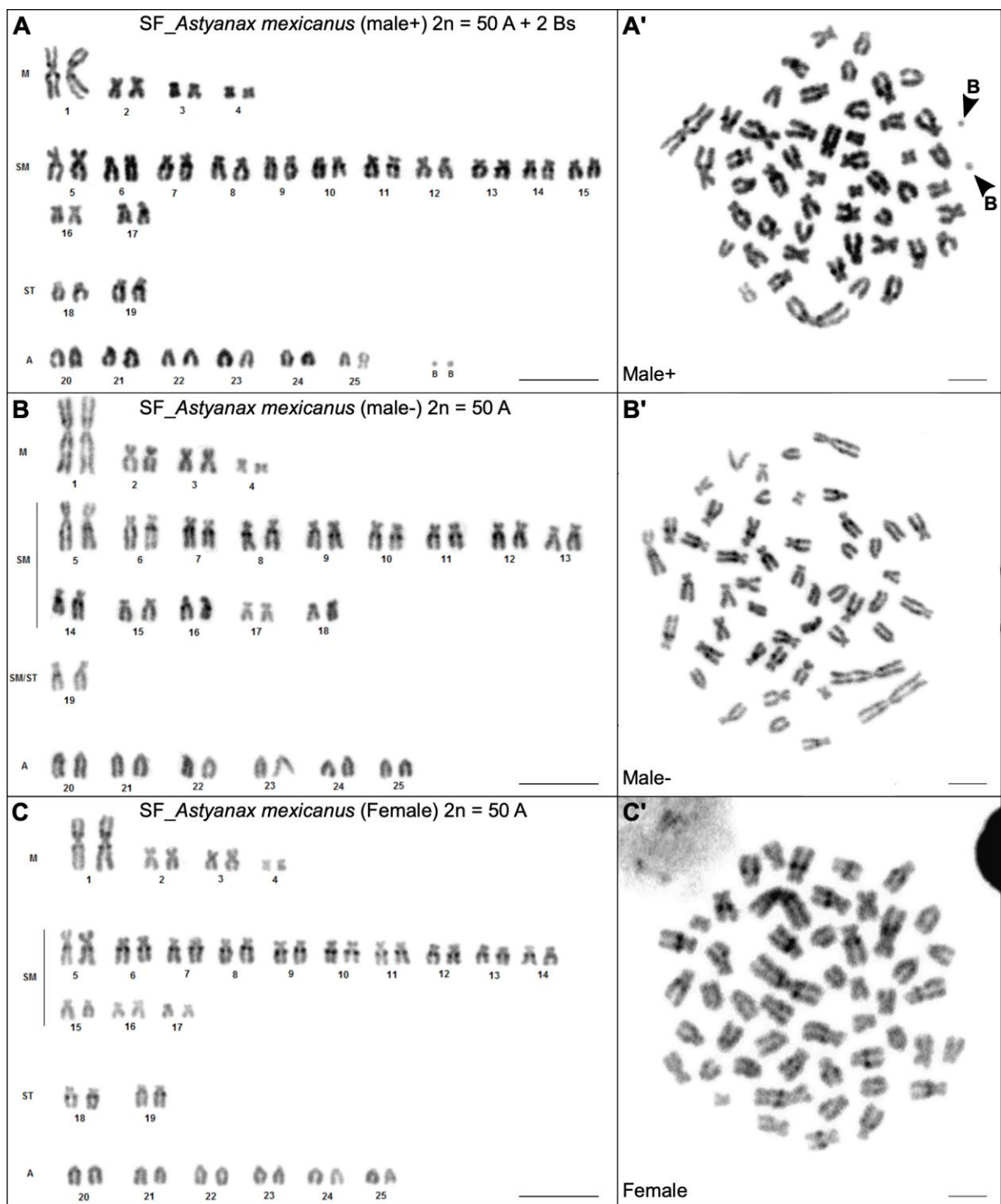


Figure 2. Karyotypes and C-banded mitotic metaphases of *Astyanax mexicanus* Texas surface fish.

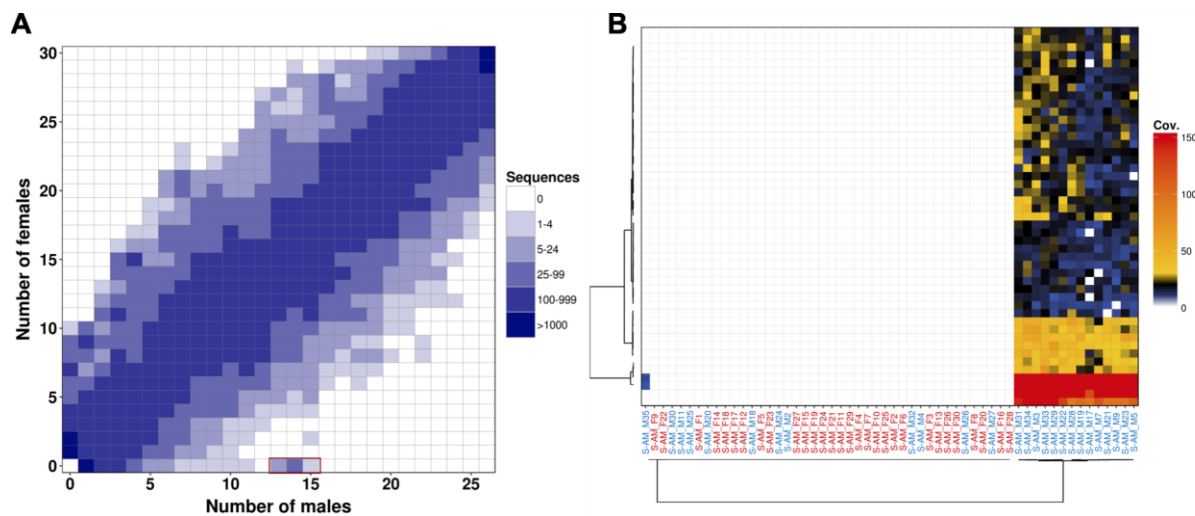


Figure 3. RAD-seq haplotypes distribution and male⁺-specific markers in *A. mexicanus* Texas surface fish.

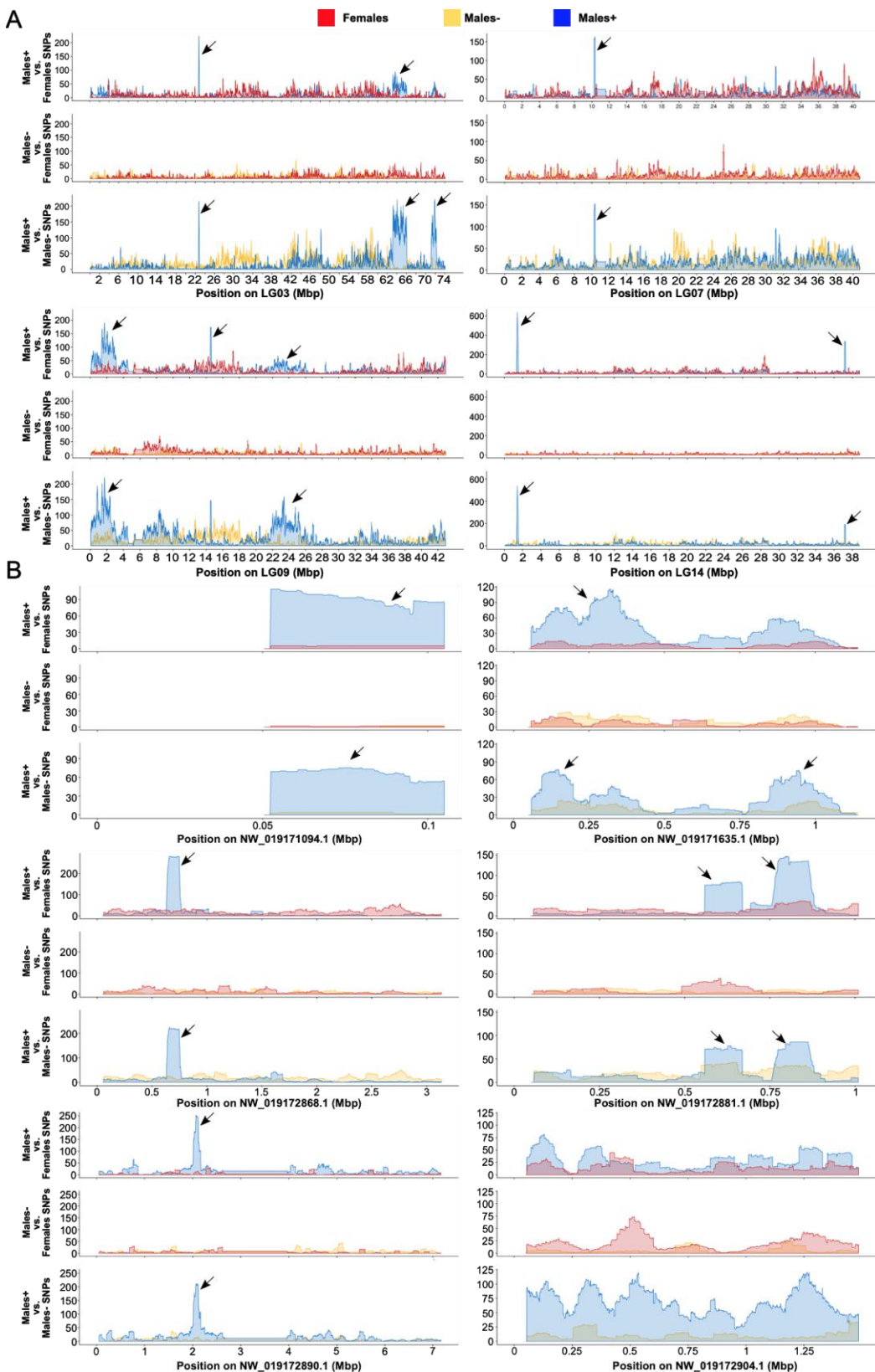


Figure 4. Pool-seq data mapped onto a female genome surface fish assembly (GCF_000372685.2) illustrating the “apparent” male⁺-specific SNPs (blue) across the different LGs and unplaced scaffolds.

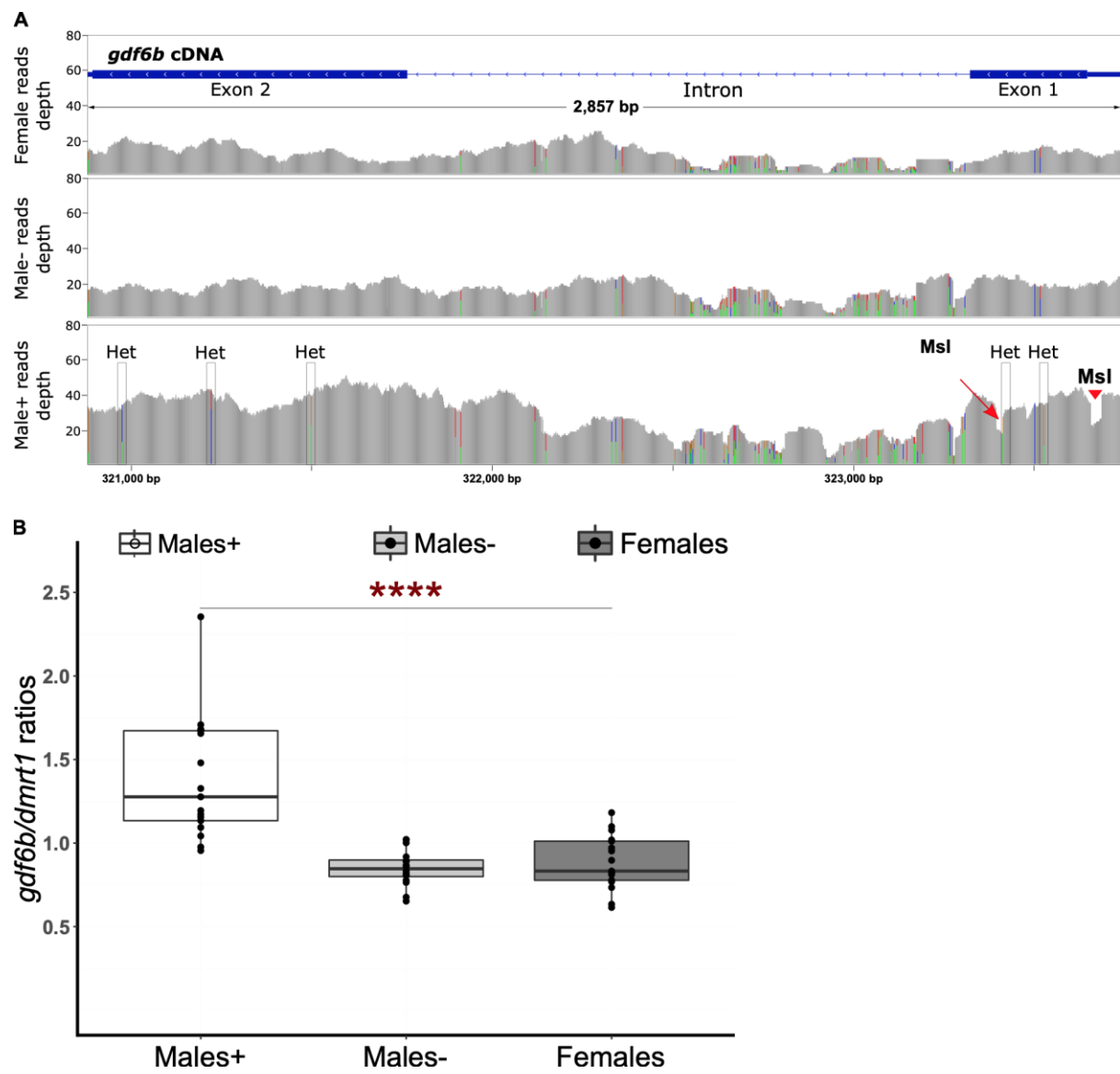
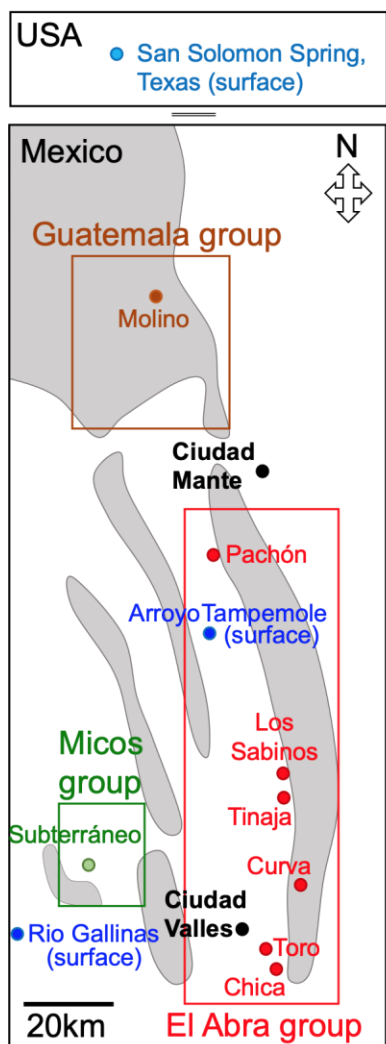


Figure 5. The specific duplication of *gdf6b* in male⁺ compared to males⁻ and females.

A



B

	Phenotypic males	Phenotypic females	Undetermined sex
	<i>gdf6b-B</i> positive	<i>gdf6b-B</i> positive	<i>gdf6b-B</i> positive
El Abra group			
Pachón (CF) *	11/11	0/9	7/15
Los Sabinos (CF) *	12/12	0/10	6/30
Tinaja (CF) *	2/2	0/6	0/3
Curva (CF) *	5/5	0/6	7/12
Toro (hybrids)	5/5	0/1	8/24
Chica (hybrids)	/	/	12/27
Guatemala group			
Molino (CF)	/	/	0/9
Jineo (CF)	/	/	0/6
Escondido (CF)	/	/	0/8
Micos group			
Subterraneo	/	/	1/16
Surface fish			
Rio Gallinas (CF) *	26/26	0/10	/
Arroyo Tampemole *	9/9	0/29	/

Figure 6. *gdf6b-B* sex-linkage in wild cavefish and surface fish populations.

SUPPLEMENTARY DATA

Table S1. Primer names, sequences, target genes, and their corresponding experiments

Primer name: Forward (Fw) and Reverse (Rv) and TaqMan probes	Sequence	Target gene	Experiment
Gdf6b_Intron_Fw	CATCACCAAGCTTCGTAGATAACG	<i>Gdf6b</i>	gdf6b Intron for surface fish genotyping
Gdf6b_Intron_Rv	GAAGCTTCCAGAGACCTTCGTGT	<i>Gdf6b</i>	
Gdf6b-B_Fw	CGTTTGATGTGTCTACGCTCTCTGA	<i>Gdf6b-B</i>	Wild populations genotyping
Gdf6b-B_Rv	GAGGGAGGGTATTTCAGCAGGT	<i>Gdf6b-B</i>	
dmrt1_TaqMan_Fw	AGGCCAACTCTGATTCTGGA	<i>dmrt1</i>	TaqMan_ assay (autosomal reference gene)
dmrt1_TaqMan_Probe	GGATTCCATCATAGAGGGAGCGGCC	<i>dmrt1</i>	
dmrt1_TaqMan_Rv	TGGCTCTCAGATACGTCACT	<i>dmrt1</i>	
gdf6b_TaqMan_Primer_Fw	CTTCAGCTTCATTCCCTGCCA	<i>Gdf6b-B</i>	TaqMan_ assay (gdf6b)
gdf6b_TaqMan_Probe	CCCACAAGCTTCTAGACTCCAGAACCC	<i>Gdf6b-B</i>	
gdf6b_TaqMan_Primer_Rv	ATCGTGGTTGTGGGAGTTC	<i>Gdf6b-B</i>	

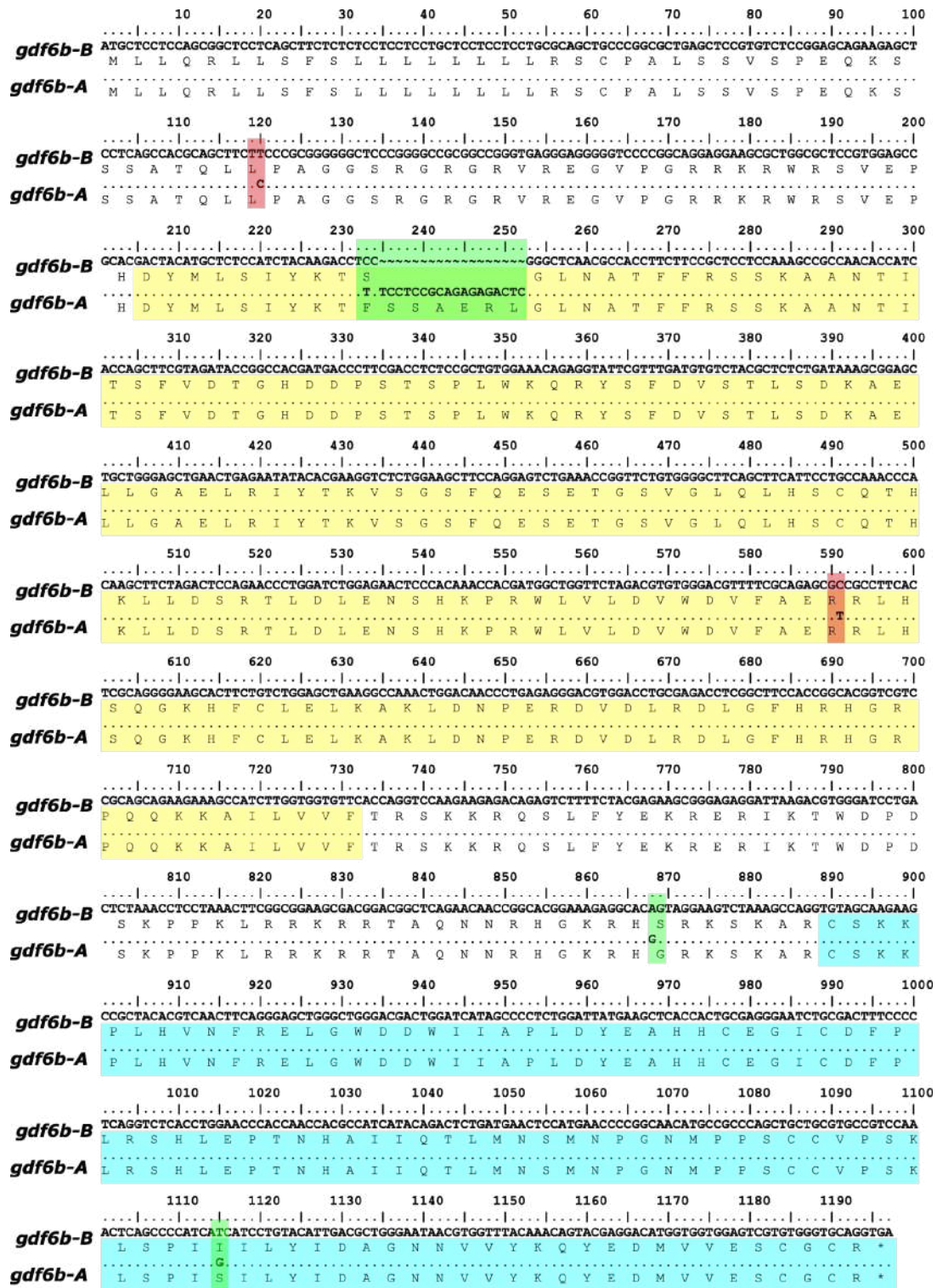


Figure S1. Alignment of nucleotide and protein sequences of the *gdf6b-A* and *gdf6b-B* genes. Sequences were aligned with BioEdit 7.2. The *gdf6b-B* variation sites are boxed (green for nonsynonymous sites and red for synonymous sites). Regions highlighted in yellow and blue indicated the Pfam “TGF-b propeptide” and “TGF-b-like” domains (El-Gebali et al., 2019). “.”: Identical nucleotides; “*”: stop codon.

DISCUSSION

DISCUSSION / PERSPECTIVES

Le tétra mexicain, *Astyanax mexicanus* fait partie des 258 espèces connues de poissons cavernicoles vivant dans l'obscurité totale et permanente (www.cavefishes.org.uk). Sa particularité par rapport à toutes ces espèces troglomorphiques, réside dans l'existence de deux morphotypes qui sont aujourd'hui toujours accessibles : morphotype cavernicole et morphotype de surface (probablement très proche de l'ancêtre commun à partir duquel les deux morphotypes actuels ont évolué). Cette particularité représente un avantage majeur et fait d'*A. mexicanus* un “modèle” quasi-unique pour des études comparatives à une échelle micro-évolutive des aspects biologiques en lien avec un changement drastique de l'environnement. De plus, il offre la possibilité d'explorer ces processus dans un contexte d'évolution convergente, parallèle et répétée grâce à l'existence d'une trentaine de populations cavernicoles qui semblent avoir des origines, en partie au moins, indépendantes et très récentes. Ainsi, la question majeure de mes travaux de thèse a été d'explorer le ou les systèmes de déterminisme du sexe chez les populations de surface (poissons originaires du Texas) et les populations cavernicoles, en l'occurrence celle de la grotte Pachón.

Dans cette section, nous discuterons les principaux résultats obtenus et proposerons des perspectives pour les travaux futurs sur les mécanismes de détermination du sexe des différentes populations d'*Astyanax mexicanus*.

La différenciation sexuelle chez Astyanax mexicanus de la grotte Pachón

La démarche scientifique menée pour répondre à cette question nous a conduit à explorer, en absence de données préalables sur le sujet, la différenciation sexuelle mâle et femelle d'un point de vue cellulaire, morphologique et moléculaire chez la population de la grotte Pachón (**Article 1**). Ainsi, nous nous sommes intéressés au suivi de la trajectoire migratoire des cellules germinales primordiales (CGPs), l'une des étapes précoces de la formation des gonades, et ce dès les premiers stades de développement embryonnaire jusqu'à leur arrivée dans le territoire présomptif des gonades. Cette détection des CGPs s'est faite dès le stade 80 % épibolie chez *A. mexicanus* grâce à l'injection de l'ARN messager de la partie 3'UTR du gène *nanos1* du poisson zèbre couplé à la GFP (Herpin et al., 2007, 2008). Dans la littérature, il a été rapporté que le chemin migratoire des CGPs est spécifique à chaque espèce (Coelho et al., 2019; Kurokawa et al., 2006; Saito et al., 2006), même si les mécanismes contrôlant leurs mouvements et leur spécification semblent être très conservés dans le règne animal (Xu et al., 2010). Or, contrairement à ce qui a été rapporté chez d'autres espèces, l'une

des particularités d'*A. mexicanus* réside dans l'augmentation du nombre de CGPs détectées entre le stade neurula précoce et les stades 8-9 somites. Cette augmentation marque une première étape de prolifération, et très probablement de spécification, suggérant que la prolifération des CGPs pourrait avoir lieu avant la colonisation des crêtes génitales chez certaines espèces dont l'*Astyanax*. Toutefois, cette étude devrait être complétée par une analyse plus fine de l'expression d'autres marqueurs moléculaires qui sous-tendent la migration et la prolifération des CGPs afin de confirmer ou d'infirmier cette hypothèse. En ce sens, plusieurs marqueurs moléculaires sont connus pour être impliqués dans le processus migratoire *e.g.*, *sdf1* (stromal cell-derived factor 1) et son récepteur transmembranaire couplé aux protéines G, *cxcr4* ou encore *vasa* qui est un marqueur spécifique des cellules germinales (Braat et al., 1999; Herpin et al., 2008; Knaut et al., 2003).

Dans un second temps, nous avons caractérisé la fenêtre de différenciation gonadique par l'association d'approches histologique et moléculaire. D'un point de vue histologique, nos résultats ne montrent aucun signe de différenciation gonadique avant 65 jours post-fécondation (jpf) chez les femelles et 90 jpf chez les mâles. Néanmoins, à 45 jpf et 65 jpf, respectivement chez les femelles et les mâles, le nombre de cellules germinales (CGs) augmente dans les ovaires et les testicules indifférenciés. Cette augmentation du nombre de CGs pourrait être un signe de prolifération des cellules germinales, qui est souvent associé au début de la différenciation sexuelle. À ce stade, il nous semble évident que des expérimentations supplémentaires seraient nécessaires entre 23 jpf et 65 jpf afin de mieux préciser la période à laquelle les cellules germinales entrent activement dans le processus de division conduisant ainsi à la différenciation gonadique.

Par ailleurs, cette étude de la différenciation histologique a été accompagnée par la caractérisation des profils d'expression de marqueurs moléculaires qui sont connus pour contrôler ce processus chez les vertébrés. Nous avons étudié notamment l'expression des gènes *dmrt1* (doublesex and mab-3 related transcription factor 1), *gsdf* (gonadal somatic cell derived factor) et *amh* (anti-Mullerian hormone) impliqués dans la différenciation testiculaire et des gènes *cyp19a1a* (cytochrome P450, family 19, subfamily A, polypeptide 1a), *foxl2a* (forkhead box L2a) et *wnt4b* (Wnt Family Member 4b) jouant un rôle crucial dans la différenciation ovarienne (Bertho et al., 2016; Guerrero-Estevez & Moreno-Mendoza, 2010; Guiguen et al., 2010; Herpin et al., 2013; Ijiri et al., 2008; Sreenivasan et al., 2014). Nos données montrent clairement l'implication de *dmrt1*, *gsdf* et de l'*amh* dans la différenciation testiculaire puisque ces gènes sont exprimés plus fortement chez les mâles que chez les femelles avant les premiers

signes de différenciation histologique. En revanche, et de manière assez intrigante, aucun des marqueurs femelles que nous avons étudié *e.g.*, *cyp19a1a*, *foxl2a*, et *wnt4b* n'est exprimé de manière dimorphique chez les femelles. Des résultats similaires chez d'autres espèces ont rapporté l'expression non-dimorphique de ces trois marqueurs *e.g.*, *foxl2* chez *Acipenser stellatus* (Burcea et al., 2018), *cyp19a1a* chez *Colossoma macropomum* (Lobo et al., 2020) ou encore chez *Astyanax altiparanae* (Martinez-Bengochea et al., 2020) et enfin *wnt4b* chez *Oncorhynchus mykiss* (Nicol et al., 2012). Ces résultats renforcent l'hypothèse selon laquelle le contrôle moléculaire de la différenciation gonadique n'est pas si conservé qu'on le pensait chez les vertébrés (Herpin et al., 2013). En lien avec cette hypothèse, ce travail ajoute de manière inattendue une autre dimension à cette non-conservation en montrant que ces marqueurs femelles sont, chez *Astyanax mexicanus*, tous exprimés plus fortement dans les testicules adultes que dans les ovaires.

Outre ces données discutées dans (Imarazene et al., *accepted*; **Article 1**), nous avons récemment élargi notre analyse (données non présentées) à d'autres gènes qui jouent également un rôle dans la différenciation mâle : *sox3* (SRY-box 3) et *sox9* (SRY-box 9) (Jiang et al., 2013; Nakamoto et al., 2005, 2009)mais aussi dans la voie ovarienne: *rspo1* (R-spondin 1), *wnt4a* (Wnt family member 4 a), *fsta* (Follistatin a) et *fstb* (Follistatin b) (Chassot et al., 2008; Chassot et al., 2012; Nicol et al., 2012, 2012, 2013; Yao et al., 2004). Bien qu'il serait probablement nécessaire de les confirmer, nos premiers résultats montrent une surexpression de l'ensemble de ces marqueurs dans les testicules matures par rapport aux ovaires matures. De plus, *sox3*, *sox9* et *wnt4a* ne présentent aucune expression dimorphique au cours de la différenciation gonadique (données non présentées). À notre connaissance, *A. mexicanus* est la seule espèce chez qui, non seulement aucun de ces marqueurs "classiques" de la différenciation femelle n'est impliqué dans la différenciation ovarienne, mais qui exprime de plus très fortement ces marqueurs "femelles" dans les testicules (adultes et en différenciation). Au vu de ces résultats, il nous paraît primordial de caractériser les acteurs moléculaires responsables de la différenciation gonadique, en particulier celle des ovaires chez *A. mexicanus*. Pour cela, il existe des approches méthodologiques plus puissantes voire "exhaustives", qui ont été utilisées chez d'autres espèces, permettant de quantifier de manière simultanée l'expression de nombreux gènes à différents stades gonadiques telles que les microarray (Depiereux et al., 2015; Douglas, 2006) ou encore les techniques de séquençage type RNA-seq (Böhne et al., 2014; Lobo et al., 2020; Tao et al., 2018; Zhang et al., 2019). L'utilisation d'une telle démarche serait très intéressante afin de valider nos résultats surprenants avec une autre approche, et aussi

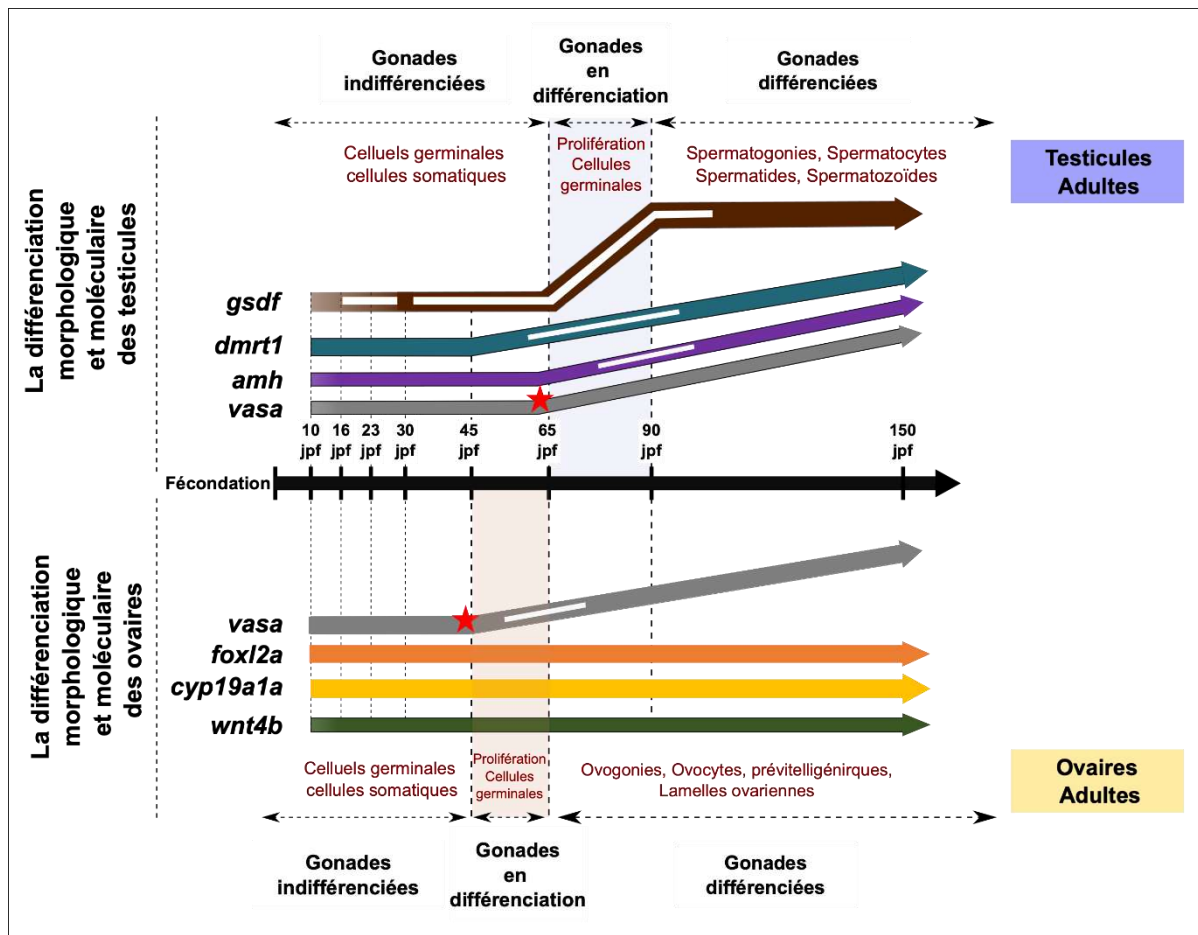


Figure 9. Représentation schématique illustrant les facteurs moléculaires et les principaux changements morphologiques au cours du développement des gonades chez *Astyanax mexicanus* de la grotte Pachón entre 10 jours post-fécondation (jpf) et 150 jpf (flèche noire graduée). Les parties supérieure et inférieure de la flèche représentent respectivement le développement testiculaire et ovarien. Les lignes verticales pointillées délimitent les stades analysés. Les flèches horizontales pointillées délimitent les principales phases de la différenciation gonadique (indiquées au-dessus pour les mâles et en dessous pour les femelles) en fonction des profils d'expression des gènes et des changements morphologiques. Les changements morphologiques à chaque phase sont indiqués en caractères rouges. Les profils d'expression des gènes impliqués dans la différenciation sexuelle mâle et femelle sont illustrés par des flèches de couleur : *gsdf* (marron), *dmrt1* (bleu), *amh* (violet), *vasa* (gris), *foxl2a* (orange), *cyp19a1a* (jaune), *wnt4b* (vert). Les flèches droites correspondent aux gènes qui ne présentent aucune expression différentielle entre les mâles et les femelles, et les flèches non-linéaires illustrent les stades à partir desquels l'expression des gènes correspondants est régulée à la hausse chez les mâles (*gsdf*, *dmrt1*, *amh* et *vasa*), chez les femelles (*vasa*). Les profils d'expression de *gsdf*, *dmrt1*, *amh* et *vasa* sont illustrés chez les mâles, et ceux de *vasa*, *foxl2a*, *cyp19a1a* et *wnt4b* chez les femelles. Les étoiles rouges indiquent les stades à partir desquels l'expression de *vasa* augmente chez les mâles et les femelles, marquant respectivement la prolifération des cellules germinales. Les lignes blanches à l'intérieur des flèches colorées indiquent les stades où l'expression du gène correspondant est plus élevée chez les mâles ou les femelles. Les zones verticales colorées en bleu et en beige indiquent les fenêtres de la différenciation gonadique précoce chez les mâles et les femelles, respectivement.

d'établir une liste de gènes candidats potentiellement impliqués dans la différenciation gonadique. Cette identification pourrait être complétée par des analyses quantitatives type qPCR et de l'hybridation *in situ* afin de caractériser aussi bien d'un point de vue quantitatif que spatial l'expression de ces gènes.

Notons tout de même que malgré ces divergences observées par rapport aux autres espèces de vertébrés, l'ensemble de nos résultats (**Article 1**) nous ont permis de proposer un schéma illustrant les grandes étapes de la différenciation histologique mâle et femelle ainsi que l'expression concomitante des principaux marqueurs moléculaires explorés dans la présente étude (Figure 9).

La détermination du sexe chez *Astyanax mexicanus* originaire de la grotte Pachón

Comme nous venons de le voir dans les sections précédentes, les mécanismes de détermination génétique du sexe chez les vertébrés, et les poissons téléostéens en particulier, sont extrêmement diversifiés (Bachtrog et al., 2014; Heule et al., 2014; Moore & Roberts, 2013). Cette diversité est caractérisée à la fois par des changements rapides des gènes déterminants majeurs du sexe et de leurs chromosomes sexuels associés (Herpin & Schartl, 2015; Kikuchi & Hamaguchi, 2013; Schartl, 2004). À ce jour, la quasi-totalité des systèmes et des gènes SD décrits reposent sur des chromosomes sexuels “classiques” (XX/YY et ZZ/ZW) d'autosomes standards qui sont des chromosomes de type A (Kitano & Peichel, 2012; Pan et al., 2018). Cependant, certaines études ont rapporté l'éventuelle implication de chromosomes Bs dans la détermination du sexe chez les poissons (Clark & Kocher, 2019; Yoshida et al., 2011). Les hypothèses avancées sur le rôle des chromosomes B dans la détermination du sexe sont, soit fondées sur une présence des Bs restreinte à un sexe, soit sur l'origine putative de chromosomes sexuels qui pourraient dériver d'anciens chromosomes Bs (Camacho et al., 2011; Mizoguchi & Martins-Santos, 1997; Pansonato-Alves et al., 2014; Serrano-Freitas et al., 2020; Utsunomia et al., 2016; Vujošević et al., 2018; Yoshida et al., 2011; Zhou et al., 2012).

Notre étude apporte, pour la toute première fois chez les poissons, des preuves fonctionnelles de l'implication directe de ces chromosomes B dans la détermination du sexe mâle. En effet, par la combinaison de plusieurs approches, génomiques, moléculaires et cytogénétiques, nous avons caractérisé et localisé un potentiel gène déterminant majeur du sexe, *gdf6b-B* porté par les chromosomes B des mâles chez *Astyanax mexicanus* de la grotte Pachón. Nous avons montré également une association complète de *gdf6b-B* au sexe mâle et une absence totale de liaison avec le sexe femelle sur des centaines d'individus suggérant que ce gène pourrait être

le déterminant majeur du sexe. L'ensemble de nos données montrent la duplication de *gdf6b-B* sur les chromosomes B avec au moins deux copies supplémentaires à la copie autosomale (*gdf6b-A*). Chez *Nothobranchius furzeri*, le paralogue de *gdf6b*, *gdf6a-Y* a été supposé être le potentiel déterminant majeur du sexe chez cette espèce (Reichwald et al., 2015).

Contrairement à ce qui a été rapporté chez une autre population cavernicole d'origine commerciale et inconnue d'*A. mexicanus* (Ahmad et al., 2020), nos données montrent la présence dominante de chromosomes B chez les mâles par rapport aux femelles (**Article 2**). Cette présence de chromosomes B chez les femelles, qui devra être vérifiée par l'analyse de métaphases ovariennes, pourrait être restreinte aux tissus somatiques uniquement. Un tel mécanisme a été décrit précédemment chez les plantes où les Bs sont éliminés spécifiquement des racines très précocement, tandis que les autres tissus contiennent jusqu'à 8 copies de Bs (Ruban et al., 2020). D'un autre côté, des séquençages de génomes de plusieurs mâles et de femelles avec des fréquences variables en chromosomes B (de 0 à 2 Bs par individu) sont en cours. Ces données devraient permettre de caractériser la séquence des chromosomes Bs et de déterminer si oui ou non les chromosomes Bs spécifiques des mâles et ceux des femelles sont différents. Grâce à ces séquençages, nous serons en mesure de vérifier si les *gdf6b-B* localisés sur les chromosomes B des femelles sont des copies tronquées du fait de leur non-liaison au sexe mâle.

Les chromosomes Bs sont connus pour être riches en séquences répétitives telles que les ADNs ribosomaux et satellites ou encore les éléments transposables (ETs) (Houben et al., 2019). Ainsi, l'annotation fine de la séquence des chromosomes B chez *A. mexicanus* permettra également d'estimer sa teneur en séquences répétitives et particulièrement celle des ETs. Certains de ces ETs pourraient d'ailleurs être les moteurs des mécanismes de duplications / insertions du chromosome B. L'une des caractéristiques de l'évolution des chromosomes sexuels est la suppression de la recombinaison méiotique pour ne pas transférer les gènes SD sur d'autres chromosomes, l'accumulation d'éléments transposables et la fixation de gènes spécifiques au sexe (Bachtrog et al., 2008; Charlesworth et al., 2005; Natri et al., 2013). À cet égard, les chromosomes B ont souvent été comparés aux chromosomes sexuels de par leur comportement méiotique ainsi que du fait de leur accumulation de séquences répétitives dont les ETs (Camacho et al., 2011; Camacho et al., 2000). De plus, plusieurs études ont avancé l'hypothèse selon laquelle les éléments transposables joueraient un rôle important dans l'émergence de nouveaux gènes déterminant du sexe (Faber-Hammond et al., 2015; Herpin et al., 2010; Lubieniecki et al., 2015; Marshall Graves & Peichel, 2010; Yano et al., 2013). En ce

sens, nos résultats montrent le non-appariement des chromosomes B avec les chromosomes A chez les mâles lors de la prophase de la première division méiotique et plus précisément au stade pachytène. Une évaluation plus précise de la teneur en ETs de *A. mexicanus* sur les chromosomes B et plus particulièrement autour du locus *gdf6b-B* serait d'une importance majeure afin de conclure sur le rôle de ces éléments transposables dans l'émergence de *gdf6b-B* mais aussi de sa duplication sur les Bs.

Chez de nombreuses espèces, les chromosomes B sont partiellement ou totalement hétérochromatiques (Burt & Trivers, 2006; Camacho et al., 2000). Or, chez *Astyanax mexicanus*, nos observations montrent clairement que les Bs sont largement euchromatiques et comportent des dizaines de gènes entiers (séquences codantes entières) et des gènes tronqués dont les séquences codantes sont partielles. Des résultats similaires ont été observés chez d'autres espèces où les Bs portent plusieurs gènes intacts mais aussi des pseudogènes (séquences tronquées) (Makunin et al., 2018; Navarro-Domínguez et al., 2017; Valente et al., 2014) y compris chez *A. mexicanus* (Ahmad et al., 2020). En plus des séquences génomiques, certaines études ont montré que de nombreux gènes localisés sur les Bs sont exprimés, ouvrant ainsi la perspective d'un rôle fonctionnel des chromosomes B dans divers processus physiologiques, alors qu'ils sont souvent considérés comme inertes et sans fonction propre (Dalla Benetta et al., 2019). Les banques transcriptomiques sur différents tissus adultes ainsi que sur des stades embryonnaires d'*A. mexicanus* dont nous disposons (Hinaux et al., 2013; Pasquier et al., 2016), devront permettre une annotation fine des gènes exprimés sur le chromosome B et à moyen terme de mieux comprendre le(s) rôle(s) fonctionnel(s) de ces chromosomes B chez notre espèce modèle. D'un autre côté, différentes hypothèses indiquant que les Bs pourraient être dérivés soit d'un seul ou de plusieurs chromosomes A ont été avancées (Hanlon et al., 2018; Martis et al., 2012; Ruban et al., 2020; Valente et al., 2014). Nos analyses, en accord avec celles d'Ahmad et al (Ahmad et al., 2020) montrent plutôt que ces Bs partagent de nombreux segments avec plusieurs chromosomes A, suggérant ainsi que les Bs sont probablement constitués d'une mosaïque de nombreux fragments autosomaux. De façon intéressante, les chromosomes B de *Drosophila melanogaster* et d'*Astatotilapia latifasciata* auraient la structure d'un isochromosome constitué de deux bras identiques ce qui pourrait être une indication de la duplication du contenu de ces Bs (Hanlon et al., 2018; Valente et al., 2014). Là aussi, des études supplémentaires sur l'analyse approfondie et l'annotation du chromosome B chez *A. mexicanus*, devraient aider à savoir si oui ou non la structure du B ressemble à celle d'un isochromosome. Cette analyse est actuellement en cours et permettra

d'esquisser de nouvelles hypothèses quant à l'origine et la formation du B, mais aussi de comprendre le processus évolutif à l'origine de la duplication de *gdf6b-B* sur les chromosomes B.

Parmi les caractéristiques classiques d'un gène déterminant majeur du sexe, son expression spécifique durant les phases précoce de la différenciation de la gonade du sexe hétérogamétique est un critère important à évaluer. Nos résultats de profils d'expression de *gdf6b*, en accord avec ceux de *gdf6aY* rapportés chez *Nothobranchius furzeri* (Reichwald et al., 2015), vont dans le sens de cette hypothèse puisqu'il est exprimé très précocement et plus fortement chez les mâles que chez les femelles. Notons toutefois, que vu la très forte homologie entre *gdf6b-A* et *gdf6b-B*, nous n'avons pas pu quantifier l'expression spécifique de ces deux copies de *gdf6b* lors du développement gonadique. Des expérimentations supplémentaires (qPCR) sont en cours afin de quantifier spécifiquement les deux copies de *gdf6b* et confirmer leurs profils d'expression durant le développement gonadique. Notons également que l'analyse de l'expression spatiale de *gdf6b* par hybridation *in situ* dans les gonades de poissons âgés de 16, 23 et 30 jpf (Annexe 2) est initiée et ces résultats pourraient apporter une preuve supplémentaire d'une expression restreinte de ce gène dans des testicules en cours de différenciation.

Nous avons aussi apporté des premières preuves fonctionnelles qui sous-tendent l'hypothèse que *gdf6b* soit bien le déterminant majeur du sexe chez *A. mexicanus*. Ainsi, nos résultats d'inactivation par la méthode CRISPR-Cas9 de *gdf6b* montrent clairement que ce gène est bien nécessaire à la différenciation testiculaire et ce dès la génération fondatrice G0 (**Article 2**). Des fondateurs ont été sélectionnés parmi les mutants positifs et une 1^{ère} génération (F1) a été générée résultant en 23,5 % de femelles phénotypiques qui sont génétiquement mâles (données non présentées). Ces résultats apportent une preuve solide de la nécessité de *gdf6b-B* et renforce notre hypothèse selon laquelle ce gène est potentiellement le déterminant majeur du sexe. Cependant, il est important de noter que nous n'avons pas pu caractériser les mutations spécifiques à *gdf6b-B* après l'inactivation. La présence de plusieurs copies de chromosomes B chez les mâles mutants inversés en femelles (1 à 3 Bs) ainsi que la duplication de *gdf6b-B* sur chacune des copies des Bs rend l'identification des mutations obtenues par CRISPR-Cas9 plus complexe. Néanmoins, nous essayons activement de trouver une méthode efficace qui pourrait nous permettre d'identifier ces mutations plus facilement. Une autre option, mais plus longue, consisterait à effectuer des croisements des animaux G0 ou F1 avec des animaux sauvages pour ségrégner ces différentes mutations et réduire la complexité du génotypage.

Par ailleurs, maintenant que nous connaissons mieux la structure des loci *gdf6b*, des approches plus ciblées pourraient peut-être être mises en place pour effectuer des inactivations ciblées sur les copies du chromosome B. Cette technique a été mise au point au laboratoire sur le médaka (Schartl et al., 2018) mais aussi chez notre modèle d'étude par Torres-Taz et al., (Torres-Taz et al., non publié). Cette approche serait particulièrement intéressante dans le cas du polymorphisme nucléotidique sur *gdf6b-B* ayant abouti à une transition d'une sérine (Ser227) présente uniquement sur la copie autosomale (*gdf6b-A*) des *A. mexicanus* de la grotte Pachón, par une glycine (Gly227) qui elle, est conservée chez l'ensemble des *gdf6* de vertébrés. Chez *Takifugu rubripes* et *Oreochromis niloticus*, des mutations ponctuelles respectivement dans l'*amhr2Y* et l'*amhY*, ont été décrites comme étant directement responsables de la détermination du sexe mâle (Kamiya et al., 2012; Li et al., 2015). Ainsi, il serait important d'envisager une édition de génome spécifique de cette variation nucléotidique chez les mâles (*gdf6b-B*) ou son remplacement sur *gdf6b-A* de façon à y intégrer la variation qui code pour la glycine. Une telle approche permettrait d'examiner les conséquences fonctionnelles d'une telle modification en faisant la connexion entre la causalité de cette variation et le phénotype mâle. De plus, elle permettrait de confirmer ou d'infirmer notre hypothèse d'une fonction hypoactive de *gdf6b-A* qui pourrait conduire à la féminisation des animaux qui n'ont pas de chromosome B et les loci *gdf6b-B* associés.

Pour confirmer le rôle de *gdf6b-B* dans la détermination du sexe, la preuve fonctionnelle de sa surexpression chez les femelles qui conduirait au phénotype mâle serait également importante. Depuis quelques années, la transgénèse additive a été mise au point chez *Astyanax mexicanus*, ce qui fait de cette espèce, un modèle attractif pour envisager des études fonctionnelles (Elipot et al., 2014). À cette fin, nous avons d'ores et déjà généré quatre lignées transgéniques d'*Astyanax mexicanus* (voir la démarche méthodologique en Annexe 3). Ces constructions ont pour objectif de surexprimer différentes combinaisons de promoteurs et cDNA de *gdf6b-B* et *gdf6b-A* e.g., : 1) promoteur-*gdf6b-B* + cDNA-*gdf6b-B*; 2) promoteur-*gdf6b-A* + cDNA-*gdf6b-B*; 3) promoteur-*gdf6b-B* + cDNA-*gdf6b-A*; 4) promoteur-*gdf6b-A* + cDNA-*gdf6b-B*. Ainsi, l'analyse de ces lignées devrait apporter des éléments de réponse quant au contrôle de la détermination du sexe par les séquences codantes (cDNA), la régulation par des régions promotrices (promoteurs) ou l'action combinée des deux à la fois. De plus, en tenant compte de la duplication de *gdf6b-B* sur les chromosomes B, la surexpression des différentes combinaisons permettrait de déterminer, si oui ou non *gdf6b* agirait par un effet de dosage sur la détermination du sexe chez *A. mexicanus*.

Enfin, il nous semble important de comprendre l'impact de l'ensemble des changements d'acides aminés détectés sur *gdf6b-B* par une approche de modélisation de la structure de ces deux protéines Gdf6b-A et Gdf6b-B. En effet, la modélisation de la structure 3D de *gdf6aY* et *gdf6aX* chez *N. furzeri* a révélé que les changements d'acides aminés observés sur *gdf6aY* pourraient affecter potentiellement l'interaction de la protéine au niveau de son récepteur ou pendant la phase de dimérisation. Il a été suggéré que ces variations alléliques pourraient modifier de manière globale la fonction de la protéine Gdf6aY en lui conférant le rôle de déterminant majeur du sexe chez cette espèce (Reichwald et al., 2015).

L'ensemble de nos résultats apportent donc, pour la toute première fois, des premières preuves fonctionnelles sur l'existence de microchromosomes B sexuels que nous avons baptisés "B-sex chromosomes" chez les poissons. Chez *A. mexicanus*, ces B-sex contiennent des copies dupliquées du gène *gdf6b* (*gdf6b-B*), qui agiraient comme un potentiel gène SD pour contrôler la détermination du sexe. Ce résultat constitue un second cas de l'implication des gènes *gdf6* dans la détermination du sexe chez les poissons, mais aussi un exemple supplémentaire de recrutement récurrent et indépendant des membres de la famille des TGF- β , dont l'importance dans la voie SD est de plus en plus mise en évidence. En outre, en apportant des arguments forts sur leur rôle dans la détermination du sexe chez *A. mexicanus*, nos travaux apportent un changement conceptuel important sur la biologie des chromosomes B qui sont souvent qualifiés d'inertes, de non-essentiels ou encore de chromosomes accessoires. Nos données, ajoutent aussi une dimension supplémentaire à la diversité étonnante des systèmes de détermination du sexe chez les vertébrés en particulier celle des chromosomes sexuels. Elles ouvrent aussi de nombreuses perspectives pour explorer l'origine des chromosomes B et les mécanismes évolutifs qui sont à l'origine de leur émergence en tant que chromosomes sexuels par l'acquisition d'un gène candidat à la SD. De plus, notre étude pourrait servir de base pour explorer l'implication des chromosomes B dans la détermination du sexe dans d'autres groupes de poissons, particulièrement les espèces chez lesquelles une liaison complète ou partielle des Bs avec le sexe avait déjà été montrée.

Évolution des systèmes de détermination du sexe chez les populations et morphotypes d'*A. mexicanus*

Suite à l'identification de l'implication potentielle du chromosome B et de ses loci *gdf6b-B* dans la détermination du sexe chez la population d'*A. mexicanus* de la grotte Pachón, nous avons élargi nos investigations à des populations sauvages cavernicoles et de surfaces du Nord-

Est du Mexique ainsi qu'à la population de laboratoire originaire de San Solomon Spring au Texas (Sud des Etats Unis) (**Article 3**). Les résultats obtenus chez les populations sauvages cavernicoles et de surface de la région de El Abra et de ses environs montrent une liaison forte entre le sexe mâle et le *gdf6b-B* putatif, suggérant ainsi un système de détermination génétique du sexe. Cette même hypothèse a été avancée chez les populations de laboratoire originaires de certaines grottes de cette région (Wilkens & Strecker, 2017). Ces résultats, bien qu'ils ne confirment en aucun cas la présence de chromosomes B ni de *gdf6b-B*, suggèrent néanmoins, l'existence d'un “*gdf6b-B* putatif” qui serait lié au sexe mâle dans les populations cavernicoles de Pachón, Los Sabinos, Tinaja, Curva, Toro et Chica et les deux populations de surface d'Arroyo Tampemole et de Rio Gallinas.

Cependant, dans les populations de la région de Guatemala (Molino, Jineo et Escondido), nous n'avons pas pu détecter la présence de *gdf6b-B* chez l'ensemble des individus analysés. Il est important de souligner que pour les populations cavernicoles sauvages analysées, les échantillonnages sont très réduits et constitués d'individus dont le sexe phénotypique n'est pas identifié soit majoritairement ou partiellement (Pachón, Los Sabinos, Tinaja, Curva, Toro and Chica), voire totalement (Subterraneo, Molino, Jineo et Escondido). Nous ne pouvons donc pas exclure que cette absence de détection du *gdf6b-B*, soit liée au fait que tous les individus échantillonés soient de sexe femelle, mais cette hypothèse qui reste possible à l'échelle d'une grotte n'est cependant que peu probable pour l'ensemble de nos prélèvements. Bien qu'un système GSD ait déjà été suggéré pour cette population (Wilkens & Strecker, 2017), les analyses des re-séquençages de 14 individus originaires de la grotte Molino (données publiques NCBI) ne montrent aucun signal au niveau du locus *gdf6b-B* qui serait lié au sexe (données non présentées). Ces données soutiennent donc l'hypothèse d'une absence complète de *gdf6b-B* et peut-être du chromosome B chez cette population de Molino.

La difficulté de travailler sur des populations cavernicoles sauvages protégées réside dans le fait que les poissons ne peuvent pas être prélevés entièrement pour des analyses au laboratoire. Du fait des tailles réduites estimées de certaines populations (de quelques dizaines à quelques centaines de poissons) (Bradic et al., 2012; Fumey et al., 2018), il est strictement interdit de prélever des poissons sauvages. Depuis quelques années (2013), Sylvie Rétaux et son équipe organisent des campagnes d'échantillonnages dans les grottes mexicaines afin de constituer une “banque de fin-clips” avec toutes les informations relatives à chacun des individus échantillonés telles que le poids, la taille, et le sexe lorsqu'il est identifiable selon les critères décrits précédemment (Eliot et al., 2014). Grâce à ces échantillonnages, des séquençages de

génomes d'individus dont le sexe est identifié dans l'ensemble des grottes y compris celle de Molino (échantillons obtenus par un collaborateur de S.R) sont prévus à court terme. Les données des séquençages devraient nous aider à caractériser les loci *gdf6b* chez les mâles et les femelles, afin de tenter d'établir si oui ou non, il existe un lien entre le phénotype mâle et un ou des loci *gdf6b-B* chez l'ensemble de ces populations.

Par ailleurs, dans la population de surface élevée en laboratoire depuis 2004 (originaire du Texas), nos données indiquent l'existence de microchromosomes B avec au moins un locus *gdf6b-B*, qui présentent une liaison partielle (~50 %) au sexe mâle. L'ensemble de ces résultats, suggèrent fortement que la détermination du sexe de certaines populations d'*A. mexicanus* de la région de Guatemala au Mexique et du Texas soit différente de la détermination GSD monofactorielle chez les populations cavernicoles de la région de El Abra.

Bien que nos données sur un éventuel effet de la température sur la détermination du sexe ne soient pas concluantes chez la population Texane (2 réplicats d'expérimentation avec des effets différents), nous ne pouvons pas complètement exclure que la température ou un autre facteur environnemental pourrait influencer la SD chez cette population. D'autres facteurs environnementaux tels que le pH, le comportement social, le taux d'oxygène et la densité ont été décrits comme pouvant avoir un effet sur la détermination du sexe chez de nombreuses espèces de poissons (Baroiller et al., 2009; Cheung et al., 2014; Devlin & Nagahama, 2002; Sato et al., 2005). Nos données pourraient aussi suggérer une détermination du sexe de type polygénique comme cela a déjà été décrit chez certaines espèces de poissons (Kallman, 1984; Moore & Roberts, 2013; Roberts et al., 2016). Des évolutions rapides des systèmes de détermination du sexe entre des populations sauvages et des populations de laboratoire nouvellement domestiquées ont été également rapportées. C'est le cas par exemple chez le poisson zèbre, où les populations sauvages auraient un système hétérogamétique femelle (ZZ/ZW), tandis que celles du laboratoire auraient perdu leur chromosome W (Wilson et al., 2014) et auraient évolué vers un système plus complexe combinant un déterminisme polygénique (Liew et al., 2012; Liew & Orbán, 2014) avec une influence environnementale (Ribas et al., 2017; Santos et al., 2017). Une perte partielle des chromosomes B en lien avec la domestication pourrait être aussi envisagée dans notre population de surface. Un tel événement aurait pu également faire évoluer le système SD d'un système monofactoriel simple vers un système plus complexe (une combinaison environnementale et polygénique de manière simultanée). Cependant, nos premières analyses ne nous ont pas permis de détecter un signal additionnel de celui du chromosome B et de son *gdf6b-B* qui pourrait supporter cette hypothèse.

Pour tenter de décrypter ce système complexe chez la population Texane, il serait intéressant dans un premier temps d'échantillonner des *A. mexicanus* sauvages au Texas afin de vérifier si l'on confirme ou infirme les résultats que nous avons obtenus sur une population de laboratoire. Pour cela, nous travaillons activement avec nos collaborateurs aux Etats Unis (Manfred Schartl) afin d'obtenir des individus entiers qui pourront être identifiés et analysés au laboratoire. De plus, avec un nouveau génome (mâle de la grotte Pachón) de meilleure qualité en termes de continuité, nous sommes maintenant en mesure de réanalyser toutes nos données de pool-seq et de RAD-seq pour tenter d'identifier le ou les loci sexuels dans la population de laboratoire. Pour comprendre si oui ou non l'environnement pourrait influencer la détermination du sexe, des croisements entre mâles et femelles de génotypes différents, avec un focus sur d'autres facteurs environnementaux, pourraient apporter des éléments de réponse quant au rôle de la composante environnementale.

Dans l'ensemble, nos données révèlent des différences majeures dans l'implication des microchromosomes B et de leurs loci *gdf6b-B* dans la détermination du sexe entre les populations cavernicoles d'El Abra et celles se trouvant dans la région de Guatemala et plus au nord au Texas. Ces différences sont également reflétées par les variations substantielles observées dans les séquences de *gdf6b-B*, par exemple chez la population Texane et la population de la grotte de la grotte Pachón. Des séquençages de génomes de mâles texans avec des génotypes différents seraient d'une importance primordiale. La comparaison des séquences des microchromosomes B ainsi que des loci *gdf6b-B* chez les différentes populations de surface et cavernicoles explorées dans mes travaux de thèse permettra de proposer des scénarios sur la dynamique évolutive des chromosomes B décrits dans notre étude comme des potentiels chromosomes sexuels à une échelle micro-évolutive très courte d'environ 20 000 ans. Ces études supplémentaires pourraient nous aider à comprendre le / les mécanisme (s) ayant abouti à la fixation de différentes mutations sur le locus sexuel au sein de la même espèce tout en gardant la fonction de déterminant majeur du sexe.

Enfin, notre étude met en évidence un nouveau cas de renouvellement intra-populationnel des systèmes de détermination du sexe chez *A. mexicanus*. Elle donne un premier aperçu d'une transition évolutive rapide entre un système de type B-sex chromosome à dominance mâle fixe vers un système plus complexe (probablement polygénique) ne reposant que partiellement sur le B-sex chromosome. Cette première étude devrait servir de base pour des futures investigations afin de mieux caractériser cette transition rapide.

BIBLIOGRAPHIE

- Ahmad, S. F., Jehangir, M., Cardoso, A. L., Wolf, I. R., Margarido, V. P., Cabral-de-Mello, D. C., O'Neill, R., Valente, G. T., & Martins, C. (2020). B chromosomes of multiple species have intense evolutionary dynamics and accumulated genes related to important biological processes. *BMC Genomics*, 21(1), 656. <https://doi.org/10.1186/s12864-020-07072-1>
- Ahmad, S., & Martins, C. (2019). The Modern View of B Chromosomes Under the Impact of High Scale Omics Analyses. *Cells*, 8(2), 156. <https://doi.org/10.3390/cells8020156>
- Altmanová, M., Rovatsos, M., Johnson Pokorná, M., Veselý, M., Wagner, F., & Kratochvíl, L. (2018). All iguana families with the exception of basilisks share sex chromosomes. *Zoology*, 126, 98–102. <https://doi.org/10.1016/j.zool.2017.11.007>
- Álvarez, J. (1947). Descripción de Anoptichthys hubbsi caracínido ciego de la cueva de los Sabinos (SLP). *Rev Soc Mex Hist Nat*
- Álvarez, J. (1946). Revision del genero Anoptichthys con descripcion de una especia nueva (Pisces, Characidae). *An. Esc. Nac. Cien. Biol. Mex.* 4 :263-282.
- Anderson, J. L., Marí, A. R., Braasch, I., Amores, A., Hohenlohe, P., Batzel, P., & Postlethwait, J. H. (2012). Multiple Sex-Associated Regions and a Putative Sex Chromosome in Zebrafish Revealed by RAD Mapping and Population Genomics. *PLOS ONE*, 7(7), e40701. <https://doi.org/10.1371/journal.pone.0040701>
- Aspiras, A. C., Rohner, N., Martineau, B., Borowsky, R. L., & Tabin, C. J. (2015). Melanocortin 4 receptor mutations contribute to the adaptation of cavefish to nutrient-poor conditions. *Proceedings of the National Academy of Sciences of the United States of America*, 112(31), 9668–9673. <https://doi.org/10.1073/pnas.1510802112>
- Avise, J. C., & Selander, R. K. (1972). EVOLUTIONARY GENETICS OF CAVE-DWELLING FISHES OF THE GENUS ASTYANAX. *Evolution; International Journal of Organic Evolution*, 26(1), 1–19. <https://doi.org/10.1111/j.1558-5646.1972.tb00170.x>
- Bachtrog, D., Hom, E., Wong, K. M., Maside, X., & de Jong, P. (2008). Genomic degradation of a young Y chromosome in *Drosophila miranda*. *Genome Biology*, 9(2), R30. <https://doi.org/10.1186/gb-2008-9-2-r30>
- Bachtrog, D., Mank, J. E., Peichel, C. L., Kirkpatrick, M., Otto, S. P., Ashman, T.-L., Hahn, M. W., Kitano, J., Mayrose, I., Ming, R., Perrin, N., Ross, L., Valenzuela, N., Vamosi, J. C., & Consortium, T. T. of S. (2014). Sex Determination: Why So Many Ways of Doing It? *PLOS Biology*, 12(7), e1001899. <https://doi.org/10.1371/journal.pbio.1001899>
- Bakkali, M., & Camacho, J. P. M. (2004). The B chromosome polymorphism of the grasshopper *Eyprepocnemis plorans* in North Africa. IV. Transmission of rare B chromosome variants. *Cytogenetic and Genome Research*, 106(2–4), 332–337. <https://doi.org/10.1159/000079308>
- Baroiller, J. F., & D'Cotta, H. (2001). Environment and sex determination in farmed fish. *Comparative Biochemistry and Physiology Part C: Toxicology & Pharmacology*, 130(4), 399–409. [https://doi.org/10.1016/S1532-0456\(01\)00267-8](https://doi.org/10.1016/S1532-0456(01)00267-8)
- Baroiller, Jean., D'Cotta, & E, S. (2009). Environmental effects on fish sex determination and differentiation. *Sexual Development: Genetics, Molecular Biology, Evolution, Endocrinology, Embryology, and Pathology of Sex Determination and Differentiation; Sex Dev*. <https://doi.org/10.1159/000223077>
- Baroiller, Jean-François, & D'Cotta, H. (2016). The Reversible Sex of Gonochoristic Fish: Insights and Consequences. *Sexual Development*, 10(5–6), 242–266. <https://doi.org/10.1159/000452362>
- Baroiller, J.-F., Guiguen, Y., & Fostier, A. (1999). Endocrine and environmental aspects of sex

- differentiation in fish. *Cellular and Molecular Life Sciences* CMS, 55(6), 910–931. <https://doi.org/10.1007/s000180050344>
- Bauerly, E., Hughes, S. E., Vietti, D. R., Miller, D. E., McDowell, W., & Hawley, R. S. (2014). Discovery of Supernumerary B Chromosomes in *Drosophila melanogaster*. *Genetics*, 196(4), 1007–1016. <https://doi.org/10.1534/genetics.113.160556>
- Becker, S. E. D., Thomas, R., Trifonov, V. A., Wayne, R. K., Graphodatsky, A. S., & Breen, M. (2011). Anchoring the dog to its relatives reveals new evolutionary breakpoints across 11 species of the Canidae and provides new clues for the role of B chromosomes. *Chromosome Research: An International Journal on the Molecular, Supramolecular and Evolutionary Aspects of Chromosome Biology*, 19(6), 685–708. <https://doi.org/10.1007/s10577-011-9233-4>
- Bertho, S., Herpin, A., Branthonne, A., Jouanno, E., Yano, A., Nicol, B., Muller, T., Pannetier, M., Pailhoux, E., Miwa, M., Yoshizaki, G., Schartl, M., & Guiguen, Y. (2018). The unusual rainbow trout sex determination gene hijacked the canonical vertebrate gonadal differentiation pathway. *Proceedings of the National Academy of Sciences*, 115(50), 12781–12786. <https://doi.org/10.1073/pnas.1803826115>
- Bertho, S., Pasquier, J., Pan, Q., Trionnaire, G. L., Bobe, J., Postlethwait, J. H., Pailhoux, E., Schartl, M., Herpin, A., & Guiguen, Y. (2016). Foxl2 and Its Relatives Are Evolutionary Conserved Players in Gonadal Sex Differentiation. *Sexual Development*, 10(3), 111–129. <https://doi.org/10.1159/000447611>
- Bibliowicz, J., Alié, A., Espinasa, L., Yoshizawa, M., Blin, M., Hinaux, H., Legendre, L., Père, S., & Rétaux, S. (2013). Differences in chemosensory response between eyed and eyeless *Astyanax mexicanus* of the Rio Subterráneo cave. *EvoDevo*, 4(1), 25. <https://doi.org/10.1186/2041-9139-4-25>
- Bilandžija, H., Ma, L., Parkhurst, A., & Jeffery, W. R. (2013). A Potential Benefit of Albinism in *Astyanax* Cavefish: Downregulation of the oca2 Gene Increases Tyrosine and Catecholamine Levels as an Alternative to Melanin Synthesis. *PLoS ONE*, 8(11). <https://doi.org/10.1371/journal.pone.0080823>
- Blin, M., Fumey, J., Lejeune, C., Pollicarpo, M., Leclercq, J., Père, S., Torres-Paz, J., Pierre, C., Imarazene, B., & Rétaux, S. (2020). Diversity of Olfactory Responses and Skills in *Astyanax Mexicanus* Cavefish Populations Inhabiting different Caves. *Diversity*, 12(10), 395. <https://doi.org/10.3390/d12100395>
- Blin, M., Tine, E., Meister, L., Elipot, Y., Bibliowicz, J., Espinasa, L., & Rétaux, S. (2018). Developmental evolution and developmental plasticity of the olfactory epithelium and olfactory skills in Mexican cavefish. *Developmental Biology*, 441(2), 242–251. <https://doi.org/10.1016/j.ydbio.2018.04.019>
- Böhne, A., Sengstag, T., & Salzburger, W. (2014). Comparative Transcriptomics in East African Cichlids Reveals Sex- and Species-Specific Expression and New Candidates for Sex Differentiation in Fishes. *Genome Biology and Evolution*, 6(9), 2567–2585. <https://doi.org/10.1093/gbe/evu200>
- Borowsky, R. (2008). Restoring sight in blind cavefish. *Current Biology*, 18(1), R23–R24. <https://doi.org/10.1016/j.cub.2007.11.023>
- Braat, A. K., Zandbergen, T., van de Water, S., Goos, H. J., & Zivkovic, D. (1999). Characterization of zebrafish primordial germ cells: Morphology and early distribution of vasa RNA. *Developmental Dynamics: An Official Publication of the American Association of Anatomists*, 216(2), 153–167. [https://doi.org/10.1002/\(SICI\)1097-0177\(199910\)216:2<153::AID-DVDY6>3.0.CO;2-1](https://doi.org/10.1002/(SICI)1097-0177(199910)216:2<153::AID-DVDY6>3.0.CO;2-1)
- Bradic, M., Beerli, P., García-de León, F. J., Esquivel-Bobadilla, S., & Borowsky, R. L. (2012). Gene flow and population structure in the Mexican blind cavefish complex (*Astyanax mexicanus*). *BMC Evolutionary Biology*, 12, 9. <https://doi.org/10.1186/1471-2148-12-9>

- Brown, E. E., Conover, D. O., & Baumann, H. (2014). Temperature and photoperiod effects on sex determination in a fish. *Journal of Experimental Marine Biology and Ecology*. <https://agris.fao.org/agris-search/search.do?recordID=US201700163352>
- Burcea, A., Popa, G.-O., Florescu Gune, I. E., Maereanu, M., Dudu, A., Georgescu, S. E., & Costache, M. (2018). Expression Characterization of Six Genes Possibly Involved in Gonad Development for Stellate Sturgeon Individuals (*Acipenser stellatus*, Pallas 1771). *International Journal of Genomics*, 2018, 7835637. <https://doi.org/10.1155/2018/7835637>
- Burt, A., & Trivers, R. (2006). *Genes in Conflict: The Biology of Selfish Genetic Elements*. Harvard University Press.
- Camacho, J. P.M., Shaw, M. W., López-León, M. D., Pardo, M. C., & Cabrero, J. (1997). Population dynamics of a selfish B chromosome neutralized by the standard genome in the grasshopper *Eyprepocnemis plorans*. *The American Naturalist*, 149(6), 1030–1050. <https://doi.org/10.1086/286037>
- Camacho, J.P.M., Cabrero, J., López-León, M. D., Bakkali, M., & Perfectti, F. (2003). The B Chromosomes of the Grasshopper *Eyprepocnemis Plorans* and the Intrageneric Conflict. *Genetica*, 117(1), 77–84. <https://doi.org/10.1023/A:1022311320394>
- Camacho, J.P.M., Schmid, M., & Cabrero, J. (2011). B Chromosomes and Sex in Animals. *Sexual Development*, 5(3), 155–166. <https://doi.org/10.1159/000324930>
- Camacho, J.P.M. (2005). CHAPTER 4—B Chromosomes. In T. R. Gregory (Éd.), *The Evolution of the Genome* (p. 223–286). Academic Press. <https://doi.org/10.1016/B978-012301463-4/50006-1>
- Camacho, J.P.M., Sharbel, T. F., & Beukeboom, L. W. (2000). B-chromosome evolution. *Philosophical Transactions of the Royal Society of London. Series B: Biological Sciences*, 355(1394), 163–178. <https://doi.org/10.1098/rstb.2000.0556>
- Capel, B. (2017). Vertebrate sex determination: Evolutionary plasticity of a fundamental switch. *Nature Reviews Genetics*, 18(11), 675–689. <https://doi.org/10.1038/nrg.2017.60>
- Carvalho, A. B. (2002). Origin and evolution of the *Drosophila* Y chromosome. *Current Opinion in Genetics & Development*, 12(6), 664–668. [https://doi.org/10.1016/s0959-437x\(02\)00356-8](https://doi.org/10.1016/s0959-437x(02)00356-8)
- Carvalho, A. B., Koerich, L. B., & Clark, A. G. (2009). Origin and Evolution of Y chromosomes: *Drosophila* tales. *Trends in genetics: TIG*, 25(6), 270–277. <https://doi.org/10.1016/j.tig.2009.04.002>
- Carvalho, R. A., Martins-Santos, I. C., & Dias, A. L. (2008). B chromosomes: An update about their occurrence in freshwater Neotropical fishes (Teleostei). *Journal of Fish Biology*, 72(8), 1907–1932. <https://doi.org/10.1111/j.1095-8649.2008.01835.x>
- Casane, D., & Rétaux, S. (2016). Evolutionary Genetics of the Cavefish *Astyanax mexicanus*. *Advances in Genetics*, 95, 117–159. <https://doi.org/10.1016/bs.adgen.2016.03.001>
- Castro, J. P., Hattori, R. S., Yoshinaga, T. T., Silva, D. M. Z. de A., Ruiz-Ruano, F. J., Foresti, F., Santos, M. H., Almeida, M. C. de, Moreira-Filho, O., & Artoni, R. F. (2019). Differential Expression of Genes Related to Sexual Determination Can Modify the Reproductive Cycle of *Astyanax scabripinnis* (Characiformes: Characidae) in B Chromosome Carrier Individuals. *Genes*, 10(11), 909. <https://doi.org/10.3390/genes10110909>
- Charlesworth, D., Charlesworth, B., & Marais, G. (2005). Steps in the evolution of heteromorphic sex chromosomes. *Heredity*, 95(2), 118–128. <https://doi.org/10.1038/sj.hdy.6800697>

- Charnov, E. L., & Bull, J. (1977). When is sex environmentally determined? *Nature*, 266(5605), 828–830. <https://doi.org/10.1038/266828a0>
- Chassot, A. A., Gregoire, E. P., Magliano, M., Lavery, R., & Chaboissier, M. C. (2008). Genetics of ovarian differentiation: Rspo1, a major player. *Sexual Development: Genetics, Molecular Biology, Evolution, Endocrinology, Embryology, and Pathology of Sex Determination and Differentiation*, 2(4–5), 219–227. <https://doi.org/10.1159/000152038>
- Chassot, A.-A., Bradford, S. T., Auguste, A., Gregoire, E. P., Pailhoux, E., Rooij, D. G. de, Schedl, A., & Chaboissier, M.-C. (2012). WNT4 and RSPO1 together are required for cell proliferation in the early mouse gonad. *Development*, 139(23), 4461–4472. <https://doi.org/10.1242/dev.078972>
- Chen, S., Zhang, G., Shao, C., Huang, Q., Liu, G., Zhang, P., Song, W., An, N., Chalopin, D., Volff, J.-N., Hong, Y., Li, Q., Sha, Z., Zhou, H., Xie, M., Yu, Q., Liu, Y., Xiang, H., Wang, N., ... Wang, J. (2014). Whole-genome sequence of a flatfish provides insights into ZW sex chromosome evolution and adaptation to a benthic lifestyle. *Nature Genetics*, 46(3), 253–260. <https://doi.org/10.1038/ng.2890>
- Cheung, C. H. Y., Chiu, J. M. Y., & Wu, R. S. S. (2014). Hypoxia turns genotypic female medaka fish into phenotypic males. *Ecotoxicology*, 23(7), 1260–1269. <https://doi.org/10.1007/s10646-014-1269-8>
- Clark, F. E., Conte, M. A., Ferreira-Bravo, I. A., Poletto, A. B., Martins, C., & Kocher, T. D. (2017). Dynamic Sequence Evolution of a Sex-Associated B Chromosome in Lake Malawi Cichlid Fish. *Journal of Heredity*, 108(1), 53–62. <https://doi.org/10.1093/jhered/esw059>
- Clark, F. E., Conte, M. A., & Kocher, T. D. (2018). Genomic Characterization of a B Chromosome in Lake Malawi Cichlid Fishes. *Genes*, 9(12). <https://doi.org/10.3390/genes9120610>
- Clark, F. E., & Kocher, T. D. (2019). Changing sex for selfish gain: B chromosomes of Lake Malawi cichlid fish. *Scientific Reports*, 9(1), 20213. <https://doi.org/10.1038/s41598-019-55774-8>
- Clelland, E. S., & Kelly, S. P. (2011). Exogenous GDF9 but not Activin A, BMP15 or TGF β alters tight junction protein transcript abundance in zebrafish ovarian follicles. *General and Comparative Endocrinology*, 171(2), 211–217. <https://doi.org/10.1016/j.ygcen.2011.01.009>
- Cnaani, A., Lee, B.-Y., Zilberman, N., Ozouf-Costaz, C., Hulata, G., Ron, M., D'Hont, A., Baroiller, J.-F., D'Cotta, H., Penman, D. J., Tomasino, E., Coutanceau, J.-P., Pepey, E., Shirak, A., & Kocher, T. D. (2008). Genetics of Sex Determination in Tilapiine Species. *Sexual Development*, 2(1), 43–54. <https://doi.org/10.1159/000117718>
- Coelho, G. C. Z., Yo, I. S., Mira-López, T. M., Monzani, P. S., Arashiro, D. R., Fujimoto, T., Senhorini, J. A., & Yasui, G. S. (2019). Preparation of a fish embryo for micromanipulation: Staging of development, removal of the chorion and traceability of PGCs in Prochilodus lineatus. *The International Journal of Developmental Biology*, 63(1–2), 57–65. <https://doi.org/10.1387/ijdb.180348gc>
- Coghill, L. M., Darrin Hulsey, C., Chaves-Campos, J., García de Leon, F. J., & Johnson, S. G. (2014). Next generation phylogeography of cave and surface *Astyanax mexicanus*. *Molecular Phylogenetics and Evolution*, 79, 368–374. <https://doi.org/10.1016/j.ympev.2014.06.029>
- Conover, D. O., & Kynard, B. E. (1981). Environmental sex determination: Interaction of temperature and genotype in a fish. *Science (New York, N.Y.)*, 213(4507), 577–579. <https://doi.org/10.1126/science.213.4507.577>

- Culver, D. C., & Pipan, T. (2009). David C. Culver and Tanja Pipan 2009: The Biology of Caves and Other Subterranean Habitats. *Acta Carsologica*, 38(2 3), Article 2 3. <https://doi.org/10.3986/ac.v38i2-3.168>
- Dalla Benetta, E., Akbari, O. S., & Ferree, P. M. (2019). Sequence Expression of Supernumerary B Chromosomes: Function or Fluff? *Genes*, 10(2), 123. <https://doi.org/10.3390/genes10020123>
- Depiereux, S., Gac, F. L., Meulder, B. D., Pierre, M., Helaers, R., Guiguen, Y., Kestemont, P., & Depiereux, E. (2015). Meta-Analysis of Microarray Data of Rainbow Trout Fry Gonad Differentiation Modulated by Ethynylestradiol. *PLOS ONE*, 10(9), e0135799. <https://doi.org/10.1371/journal.pone.0135799>
- D'Ambrosio, U., Alonso-Lifante, M. P., Barros, K., Kovařík, A., Mas de Xaxars, G., & Garcia, S. (2017). B-chrom: A database on B-chromosomes of plants, animals and fungi. *New Phytologist*, 216(3), 635 642. <https://doi.org/10.1111/nph.14723>
- Devlin, R. H., & Nagahama, Y. (2002). Sex determination and sex differentiation in fish: An overview of genetic, physiological, and environmental influences. *Aquaculture*, 208(3 4), 191 364. [https://doi.org/10.1016/S0044-8486\(02\)00057-1](https://doi.org/10.1016/S0044-8486(02)00057-1)
- Devos, L., KLEE, F., Edouard, J., Simon, V., Legendre, L., Khallouki, N., Blin, M., Barbachou, S., Sohm, F., & Rétaux, S. (2019). Morphogenetic and patterning defects explain the coloboma phenotype of the eye in the Mexican cavefish. <https://doi.org/10.1101/698035>
- Dong, J., Albertini, D. F., Nishimori, K., Kumar, T. R., Lu, N., & Matzuk, M. M. (1996). Growth differentiation factor-9 is required during early ovarian folliculogenesis. *Nature*, 383(6600), 531 535. <https://doi.org/10.1038/383531a0>
- Douglas, S. E. (2006). Microarray Studies of Gene Expression in Fish. *OMICS: A Journal of Integrative Biology*, 10(4), 474 489. <https://doi.org/10.1089/omi.2006.10.474>
- Dowling, T. E., Martasian, D. P., & Jeffery, W. R. (2002). Evidence for multiple genetic forms with similar eyeless phenotypes in the blind cavefish, *Astyanax mexicanus*. *Molecular Biology and Evolution*, 19(4), 446 455. <https://doi.org/10.1093/oxfordjournals.molbev.a004100>
- Duboué, E. R., Keene, A. C., & Borowsky, R. L. (2011). Evolutionary convergence on sleep loss in cavefish populations. *Current Biology: CB*, 21(8), 671 676. <https://doi.org/10.1016/j.cub.2011.03.020>
- Elipot, Y., Hinaux, H., Callebert, J., & Rétaux, S. (2012). Evolutionary Shift from Fighting to Foraging in Blind Cavefish through Changes in the Serotonin Network. *Current biology: CB*, 23. <https://doi.org/10.1016/j.cub.2012.10.044>
- Elipot, Y., Hinaux, H., Callebert, J., Launay, J.-M., Blin, M., & Rétaux, S. (2014). A mutation in the enzyme monoamine oxidase explains part of the *Astyanax* cavefish behavioural syndrome. *Nature Communications*, 5(1), 3647. <https://doi.org/10.1038/ncomms4647>
- Elipot, Y., Legendre, L., Père, S., Sohm, F., & Rétaux, S. (2014). Astyanax transgenesis and husbandry: How cavefish enters the laboratory. *Zebrafish*, 11(4), 291 299. <https://doi.org/10.1089/zeb.2014.1005>
- Elliott, W. R. (2019). The *Astyanax* Caves of Mexico: Cavefishes of Tamaulipas, San Luis Potosí, and Guerrero. *Journal of Fish Biology*, 94(1), 205 205. <https://doi.org/10.1111/jfb.13889>
- Elliott, William R. (2016a). Cave Biodiversity and Ecology of the Sierra de El Abra Region. In A. C. Keene, M. Yoshizawa, & S. E. McGaugh (Éds.), *Biology and Evolution of the Mexican Cavefish* (p. 59 76). Academic Press. <https://doi.org/10.1016/B978-0-12-802148-4.00003-7>
- Elliott, William R. (2016b). Cave Exploration and Mapping in the Sierra de El Abra Region. In A. C. Keene, M. Yoshizawa, & S. E. McGaugh (Éds.), *Biology and Evolution of the*

- Mexican Cavefish (p. 9–40). Academic Press. <https://doi.org/10.1016/B978-0-12-802148-4.00001-3>
- Eschmeyer, W. (accessed on March 2020). Catalog of Fishes: Genera, Species, References. Available online: <http://researcharchive.calacademy.org/research/ichthyology/catalog/fishcatmain.asp>
- Espinasa, L., Bonaroti, N., Wong, J., Pottin, K., Queinnec, E., & Rétaux, S. (2017). Contrasting feeding habits of post-larval and adult *Astyanax* cavefish. *Subterranean Biology*, 21, 1–17. <https://doi.org/10.3897/subtbiol.21.11046>
- Espinasa, L., Legendre, L., Fumey, J., Blin, M., Rétaux, S., & Espinasa, M. (2018). A new cave locality for *Astyanax* cavefish in Sierra de El Abra, Mexico. *Subterranean Biology*, 26, 39–53. <https://doi.org/10.3897/subtbiol.26.26643>
- Faber-Hammond, J. J., Phillips, R. B., & Brown, K. H. (2015). Comparative Analysis of the Shared Sex-Determination Region (SDR) among Salmonid Fishes. *Genome Biology and Evolution*, 7(7), 1972–1987. <https://doi.org/10.1093/gbe/evv123>
- Feldberg, E., Porto, J. I. R., Alves-Brinn, M. N., Mendonça, M. N. C., & Benzaquem, D. C. (2004). B chromosomes in Amazonian cichlid species. *Cytogenetic and Genome Research*, 106(2–4), 195–198. <https://doi.org/10.1159/000079287>
- Feron, R., Zahm, M., Cabau, C., Klopp, C., Roques, C., Bouchez, O., Eché, C., Valière, S., Donnadieu, C., Haffray, P., Bestin, A., Morvezen, R., Acloque, H., Euclide, P. T., Wen, M., Jouano, E., Schartl, M., Postlethwait, J. H., Schraadt, C., ... Guiguen, Y. (2020). Characterization of a Y-specific duplication/insertion of the anti-Mullerian hormone type II receptor gene based on a chromosome-scale genome assembly of yellow perch, *Perca flavescens*. *Molecular Ecology Resources*, 20(2), 531–543. <https://doi.org/10.1111/1755-0998.13133>
- Forconi, M., Canapa, A., Barucca, M., Biscotti, M. A., Capriglione, T., Buonocore, F., Fausto, A. M., Makapedua, D. M., Pallavicini, A., Gerdol, M., De Moro, G., Scapigliati, G., Olmo, E., & Schartl, M. (2013). Characterization of Sex Determination and Sex Differentiation Genes in Latimeria. *PLoS ONE*, 8(4), e56006. <https://doi.org/10.1371/journal.pone.0056006>
- Foresti, F., Almeida-Tolcdo, L. F., & Toledo, S. A. (1989). Supernumerary chromosome system, C-banding pattern characterization and multiple nucleolus organizer regions in *Moenkhausia sanctaefilomenae* (Pisces, Characidae). *Genetica*, 79(2), 107–114. <https://doi.org/10.1007/BF00057927>
- Fowler, B. L. S., & Buonaccorsi, V. P. (2016). Genomic characterization of sex-identification markers in *Sebastes carnatus* and *Sebastes chrysomelas* rockfishes. *Molecular Ecology*, 25(10), 2165–2175. <https://doi.org/10.1111/mec.13594>
- Francis, R. C. (1984). The Effects of Bidirectional Selection for Social Dominance on Agonistic Behavior and Sex Ratios in the Paradise Fish (*Macropodus Opercularis*). *Behaviour*, 90(1–3), 25–44. <https://doi.org/10.1163/156853984X00542>
- Fricke, R., Eschmeyer, W. N. & R. van der Laan. (accessed: on march 2020). Eschmeyer's catalog of fishes: genera, species, references. Available online: (<http://researcharchive.calacademy.org/research/ichthyology/catalog/fishcatmain.asp>)
- Fumey, J., Hinaux, H., Noirot, C., Thermes, C., Rétaux, S., & Casane, D. (2018). Evidence for late Pleistocene origin of *Astyanax mexicanus* cavefish. *BMC Evolutionary Biology*, 18(1), 43. <https://doi.org/10.1186/s12862-018-1156-7>
- Gross, J. B. (2012). The complex origin of *Astyanax* cavefish. *BMC Evolutionary Biology*, 12, 105. <https://doi.org/10.1186/1471-2148-12-105>
- Gross, J. B., Borowsky, R., & Tabin, C. J. (2009). A novel role for Mc1r in the parallel evolution of depigmentation in independent populations of the cavefish *Astyanax mexicanus*. *PLoS Genetics*, 5(1), e1000326.

- <https://doi.org/10.1371/journal.pgen.1000326>
- Gross, J. B., Krutzler, A. J., & Carlson, B. M. (2014). Complex craniofacial changes in blind cave-dwelling fish are mediated by genetically symmetric and asymmetric loci. *Genetics*, 196(4), 1303–1319. <https://doi.org/10.1534/genetics.114.161661>
- Guerrero-Estevez, S., & Moreno-Mendoza, N. (2010). Sexual determination and differentiation in teleost fish. *Reviews in Fish Biology and Fisheries*, 20(1), 101–121. <https://doi.org/10.1007/s11160-009-9123-4>
- Gui, J., & Zhou, L. (2010). Genetic basis and breeding application of clonal diversity and dual reproduction modes in polyploid *Carassius auratus gibelio*. *Science China. Life Sciences*, 53(4), 409–415. <https://doi.org/10.1007/s11427-010-0092-6>
- Guiguen, Y., Fostier, A., & Herpin, A. (2018). Sex Determination and Differentiation in Fish. In *Sex Control in Aquaculture* (p. 35–63). John Wiley & Sons, Ltd. <https://doi.org/10.1002/9781119127291.ch2>
- Guiguen, Y., Fostier, A., Piferrer, F., & Chang, C.-F. (2010). Ovarian aromatase and estrogens: A pivotal role for gonadal sex differentiation and sex change in fish. *General and Comparative Endocrinology*, 165(3), 352–366. <https://doi.org/10.1016/j.ygcen.2009.03.002>
- Hackstein, J. H., Hochstenbach, R., Hauschteck-Jungen, E., & Beukeboom, L. W. (1996). Is the Y chromosome of *Drosophila* an evolved supernumerary chromosome? *BioEssays: News and Reviews in Molecular, Cellular and Developmental Biology*, 18(4), 317–323. <https://doi.org/10.1002/bies.950180410>
- Hafez R, Labat R, Quiller R. (1981). Reserches sur les chromosomes supernuméraires de l'ablette (*Alburnus alburnus* L.). *Cybium* 5: 81-87.
- Hanlon, S. L., Miller, D. E., Eche, S., & Hawley, R. S. (2018). Origin, Composition, and Structure of the Supernumerary B Chromosome of *Drosophila melanogaster*. *Genetics*, 210(4), 1197–1212. <https://doi.org/10.1534/genetics.118.301478>
- Hattori, R. S., Strüssmann, C. A., Fernandino, J. I., & Somoza, G. M. (2013). Genotypic sex determination in teleosts: Insights from the testis-determining amhy gene. *General and Comparative Endocrinology*, 192, 55–59. <https://doi.org/10.1016/j.ygcen.2013.03.019>
- Hausdorf, B., Wilkens, H., & Strecker, U. (2011). Population genetic patterns revealed by microsatellite data challenge the mitochondrial DNA based taxonomy of *Astyanax* in Mexico (Characidae, Teleostei). *Molecular Phylogenetics and Evolution*, 60(1), 89–97. <https://doi.org/10.1016/j.ympev.2011.03.009>
- Hayes, T. B. (1998). Sex determination and primary sex differentiation in amphibians: Genetic and developmental mechanisms. <https://onlinelibrary.wiley.com/doi/10.1002/%28SICI%291097-010X%2819980801%29281%3A5%3C373%3A%3AAID-JEZ4%3E3.0.CO%3B2-L>
- Herman, A., Brandvain, Y., Weagley, J., Jeffery, W. R., Keene, A. C., Kono, T. J. Y., Bilandžija, H., Borowsky, R., Espinasa, L., O’Quin, K., Ornelas-García, C. P., Yoshizawa, M., Carlson, B., Maldonado, E., Gross, J. B., Cartwright, R. A., Rohner, N., Warren, W. C., & McGaugh, S. E. (2018). The role of gene flow in rapid and repeated evolution of cave-related traits in Mexican tetra, *Astyanax mexicanus*. *Molecular Ecology*, 27(22), 4397–4416. <https://doi.org/10.1111/mec.14877>
- Herpin, A., & Schartl, M. (2009). Molecular mechanisms of sex determination and evolution of the Y-chromosome: Insights from the medakafish (*Oryzias latipes*). *Molecular and Cellular Endocrinology*, 306(1–2), 51–58. <https://doi.org/10.1016/j.mce.2009.02.004>
- Herpin, A., Adolfi, M. C., Nicol, B., Hinzmamn, M., Schmidt, C., Klughammer, J., Engel, M., Tanaka, M., Guiguen, Y., & Schartl, M. (2013). Divergent Expression Regulation of Gonad Development Genes in Medaka Shows Incomplete Conservation of the Downstream Regulatory Network of Vertebrate Sex Determination. *Molecular Biology*

- and Evolution, 30(10), 2328–2346. <https://doi.org/10.1093/molbev/mst130>
- Herpin, A., Braasch, I., Kraeussling, M., Schmidt, C., Thoma, E. C., Nakamura, S., Tanaka, M., & Schartl, M. (2010). Transcriptional Rewiring of the Sex Determining dmrt1 Gene Duplicate by Transposable Elements. *PLOS Genetics*, 6(2), e1000844. <https://doi.org/10.1371/journal.pgen.1000844>
- Herpin, A., Fischer, P., Liedtke, D., Kluever, N., Neuner, C., Raz, E., & Schartl, M. (2008). Sequential SDF1a and b-induced mobility guides Medaka PGC migration. *Developmental Biology*, 320(2), 319–327. <https://doi.org/10.1016/j.ydbio.2008.03.030>
- Herpin, A., Rohr, S., Riedel, D., Kluever, N., Raz, E., & Schartl, M. (2007). Specification of primordial germ cells in medaka (*Oryzias latipes*). *BMC Developmental Biology*, 7(1), 3. <https://doi.org/10.1186/1471-213X-7-3>
- Herpin, A., & Schartl, M. (2011). Dmrt1 genes at the crossroads: A widespread and central class of sexual development factors in fish. *The FEBS Journal*, 278(7), 1010–1019. <https://doi.org/10.1111/j.1742-4658.2011.08030.x>
- Herpin, A., & Schartl, M. (2015). Plasticity of gene-regulatory networks controlling sex determination: Of masters, slaves, usual suspects, newcomers, and usurpators. *EMBO Reports*, 16(10), 1260–1274. <https://doi.org/10.15252/embr.201540667>
- Herrera, J. A., López-León, M. D., Cabrero, J., Shaw, M. W., & Camacho, J. P. M. (1996). Evidence for B chromosome drive suppression in the grasshopper *Eyprepocnemis plorans*. *Heredity*, 76(6), 633–639. <https://doi.org/10.1038/hdy.1996.90>
- Heule, C., Salzburger, W., & Böhne, A. (2014). Genetics of Sexual Development: An Evolutionary Playground for Fish. *Genetics*, 196(3), 579–591. <https://doi.org/10.1534/genetics.114.161158>
- Hinaux, H., Blin, M., Fumey, J., Legendre, L., Heuzé, A., Casane, D., & Rétaux, S. (2015). Lens defects in *Astyanax mexicanus* Cavefish: Evolution of crystallins and a role for alphaA-crystallin. *Developmental Neurobiology*, 75(5), 505–521. <https://doi.org/10.1002/dneu.22239>
- Hinaux, H., Devos, L., Blin, M., Elipot, Y., Bibliowicz, J., Alié, A., & Rétaux, S. (2016). Sensory evolution in blind cavefish is driven by early embryonic events during gastrulation and neurulation. *Development* (Cambridge, England), 143(23), 4521–4532. <https://doi.org/10.1242/dev.141291>
- Hinaux, H., Poulain, J., Da Silva, C., Noirot, C., Jeffery, W. R., Casane, D., & Rétaux, S. (2013). De novo sequencing of *Astyanax mexicanus* surface fish and Pachón cavefish transcriptomes reveals enrichment of mutations in cavefish putative eye genes. *PloS One*, 8(1). <https://doi.org/10.1371/journal.pone.0053553>
- Houben, A., Jones, N., Martins, C., & Trifonov, V. (2019). Evolution, Composition and Regulation of Supernumerary B Chromosomes. *Genes*, 10(2). <https://doi.org/10.3390/genes10020161>
- Houben, A., Banaei-Moghaddam, A. M., Klemme, S., & Timmis, J. N. (2014). Evolution and biology of supernumerary B chromosomes. *Cellular and Molecular Life Sciences*, 71(3), 467–478. <https://doi.org/10.1007/s00018-013-1437-7>
- Huang, W., Du, Y., Zhao, X., & Jin, W. (2016). B chromosome contains active genes and impacts the transcription of A chromosomes in maize (*Zea mays* L.). *BMC Plant Biology*, 16, 88. <https://doi.org/10.1186/s12870-016-0775-7>
- Hubbs, C.L and W.T. Innes. (1936). The first known blind fish of the family Characidae: A new genus from Mexico. *Occ. Pap. Mus. Zool. Mich.* No. 342:1-7.
- Huminiecki, L., Goldovsky, L., Freilich, S., Moustakas, A., Ouzounis, C., & Heldin, C.-H. (2009). Emergence, development and diversification of the TGF- β signalling pathway within the animal kingdom. *BMC Evolutionary Biology*, 9(1), 28. <https://doi.org/10.1186/1471-2148-9-28>

- Hüppop, K., & Wilkens, H. (1991). Bigger eggs in subterranean *Astyanax fasciatus* (Characidae, Pisces). *Journal of Zoological Systematics and Evolutionary Research*, 29(4), 280–288. <https://doi.org/10.1111/j.1439-0469.1991.tb00673.x>
- Ikushima, H., & Miyazono, K. (2010). TGFbeta signaling: A complex web in cancer progression. *Nature Reviews Cancer*, 10(6), 415–424. <https://doi.org/10.1038/nrc2853>
- Ijiri, S., Kaneko, H., Kobayashi, T., Wang, D.-S., Sakai, F., Paul-Prasanth, B., Nakamura, M., & Nagahama, Y. (2008). Sexual Dimorphic Expression of Genes in Gonads During Early Differentiation of a Teleost Fish, the Nile Tilapia *Oreochromis niloticus*. *Biology of Reproduction*, 78(2), 333–341. <https://doi.org/10.1095/biolreprod.107.064246>
- Itman, C., & Loveland, K. L. (2008). SMAD expression in the testis: An insight into BMP regulation of spermatogenesis. *Developmental Dynamics*, 237(1), 97–111. <https://doi.org/10.1002/dvdy.21401>
- Janzen, F. J., & Paukstis, G. L. (1991). Environmental Sex Determination in Reptiles: Ecology, Evolution, and Experimental Design. *The Quarterly Review of Biology*, 66(2), 149–179. JSTOR.
- Jeffery, W. R. (2009). Regressive evolution in *Astyanax* cavefish. *Annual Review of Genetics*, 43, 25–47. <https://doi.org/10.1146/annurev-genet-102108-134216>
- Jeffery, W. R. (2020). *Astyanax* surface and cave fish morphs. *EvoDevo*, 11, 14. <https://doi.org/10.1186/s13227-020-00159-6>
- Jiang, T., Hou, C.-C., She, Z.-Y., & Yang, W.-X. (2013). The SOX gene family: Function and regulation in testis determination and male fertility maintenance. *Molecular Biology Reports*, 40(3), 2187–2194. <https://doi.org/10.1007/s11033-012-2279-3>
- Jin, W., Lamb, J. C., Vega, J. M., Dawe, R. K., Birchler, J. A., & Jiang, J. (2005). Molecular and Functional Dissection of the Maize B Chromosome Centromere. *The Plant Cell*, 17(5), 1412–1423. <https://doi.org/10.1105/tpc.104.030643>
- Jones, N. (2017). New species with B chromosomes discovered since 1980. *The Nucleus*, 60(3), 263–281. <https://doi.org/10.1007/s13237-017-0215-6>
- Jones, R. N. (1991). B-Chromosome Drive. *The American Naturalist*, 137(3), 430–442. <https://doi.org/10.1086/285175>
- Jones, R. N., & Rees, H. (1982). B chromosomes. B Chromosomes. <https://www.cabdirect.org/cabdirect/abstract/19831625314>
- Kallman, K. D. (1984). A New Look at Sex Determination in Poeciliid Fishes. In B. J. Turner (Ed.), *Evolutionary Genetics of Fishes* (p. 95–171). Springer US. https://doi.org/10.1007/978-1-4684-4652-4_3
- Kamiya, T., Kai, W., Tasumi, S., Oka, A., Matsunaga, T., Mizuno, N., Fujita, M., Suetake, H., Suzuki, S., Hosoya, S., Tohari, S., Brenner, S., Miyadai, T., Venkatesh, B., Suzuki, Y., & Kikuchi, K. (2012). A Trans-Species Missense SNP in Amhr2 Is Associated with Sex Determination in the Tiger Pufferfish, *Takifugu rubripes* (Fugu). *PLOS Genetics*, 8(7), e1002798. <https://doi.org/10.1371/journal.pgen.1002798>
- Katoh, K., & Miyata, T. (1999). A heuristic approach of maximum likelihood method for inferring phylogenetic tree and an application to the mammalian SOX-3 origin of the testis-determining gene SRY. *FEBS Letters*, 463(1–2), 129–132. [https://doi.org/10.1016/S0014-5793\(99\)01621-X](https://doi.org/10.1016/S0014-5793(99)01621-X)
- Keene, A. C., Yoshizawa, M., & McGaugh, S. E. (2016). *Biology and Evolution of the Mexican Cavefish*. Elsevier. <https://doi.org/10.1016/C2014-0-01426-8>
- Kikuchi, K., & Hamaguchi, S. (2013). Novel sex-determining genes in fish and sex chromosome evolution. *Developmental Dynamics: An Official Publication of the American Association of Anatomists*, 242(4), 339–353. <https://doi.org/10.1002/dvdy.23927>

- Kimura, R., Murata, C., Kuroki, Y., & Kuroiwa, A. (2014). Mutations in the Testis-Specific Enhancer of SOX9 in the SRY Independent Sex-Determining Mechanism in the Genus Tokudaia. *PLOS ONE*, 9(9), e108779. <https://doi.org/10.1371/journal.pone.0108779>
- Kitano, J., & Peichel, C. L. (2012). Turnover of sex chromosomes and speciation in fishes. *Environmental Biology of Fishes*, 94(3), 549–558. <https://doi.org/10.1007/s10641-011-9853-8>
- Knaut, H., Werz, C., Geisler, R., & Nüsslein-Volhard, C. (2003). A zebrafish homologue of the chemokine receptor Cxcr4 is a germ-cell guidance receptor. *Nature*, 421(6920), 279–282. <https://doi.org/10.1038/nature01338>
- Koopman, P., Gubbay, J., Vivian, N., Goodfellow, P., & Lovell-Badge, R. (1991). Male development of chromosomally female mice transgenic for Sry. *Nature*, 351(6322), 117–121. <https://doi.org/10.1038/351117a0>
- Kosswig, C. (1964). Polygenic sex determination. *Experientia*, 20(4), 190–199. <https://doi.org/10.1007/BF02135395>
- Kowalko, J. E., Rohner, N., Linden, T. A., Rompani, S. B., Warren, W. C., Borowsky, R., Tabin, C. J., Jeffery, W. R., & Yoshizawa, M. (2013). Convergence in feeding posture occurs through different genetic loci in independently evolved cave populations of *Astyanax mexicanus*. *Proceedings of the National Academy of Sciences of the United States of America*, 110(42), 16933–16938. <https://doi.org/10.1073/pnas.1317192110>
- Koyama, T., Nakamoto, M., Morishima, K., Yamashita, R., Yamashita, T., Sasaki, K., Kuruma, Y., Mizuno, N., Suzuki, M., Okada, Y., Ieda, R., Uchino, T., Tasumi, S., Hosoya, S., Uno, S., Koyama, J., Toyoda, A., Kikuchi, K., & Sakamoto, T. (2019). A SNP in a Steroidogenic Enzyme Is Associated with Phenotypic Sex in Seriola Fishes. *Current Biology*, 29(11), 1901–1909.e8. <https://doi.org/10.1016/j.cub.2019.04.069>
- Kurokawa, H., Aoki, Y., Nakamura, S., Ebe, Y., Kobayashi, D., & Tanaka, M. (2006). Time-lapse analysis reveals different modes of primordial germ cell migration in the medaka *Oryzias latipes*. *Development, Growth and Differentiation*, 48(3), 209–221. <https://doi.org/10.1111/j.1440-169X.2006.00858.x>
- Li, M., Sun, Y., Zhao, J., Shi, H., Zeng, S., Ye, K., Jiang, D., Zhou, L., Sun, L., Tao, W., Nagahama, Y., Kocher, T. D., & Wang, D. (2015). A Tandem Duplicate of Anti-Müllerian Hormone with a Missense SNP on the Y Chromosome Is Essential for Male Sex Determination in Nile Tilapia, *Oreochromis niloticus*. *PLOS Genetics*, 11(11), e1005678. <https://doi.org/10.1371/journal.pgen.1005678>
- Li, X.-Y., Liu, X.-L., Ding, M., Li, Z., Zhou, L., Zhang, X.-J., & Gui, J.-F. (2017). A novel male-specific SET domain-containing gene setdm identified from extra microchromosomes of gibel carp males. *Science Bulletin*, 62(8), 528–536. <https://doi.org/10.1016/j.scib.2017.04.002>
- Li, X.-Y., Zhang, Q.-Y., Zhang, J., Zhou, L., Li, Z., Zhang, X.-J., Wang, D., & Gui, J.-F. (2016). Extra Microchromosomes Play Male Determination Role in Polyploid Gibel Carp. *Genetics*, 203(3), 1415–1424. <https://doi.org/10.1534/genetics.115.185843>
- Liew, W. C., Bartfai, R., Lim, Z., Sreenivasan, R., Siegfried, K. R., & Orban, L. (2012). Polygenic Sex Determination System in Zebrafish. *PLOS ONE*, 7(4), e34397. <https://doi.org/10.1371/journal.pone.0034397>
- Liew, W. C., & Orbán, L. (2014). Zebrafish sex: A complicated affair. *Briefings in Functional Genomics*, 13(2), 172–187. <https://doi.org/10.1093/bfgp/elt041>
- Lobo, I. K. C., Nascimento, Á. R. do, Yamagishi, M. E. B., Guiguen, Y., Silva, G. F. da, Severac, D., Amaral, A. da C., Reis, V. R., & Almeida, F. L. de. (2020). Transcriptome of tambaqui *Colossoma macropomum* during gonad differentiation: Different molecular signals leading to sex identity. *Genomics*, 112(3), 2478–2488. <https://doi.org/10.1016/j.ygeno.2020.01.022>

- Lubieniecki, K. P., Lin, S., Cabana, E. I., Li, J., Lai, Y. Y. Y., & Davidson, W. S. (2015). Genomic Instability of the Sex-Determining Locus in Atlantic Salmon (*Salmo salar*). *G3* (Bethesda, Md.), 5(11), 2513–2522. <https://doi.org/10.1534/g3.115.020115>
- Luckenbach, A. J., & Yamamoto, Y. (2018). Genetic & Environmental Sex Determination in Cold-blooded Vertebrates: Fishes, Amphibians, and Reptiles. In M. K. Skinner (Ed.), *Encyclopedia of Reproduction* (Second Edition) (p. 176–183). Academic Press. <https://doi.org/10.1016/B978-0-12-809633-8.20553-0>
- Ma, L., Parkhurst, A., & Jeffery, W. R. (2014). The role of a lens survival pathway including sox2 and αA-crystallin in the evolution of cavefish eye degeneration. *EvoDevo*, 5, 28. <https://doi.org/10.1186/2041-9139-5-28>
- Ma, L., Gore, A. V., Castranova, D., Shi, J., Ng, M., Tomins, K. A., van der Weele, C. M., Weinstein, B. M., & Jeffery, W. R. (2020). A hypomorphic cystathionine β-synthase gene contributes to cavefish eye loss by disrupting optic vasculature. *Nature Communications*, 11(1), 2772. <https://doi.org/10.1038/s41467-020-16497-x>
- Makunin, A. I., Rajičić, M., Karamysheva, T. V., Romanenko, S. A., Druzhkova, A. S., Blagojević, J., Vujošević, M., Rubtsov, N. B., Graphodatsky, A. S., & Trifonov, V. A. (2018). Low-pass single-chromosome sequencing of human small supernumerary marker chromosomes (sSMCs) and Apodemus B chromosomes. *Chromosoma*, 127(3), 301–311. <https://doi.org/10.1007/s00412-018-0662-0>
- Mank, J. E., & Avise, J. C. (2009). Evolutionary diversity and turn-over of sex determination in teleost fishes. *Sexual Development: Genetics, Molecular Biology, Evolution, Endocrinology, Embryology, and Pathology of Sex Determination and Differentiation*, 3(2–3), 60–67. <https://doi.org/10.1159/000223071>
- Marques, A., Banaei-Moghaddam, A. M., Klemme, S., Blattner, F. R., Niwa, K., Guerra, M., & Houben, A. (2013). B chromosomes of rye are highly conserved and accompanied the development of early agriculture. *Annals of Botany*, 112(3), 527–534. <https://doi.org/10.1093/aob/mct121>
- Marshall Graves, J. A., & Peichel, C. L. (2010). Are homologies in vertebrate sex determination due to shared ancestry or to limited options? *Genome Biology*, 11(4), 205. <https://doi.org/10.1186/gb-2010-11-4-205>
- Martinez-Bengochea, A., Doretto, L., Rosa, I. F., Oliveira, M. A., Silva, C., Silva, D. M. Z. A., Santos, G. R., Santos, J. S. F., Avelar, M. M., Silva, L. V., Lucianelli-Junior, D., Souza, E. R. B., Silva, R. C., Stewart, A. B., Nakaghi, L. S. O., Valentin, F. N., & Nóbrega, R. H. (2020). Effects of 17β-estradiol on early gonadal development and expression of genes implicated in sexual differentiation of a South American teleost, *Astyanax altiparanae*. *Comparative Biochemistry and Physiology Part B: Biochemistry and Molecular Biology*, 248–249, 110467. <https://doi.org/10.1016/j.cbpb.2020.110467>
- Martis, M. M., Klemme, S., Banaei-Moghaddam, A. M., Blattner, F. R., Macas, J., Schmutz, T., Scholz, U., Gundlach, H., Wicker, T., Šimková, H., Novák, P., Neumann, P., Kubaláková, M., Bauer, E., Haseneyer, G., Fuchs, J., Doležel, J., Stein, N., Mayer, K. F. X., & Houben, A. (2012). Selfish supernumerary chromosome reveals its origin as a mosaic of host genome and organellar sequences. *Proceedings of the National Academy of Sciences of the United States of America*, 109(33), 13343–13346. <https://doi.org/10.1073/pnas.1204237109>
- Matson, C. K., & Zarkower, D. (2012). Sex and the singular DM domain: Insights into sexual regulation, evolution and plasticity. *Nature Reviews. Genetics*, 13(3), 163–174. <https://doi.org/10.1038/nrg3161>
- Matsuda, M., Nagahama, Y., Kobayashi, T., Matsuda, C., Hamaguchi, S., & Sakaizumi, M. (2003). The sex determining gene of medaka: A Y-specific DM domain gene (DMY) is required for male development. *Fish Physiology and Biochemistry*, 28(1), 135–139.

<https://doi.org/10.1023/B:FISH.0000030500.29914.7a>

- Matsuda, M., Nagahama, Y., Shinomiya, A., Sato, T., Matsuda, C., Kobayashi, T., Morrey, C. E., Shibata, N., Asakawa, S., Shimizu, N., Hori, H., Hamaguchi, S., & Sakaizumi, M. (2002). DMY is a Y-specific DM-domain gene required for male development in the medaka fish. *Nature*, 417(6888), 559–563. <https://doi.org/10.1038/nature751>
- Miller, R.R. and M.L. Smith. (1986). Origin and geography of the fishes of central Mexico, p. 487–517. In: *The zoogeography of North American freshwater fishes*. Hocutt, H.C. and E.O. Wiley (eds.).
- Mishima, Y., Giraldez, A. J., Takeda, Y., Fujiwara, T., Sakamoto, H., Schier, A. F., & Inoue, K. (2006). Differential regulation of germline mRNAs in soma and germ cells by zebrafish miR-430. *Current Biology: CB*, 16(21), 2135–2142. <https://doi.org/10.1016/j.cub.2006.08.086>
- Mitchell, R. W., Russell, W. H., & Elliott, W. R. (1977). Mexican eyeless characin fishes, genus *Astyanax*: Environment, distribution, and evolution. Texas Tech Press.
- Miura, I. (2007). An evolutionary witness: The frog *Rana rugosa* underwent change of heterogametic sex from XY male to ZW female. *Sexual Development: Genetics, Molecular Biology, Evolution, Endocrinology, Embryology, and Pathology of Sex Determination and Differentiation*, 1(6), 323–331. <https://doi.org/10.1159/000111764>
- Miura, I. (2017). Sex Determination and Sex Chromosomes in Amphibia. *Sexual Development*, 11(5–6), 298–306. <https://doi.org/10.1159/000485270>
- Mizoguchi, S. M. H. N., & Martins-Santos, I. C. (1997). Macro- and Microchromosomes B in Females of *Astyanax scabripinnis* (Pisces, Characidae). *Hereditas*, 127(3), 249–253. <https://doi.org/10.1111/j.1601-5223.1997.00249.x>
- Moore, E. C., & Roberts, R. B. (2013). Polygenic sex determination. *Current Biology*, 23(12), R510–R512. <https://doi.org/10.1016/j.cub.2013.04.004>
- Moran, D., Softley, R., & Warrant, E. J. (2014). Eyeless Mexican Cavefish Save Energy by Eliminating the Circadian Rhythm in Metabolism. *PLOS ONE*, 9(9), e107877. <https://doi.org/10.1371/journal.pone.0107877>
- Muratova, E. N. (2000). B-chromosomes of gymnosperms. *Uspekhi Sovremennoi Biologii*, 120(5), 452–465.
- Myoshio, T., Otake, H., Masuyama, H., Matsuda, M., Kuroki, Y., Fujiyama, A., Naruse, K., Hamaguchi, S., & Sakaizumi, M. (2012). Tracing the Emergence of a Novel Sex-Determining Gene in Medaka, *Oryzias luzonensis*. *Genetics*, 191(1), 163–170. <https://doi.org/10.1534/genetics.111.137497>
- Nakamoto, M., Muramatsu, S., Yoshida, S., Matsuda, M., Nagahama, Y., & Shibata, N. (2009). Gonadal sex differentiation and expression of Sox9a2, Dmrt1, and Foxl2 in *Oryzias luzonensis*. *Genesis*, 47(5), 289–299. <https://doi.org/10.1002/dvg.20498>
- Nakamoto, M., Suzuki, A., Matsuda, M., Nagahama, Y., & Shibata, N. (2005). Testicular type Sox9 is not involved in sex determination but might be in the development of testicular structures in the medaka, *Oryzias latipes*. *Biochemical and Biophysical Research Communications*, 333(3), 729–736. <https://doi.org/10.1016/j.bbrc.2005.05.158>
- Nanda, I., Kondo, M., Hornung, U., Asakawa, S., Winkler, C., Shimizu, A., Shan, Z., Haaf, T., Shimizu, N., Shima, A., Schmid, M., & Schartl, M. (2002). A duplicated copy of DMRT1 in the sex-determining region of the Y chromosome of the medaka, *Oryzias latipes*. *Proceedings of the National Academy of Sciences of the United States of America*, 99(18), 11778–11783. <https://doi.org/10.1073/pnas.182314699>
- Natri, H. M., Shikano, T., & Merilä, J. (2013). Progressive Recombination Suppression and Differentiation in Recently Evolved Neo-Sex Chromosomes. *Molecular Biology and Evolution*, 30(5), 1131–1144. <https://doi.org/10.1093/molbev/mst035>
- Navarro-Domínguez, B., Ruiz-Ruano, F. J., Cabrero, J., Corral, J. M., López-León, M. D.,

- Sharbel, T. F., & Camacho, J. P. M. (2017). Protein-coding genes in B chromosomes of the grasshopper *Eyprepocnemis plorans*. *Scientific Reports*, 7(1), 45200. <https://doi.org/10.1038/srep45200>
- Nelson, J. S., Grande, T. C., & Wilson, M. V. H. (2016). Phylum Chordata. In *Fishes of the World* (p. 13–526). John Wiley & Sons, Ltd. <https://doi.org/10.1002/9781119174844.ch2>
- Néo, D. M., Bertollo, L. A. C., & Filho, O. M. (2000). Morphological Differentiation and Possible Origin of B Chromosomes in Natural Brazilian Population of *Astyanax Scabripinnis* (PISCES, CHARACIDAE). *Genetica*, 108(3), 211–215. <https://doi.org/10.1023/A:1004157901097>
- Nicol, B., Guerin, A., Fostier, A., & Guiguen, Y. (2012). Ovary-predominant wnt4 expression during gonadal differentiation is not conserved in the rainbow trout (*Oncorhynchus mykiss*). *Molecular Reproduction and Development*, 79(1), 51–63. <https://doi.org/10.1002/mrd.21404>
- Nicol, B., Yano, A., Jouanno, E., Guérin, A., Fostier, A., & Guiguen, Y. (2013). Follistatin Is an Early Player in Rainbow Trout Ovarian Differentiation and Is Both Colocalized with Aromatase and Regulated by the Wnt Pathway. *Sexual Development*, 7(5), epub ahead of print. <https://doi.org/10.1159/000350687>
- Niwa, K., & Sakamoto, S. (1995). Origin of B chromosomes in cultivated rye. *Genome*, 38(2), 307–312. <https://doi.org/10.1139/g95-038>
- Oliveira, C., Maria Rodrigues Saboya, S., Foresti, F., Augusto Senhorini, J., & Bernardino, G. (1997). Increased B chromosome frequency and absence of drive in the fish *Prochilodus lineatus*. *Heredity*, 79(5), 473–476. <https://doi.org/10.1038/hdy.1997.186>
- Ornelas-García, C. P., Domínguez-Domínguez, O., & Doadrio, I. (2008). Evolutionary history of the fish genus *Astyanax* Baird & Girard (1854) (Actinopterygii, Characidae) in Mesoamerica reveals multiple morphological homoplasies. *BMC Evolutionary Biology*, 8, 340. <https://doi.org/10.1186/1471-2148-8-340>
- Ospina-Alvarez, N., & Piferrer, F. (2008). Temperature-dependent sex determination in fish revisited: Prevalence, a single sex ratio response pattern, and possible effects of climate change. *PloS One*, 3(7), e2837. <https://doi.org/10.1371/journal.pone.0002837>
- Otsuka, F., McTavish, K., & Shimasaki, S. (2011). Integral Role of GDF-9 and BMP-15 in Ovarian Function. *Molecular reproduction and development*, 78(1), 9–21. <https://doi.org/10.1002/mrd.21265>
- Otto, S. P., & Lenormand, T. (2002). Resolving the paradox of sex and recombination. *Nature Reviews Genetics*, 3(4), 252–261. <https://doi.org/10.1038/nrg761>
- Palaiokostas, C., Bekaert, M., Taggart, J. B., Gharbi, K., McAndrew, B. J., Chatain, B., Penman, D. J., & Vandepitte, M. (2015). A new SNP-based vision of the genetics of sex determination in European sea bass (*Dicentrarchus labrax*). *Genetics Selection Evolution*, 47(1), 68. <https://doi.org/10.1186/s12711-015-0148-y>
- Pan, Q., Anderson, J., Bertho, S., Herpin, A., Wilson, C., Postlethwait, J. H., Schartl, M., & Guiguen, Y. (2016). Vertebrate sex-determining genes play musical chairs. *Comptes Rendus Biologies*, 339(7), 258–262. <https://doi.org/10.1016/j.crvi.2016.05.010>
- Pan, Q., Feron, R., Yano, A., Guyomard, R., Jouanno, E., Vigouroux, E., Wen, M., Busnel, J.-M., Bobe, J., Concorde, J.-P., Parrinello, H., Journot, L., Klopp, C., Lluch, J., Roques, C., Postlethwait, J., Schartl, M., Herpin, A., & Guiguen, Y. (2019). Identification of the master sex determining gene in Northern pike (*Esox lucius*) reveals restricted sex chromosome differentiation. *PLOS Genetics*, 15(8), e1008013. <https://doi.org/10.1371/journal.pgen.1008013>
- Pan, Q., Guiguen, Y., & Herpin, A. (2018). Evolution of Sex Determining Genes in Fish. In M. K. Skinner (Ed.), *Encyclopedia of Reproduction* (Second Edition) (p. 168–175).

- Academic Press. <https://doi.org/10.1016/B978-0-12-809633-8.20552-9>
- Pangas, S. A. (2012). Regulation of the ovarian reserve by members of the transforming growth factor beta family. *Molecular Reproduction and Development*, 79(10), 666–679. <https://doi.org/10.1002/mrd.22076>
- Pansonato-Alves, J. C., Serrano, É. A., Utsunomia, R., Camacho, J. P. M., Costa Silva, G. J. da, Vicari, M. R., Artoni, R. F., Oliveira, C., & Foresti, F. (2014). Single Origin of Sex Chromosomes and Multiple Origins of B Chromosomes in Fish Genus Characidium. *PLoS ONE*, 9(9), e107169. <https://doi.org/10.1371/journal.pone.0107169>
- Pasquier, J., Cabau, C., Nguyen, T., Jouanno, E., Severac, D., Braasch, I., Journot, L., Pontarotti, P., Klopp, C., Postlethwait, J. H., Guiguen, Y., & Bobe, J. (2016). Gene evolution and gene expression after whole genome duplication in fish: The PhyloFish database. *BMC Genomics*, 17(1), 368. <https://doi.org/10.1186/s12864-016-2709-z>
- Pauls, E., & Bertollo, L. A. C. (1983). Evidence for a System of Supernumerary Chromosomes in Prochilodus Scrofa Steindachner, 1881 (Pisces, Prochilodontidae). *Caryologia*, 36(4), 307–314. <https://doi.org/10.1080/00087114.1983.10797671>
- Pierre, C., Pradère, N., Froc, C., Ornelas-García, P., Callebert, J., & Rétaux, S. (2020). A mutation in monoamine oxidase (MAO) affects the evolution of stress behavior in the blind cavefish *Astyanax mexicanus*. *Journal of Experimental Biology*, 223(18). <https://doi.org/10.1242/jeb.226092>
- Piferrer, F., Blázquez, M., Navarro, L., & González, A. (2005). Genetic, endocrine, and environmental components of sex determination and differentiation in the European sea bass (*Dicentrarchus labrax* L.). *General and Comparative Endocrinology*, 142(1–2), 102–110. <https://doi.org/10.1016/j.ygcen.2005.02.011>
- Pires, L. B., Sampaio, T. R., & Dias, A. L. (2015). Mitotic and Meiotic Behavior of B Chromosomes in *Crenicichla lepidota*: New Report in the Family Cichlidae. *Journal of Heredity*, 106(3), 289–295. <https://doi.org/10.1093/jhered/esv007>
- Pokorná, M. J., Altmanová, M., Rovatsos, M., Velenský, P., Vodička, R., Rehák, I., & Kratochvíl, L. (2016). First Description of the Karyotype and Sex Chromosomes in the Komodo Dragon (*Varanus komodoensis*). *Cytogenetic and Genome Research*, 148(4), 284–291. <https://doi.org/10.1159/000447340>
- Poletto, A. B., Ferreira, I. A., & Martins, C. (2010). The B chromosomes of the African cichlid fish *Haplochromis obliquidens* harbour 18S rRNA gene copies. *BMC Genetics*, 11(1), 1. <https://doi.org/10.1186/1471-2156-11-1>
- Policarpo, M., Fumey, J., Lafargeas, P., Naquin, D., Thermes, C., Naville, M., Dechaud, C., Volff, J.-N., Cabau, C., Klopp, C., Moller, P., Bernatchez, L., García-Machado, E., Rétaux, S., & Casane, D. (2020). Contrasting gene decay in subterranean vertebrates: Insights from cavefishes and fossorial mammals. *Molecular biology and evolution*. <https://doi.org/10.1093/molbev/msaa249>
- Portela-Castro, A. L. de B., Júnior, H. F. J., & Nishiyama, P. B. (2000). New occurrence of microchromosomes B in *Moenkhausia sanctaefilomenae* (Pisces, Characidae) from the Paraná River of Brazil: Analysis of the synaptonemal complex. *Genetica*, 110(3), 277–283. <https://doi.org/10.1023/A:1012742717240>
- Porter, M. L., Dittmar, K., & Pérez-Losada, M. (2007). How Long Does Evolution of the Troglomorphic Form Take? Estimating Divergence Times in *Astyanax Mexicanus*. *Acta Carsologica*, 36(1), Article 1. <https://doi.org/10.3986/ac.v36i1.219>
- Protas, M. E., Hersey, C., Kochanek, D., Zhou, Y., Wilkens, H., Jeffery, W. R., Zon, L. I., Borowsky, R., & Tabin, C. J. (2006). Genetic analysis of cavefish reveals molecular convergence in the evolution of albinism. *Nature Genetics*, 38(1), 107–111. <https://doi.org/10.1038/ng1700>
- Purcell, C. M., Seetharam, A. S., Snodgrass, O., Ortega-García, S., Hyde, J. R., & Severin, A.

- J. (2018). Insights into teleost sex determination from the *Seriola dorsalis* genome assembly. *BMC Genomics*, 19(1), 31. <https://doi.org/10.1186/s12864-017-4403-1>
- Randolph, L.F. (1928). Types of supernumerary chromosomes in maize. *Anat. Rec.* 41, 102.
- Reed, K. M. (1993). Cytogenetic analysis of the paternal sex ratio chromosome of *Nasonia vitripennis*. *Genome*, 36(1), 157–161. <https://doi.org/10.1139/g93-020>
- Reed, K. M., & Werren, J. H. (1995). Induction of paternal genome loss by the paternal-sex-ratio chromosome and cytoplasmic incompatibility bacteria (Wolbachia): A comparative study of early embryonic events. *Molecular Reproduction and Development*, 40(4), 408–418. <https://doi.org/10.1002/mrd.1080400404>
- Reichwald, K., Petzold, A., Koch, P., Downie, B. R., Hartmann, N., Pietsch, S., Baumgart, M., Chalopin, D., Felder, M., Bens, M., Sahm, A., Szafranski, K., Taudien, S., Groth, M., Arisi, I., Weise, A., Bhatt, S. S., Sharma, V., Kraus, J. M., ... Platzer, M. (2015). Insights into Sex Chromosome Evolution and Aging from the Genome of a Short-Lived Fish. *Cell*, 163(6), 1527–1538. <https://doi.org/10.1016/j.cell.2015.10.071>
- Rétaux, S., & Elipot, Y. (2013). Feed or fight: A behavioral shift in blind cavefish. *Communicative & integrative biology*, 6, e23166. <https://doi.org/10.4161/cib.23166>
- Ribas, L., Liew, W. C., Díaz, N., Sreenivasan, R., Orbán, L., & Piferrer, F. (2017). Heat-induced masculinization in domesticated zebrafish is family-specific and yields a set of different gonadal transcriptomes. *Proceedings of the National Academy of Sciences of the United States of America*, 114(6), E941–E950. <https://doi.org/10.1073/pnas.1609411114>
- Ribas, L., Valdivieso, A., Díaz, N., & Piferrer, F. (2017). Appropriate rearing density in domesticated zebrafish to avoid masculinization: Links with the stress response. *The Journal of Experimental Biology*, 220(Pt 6), 1056–1064. <https://doi.org/10.1242/jeb.144980>
- Riddle, M. R., Aspiras, A. C., Gaudenz, K., Peuß, R., Sung, J. Y., Martineau, B., Peavey, M., Box, A. C., Tabin, J. A., McGaugh, S., Borowsky, R., Tabin, C. J., & Rohner, N. (2018). Insulin resistance in cavefish as an adaptation to a nutrient-limited environment. *Nature*, 555(7698), 647–651. <https://doi.org/10.1038/nature26136>
- Riddle, M. R., Boesmans, W., Caballero, O., Kazwiny, Y., & Tabin, C. J. (2018). Morphogenesis and motility of the *Astyanax mexicanus* gastrointestinal tract. *Developmental Biology*, 441(2), 285–296. <https://doi.org/10.1016/j.ydbio.2018.06.004>
- Roberts, N. B., Juntti, S. A., Coyle, K. P., Dumont, B. L., Stanley, M. K., Ryan, A. Q., Fernald, R. D., & Roberts, R. B. (2016). Polygenic sex determination in the cichlid fish *Astatotilapia burtoni*. *BMC Genomics*, 17(1), 835. <https://doi.org/10.1186/s12864-016-3177-1>
- Roberts, R. B., Ser, J. R., & Kocher, T. D. (2009). Sexual Conflict Resolved by Invasion of a Novel Sex Determiner in Lake Malawi Cichlid Fishes. *Science*, 326(5955), 998–1001. <https://doi.org/10.1126/science.1174705>
- Rondeau, E. B., Messmer, A. M., Sanderson, D. S., Jantzen, S. G., von Schalburg, K. R., Minkley, D. R., Leong, J. S., Macdonald, G. M., Davidsen, A. E., Parker, W. A., Mazzola, R. S., Campbell, B., & Koop, B. F. (2013). Genomics of sablefish (*Anoplopoma fimbriae*): Expressed genes, mitochondrial phylogeny, linkage map and identification of a putative sex gene. *BMC Genomics*, 14(1), 452. <https://doi.org/10.1186/1471-2164-14-452>
- Ruban, A., Schmutzler, T., Wu, D. D., Fuchs, J., Boudichevskaia, A., Rubtsova, M., Pistrick, K., Melzer, M., Himmelbach, A., Schubert, V., Scholz, U., & Houben, A. (2020). Supernumerary B chromosomes of *Aegilops speltoides* undergo precise elimination in roots early in embryo development. *Nature Communications*, 11(1), 2764. <https://doi.org/10.1038/s41467-020-16594-x>

- Rubin, D. A. (1985). Effect of ph on Sex Ratio in Cichlids and a Poeciliid (Teleostei). *Copeia*, 1985(1), 233–235. JSTOR. <https://doi.org/10.2307/1444818>
- Şadoğlu P. (1957). Mendelian inheritance in the hybrids between the Mexican blind cave fishes and their overground ancestor. *Verh Dtsch Zool Ges Graz*. 1957:432–439.
- Saillant, E., Fostier, A., Haffray, P., Menu, B., & Chatain, B. (2003). Saline preferendum for the European sea bass, *Dicentrarchus labrax*, larvae and juveniles: Effect of salinity on early development and sex determination. *Journal of Experimental Marine Biology and Ecology*, 287(1), 103–117. [https://doi.org/10.1016/S0022-0981\(02\)00502-6](https://doi.org/10.1016/S0022-0981(02)00502-6)
- Saillant, E., Fostier, A., Haffray, P., Menu, B., Thimonier, J., & Chatain, B. (2002). Temperature effects and genotype-temperature interactions on sex determination in the European sea bass (*Dicentrarchus labrax* L.). *Journal of Experimental Zoology*, 292(5), 494–505. <https://doi.org/10.1002/jez.10071>
- Saito, T., Fujimoto, T., Maegawa, S., Inoue, K., Tanaka, M., Arai, K., & Yamaha, E. (2006). Visualization of primordial germ cells in vivo using GFP-nos1 3'UTR mRNA. *The International Journal of Developmental Biology*, 50(8), 691–699. <https://doi.org/10.1387/ijdb.062143ts>
- Salin, K., Voituron, Y., Mourin, J., & Hervant, F. (2010). Cave colonization without fasting capacities: An example with the fish *Astyanax fasciatus mexicanus*. *Comparative Biochemistry and Physiology Part A: Molecular & Integrative Physiology*, 156(4), 451–457. <https://doi.org/10.1016/j.cbpa.2010.03.030>
- Santos, D., Luzio, A., & Coimbra, A. M. (2017). Zebrafish sex differentiation and gonad development: A review on the impact of environmental factors. *Aquatic Toxicology*, 191, 141–163. <https://doi.org/10.1016/j.aquatox.2017.08.005>
- Sato, T., Endo, T., Yamahira, K., Hamaguchi, S., & Sakaizumi, M. (2005). Induction of female-to-male sex reversal by high temperature treatment in Medaka, *Oryzias latipes*. *Zoological Science*, 22(9), 985–988. <https://doi.org/10.2108/zsj.22.985>
- Schartl, M. (2004). Sex chromosome evolution in non-mammalian vertebrates. *Current Opinion in Genetics & Development*, 14(6), 634–641. <https://doi.org/10.1016/j.gde.2004.09.005>
- Schartl, M., & Herpin, A. (2018). Sex Determination in Vertebrates. In M. K. Skinner (Ed.), *Encyclopedia of Reproduction* (Second Edition) (p. 159–167). Academic Press. <https://doi.org/10.1016/B978-0-12-809633-8.20551-7>
- Schartl, M., Nanda, I., Schlupp, I., Wilde, B., Epplen, J. T., Schmid, M., & Parzefall, J. (1995). Incorporation of subgenomic amounts of DNA as compensation for mutational load in a gynogenetic fish. *Nature*, 373(6509), 68–71. <https://doi.org/10.1038/373068a0>
- Schartl, M., Schories, S., Wakamatsu, Y., Nagao, Y., Hashimoto, H., Bertin, C., Mourot, B., Schmidt, C., Wilhelm, D., Centanin, L., Guiguen, Y., & Herpin, A. (2018). Sox5 is involved in germ-cell regulation and sex determination in medaka following co-option of nested transposable elements. *BMC Biology*, 16(1), 16. <https://doi.org/10.1186/s12915-018-0485-8>
- Schemmel, C. (1980). Studies on the genetics of feeding behaviour in the cave fish *Astyanax mexicanus* f. *Anoptichthys*. An example of apparent monofactorial inheritance by polygenes. *Zeitschrift Fur Tierpsychologie*, 53(1), 9–22. <https://doi.org/10.1111/j.1439-0310.1980.tb00730.x>
- Schepers, G. E., Teasdale, R. D., & Koopman, P. (2002). Twenty pairs of sox: Extent, homology, and nomenclature of the mouse and human sox transcription factor gene families. *Developmental Cell*, 3(2), 167–170. [https://doi.org/10.1016/s1534-5807\(02\)00223-x](https://doi.org/10.1016/s1534-5807(02)00223-x)
- Schmid, M., Ziegler, C. G., Steinlein, C., Nanda, I., & Schartl, M. (2006). Cytogenetics of the bleak (*Alburnus alburnus*), with special emphasis on the B chromosomes. *Chromosome*

- Research, 14(3), 231–242. <https://doi.org/10.1007/s10577-006-1038-5>
- Schultheis, C., Böhne, A., Schartl, M., Volff, J. N., & Galiana-Arnoux, D. (2009). Sex Determination Diversity and Sex Chromosome Evolution in Poeciliid Fish. *Sexual Development*, 3(2/3), 68–77. <https://doi.org/10.1159/000223072>
- Ser, J. R., Roberts, R. B., & Kocher, T. D. (2010). Multiple Interacting Loci Control Sex Determination in Lake Malawi Cichlid Fish. *Evolution*, 64(2), 486–501. <https://doi.org/10.1111/j.1558-5646.2009.00871.x>
- Serrano-Freitas, É. A., Silva, D. M. Z. A., Ruiz-Ruano, F. J., Utsunomia, R., Araya-Jaime, C., Oliveira, C., Camacho, J. P. M., & Foresti, F. (2020). Satellite DNA content of B chromosomes in the characid fish Characidium gomesi supports their origin from sex chromosomes. *Molecular Genetics and Genomics*, 295(1), 195–207. <https://doi.org/10.1007/s00438-019-01615-2>
- Shang, E. H. H., Yu, R. M. K., & Wu, R. S. S. (2006). Hypoxia affects sex differentiation and development, leading to a male-dominated population in zebrafish (*Danio rerio*). *Environmental Science & Technology*, 40(9), 3118–3122. <https://doi.org/10.1021/es0522579>
- Sharbel, T. F., Green, D. M., & Houben, A. (1998). B-chromosome origin in the endemic New Zealand frog *Leiopelma hochstetteri* through sex chromosome devolution. 41, 9.
- Shen, Z.-G., & Wang, H.-P. (2014). Molecular players involved in temperature-dependent sex determination and sex differentiation in Teleost fish. *Genetics, Selection, Evolution: GSE*, 46(1), 26. <https://doi.org/10.1186/1297-9686-46-26>
- Silva, D. M. Z. de A., Pansonato-Alves, J. C., Utsunomia, R., Araya-Jaime, C., Ruiz-Ruano, F. J., Daniel, S. N., Hashimoto, D. T., Oliveira, C., Camacho, J. P. M., Porto-Foresti, F., & Foresti, F. (2014). Delimiting the Origin of a B Chromosome by FISH Mapping, Chromosome Painting and DNA Sequence Analysis in *Astyanax paranae* (Teleostei, Characiformes). *PLoS ONE*, 9(4), e94896. <https://doi.org/10.1371/journal.pone.0094896>
- Simon, V., Elleboode, R., Mahé, K., Legendre, L., Ornelas-Garcia, P., Espinasa, L., & Rétaux, S. (2017). Comparing growth in surface and cave morphs of the species *Astyanax mexicanus*: Insights from scales. *EvoDevo*, 8, 23. <https://doi.org/10.1186/s13227-017-0086-6>
- Simon, V., Hyacinthe, C., & Rétaux, S. (2019). Breeding behavior in the blind Mexican cavefish and its river-dwelling conspecific. *PloS One*, 14(2), e0212591. <https://doi.org/10.1371/journal.pone.0212591>
- Sinclair, A. H., Berta, P., Palmer, M. S., Hawkins, J. R., Griffiths, B. L., Smith, M. J., Foster, J. W., Frischaufl, A. M., Lovell-Badge, R., & Goodfellow, P. N. (1990). A gene from the human sex-determining region encodes a protein with homology to a conserved DNA-binding motif. *Nature*, 346(6281), 240–244. <https://doi.org/10.1038/346240a0>
- Smith, C. A., Roeszler, K. N., Ohnesorg, T., Cummins, D. M., Farlie, P. G., Doran, T. J., & Sinclair, A. H. (2009). The avian Z-linked gene DMRT1 is required for male sex determination in the chicken. *Nature*, 461(7261), 267–271. <https://doi.org/10.1038/nature08298>
- Sreenivasan, R., Jiang, J., Wang, X., Bártfai, R., Kwan, H. Y., Christoffels, A., & Orbán, L. (2014). Gonad Differentiation in Zebrafish Is Regulated by the Canonical Wnt Signaling Pathway. *Biology of Reproduction*, 90(2). <https://doi.org/10.1095/biolreprod.113.110874>
- Stahl, B., Jaggard, J., Chin, J., Kowalko, J., Keene, A., & Duboue, E. (2019). Manipulation of Gene Function in Mexican Cavefish. *Journal of Visualized Experiments*. <https://doi.org/10.3791/59093>
- Stockdale, W. T., Lemieux, M. E., Killen, A. C., Zhao, J., Hu, Z., Riepsaame, J., Hamilton, N.,

- Kudoh, T., Riley, P. R., van Aerle, R., Yamamoto, Y., & Mommersteeg, M. T. M. (2018). Heart Regeneration in the Mexican Cavefish. *Cell Reports*, 25(8), 1997-2007.e7. <https://doi.org/10.1016/j.celrep.2018.10.072>
- Strecker, U., Bernatchez, L., & Wilkens, H. (2003). Genetic divergence between cave and surface populations of *Astyanax* in Mexico (Characidae, Teleostei). *Molecular Ecology*, 12(3), 699–710. <https://doi.org/10.1046/j.1365-294x.2003.01753.x>
- Strecker, Ulrike, Faúndez, V. H., & Wilkens, H. (2004). Phylogeography of surface and cave *Astyanax* (Teleostei) from Central and North America based on cytochrome b sequence data. *Molecular Phylogenetics and Evolution*, 33(2), 469–481. <https://doi.org/10.1016/j.ympev.2004.07.001>
- Strecker, Ulrike, Hausdorf, B., & Wilkens, H. (2012). Parallel speciation in *Astyanax* cave fish (Teleostei) in Northern Mexico. *Molecular Phylogenetics and Evolution*, 62(1), 62–70. <https://doi.org/10.1016/j.ympev.2011.09.005>
- Takehana, Y., Matsuda, M., Myosho, T., Suster, M. L., Kawakami, K., Shin-I, T., Kohara, Y., Kuroki, Y., Toyoda, A., Fujiyama, A., Hamaguchi, S., Sakaizumi, M., & Naruse, K. (2014). Co-option of Sox3 as the male-determining factor on the Y chromosome in the fish *Oryzias dancena*. *Nature Communications*, 5(1), 4157. <https://doi.org/10.1038/ncomms5157>
- Tao, W., Chen, J., Tan, D., Yang, J., Sun, L., Wei, J., Conte, M., Kocher, T., & Wang, D. (2018). Transcriptome display during tilapia sex determination and differentiation as revealed by RNA-Seq analysis. *BMC Genomics*, 19. <https://doi.org/10.1186/s12864-018-4756-0>
- Terán, G., Benítez, M., & Mirande, juan marcos. (2020). Opening the Trojan horse: Phylogeny of *Astyanax*, two new genera and resurrection of *Psalidodon* (Teleostei: Characidae). *Zoological Journal of the Linnean Society*, 1–18. <https://doi.org/10.1093/zoolinnean/zlaa019/5819054>
- Torres-Paz, J., Hyacinthe, C., Pierre, C., & Rétaux, S. (2018). Towards an integrated approach to understand Mexican cavefish evolution. *Biology Letters*, 14(8), 20180101. <https://doi.org/10.1098/rsbl.2018.0101>
- Tree of Sex Consortium. (2014). Tree of Sex: A database of sexual systems. *Scientific Data*, 1, 140015. <https://doi.org/10.1038/sdata.2014.15>
- Uhl, C. H., & Moran, R. (1973). The Chromosomes of *Pachyphytum* (Crassulaceae). *American Journal of Botany*, 60(7), 648–656. JSTOR. <https://doi.org/10.2307/2441442>
- Utsunomia, R., Silva, D. M. Z. de A., Ruiz-Ruano, F. J., Araya-Jaime, C., Pansonato-Alves, J. C., Scacchetti, P. C., Hashimoto, D. T., Oliveira, C., Trifonov, V. A., Porto-Foresti, F., Camacho, J. P. M., & Foresti, F. (2016). Uncovering the Ancestry of B Chromosomes in *Moenkhausia sanctaefilomenae* (Teleostei, Characidae). *PLoS One*, 11(3), e0150573. <https://doi.org/10.1371/journal.pone.0150573>
- Valente, G. T., Conte, M. A., Fantinatti, B. E. A., Cabral-de-Mello, D. C., Carvalho, R. F., Vicari, M. R., Kocher, T. D., & Martins, C. (2014). Origin and Evolution of B Chromosomes in the Cichlid Fish *Astatotilapia latifasciata* Based on Integrated Genomic Analyses. *Molecular Biology and Evolution*, 31(8), 2061–2072. <https://doi.org/10.1093/molbev/msu148>
- Valente, G. T., Nakajima, R. T., Fantinatti, B. E. A., Marques, D. F., Almeida, R. O., Simões, R. P., & Martins, C. (2017). B chromosomes: From cytogenetics to systems biology. *Chromosoma*, 126(1), 73–81. <https://doi.org/10.1007/s00412-016-0613-6>
- Valenzuela, N., Adams, D. C., & Janzen, F. J. (2003). Pattern does not equal process: Exactly when is sex environmentally determined? *The American Naturalist*, 161(4), 676–683. <https://doi.org/10.1086/368292>
- Vandeputte, M., Dupont-Nivet, M., Chavanne, H., & Chatain, B. (2007). A Polygenic

- Hypothesis for Sex Determination in the European Sea Bass *Dicentrarchus labrax*. *Genetics*, 176(2), 1049–1057. <https://doi.org/10.1534/genetics.107.072140>
- Varatharasan, N., Croll, R. P., & Franz-Odendaal, T. (2009). Taste bud development and patterning in sighted and blind morphs of *Astyanax mexicanus*. *Developmental Dynamics: An Official Publication of the American Association of Anatomists*, 238(12), 3056–3064. <https://doi.org/10.1002/dvdy.22144>
- Ventura, K., O'Brien, P. C. M., Moreira, C. do N., Yonenaga-Yassuda, Y., & Ferguson-Smith, M. A. (2015). On the Origin and Evolution of the Extant System of B Chromosomes in Oryzomyini Radiation (Rodentia, Sigmodontinae). *PLOS ONE*, 10(8), e0136663. <https://doi.org/10.1371/journal.pone.0136663>
- Veyrunes, F., Chevret, P., Catalan, J., Castiglia, R., Watson, J., Dobigny, G., Robinson, T. J., & Britton-Davidian, J. (2010). A novel sex determination system in a close relative of the house mouse. *Proceedings of the Royal Society B: Biological Sciences*, 277(1684), 1049–1056. <https://doi.org/10.1098/rspb.2009.1925>
- Vicente, V. E., Moreira-Filho, O., & Camacho, J. P. (1996). Sex-ratio distortion associated with the presence of a B chromosome in *Astyanax scabripinnis* (Teleostei, Characidae). *Cytogenetics and Cell Genetics*, 74(1–2), 70–75. <https://doi.org/10.1159/000134385>
- Volff, J.-N., Nanda, I., Schmid, M., & Schartl, M. (2007). Governing Sex Determination in Fish: Regulatory Putsches and Ephemeral Dictators. *Sexual Development*, 1(2), 85–99. <https://doi.org/10.1159/000100030>
- Volff, J.-N., & Schartl, M. (2001). Variability of genetic sex determination in poeciliid fishes. *Genetica*, 111(1), 101–110. <https://doi.org/10.1023/A:1013795415808>
- Vujošević, M., Rajičić, M., & Blagojević, J. (2018). B Chromosomes in Populations of Mammals Revisited. *Genes*, 9(10), 487. <https://doi.org/10.3390/genes9100487>
- Wang, W., Zhu, H., Dong, Y., Tian, Z., Dong, T., Hu, H., & Niu, C. (2017). Dimorphic expression of sex-related genes in different gonadal development stages of sterlet, *Acipenser ruthenus*, a primitive fish species. *Fish Physiology and Biochemistry*, 43(6), 1557–1569. <https://doi.org/10.1007/s10695-017-0392-x>
- Weiss, A., & Attisano, L. (2013). The TGFbeta superfamily signaling pathway. *Wiley Interdisciplinary Reviews: Developmental Biology*, 2(1), 47–63. <https://doi.org/10.1002/wdev.86>
- Wexler, J. R., Plachetzki, D. C., & Kopp, A. (2014). Pan-metazoan phylogeny of the DMRT gene family: A framework for functional studies. *Development Genes and Evolution*, 224(3), 175–181. <https://doi.org/10.1007/s00427-014-0473-0>
- Wilhelm, D., & Pask, A. J. (2018). Genetic Mechanisms of Sex Determination. In M. K. Skinner (Ed.), *Encyclopedia of Reproduction* (Second Edition) (p. 245–249). Academic Press. <https://doi.org/10.1016/B978-0-12-801238-3.64460-4>
- Wilkens, H., & Strecker, U. (2017). *Evolution in the Dark: Darwin's Loss Without Selection*. Springer-Verlag. <https://doi.org/10.1007/978-3-662-54512-6>
- Wilson, E.B. (1907). The supernumerary chromosomes of Hemiptera. *Sci. New Ser.*
- Wilson, C. A., High, S. K., McCluskey, B. M., Amores, A., Yan, Y., Titus, T. A., Anderson, J., Batzel, P., Carvan III, M. J., Schartl, M., & Postlethwait, J. H. (2014). Wild sex in Zebrafish: Loss of the natural sex determinant in domesticated strains. *Genetics*, 198(3), 1291–1308. <https://doi.org/10.1534/genetics.114.169284>
- Xiong, S., Krishnan, J., Peuß, R., & Rohner, N. (2018). Early adipogenesis contributes to excess fat accumulation in cave populations of *Astyanax mexicanus*. *Developmental Biology*, 441(2), 297–304. <https://doi.org/10.1016/j.ydbio.2018.06.003>
- Xu, H., Li, M., Gui, J., & Hong, Y. (2010). Fish germ cells. *Science China Life Sciences*, 53(4), 435–446. <https://doi.org/10.1007/s11427-010-0058-8>
- Yamamoto, Y., & Jeffery, W. R. (2000). Central role for the lens in cave fish eye degeneration.

- Science (New York, N.Y.), 289(5479), 631 633.
<https://doi.org/10.1126/science.289.5479.631>
- Yamamoto, Yoji, Zhang, Y., Sarida, M., Hattori, R. S., & Strüssmann, C. A. (2014). Coexistence of Genotypic and Temperature-Dependent Sex Determination in Pejerrey *Odontesthes bonariensis*. PLOS ONE, 9(7), e102574.
<https://doi.org/10.1371/journal.pone.0102574>
- Yamamoto, Yoshiyuki, Byerly, M. S., Jackman, W. R., & Jeffery, W. R. (2009). Pleiotropic functions of embryonic sonic hedgehog expression link jaw and taste bud amplification with eye loss during cavefish evolution. Developmental biology, 330(1), 200 211.
<https://doi.org/10.1016/j.ydbio.2009.03.003>
- Yamamoto, Yoshiyuki, Espinasa, L., Stock, D. W., & Jeffery, W. R. (2003). Development and evolution of craniofacial patterning is mediated by eye-dependent and -independent processes in the cavefish *Astyanax*. Evolution & Development, 5(5), 435 446.
<https://doi.org/10.1046/j.1525-142X.2003.03050.x>
- Yan, C., Wang, P., DeMayo, J., DeMayo, F. J., Elvin, J. A., Carino, C., Prasad, S. V., Skinner, S. S., Dunbar, B. S., Dube, J. L., Celeste, A. J., & Matzuk, M. M. (2001). Synergistic roles of bone morphogenetic protein 15 and growth differentiation factor 9 in ovarian function. Molecular Endocrinology (Baltimore, Md.), 15(6), 854 866.
<https://doi.org/10.1210/mend.15.6.0662>
- Yano, A., Guyomard, R., Nicol, B., Jouanno, E., Quillet, E., Klopp, C., Cabau, C., Bouchez, O., Fostier, A., & Guiguen, Y. (2012). An immune-related gene evolved into the master sex-determining gene in rainbow trout, *Oncorhynchus mykiss*. Current Biology: CB, 22(15), 1423 1428. <https://doi.org/10.1016/j.cub.2012.05.045>
- Yano, A., Nicol, B., Jouanno, E., Quillet, E., Fostier, A., Guyomard, R., & Guiguen, Y. (2013). The sexually dimorphic on the Y-chromosome gene (sdY) is a conserved male-specific Y-chromosome sequence in many salmonids. Evolutionary Applications, 6(3), 486 496. <https://doi.org/10.1111/eva.12032>
- Yao, H. H. C., Matzuk, M. M., Jorgez, C. J., Menke, D. B., Page, D. C., Swain, A., & Capel, B. (2004). Follistatin Operates Downstream of Wnt4 in Mammalian Ovary Organogenesis. Developmental dynamics: an official publication of the American Association of Anatomists, 230(2), 210 215. <https://doi.org/10.1002/dvdy.20042>
- Yoshida, K., Terai, Y., Mizoiri, S., Aibara, M., Nishihara, H., Watanabe, M., Kuroiwa, A., Hirai, H., Hirai, Y., Matsuda, Y., & Okada, N. (2011). B Chromosomes Have a Functional Effect on Female Sex Determination in Lake Victoria Cichlid Fishes. PLoS Genetics, 7(8), e1002203. <https://doi.org/10.1371/journal.pgen.1002203>
- Yoshimoto, S., Okada, E., Umemoto, H., Tamura, K., Uno, Y., Nishida-Umebara, C., Matsuda, Y., Takamatsu, N., Shiba, T., & Ito, M. (2008). A W-linked DM-domain gene, DM-W, participates in primary ovary development in *Xenopus laevis*. Proceedings of the National Academy of Sciences, 105(7), 2469 2474.
<https://doi.org/10.1073/pnas.0712244105>
- Yoshizawa, M., Ashida, G., & Jeffery, W. R. (2012). Parental genetic effects in a cavefish adaptive behavior explain disparity between nuclear and mitochondrial DNA. Evolution; International Journal of Organic Evolution, 66(9), 2975 2982.
<https://doi.org/10.1111/j.1558-5646.2012.01651.x>
- Yoshizawa, M., Goricki, S., Soares, D., & Jeffery, W. R. (2010). Evolution of a behavioral shift mediated by superficial neuromasts helps cavefish find food in darkness. Current Biology: CB, 20(18), 1631 1636. <https://doi.org/10.1016/j.cub.2010.07.017>
- Yoshizawa, M., Yamamoto, Y., O'Quin, K. E., & Jeffery, W. R. (2012). Evolution of an adaptive behavior and its sensory receptors promotes eye regression in blind cavefish. BMC Biology, 10(1), 108. <https://doi.org/10.1186/1741-7007-10-1>

- Zhang, K., Xu, J., Zhang, Z., Huang, Y., Ruan, Z., Chen, S., Zhu, F., You, X., Jia, C., Meng, Q., Gu, R., Lin, X., Xu, J., Xu, P., Zhang, Z., & Shi, Q. (2019). A comparative transcriptomic study on developmental gonads provides novel insights into sex change in the protandrous black porgy (*Acanthopagrus schlegelii*). *Genomics*, 111(3), 277–283. <https://doi.org/10.1016/j.ygeno.2018.11.006>
- Zheng, S., Long, J., Liu, Z., Tao, W., & Wang, D. (2018). Identification and Evolution of TGF- β Signaling Pathway Members in Twenty-Four Animal Species and Expression in Tilapia. *International Journal of Molecular Sciences*, 19(4), 1154. <https://doi.org/10.3390/ijms19041154>
- Zhou, Q., Zhu, H., Huang, Q., Xuan, Z., Zhang, G., Zhao, L., Ding, Y., Roy, S., Vicoso, B., Ruan, J., Zhang, Y., Zhao, R., Mu, B., Min, J., Zhang, Q., Li, J., Luo, Y., Liang, Z., Ye, C., ... Bachtrog, D. (2012). Deciphering neo-sex and B chromosome evolution by the draft genome of *Drosophila albomicans*. *BMC Genomics*, 13(1), 109. <https://doi.org/10.1186/1471-2164-13-109>
- Ziegler, C. G., Lamatsch, D. K., Steinlein, C., Engel, W., Schartl, M., & Schmid, M. (2003). The giant B chromosome of the cyprinid fish *Alburnus alburnus* harbours a retrotransposon-derived repetitive DNA sequence. *Chromosome Research*, 11(1), 23–35. <https://doi.org/10.1023/A:1022053931308>

ANNEXES

Article

Diversity of Olfactory Responses and Skills in *Astyanax mexicanus* Cavefish Populations Inhabiting different Caves

Maryline Blin ¹, Julien Fumey ^{2,‡}, Camille Lejeune ^{1,‡}, Maxime Policarpo ^{1,3}, Julien Leclercq ¹, Stéphane Père ¹, Jorge Torres-Paz ¹, Constance Pierre ¹, Boudjema Imarazene ^{1,4} and Sylvie Rétaux ^{1,*}

¹ Paris-Saclay Institute of Neuroscience, CNRS and University Paris-Saclay, 91190, Gif-sur-Yvette, France; blin@inaf.cnrs-gif.fr (M.B.); camille.sabine.lejeune@orange.fr (C.L.); Maxime.Policarpo@egce.cnrs-gif.fr (M.P.); julien.leclercq@u-psud.fr (J.L.); Stephane.pere@inaf.cnrs-gif.fr (S.P.); jorge.torres-paz@cnrs.fr (J.T.-P.); constance.pierre@free.fr (C.P.); boudjema.imarazene@gmail.com (B.I.)

² Human Genetics and Cognitive Functions, Institut Pasteur, UMR3571 CNRS, Université de Paris, 75015, Paris, France; julien.fumey@pasteur.fr

³ Évolution, Génomes, Comportement et Écologie, IRD, CNRS and Université Paris-Saclay, 91190, Gif-sur-Yvette, France

⁴ INRAE, Laboratoire de Physiologie et Génomique des Poissons, 35000, Rennes, France

* Correspondence: retaux@inaf.cnrs-gif.fr; Tel.: +33(0)-1-69-82-34-52

‡ Equal contribution to this work

Received: 15 September 2020; Accepted: 08 October 2020; Published: 13 October 2020

Abstract: Animals in many phyla are adapted to and thrive in the constant darkness of subterranean environments. To do so, cave animals have presumably evolved mechano- and chemosensory compensations to the loss of vision, as is the case for the blind characiform cavefish, *Astyanax mexicanus*. Here, we systematically assessed the olfactory capacities of cavefish and surface fish of this species in the lab as well as in the wild, in five different caves in northeastern Mexico, using an olfactory setup specially developed to test and record olfactory responses during fieldwork. Overall cavefish showed lower (i.e., better) olfactory detection thresholds than surface fish. However, wild adult cavefish from the Pachón, Sabinos, Tinaja, Chica and Subterráneo caves showed highly variable responses to the three different odorant molecules they were exposed to. Pachón and Subterráneo cavefish showed the highest olfactory capacities, and Chica cavefish showed no response to the odors presented. We discuss these data with regard to the environmental conditions in which these different cavefish populations live. Our experiments in natural settings document the diversity of cave environments inhabited by a single species of cavefish, *A. mexicanus*, and highlight the complexity of the plastic and genetic mechanisms that underlie cave adaptation.

Keywords: fieldwork; wild fish; comparative biology; behavior; troglomorphism; olfactory test; infrared movies; amino acids; chondroitin; plasticity

1. Introduction

A very broad diversity of fauna (micro-organisms, insects, vertebrates) lives in underground environments in a more or less permanent manner. Among various niches in the subterranean milieu, caves are emblematic and attractive to human exploration. Species living there permanently display striking phenotypic convergences in their morphology, physiology, or behaviors, with the hallmarks of troglomorphism being the loss of eyes and pigmentation [1]. Caves are often considered as an extreme environment. In the absence of photoautotrophic production, the quantity of food available is limited or

irregular, the space available is finite, and reproduction seems difficult. Finding food and mates in the absence of vision are the two main challenges faced by cave animals and must limit cave colonization and survival. The evolutionary forces at play during cave adaptation and the respective contributions of natural selection and genetic drift, along with the evolutionary mechanisms, are still a matter of debate [2]. Biologists currently aim at disentangling the roles of genetic mutations and phenotypic plasticity, or epigenetics, in the process. Finally, the observation that some species or lineages have repeatedly adapted to the cave environment while some others never did may support the questioned idea of “pre-adaptive traits” that might favor adaptation to permanent darkness (e.g., [3,4]).

During evolution, most epigean representatives of species that became cave-adapted have become extinct, leaving the underground lineages the only representatives of their taxon, which hampers comparative or genetic studies. The teleost fish *Astyanax mexicanus* is one of the few exceptions to this rule [5,6]. Therefore, the surface-dwelling and cave-dwelling morphs of this species are increasingly used in evolutionary studies to address the developmental, genetic, or genomic mechanisms of morphological evolution and behavioral adaptation [2,7–9]. The surface form (SF) lives in the rivers of the southern United States and Central America, while the blind and depigmented cave form (CF) is endemic to caves in a karst region located in the states of San Luis Potosí and Tamaulipas in Mexico. There, 30 identified caves host *Astyanax mexicanus* cavefish populations. They are distributed into three geographically distant groups located, respectively, in the Sierra de El Abra, the Sierra de Guatemala, and the Sierra Colmena [5,10,11]. All populations of cavefish and surface fish are interfertile, indicating that they are conspecific [12,13]. In nature, the hybridization phenomenon has also been observed and documented [14]. In addition, crosses between geographically distant populations of cavefish can lead to eyed F1 offspring [13], indicating that different mutations are involved in ocular regression in different cave populations and suggesting that some of these populations have evolved independently. However, the evolutionary history of *A. mexicanus* cave populations is still poorly understood because of the geographic dispersion of caves, the lack of knowledge on the underground aquifer network, and the possibility of surface fish introgressions into caves as well as cavefish migrations between caves using underground flows. Recent studies have indicated that initial cave colonization by *A. mexicanus* surface-like ancestors occurred very recently, less than 20,000 years ago [15,16], prompting evolutionary biologists to revise some views about the (rapid) mechanisms of cave adaptation. Like most cave-adapted animals, *A. mexicanus* cavefish present sensory specializations to life without vision. The brains and sensory systems of surface fish and cavefish differ (reviewed by the authors of [7]), along with their sensory systems: Cavefish have more taste buds [17], more neuromasts [18], and larger olfactory epithelia [14,19,20]. From a behavioral point of view, these mechano- and chemosensory specializations are associated with vibratory attraction behavior to locate moving objects [18] and to an excellent sense of smell to detect low concentrations of food-related odors [20], respectively.

Most of the results described above were obtained in the laboratory, often on one or two lab-raised cave population(s). It is therefore important to extend the studies to other populations, and to validate the results on wild animals in order to avoid possible misinterpretations. Going to the field to observe the natural environment of fish, taking samples, and filming behaviors can help answer questions or revise preconceived ideas [21,22]. For instance, it is often stated that caves are a food-poor environment. However, analysis of stomach contents of wild individuals from the Pachón cave has shown that juveniles feed on small arthropods, and adults on decaying materials and bat guano. Overall and contrary to common belief, Pachón cavefish seemed relatively well fed [23]. Another study revealed that growth curves and age/size relationship are comparable in wild surface fish and wild cavefish, again indicating that cave environment is probably not as food-poor as it may seem [24]. In fact, depending on the location of the cave, its topography, and the hydraulic regime, the amounts of carbon flux can sometimes be of the same order as those reported for surface rivers [1] and, most importantly, the carbon content in the mud sampled from different *Astyanax* caves can show up to three-fold variation [24]. Energy sources can come from percolating water, animals entering caves and depositing their excrement or dead bodies, or rivers that overflow during the rainy season and carry organic matter. These energy sources are both spatially and temporally variable [1]. During several cave expeditions, our team noticed the diversity of local environments between caves—

and also between pools within a single cave—reinforcing the idea that field comparisons on fish biology between different caves can be as interesting as the comparison between cavefish and surface fish.

During a field trip in 2013, we carried out, for the first time, experiments of olfactory behavior in situ, in the Subterráneo cave [14]. We had the idea to use a small, light, compact, inflatable children's plastic pool, which was easy to bring on the field. With a rudimentary perfusion system and an infrared camera, we showed that only fish with eyeless phenotype and large olfactory epithelia swam toward an odor source consisting of a food extract. Thanks to this experience and after visits to many other caves, we set up a more complex behavioral experiment, with the aim of systematically assessing olfactory skills and responses of *A. mexicanus* cavefishes inhabiting different Mexican caves. During expeditions in 2016, 2017, and 2019, we performed olfactory tests in the Pachón, Sabinos, Tinaja, Chica, and Subterraneo caves. We found that wild adult cavefish from these five caves showed very variable responses to the three different odorant molecules they were exposed to, with Pachón and Subterraneo cavefish showing the highest olfactory capacities, and Chica cavefish showing no olfactory responses to the odors presented. We discuss these data with regard to the environmental conditions in which these different cavefish populations live.

2. Materials and Methods

2.1. Field Experimentation in Five Different Caves: Constraints and Criteria for Choice

Caves chosen to carry out olfaction experiments had to fulfill several criteria: (1) Reasonably easy access and climbing challenges, as the total weight of experimental equipment was approximately 25 kg carried in backpacks and each location had to be visited twice on two consecutive days. (2) Sufficient space inside the cave to install three experimental plastic pools near the water. Thanks to our field experience, we excluded some caves. For example, Curva's ceiling is too low, Chiquitita's entrance is too narrow, as it is located in a big tree's root [10], Toro is a fault in the rock, and Molino and other Guatemala caves are too challenging in terms of climbing ([11] and team observations). (3) Caves already known and visited by the team in the past were preferred to plan the precise place where to install plastic pools and to anticipate troubleshooting. (4) Good representative sampling of diverse local environments (e.g., rocky and muddy caves). (5) Good representative sampling of diverse cavefish population histories (e.g., with or without surface gene flow, or mountain range in which the cave is located). (6) Possibility to compare with our lab studies performed on Pachón cavefish.

Consequently, we decided to perform experiments in four caves: Pachón and Sabinos (fully troglomorphic fish morphotypes in muddy caves), Chica (introgressed fish population in "dirty" cave), and Subterráneo (introgressed population in rocky cave). We also performed some preliminary experiments in Tinaja (fully troglomorphic fish morphotypes in rocky or muddy cave ponds).

2.2. Cavefishes in the Wild

Olfactory behavior tests were carried out during three field trips to San Luis Potosí and Tamaulipas States, Mexico, in March 2016, March 2017, and March 2019, in five cave localities. Fieldwork Mexican permits 02438/16, 05389/17 and 1893/19 (to SR and Patricia Ornelas-Garcia) were delivered by the Secretaría de Medio Ambiente y Recursos Naturales. The history of the discovery and precise descriptions of *Astyanax* caves are given by the authors of [5,11].

The Pachón cave is located in altitude near the village of Praxedis Guerrero ($22^{\circ}37' N$ latitude and $99^{\circ}01' W$ longitude, about 16 km SW of Ciudad Mante), in the north Sierra de El Abra, and is easy to access [11]. The cave is small, and the water is stagnant on a muddy bottom. Fish from the Pachón cave (named here CF-Pachón) present a fully troglomorphic type.

The Sabinos cave is located near the village of El Sabino, in the central Sierra de El Abra ($22^{\circ}06' N$ latitude and $89^{\circ} 56' W$ longitude, about 13 km NNE of Ciudad Valles) [11]. Villagers installed a padlock grid to exploit this cave and the access is chargeable. The entrance is majestic and the succession of two pits involves bringing harnesses and ropes to abseil down. Fish from the Sabinos cave (CF-Sabinos) are also fully troglomorphic.

The Chica cave is located at the south Sierra de El Abra, on the property of a farmer, at about 21°52' N latitude and 89° 56' W longitude, near the village of El Pujal. It is easy to access, and the entrance and the first cavity are wide. Fish from the Chica cave (CF-Chica) are phenotypically diverse because of surface fish introgression and hybridization. We worked on cavefish from the Chica superficial pool, which are the most troglomorphic/least introgressed among the three natural pools of this cave.

The Subterráneo cave is located in the Micos region, in the Sierra de Colmena (22°03' N latitude and 99°14' W longitude, about 10 km SSW of Micos). Access to this cave is not difficult and the entrance is easy, at the level of the polje or sugar cane field. Fish from the Subterráneo cave (CF-SubT) also occasionally hybridize with surface fish. Hence, they show variable levels of eye regression and pigmentation.

The Tinaja cave is very close to the Sabinos cave, also located in the territory of El Sabino (entrance is free). The cave is located at 22°05' N latitude and 89°57' W longitude, about 10.5 km NE of Ciudad Valles on the Rancho de La Tinaja. Access is via a sugar cane field and permission must be obtained from the owner before crossing it. The cave entrance is accessible after a 2-h hike through a thorny tree forest and a dry canyon covered with jungle. According to Elliott, 2016 [6], the underground hydraulic systems of Tinaja, Sabinos and Sótano de Soyate caves are connected. It has been suggested indeed that the cavefish populations of Tinaja and Sabinos are genetically close [25,26]. The cave entrance is majestic. Climbing equipment is not needed but hiking is difficult due to a very slippery mud covering a stony soil. The air is charged with CO₂ and renders physical effort somewhat difficult. Fish from the Tinaja cave (CF-Tinaja) show a full cave morphotype.

2.3. Fishes from the Lab Facility

Laboratory *Astyanax mexicanus* surface fish (origin: San Salomon spring, Reeves County, TX, USA) and cavefish (Pachón population) were obtained in 2004 from the Jeffery laboratory at the University of Maryland, College Park, Prince George's County, MD, USA. Here, we also used F1 hybrids, which were the progeny of a cross between a Pachón female and a surface fish male. Colonies were maintained at 22 °C (cavefish and F1 hybrids) or 26 °C (surface fish) on a 12:12 h light:dark cycle. In the present paper, lab-raised fish are named Lab-Pachón, Lab-SF, and Lab-Hyb, respectively. SR's authorization for use of *Astyanax mexicanus* in research is 91–116 and the Paris Centre-Sud Ethic Committee protocol authorization number related to this work is 2017-04#~8545. The animal facility of the Institute received authorization 91272105 from the Veterinary Services of Essonne, France, in 2015.

2.4. Sampling and Photography

Wild and lab fish were caught with a net (hand net or seine). In order to record their phenotypes after the behavioral tests, wild cavefish were photographed individually in a small aquarium or a plastic support with a graduated ruler and immediately returned to their pond of origin. Total body lengths were measured from these pictures using the ImageJ software. In the Pachón and Sabinos caves, we also weighed the fish using a portable balance. Taring of the balance was carried out with a glass of water, and each fish was weighed inside the glass of water.

2.5. Odor Choice

The general principle of the experiment was to place eight fish in an experimental square plastic pool, and to successively perfuse three odorant compounds, each in a different corner of the pool (Figure 1). Each odor perfusion was preceded and followed by a perfusion of water, and a water counterflow flowed permanently from the corner opposite to the perfusion of odor. The odors used were L-alanine and L-serine amino acids, and chondroitin (all from Sigma). They correspond to degradation products of organic compounds assimilated to food odors and serve as attractants to fish.

The rationale for choosing alanine and serine as odorant molecules were: (i) To compare them with the results already obtained in the laboratory [19,20]; (ii) due to the fact that attraction and food-searching behavior are easier to identify than repulsion behavior; (iii) because finding food is a matter of survival for these fish and the sense of smell probably plays a major role in this quest. Indeed, previous experiments

performed in the lab had shown that responses to alanine and serine are olfactory-mediated in *Astyanax* larvae [20].

We chose working concentrations of 10^{-7} M for alanine and serine because it is intermediate between the detection threshold for larvae of surface fish (10^{-5} M) and Pachón cavefish (10^{-10} M) in the lab. We also reasoned that it would be “risky” to use a very low concentration close to the cavefish detection threshold in non-controlled cave/field experimental conditions (in particular, water cleanliness, more or less charged with natural odors).

As chondroitin induces freezing in zebrafish [27], we tested this molecule in the lab assuming that *A. mexicanus* would also adopt a freezing behavior [28,29]. Surprisingly, both surface fish and Pachón cavefish instead showed a pronounced and persisting foraging behavior (see Video S1). Preliminary tests in the lab showed that Pachón cavefish have a chondroitin detection threshold at 10^{-4} M.

2.6. Setup Design

With the conditions for setting up and carrying out the experiments *in situ* being difficult, the setup was meant to be light, easy to assemble and dismantle, and not too bulky. Plastic pools (Intex, 85 cm × 85 cm × 23 cm; thoroughly rinsed several times in the lab before use to eliminate inorganic volatile odors) were inflated and placed on the ground after adjusting for horizontality with mud or rocks if necessary. They were filled with 40 L of local cave pond water where cavefish swim. Before pouring into the plastic pools, water was filtered on a coffee filter paper to remove large suspended particles and to ensure cleanliness and good video quality.

A tripod was placed near the corner #1 of the plastic pool. Two infrared lamps (IR Torch 850nm, (Maketheone, LA, USA) and the syringe holder were attached to the tripod at a height of 110 cm. The pool was enlightened from above to reduce shadows and filmed from the top to avoid blind spots. For the 2016–2017 campaigns, we built our own infrared camera using a Raspberry pi 3 model B and a Pi-NoIR V2.1 camera. We used a 5-V power bank to supply electricity to this camera, which was controlled from a computer connected in ethernet via a SSH connection. Using Python 2.7.9 and the PiCamera V1.12 package, we wrote two scripts (available at <https://github.com/julienfumey/PiCaveRecord>) to frame on the pool and to record the video. Videos were converted from h264 to mp4 with VLC software [30]. In 2019, to avoid having to use a computer in caves and to save time, we opted for an infrared hunting camera (nature camera Full HD WK-590, VisorTech, Nairobi, Kenya) which records films in AVI format.

For each plastic pool, we constructed a set of four tubing lines consisting of four 50-mL syringes connected to a 180-cm-long medical solution administration tubing (Infusion device, Intrafix® SafeSet; B. Braun; inside volume of 20 mL) and terminated by a 0.6-mm-diameter needle (protected by a plastic cap to avoid wounding the fish). The opening of the perfusion was controlled by a Luer stopper and the perfusion rate was regulated by the needle. The end of the tubing was attached to a metal guide (which did not touch the water) to hold the needle in the corner of the plastic pool. Each perfusion line was guided to its respective corner.

A set of three pools was installed in the visited cave, with eight cavefish in each ($n = 24$ total). The installation of three experimental setups was completed in ~4 h by four people. Fish were left for a 20-h habituation period (from approximately 5 p.m. day 1 to 1 p.m. day 2). The next day, behavioral tests were carried out in the dark (IR recordings) and in silence, in parallel, by three experimenters.

2.7. Procedure

Chemicals were weighed in the laboratory on the day before field trip departure. In a hermetically closed 50-mL tube, 10 mg of L-alanine (CAS 56-41-7, Sigma-Aldrich, Saint-Quentin Fallavier, France), 10 mg of L-serine (CAS 56-45-1, Sigma-Aldrich), and 5 mg or 110 mg of chondroitin (CAS 9082-07-9, Sigma-Aldrich) were each placed (a series of three tubes of powder per cave were thus prepared in advance). Solutions were prepared extemporaneously by adding 50 mL of filtered cave water to each tube. Chondroitin concentration was 10^{-4} M and 10^{-3} M, respectively. For alanine and serine working solutions, a second dilution (3 μ L in 50 mL) was prepared to obtain 10^{-7} M solutions. For experiments performed in the

lab with surface fish, we prepared a different dilution (300 μ L in 50 mL) to obtain 10⁻⁵ M alanine or serine solutions.

The experimenter seated near the pool took care not to move and not to speak during the whole experiment. To start the experiment, filtered water (= control) was perfused from tubing #1 and #3 (i.e., opposite corners), and then from tubing #2 and #4 (i.e., opposite corners), for 6 min each. The aim of this step was to accustom fish to flow and possible vibrations of perfusions and to reduce subsequent nonspecific responses. Indeed, thanks to their lateral line, fish perceive and are attracted by vibrations [18].

Then, water was perfused for 6 min from tubing #1 and #3. Solution flow from the two syringes was initiated simultaneously. When syringes emptied, 50 mL of alanine solution was added to syringe #1 and water was added again for counter-flow in syringe #3 (Figure 1, left panel, orange for alanine). After completion of alanine perfusion, the test continued with a new water perfusion from corners #1 and #3. Experimenters took care to ascertain a continuous flow by filling syringes with water or odor solutions before they were completely empty to avoid the introduction of air bubbles into the system.

The same principle was then applied for the perfusion of water, serine or water, and water at corners #2 and #4 (Figure 1, middle panel, green for serine). Finally, water, chondroitin or water, and water, were perfused at corners #3 and #1 (Figure 1, right panel, blue for chondroitin).

With the exact same setup and procedure, we performed series of experiments in the lab, in a dark and soundproof room, using animals from our breeding facility.

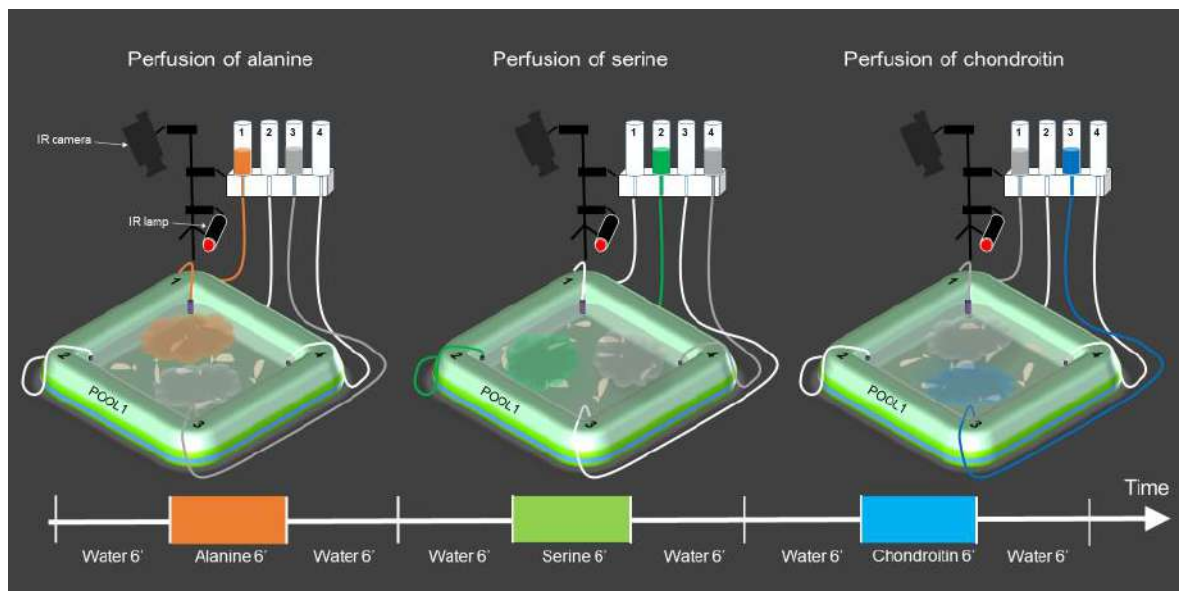


Figure 1. Establishment of a behavioral setup and protocol to test cavefish olfaction in the field. The setup allows testing olfactory responses of eight adult fish in inflatable plastic pools in the dark under infrared recordings. Three different odors were perfused sequentially by gravity flow at different corners of the plastic pool, according to the indicated timeline. See Methods and the first paragraph of Results for details.

2.8. Video Scoring

A total of ~60 h of infrared videos was recorded. We first attempted to analyze them with an automatic multiple tracking video software [31], which unfortunately did not detect the fish correctly. The reasons were probably numerous: There were eight fish in the pool, the film was in infrared, the contrast of fish on white background was not strong enough, the lamps sometimes produced lighting reflections on the water surface, and the pool edges generated blind spots. Thus, we could not satisfactorily extract the time spent by each fish in each zone and turned to manual scoring.

We first established that, after perfusion of 50 mL of blue-colored water (with a counterflow), the blue color occupied roughly half of the arena, i.e., a triangle formed by the corner from which the perfusion arrived and the diagonal of the plastic pool (Figure S1A). We therefore considered this half of the pool as

the “odorant area” and its opposite half as the “water/control area.” Videos were tracked manually through frame-by-frame analysis using Windows Media Player. The number of fish present in each half of the pool was counted every 15 s during the whole experiment. The odor Preference Index (PI) was calculated for each odor using the formula: (Fish count (odor area) – Fish count (water area) / Total fish count (Figure S1B). When all fish were in the odorant area, PI = 1 (suggesting attraction effect); when all fish were in the opposite corner, PI = -1 (suggesting repulsion effect); and when fish were distributed evenly/randomly in the two parts of the pool, PI = 0 (suggesting no effect).

2.9. Data Analyses and Statistics

When the odorous solution was poured into the syringe, 20 mL (= dead volume contained inside the 180 cm long tubing) of water flew out before the actual odorant solution entered the pool. For each perfusion, we calculated the speed of the flow to determine odor (or water) perfusion duration. Although tubing were the same length and volume perfused by gravity flow was always 50 mL, the perfusion duration (theoretically 6 min) was appreciably variable both between the four perfusion lines, between the successive water/odor/water perfusions, and between the three plastic pools in a given cave. To overcome this problem, we normalized time and calculated PI means over periods corresponding to 25% of the total perfusion time for each sequence. Thus, we obtained four PI means for each perfusion duration. To determine the statistical significance of the behavioral responses, we used Friedman nonparametric test by ranks for repeated measures in order to compare PI variations along time, during water perfusion before odor, during odor perfusion, and during water perfusion after odor. We also used Wilcoxon Mann-Whitney tests to determine the statistical significance of each PI distribution against PI = 0 (no effect) for each time segment.

Fish sizes and weights were also compared using a nonparametric Wilcoxon–Mann–Whitney test.

Statistical analyses were performed using R 3.6.1 [32] in Rstudio environment [33] with rstatix package, version 0.5.0 [34]. Plots were generated using ggplot2 package [35] from tidyverse open-source R packages [36].

3. Results

3.1. Methodological Considerations: Testing Olfactory Responses in the Lab versus in the Wild

Our previous analyses of olfactory skills and behaviors in *A. mexicanus* were mostly performed on larvae, in small 9- × 13-cm U-shaped “olfaction boxes” containing 150 mL of water, and under laboratory-controlled conditions and standards [19,20]. We had also performed a preliminary experiment on adult fish in the Subterráneo cave but the insights were limited because, among other difficulties, a single “odor” consisting of crushed food pellets was tested as odorant cue [14]. Here, to reach our goal of testing several relevant odors on adult cavefishes inhabiting several caves, we developed a novel setup and a novel experimental procedure adapted to the field.

First, we carried out laboratory experiments to establish and validate the experimental setup (Figure 1 and see Methods) and to study adult fish olfactory behavioral responses. We reasoned that such results would also help us interpreting data obtained in caves. Cavefish from our animal facility originated from the Pachón cave but have been raised under markedly different conditions (food, light, water quality) for several generations [37], and they might have been affected by captivity and environment.

Moreover, laboratory experiments were the only option we had to study surface fish olfactory responses. In our experience, it has been impossible to test wild surface fish in the field. Besides the difficulty and time needed for catching wild fish in rivers, they are highly sensitive to manipulations and stress and do not behave “normally,” displaying most signs of their stress repertoire [25]. In addition, due to daylight, setting up an experimental test near the river is complex, with a risk of predation on fish by wild animals during the habituation period or destruction/stealing of the equipment.

Finally, we also carried out tests on lab-generated F1 Hybrids. We previously showed that F1 Hybrids larvae have a relatively poor odor detection threshold, similar or even below surface fish skills [19]. In the

Subterráneo and Chica caves, wild fish present a wide variety of intermediate hybrid-like phenotypes. It was therefore interesting to perform tests on adult F1 Hybrids in the lab to compare with result obtained on larvae and on wild cavefish populations where hybridization occurs.

3.2. Responses to Odors in Laboratory-Raised *A. Mexicanus*

The results of laboratory experiments are presented in Figure 2 ($n = 8$ plastic pools averaged for each graph, hence 64 fish were tested for each morphotype).

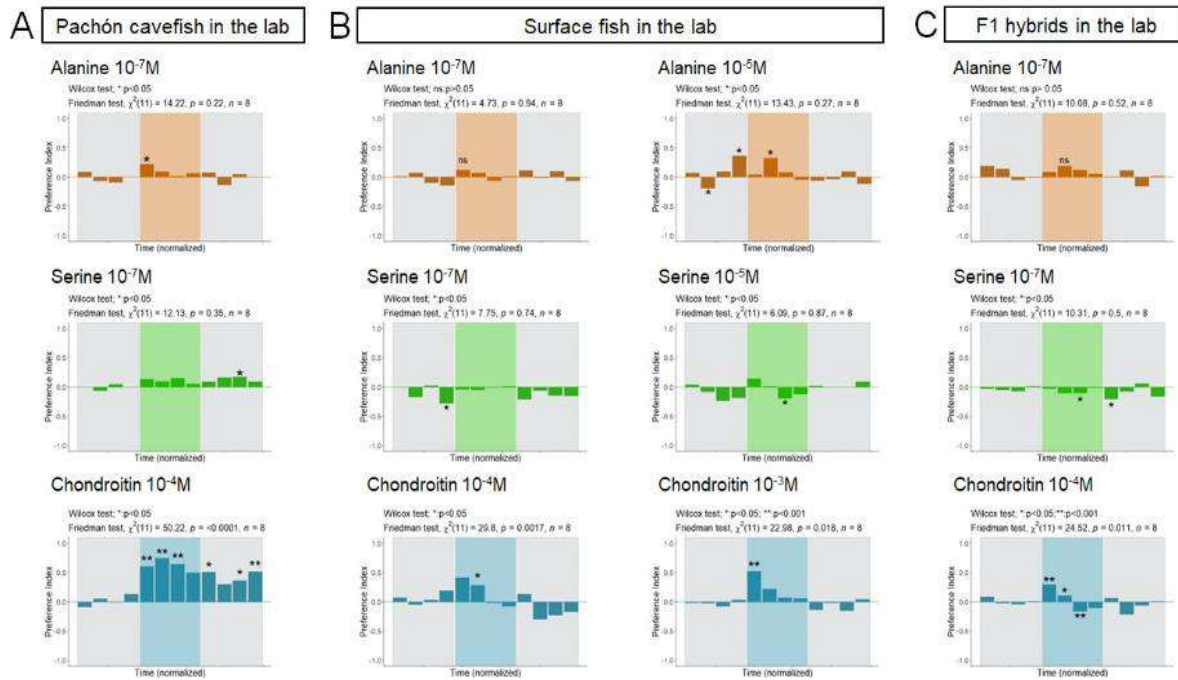


Figure 2. Testing olfactory skills in the laboratory; Olfactory responses of Pachón cavefish (A), Surface fish (B) and F1 hybrids (C) to the indicated odors at the indicated concentrations using the described olfactory setup in laboratory conditions ($n = 8$ for each); The preference index (PI; positive values suggest attraction) is shown as a function of time. Time intervals corresponding to odor perfusion are shaded. Asterisks on graphs indicate significance as compared to no response (i.e., PI = zero) for a given time interval (Wilcoxon Mann-Whitney test). The results of Wilcoxon and Friedman tests to probe the significance of the response across time with repeated measures are also indicated.

In agreement with previous experiments on larvae, only Lab-Pachón showed a positive attractive response to the low concentration of alanine 10⁻⁷ M (Figure 2A, orange). A modest but significant response was observed during the first quarter of alanine perfusion time (PI = 0.22; Wilcoxon test, $p = 0.008$; but Friedman test, NS), suggesting that Lab-Pachón detected the odor as soon as it arrived in the arena but were not attracted for more than a few minutes. On the other hand, Lab-SF did not respond to alanine 10⁻⁷ M but were significantly attracted by the higher concentration of 10⁻⁵ M alanine during the second quarter of perfusion time (Figure 2B, orange; PI = 0.32; Wilcoxon test, $p = 0.008$; but Friedman test, NS). These data suggest that, like larvae, adult Lab-Pachón have a better olfactory detection threshold than Lab-SF for alanine. Finally, Lab-Hyb did not respond to the low (10⁻⁷ M) alanine concentration, and were not further tested for a higher concentration (Figure 2C, orange).

Serine elicited very little, if any, response on surface and cave adult *Astyanax* (Figure 2A–C, green; Wilcoxon tests and Friedman tests, all NS). Of note, Lab-Pachón were present in the odor perfusion zone in a delayed manner, i.e., when water was subsequently perfused from that corner (PI = 0.16; Wilcoxon test, $p = 0.008$), suggesting that the response to serine may have different kinetics compared to the response to alanine. Surprisingly, transiently negative PIs were observed for both Lab-SF (10⁻⁵ M serine, PI = −0.2;

Wilcoxon test, $p = 0.008$) and Lab-Hyb (10^{-7} M serine, PI = -0.07 and -0.03 ; Wilcoxon test, $p = 0.008$ and 0.02), which was an unexpected result (see Discussion).

Chondroitin provoked strong positive responses in all lab-raised fish, as shown by statistical significance with both Wilcoxon tests and Friedman tests (Figure 2A–C, blue). Lab-Pachón showed intense response to 10^{-4} M chondroitin and were present in the perfusion zone as soon as the odor arrived, with very high PIs (PI = $0.6 / 0.7 / 0.6 / 0.5$; Wilcoxon test, $p = 0.0004$ at all times). The attraction was persistent, since fish remained in the odor zone during the water perfusion that followed. Lab-SF showed a comparatively more modest response to 10^{-4} M chondroitin (PI = 0.27 ; Wilcoxon test, $p = 0.008$), but a strong attraction for the higher chondroitin concentration of 10^{-3} M (PI = 0.52 ; Wilcoxon test, $p = 0.0004$). Finally, the Lab-Hyb were present in the odor zone during the first half of the chondroitin perfusion (PI = 0.29 and 0.1 ; Wilcoxon test, $p = 0.0004$ and 0.008) but then seemed to avoid the area (PI = -0.17 ; Wilcoxon test, $p = 0.0004$). Thus, all morphotypes/genotypes were attracted by chondroitin, but persistence and intensity of the response was particularly spectacular with Lab-Pachón (Video S1). Overall, these laboratory experiments showed that our setup allowed us to measure olfactory responses on adult *A. mexicanus* in a reliable manner.

3.3. Responses to Odors in Caves, in Wild *A. Mexicanus* Cavefish Populations



Figure 3. Sampling cavefish olfactory skills in their natural environment; (A) Simplified map of the region of Ciudad Valles, Mexico. Mountain ranges are in grey. The locations of visited caves are indicated by colored circles. The color code indicates the geographical group where they belong; (B) Fieldwork in the Pachón cave. The main pool was muddy and the water level was low. Note that in March 2017 and March 2019, the three plastic pools were installed and processed in the best possible reproductive manner, on the “beach” along the main pool. Close-ups show the Luer-lock perfusion system and the eight fish installed in one of the experimental plastic pools; (C) Work in pool 2 of the Subterráneo cave, located just after the 3-m pit. This pool offers a rocky substrate. There, we repeatedly observed the presence of crayfishes (predators on adult cavefish). The bottom right panel shows the infrared, hunting-type camera, used in our 2019 campaign; (D) Work in Los Sabinos cave. Pool 1 of this cave had crystal-clear water. Again, note that olfactory setups were installed in the same place in March 2017 and 2019, respectively, i.e., on a rocky plateau just above pool 1. A close-up shows the Raspberry Pi camera used during our 2017 campaign. (E) Testing olfaction on fish from

the Chica superficial pool. The top photos show the guano slope leading to the superficial pool, which was very rich in organic material (decomposing bat cadaver). On the bottom left panel, note the large size of the eight fish (compare with the equivalent picture in Pachón, and see Figure 4).

3.3.1. Pachón Cave

Despite the thick mud, it was easy to install three plastic pools near the natural main pool (Figure 3B). CF-Pachón were of relatively small size (mean: 4.6 cm) compared to other caves studied (Figure 4A, purple) and they were all eyeless and depigmented (Figure 4D). Fish used for olfaction experiments came from the small lateral pool in 2017 and from the main pool in 2019. These two pools communicate with each other when the water level is high and the fish can swim and mix between these two pieces of water. There was no difference in size (or phenotype) between the fish tested during the two expeditions (Figure 4B, purple), suggesting that the local conditions have been stable across the years in the cave. The fauna encountered there and the feeding habits of the CF-Pachón have been described by Espinasa et al., 2017 [23].

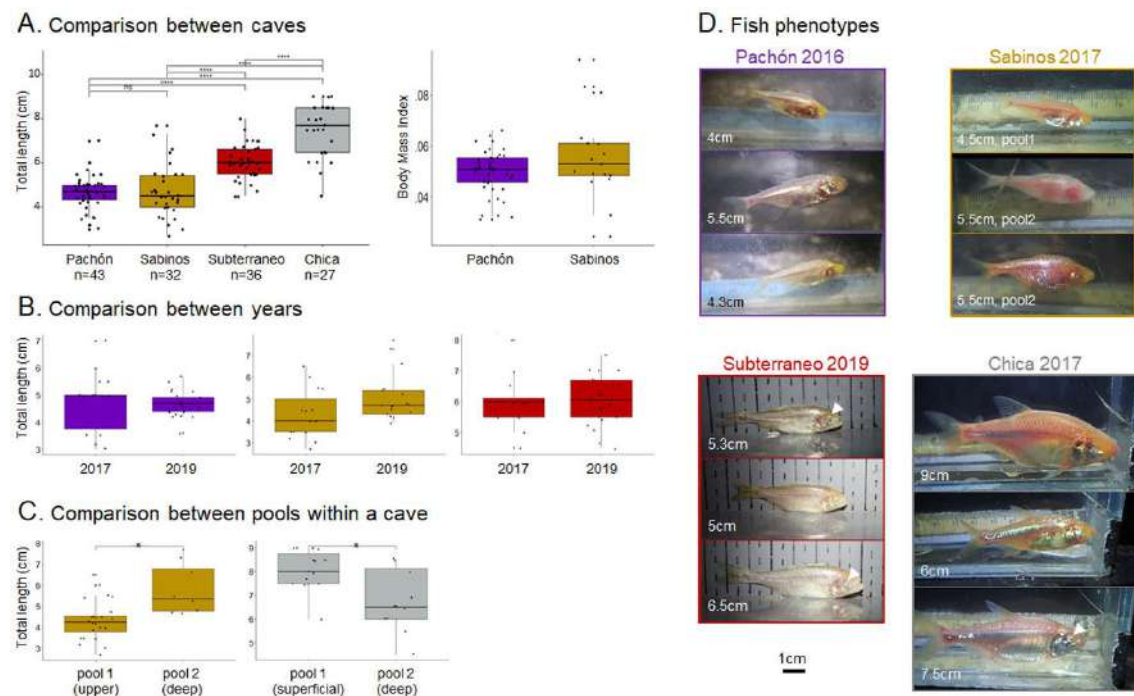


Figure 4. Cavefish sizes and phenotypes in different caves; (A) Sizes (left graph) and body mass indexes (BMI, right graph) of the cavefish individuals tested for olfactory responses in the Pachón (purple), Sabinos (brown), Subterráneo (red), and Chica (grey) caves. Asterisks indicate significant differences (Mann–Whitney test); (B) Comparison of sizes of the cavefish tested for olfactory responses in different field campaigns, in 2017 and 2019, showing that the condition of the fish tested did not vary; (C) Comparison of sizes of cavefish in different water ponds in a same cave locality, showing that fish condition varied, probably due to local trophic, environmental and/or genetic parameters; (D) Fish phenotypes are fully troglomorphic in the Pachón and Sabinos caves, whereas hybrid-type fish with small eyes (arrowheads) and some pigmentation can be seen in Subterraneo (pool 2) and Chica (superficial pool) caves. They result from hybridization with introgressed surface fish. Of note, in Subterraneo, surface fish enter by the cave entrance at the polje level, whereas, in Chica, surface fish enter the cave by the bottom. Hence, in both caves, the most troglomorphic fish are larger.

Despite fair conditions for installation of the olfactory setup, CF-Pachón from two experimental pools out of the six recorded presented an obvious place preference behavior (one in 2017 and one in 2019), for unknown reasons (Figure 5). These data were thus discarded from the analyses shown in Figure 6A.

Contrary to Lab-Pachón, CF-Pachón did not respond to alanine 10^{-7} M. Even more so, the preference index reached negative values during the perfusion. Conversely, CF-Pachón were strongly and significantly attracted by serine 10^{-7} M (PI = 0.41) and by chondroitin 10^{-4} M (PI = 0.55), as shown both by Friedman and Wilcoxon statistical tests (Figure 6A, green and blue). Moreover, the type of behavioral response elicited by chondroitin in the field was similar to the food-seeking behavior recorded in the lab (Video S2). Although slightly surprising because the alanine and serine responses seem divergent between the Lab-Pachón and the CF-Pachón, these data confirm, in the field, that CF-Pachón have excellent olfactory detection skills.

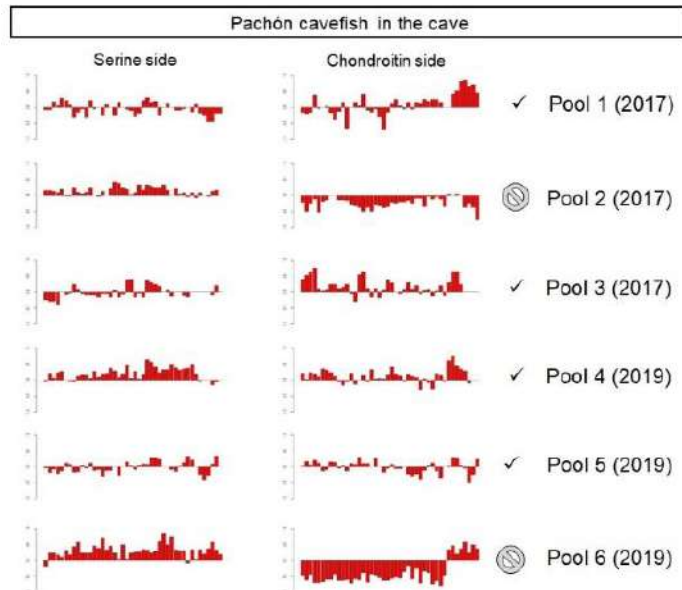


Figure 5. The place preference problem during cave experimentation. Graphs showing the position of the fish along the whole ~1 h protocol for the $n = 6$ experiments performed in the Pachón cave. The bars represent the preference of fish toward the serine perfusion side (left column) or the chondroitin perfusion side (right column). In theory, the eight fish should swim across the arena and distribute or explore randomly except for the response to the considered odor. However, in some instances (here, plastic pools 2 and 6), it was not the case: The fish remained in the same part of the plastic pool throughout the experiment, showing place preference for unknown reasons. These data were excluded from analysis.

3.3.2. Sabinos cave.

The first fish pool encountered, i.e., the upper pool, lies under a large arch and contains shallow water that disappears under the rock (Figure 3D). Exploration there revealed a large (20–30 m), continuous body of water under a low ceiling, hosting a significant cavefish population. The water was clear with a muddy substrate. Juvenile cavefish (size 1–2 cm) were observed, indicating that reproduction occurs. Large isopods and numerous mysid shrimps were present. Just above this natural pool, a natural rocky stage allowed us to install three plastic setups in the same place in 2017 and 2019 (Figure 3D). From there, a corridor led into a large and relatively low room where a second fish pool, or bottom pool, was encountered. Bats were numerous (observed in 2013, 2017, and 2019). The air was loaded with spores and the soil was covered with patches of microorganism covered with insects. CO₂ was not measured but was probably high.

All fish in the Sabinos cave had a fully troglomorphic phenotype (Figure 4D). Fish used in the experiments were sampled from both the upper and the bottom pools. Like in the Pachón cave, their size and body mass index was modest (Figure 4A, brown; mean: 4.7 cm) and did not vary between 2017 and 2019 samplings (Figure 4B, brown), suggesting that the two experimental series were performed on fish of similar condition. We noted that CF-Sabinos found in the deeper pool were significantly larger (Figure 4C, brown) and more corpulent (Body Mass Index, Wilcoxon test, $p = 0.006$) than those fished in the upper pool, suggesting that they were older [24] and/or better fed. However, this observed difference in condition could

not be correlated to their olfactory responses. As in the Pachón cave, we observed a strong place preference bias in two experiments out of six, hence these data were discarded (Figure S2). When tested for olfactory responses, CF-Sabinos were attracted neither by alanine nor by serine (Figure 6B). However, they did spend time in the odorous part of the arena after chondroitin perfusion (PI values between 0.46 and 0.28; Wilcoxon test, $p = 0.02$; but Friedman test, NS), suggesting that they were, although moderately, attracted to this molecule (Figure 6B).

3.3.3. Subterráneo Cave

A 20 min descent in a boulder tunnel filled with organic waste (including of very large size like trees) carted inside during the rainy season leads to a first small fish pool, where almost all individuals are surface-like (*A. mexicanus*, poeciliids, some cichlids, presumably washed in during flooding) and where troglomorphic fish are rare (see Simon et al., 2017 [24]). Then, the tunnel continues and leads to a small 5-m pit which descends directly into the natural pool 2, with clear water on a rocky substrate, where CF-SubT swim. All fish used and measured in 2013 [14], 2016, and 2019 came from this room (Figure 3C). The ground of the cave at this level was relatively horizontal but it was covered with pebbles. As there was no mud to flatten the ground, we installed plastic pools on small flat mounds (Figure 3C).

As we previously described [14], CF-SubT presented mixed phenotypes in terms of eye size and pigmentation as a result of hybridization with introgressed surface fish, and most of them were not fully troglomorphic (Figure 4D). We found that CF-SubT were significantly larger than CF-Pachón and CF-Sabinos (Figure 4A, red; mean: 6 cm), suggesting that they may have been overall slightly older [24] and/or in better nutritional condition. In addition, the CF-SubT tested in 2017 and 2019 were of similar sizes (Figure 4B, red). During the olfaction tests, the CF-SubT were present in the 10^{-7} M alanine perfusion area approximately 2 min after the odor arrived and they remained in this zone during the entire perfusion time (PI = 0.25/0.26/0.19; Wilcoxon test, $p = 0.007/0.118/0.025$) (Figure 6D). Conversely, they did not significantly respond to serine. Finally, CF-SubT were attracted by chondroitin (but note that the concentration perfused was higher than in other caves: 10^{-3} M), since they stayed in the odorous area with high preference indexes (PI between 0.48 and 0.33; Wilcoxon test, $p = 0.025/0.007$). Thus, overall, CF-SubT showed significant olfactory skills and responses in their natural settings. Of note, in videos, it was impossible to make any correlation between olfactory responses and the degree of troglomorphism exhibited by individual CF-SubT.

3.3.4. Chica Cave

The Chica superficial pool (or pool 1) hosting cavefishes is a large body of water with a guano slope bank, probably very rich in organic content due to a large bat colony and influx of organic materials from the surface during the rainy season (decaying bats, vegetal debris were observed; Figure 3E). A corridor with a flat rocky floor allowed us to set up experiments just above this superficial pool (Figure 3E). Further down, Chica pool 2 could be reached by following the underground river, which cascaded after a pit [11], and also contained fish that were phenotypically less troglomorphic and more surface-like or hybrid-like than the fish in superficial pool 1 (not shown).

The superficial pool CF-Chica tested were not fully troglomorphic, i.e., some individuals showed some degree of pigmentation and had tiny to small eyes (Figure 4D), probably as a result of hybridization with surface fish. CF-Chica were, by far, the largest and most corpulent fish that we tested among the different caves visited (Figure 4A, grey and 4D). The individuals fished for the olfaction experiments originated from the superficial pool, where the most extreme sizes (mean: 8.1 cm, max: 9 cm) were encountered (compare with CF-Chica from pool 2; mean: 6.8 cm, Figure 4C, grey). In this cave, olfaction experiments were performed once, in 2017. Hence, only $n = 3$ plastic pools were recorded. For the CF-Chica, Friedman tests indicated that the Preference Indexes did not vary between the perfusions of water and amino acids, and the Wilcoxon tests indicated that they were not different from 0 (Figure 6C). A video problem at the end of one recording resulted in $n = 2$ for chondroitin, for which we could not perform statistical tests. However,

for chondroitin, the pattern was flat along the whole perfusion sequence, and there was no such behavioral foraging response as visually observed in other caves. These results showed that CF-Chica did not respond to the odors used in our tests, including chondroitin that elicited strong responses in all other cavefishes tested as well as in Lab-SF and Lab-Hyb.

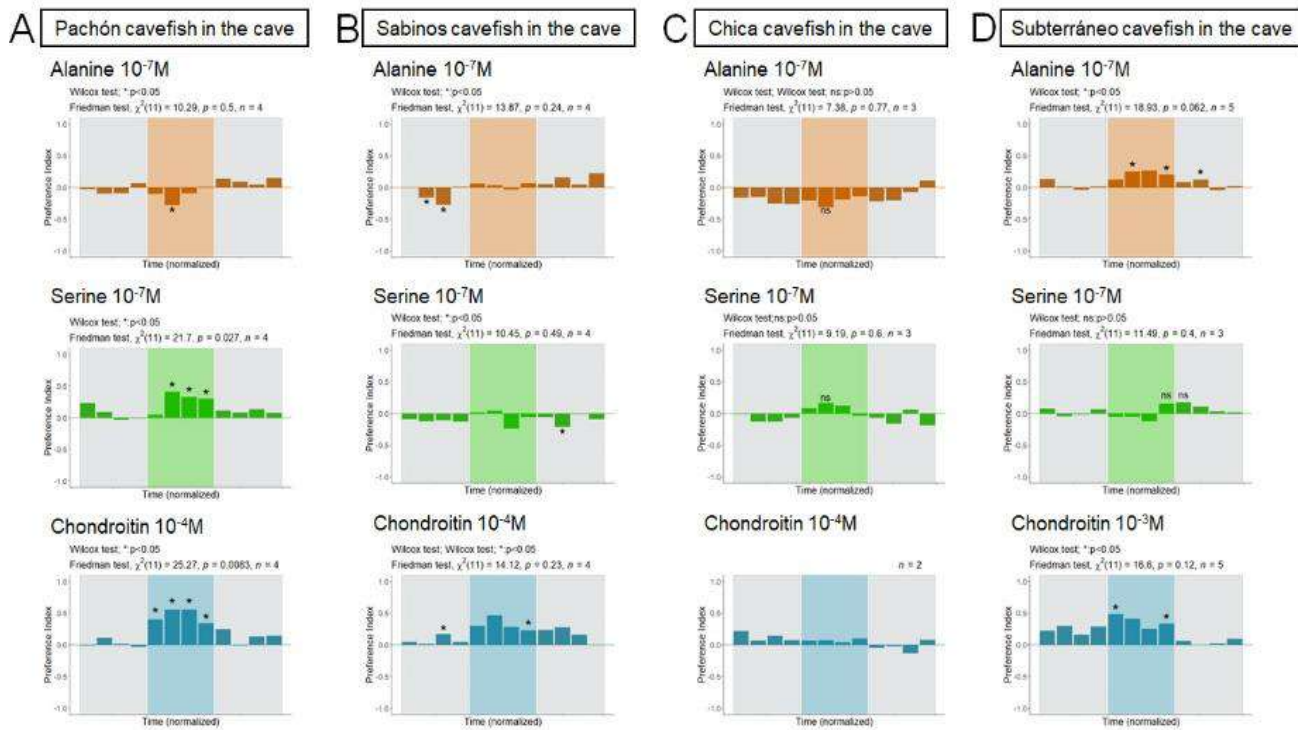


Figure 6. Olfactory responses of cavefishes in natural cave settings; (A), (B), (C), (D) Olfactory responses recorded in the Pachón (A), Sabinos (B), Chica (C), and Subterráneo (D) caves; Odors and concentrations are indicated, as well the number of replicates. The preference index (PI; positive values suggest attraction) is shown as a function of time. Time intervals corresponding to odor perfusion are shaded. Asterisks on graphs indicate significance as compared to no response (i.e., PI = zero) for a given time interval (Mann-Whitney test). The results of Wilcoxon and Friedman tests to probe the significance of the response across time with repeated measures are also indicated.

3.3.5. Tinaja Cave

The first, very small, Tinaja “perched pool” was encountered after a 20-min walk and consisted of a small piece of crystal-clear water retained between rocks (Figure 7A). We found fully troglomorphic CF-Tinaja there (approximately $n = 20\text{--}30$) in two consecutive years (2016 and 2017). After another 20 min of hiking down, the tunnel narrows before reaching a fault, at the bottom of which lies Traverse Lake (or Tinaja pool 1) (Figure 7B). A small natural beach allowed for experimental installation, but the space was small and inconvenient (~ 3 m wide). Drops of water constantly falling from the ceiling generated a very thick and sticky layer of mud. The water was cloudy. In such conditions, it was difficult to install the olfaction setup. This was partly achieved in March 2016, with only $n = 2$ plastic pools and with video recordings performed in the light (Figure 7B). The size of the fish was 6.1 cm on average ($n = 12$ measured). In 2017, we aimed to complete the Tinaja study and we performed $n = 1$ additional olfactory test directly in the small natural “perched pool 1.” Although we cannot provide statistical support ($n = 2$ and $n = 1$, respectively), the video analyses suggest that that CF-Tinaja were not attracted by any of the three perfused odors (data not shown).

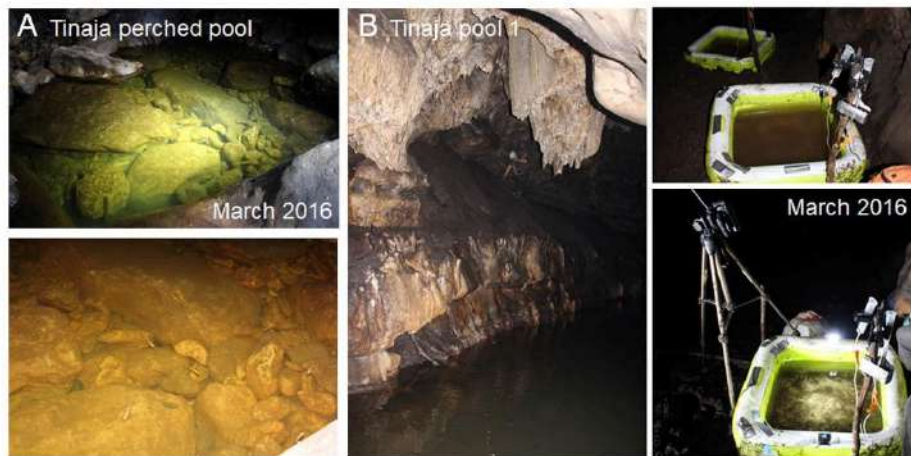


Figure 7. Experimentation in the Tinaja cave; (A) single test was “manually” performed in Tinaja perched pool, a very small (~3–4 m²) and shallow natural pool where water is retained between rocks. There, over the years, we repeatedly observed 20–30 fully troglomorphic fish, presumably trapped there during the rainy season. The water is crystal clear; (B) Preliminary experiments were performed in March 2016 in Tinaja pool 1 (called Traverse Lake), a relatively large and muddy water reservoir. At the time, films were recorded in the light (instead of in the dark with infrared) and the perfusion system and the odorant molecules perfused were still under tuning. This type of expedition was of paramount importance to improve and establish the final experimental setup and design we used successfully in 2017 and 2019 in other caves.

4. Discussion

4.1. Testing Cavefish Olfaction in the Field: A Challenge

To our knowledge, this is the first study reporting systematic, precise, and quantified olfactory responses to specific odorant molecules in behavioral tests with subterranean animals in their natural environment (but see [14,22]). The trip organization, transport of equipment, and difficulties of access, together with the struggle of setting up experiments in “natural laboratories” which were different each time and handling the unexpected, means that few researchers risk of this kind of experimentation. The interpretation of the results must also be approached with caution because the experimental parameters are far from being fully mastered or even known. Of note, we found that establishing and pretesting of protocols in the lab are mandatory steps, and the comparison between lab and field results can help reach conclusions. Finally, this type of field behavior work needs to extend over the long term, with continuous improvements and feedbacks. For example, the difficulties we encountered in Tinaja in 2016 allowed us to improve the setup. From that expedition, we concluded that the plastic pools needed to be perfectly clean and the cave water needed to be filtered before being poured into the arena or else the videos would be difficult to interpret, that we should not use rechargeable batteries for infrared lamps because the Mexican electrical network sometimes fluctuates, that we should systematically include a water counterflow at the corner opposite to odor perfusion to remove biases of lateral line driven behaviors, and that we should not plan for 2-day-long experiments in a cave where access is difficult. Hence, our Tinaja 2016 experiments ($n = 2$ only) were not performed in the dark, did not have the same perfusion sequence nor the same odor concentrations, and were not included in the main results of the present paper, but they ended up being very instructive for improving the setup and protocols, and they allowed us to draw preliminary conclusions (see Figure 7).

4.2. Alanine, Serine and Chondroitin Elicit Variable Behavioral Responses in Wild and Lab-Raised Adult *A. Mexicanus*.

The choice of odors presented to fish was critical. Whereas alanine and serine amino acids are “classically” used in fish olfaction experiments because they correspond to food degradation products and therefore serve as food-related attractive cues (e.g., [38–40]), the use of chondroitin is more novel.

Chondroitin sulfate is a glycosaminoglycan composed of a chain of alternating sugars and a component of the cartilage matrix. It is also present in zebrafish skin mucus, where it was recently discovered to serve for the long-searched active molecule of the alarm substance [27,41]. Indeed, zebrafish strongly react to chondroitin with a typical alarm behavior, including erratic swimming and freezing, and the activated brain regions are the same as those activated after presentation of skin extracts [27]. In *A. mexicanus*, it was therefore unexpected that chondroitin would elicit (1) attraction and (2) foraging, and even more so, (3) the same response in the two morphs. Along with the idea that the alarm substance is species-specific [42], our findings suggest that its composition in zebrafish and *Astyanax* must be markedly different. Moreover, early studies have suggested that alarm reaction is indeed present in surface fish but mostly lost in cavefishes, at least those originating from the Pachón and Chica caves [28,29,43]. Here, surface fish and Pachón cavefish strongly reacted to chondroitin, but Chica cavefish did not, further suggesting that this molecule is not part of the alarm substance in the species. Rather, it seems to correspond to a foraging cue, which is in line with *Astyanax* being carnivorous, eating carcasses and responding to cartilage odors. In fact, we ended up considering chondroitin as a sort of positive control: All types of fish tested, in the lab and in the field (except CF-Chica, see below), adopted an intense food search behavior, almost leaking or sucking the extremity of the tube where chondroitin flew in (Supplementary videos). Of note, chondroitin was the third and last odor presented in the protocol because we reasoned that the more modest responses elicited by amino acids may be lost after the strong stimulation caused by chondroitin. Finally, response to chondroitin also validated, in a way, the whole test, and we were confident that absence of response to amino acids sometimes observed was true because fish reliably and repeatedly responded to chondroitin at the end of the behavioral assay (Table 1).

Table 1. A summary of the results obtained in all the cave and laboratory olfaction experiments. Attractive response (+) or no response (0) is summarized for each cavefish or surface fish population, when recorded in the field or in the lab (as indicated in the different columns) for the 3 different odors studied (as indicated in the different rows; orange/alanine, green/serine, blue/chondroitin). Light and dark colors indicate response to the high concentration (light color, lower detection capacities) or the low concentration (dark color, better detection capacities) of the odor considered. The last line (grey shades) indicates to how many odors, out of the 3 tested, the fish have responded.

Fishes		Cave fishes					Surface fishes		
		Lab-Pachón	CF-Pachón	CF-SubT	CF-Sabinos	CF-Chica			
Alanine	Attraction : (+)	+	0	+	0	0	+	0	0
	No response : (0)	10 ⁻⁵ M	10 ⁻⁷ M						
Serine	Attraction : (+)	+	++	0	0	0	0	0	0
	No response : (0)	10 ⁻⁵ M	10 ⁻⁷ M						
Chondroitin	Attraction : (+)	+++	+++	++	+	0	++	+	+
	No response : (0)	10 ⁻³ M	10 ⁻⁴ M						
Olfactory performance summary		3/3	2/3	2/3	1/3	0/3	2/3	1/3	1/3

Regarding amino acids, the results we obtained with adult fish in the lab globally corroborate what has already been observed with 1-month-old larvae [20]: The adult Lab-SF had a lower olfactory detection threshold than the Lab-Pachón (Table 1). The results confirm that older and larger adult fish do not have a better detection threshold than 1 month-old-larvae [19], reinforcing the idea that olfactory detection threshold is not directly or exclusively linked to the size of the olfactory organs, or to the intrinsic properties of the olfactory system. The results also confirm that the olfactory system of the 1-month-old larvae tested in our previous studies was functionally mature.

For reasons explained earlier, adult surface fish (and F1 hybrids) could only be tested in the lab. We considered their olfactory performance to be poor (Table 1). They did respond to chondroitin—albeit less intensely than Lab-Pachón, but barely responded to amino acids, even at high concentrations. An explanation to this mitigated result might be that the olfactory response is slightly blurred by schooling behavior, even in the dark [25,44]. Indeed, for these fish, we observed transient statistically significant PI scores (positive or negative) before or after odor perfusion (see Figure 2B–C) that cannot correspond to true and specific olfactory responses, and that probably resulted from the grouping of all eight fish in the same area of the arena at some time points of some experiments. These observations further confirm the appropriateness of using 1-month-old surface fish—which do not yet school intensely—for olfactory tests with these morphotypes. Of note, such an interference of schooling in olfactory responses is irrelevant in the case of cavefish who have lost schooling behavior, as first observed by Parzefall in the field [22].

Finally, the comparative responses of Pachón cavefish from the lab and from the field to amino acids is also worth discussing. Lab-Pachón responded positively (= attraction, like larvae) to alanine, whereas CF-Pachón responded negatively (= repulsion). Moreover, Lab-Pachón response to serine was weak or delayed (if any), whereas CF-Pachón response was strong and immediate. Thus, both lab-raised and wild animals originating from the Pachón cave seem able to detect very low concentrations of amino acids (here, 10^{-7} M), thereby confirming their excellent olfactory skills. However, unexpectedly, their responses to a given odor can differ in nature or intensity. The first hypothesis we can draw relates to the distinct environment in which the lab and wild fish were grown and live, e.g., the water parameters or diet could be at the origin of their difference in reaction. Indeed, the water used in the lab tests (tap water bubbled for 24 h) is “cleaner” than the water used in the field, which, although filtered, is loaded with dissolved organic compounds. It has also been proposed that fish move toward or away from a given amino acid depending on the concentration as well as the age and the species of fish. For example, cysteine acts as a repellent for 1-month-old juvenile zebrafish (3×10^{-5} M; [45]) but as an attractant for rainbow trout (10^{-6} M; [39]). Moreover, olfactory conditioning or learning seems to play an important role in the expression of behavioral responses [46,47]. In the Pachón cave, juveniles feed on micro-arthropods and adults feed on decomposing organic debris and mud [23]. Conversely, in the lab, larvae are fed with micro-worms and artemia nauplii, and juveniles and adults are fed with granules that contain by-products of fish, cereals, vegetables, and crustaceans. Lab-raised fish eat very little decomposing food since they finish their meals in a few minutes. Such differences in feeding experience and odor exposure might explain the differential responses of Lab-Pachón and CF-Pachón. The repulsive behavior after alanine perfusion in the natural cave may suggest that CF-Pachón are exposed to an unpalatable organic matter that gives off alanine. We do not know the amino acids compositions of different organic materials found in this cave. It is therefore difficult to determine which one might be the source of this repulsion. Overall, the sometimes-contrasting responses that we observed in the lab and in the wild reinforce the interest and necessity to assess behavioral repertoires in the natural environment to discuss ecological or evolutionary relevance.

4.3. Not All Cavefish Respond the Same

Our field observations in five different caves lead to one main conclusion: Cavefish from different caves showed very distinctive responses when presented with exogenous odor cues at low concentrations (Table 1). For those that did respond (CF-Pachón, CF-SubT), we can propose that they have augmented olfactory skills when compared to their surface conspecifics, which confirms our previous studies [14,20]. For those which did not respond as well (CF-Sabinos) or did not respond at all (CF-Chica, CF-Tinaja), several questions arise. Is the lack of response due to local environment, previous experience and/or fish condition and nutritional status? Or is it due to experimental conditions?

(1) Let us start with the latter—perhaps less biologically interesting—hypothesis. We cannot rule out that CF-Chica did not respond because the cave water used (although filtered) was so loaded with debris and dissolved organic materials and endogenous olfactory cues that their olfactory

system was saturated and could not detect the low concentrations of amino acids or even chondroitin perfused (see Figure 3E). The same holds true in the Tinaja cave, where carbon content in the mud is high (32%, to be compared to 9.2% in the main pool of Pachón) [24], and, maybe to a lesser extent, in the Sabinos cave (see description in Results). A way to test directly this hypothesis would be to transport “clean” tap water into the caves to perform the experiments. However, we feel that the interest of such experiments would be rather limited, as we anticipate that they would be flawed with other problems and quite demanding in terms of logistics. Nevertheless, future studies examining the physicochemical parameters and the exact nature of compounds present in the water will be important to answer these questions.

(2) The environment-dependent and experience-dependent hypothesis is more scientifically exciting to discuss adaptation to the environment. It implies that the expression of olfactory skills depends on local environment, such as the configuration and ecological parameters of the cave and previous olfactory experiences of the fish related to these local environmental parameters, including possible interactions with other sensory systems and fish nutritional status and motivation to find food.

Indirect support for this hypothesis comes from our finding that CF-Pachón and CF-SubT, which do not belong to the same geographical group of caves and correspond to independently evolved cavefish populations [5,11,48], both show significantly augmented olfactory skills. Thus, this trait most probably corresponds to an evolutionary convergence. This result further suggests that the evolution of food-related (and maybe pheromonal, not addressed here) odor sensing is of paramount importance for cavefish life, adaptation, and survival in the dark. On the other hand, population genetic studies have shown that El Abra cave populations (Pachón, Sabinos, Tinaja, Chica) are genetically close and share many polymorphisms [25,48,49], suggesting that CF-Sab or CF-Tinaja probably carry all or part of the mutations in “olfaction genes” that genetically determine CF-Pachón olfactory skills. However, they do not necessarily express these skills as a consequence of plasticity, with expression depending on the environmental conditions at the precise time and location where we measured olfactory responses. The most striking pieces of evidences in favor of this possibility are discussed below.

CF-Pachón were the smallest among all fish assayed in this study, in agreement with previous measurements [24]. They live in a low-carbon cave (9.2% in the mud), with limited influx of organic matter from the surface. There, foraging must be challenging and strongly olfactory-driven. Conversely, CF-Chica were the largest and biggest among the cavefish that we tested and measured. The very large bat colonies in this “dirty” cave probably render foraging easy, together with fast growth and a long lifespan. CF-Tinaja are also large and old [24] and live in a carbon-rich (31.9%) environment [23]. Strikingly, and in line with these very different trophic environmental conditions, CF-Pachón and CF-Chica (and CF-Tinaja, according to preliminary results) were at the two ends of the spectrum of olfactory responses that we observed.

Vibration attraction behavior (VAB) is thought to help cavefish locate food droppings or vibrating objects at the surface of the water [18,50]. VAB is mediated by neuromasts, and therefore corresponds to a mechanosensory modality. In the field, VAB responses are variable in different caves and even in different ponds of a single cave [51]. In cave ponds where insects are numerous or where percolating water drops are abundant, food search is probably strongly guided by VAB, and less so by the chemosensory olfactory modality. Our results fit well with this idea. Indeed, in the Tinaja cave, where it literally “rains,” or in the Sabinos cave, where we personally witnessed abundant water drops over pool 1 to which the CF-Sab were systematically attracted (SR and A. Alié, pers.obs.), the olfactory sense and skills may not be solicited as much as in the Pachón or Subterráneo caves, where vibrating objects are much rarer and food must be found by the nose. Thus, we propose the possibility of a balanced use of different sensory modalities and expression of sensory skills depending on local conditions. Of note, fish may preferentially use one or the other (or both) sense across their lifespan to find a proper diet and to adapt to different locations where they can swim in a cave, or even across seasonal fluctuations of local ecological conditions.

Finally, cavefish genetics and the hybridization with introgressed surface fish is also a parameter to consider. Whereas Pachón, Sabinos, and Tinaja cavefish are fully troglomorphic (see Figure 4), CF-SubT and CF-Chica correspond to “hybrid-like” populations and carry surface fish alleles (see [14]). Interestingly, the entrance of surface individuals into these two caves does not proceed by the same end: In Subterráneo, surface fish are washed inside the cave from the surface by flooding, whereas, in Chica, surface fish enter the cave by a bottom resurgence. This probably explains why, in Chica, the pool 2 (deeper) fish, which carry more surface alleles, are smaller than the pool 1 (upper) fish, which are less hybridized and more troglomorphic and cave-adapted. In any case, we cannot exclude that the important gene flow from the surface that exists in Chica [25,48] might counteract the effects of cave alleles, favoring the evolution of augmented olfactory skills. Hence, the absence of olfactory responses in CF-Chica might correspond to truly modest olfactory capacities. Deciphering the effects of genetics (presence of surface alleles) from the effects of environmental parameters on plasticity (food-rich cave) or from experimental conditions (odor-saturated water during test) is impossible at this stage. However, it must be noted that the CF-SubT, which also carry surface alleles, responded much better than CF-Chica to the odors we presented: They strongly responded to both alanine and chondroitin. Therefore, in this later case, the effects of hybridization and introgression of surface alleles appears very limited on the behavioral phenotype.

5. Conclusion

Almost 80 years have passed since the first descriptions of ecological conditions in which Chica cavefish live by Charles Breder [52]. Since then, fieldwork in *Astyanax* caves has continuously brought novel information on caves topography, population genetics, and cavefish biology in general. Recently, important examples of insights on the evolution of cavefish behaviors or the evolution of their immune system started from field observations [53,54]. Here, by bringing the “behavior room” into the field, we highlighted the diversity and complexity of the mechanisms that underlie cave adaptation and documented the diversity of cave environments inhabited by a single species of cavefish, *A. mexicanus*. Our data confirm the classical proposal of sensory compensations to the absence of vision in the dark. Indeed, overall cavefish showed lower (i.e., better) olfactory detection thresholds than surface fish. However, the picture appears more complicated than simply “cavefish smell better.” The next challenge will be to disentangle the effects of genetics, plasticity, environment, and their interactions in the evolution of cavefish olfactory system. Then, of course, more fieldwork will be needed to refine behavioral observations and to further describe the diverse natural ecological conditions in which cavefish live.

Supplementary Materials: The following are available online at www.mdpi.com/xxx/s1, Figure S1: Rationale for olfactory scoring. Figure S2: Place preference problem in the Sabinos cave. Video S1: Behavioral response of Pachón cavefish to chondroitin in laboratory settings. Video S2: Behavioral response of Pachón cavefish to chondroitin in natural settings.

Author Contributions: Conceptualization, M.B. and S.R.; methodology, M.B., J.F. and S.R.; validation, M.B. and S.R.; formal analysis, M.B. and S.R.; investigation, all authors; data curation, M.B.; writing—original draft preparation, S.R. and M.B.; writing—review and editing, S.R.; visualization, M.B. and S.R.; supervision, S.R.; project administration, S.R.; funding acquisition, S.R. All authors have read and agreed to the published version of the manuscript.

Funding: This research was funded by CNRS, ANR (Agence Nationale pour la Recherche) grant [BLINDTEST], Fondation pour la Recherche Médicale Equipe FRM grant [DEQ20150331745] to SR, and a French-Mexican Ecos-Nord Exchange Program grant [M15A03] to SR and Patricia-Ornelas Garcia (UNAM, Mexico). The APC was funded by CNRS.

Acknowledgements: We thank Laurent Legendre, Luis Espinasa, Didier Casane, Carole Hyacinthe, Victor Simon, Eric Queinnec, Karen Pottin, Stéphane Rode, Joel Attia and all other past and present members of the Rétaux’s lab for their invaluable help and team spirit during fieldwork over the years. We are grateful to Krystel Saroul for taking care of our lab *Astyanax* colony.

Conflicts of Interest: The authors declare no conflict of interest.

References

- Culver, D.C.; Pipan, T. *The Biology of Caves and Other Subterranean Habitats*; Biology of Habitats Series; 2nd ed.; Oxford University Press: Oxford, UK, 2019. ISBN 978-0-19-882077-2.
- Rétaux, S.; Casane, D. Evolution of eye development in the darkness of caves: Adaptation, drift, or both? *EvoDevo* **2013**, *4*, 26, doi:10.1186/2041-9139-4-26.
- Romero, A. Cave Biology: Life in Darkness. *Integr. Comp. Biol.* **2010**, *50*, 689–691, doi:10.1093/icb/icq067.
- Simon, V.; Hyacinthe, C.; Rétaux, S. Breeding behavior in the blind Mexican cavefish and its river-dwelling conspecific. *PLoS ONE* **2019**, *14*, e0212591, doi:10.1371/journal.pone.0212591.
- Mitchell, R.; Russell, W.; Elliott, W. Mexican eyeless characin fishes, genus *Astyanax*: Environment, distribution, and evolution. *Spec. Publ. Mus. Texas Tech. Univ.* **1977**, *12*, 1–89.
- Elliott, W.R. Cave Biodiversity and Ecology of the Sierra de El Abra Region. In *Biology and Evolution of the Mexican Cavefish*; Elsevier: Amsterdam, The Netherlands, 2016; pp. 59–76. ISBN 978-0-12-802148-4.
- Casane, D.; Rétaux, S. Evolutionary Genetics of the Cavefish *Astyanax mexicanus*. *Adv. Genet.* **2016**, *95*, 117–159, doi:10.1016/bs.adgen.2016.03.001.
- Jeffery, W.R. Chapter 8 Evolution and Development in the Cavefish *Astyanax*. In *Current Topics in Developmental Biology*; Elsevier: Amsterdam, The Netherlands, 2009; Volume 86, pp. 191–221. ISBN 978-0-12-374455-5.
- Keene, A.; Yoshizawa, M.; Mcgaugh, S.E. *Biology and Evolution of the Mexican Cavefish*; Elsevier Science: Amsterdam, The Netherlands, 2015. ISBN 978-0-12-802148-4.
- Espinasa, L.; Legendre, L.; Fumey, J.; Blin, M.; Rétaux, S.; Espinasa, M. A new cave locality for *Astyanax* cavefish in Sierra de El Abra, Mexico. *Subterr. Biol.* **2018**, *26*, 39–53, doi:10.3897/subtbiol.26.26643.
- Elliott, W.R. *The Astyanax Caves of Mexico Cavefishes of Tamaulipas, San Luis Potosí, and Guerrero*; Association for Mexican Cave Studies, PO Box 7672, Austin, Texas 78713, USA: 2018.
- Şadoğlu, P. A mendelian gene for albinism in natural cavefish. *Experientia* **1957**, *13*, 394, doi:10.1007/BF02161111.
- Borowsky, R. Restoring sight in blind cavefish. *Curr. Biol. CB* **2008**, *18*, R23–R24, doi:10.1016/j.cub.2007.11.023.
- Bibliowicz, J.; Alié, A.; Espinasa, L.; Yoshizawa, M.; Blin, M.; Hinaux, H.; Legendre, L.; Père, S.; Rétaux, S. Differences in chemosensory response between eyed and eyeless *Astyanax mexicanus* of the Rio Subterráneo cave. *EvoDevo* **2013**, *4*, 25, doi:10.1186/2041-9139-4-25.
- Fumey, J.; Hinaux, H.; Noirot, C.; Thermes, C.; Rétaux, S.; Casane, D. Evidence for late Pleistocene origin of *Astyanax mexicanus* cavefish. *BMC Evol. Biol.* **2018**, *18*, 43, doi:10.1186/s12862-018-1156-7.
- Policarpo, M.; Fumey, J.; Lafargeas, P.; Naquin, D.; Thermes, C.; Naville, M.; Dechaud, C.; Wolff, J.-N.; Cabau, C.; Klopp, C.; et al. Contrasting gene decay in subterranean vertebrates: Insights from cavefishes and fossorial mammals. *Mol. Biol. Evol.* **2020**, doi:10.1093/molbev/msaa249.
- Yamamoto, Y.; Byerly, M.S.; Jackman, W.R.; Jeffery, W.R. Pleiotropic functions of embryonic sonic hedgehog expression link jaw and taste bud amplification with eye loss during cavefish evolution. *Dev. Biol.* **2009**, *330*, 200–211, doi:10.1016/j.ydbio.2009.03.003.
- Yoshizawa, M.; Gorički, Š.; Soares, D.; Jeffery, W.R. Evolution of a Behavioral Shift Mediated by Superficial Neuromasts Helps Cavefish Find Food in Darkness. *Curr. Biol.* **2010**, *20*, 1631–1636, doi:10.1016/j.cub.2010.07.017.
- Blin, M.; Tine, E.; Meister, L.; Eliot, Y.; Bibliowicz, J.; Espinasa, L.; Rétaux, S. Developmental evolution and developmental plasticity of the olfactory epithelium and olfactory skills in Mexican cavefish. *Dev. Biol.* **2018**, *441*, 242–251, doi:10.1016/j.ydbio.2018.04.019.
- Hinaux, H.; Devos, L.; Blin, M.; Eliot, Y.; Bibliowicz, J.; Alié, A.; Rétaux, S. Sensory evolution in blind cavefish is driven by early embryonic events during gastrulation and neurulation. *Development* **2016**, *143*, 4521–4532, doi:10.1242/dev.141291.
- Torres-Paz, J.; Hyacinthe, C.; Pierre, C.; Rétaux, S. Towards an integrated approach to understand Mexican cavefish evolution. *Biol. Lett.* **2018**, *14*, doi:10.1098/rsbl.2018.0101.
- Parzefall, J. Field observation in epigean and cave populations of the Mexican characid *Astyanax mexicanus* (Pisces, Characidae). *Mémoires de biospéologie* **1983**, *10*, 171–176.
- Espinasa, L.; Bonaroti, N.; Wong, J.; Pottin, K.; Queinnec, E.; Rétaux, S. Contrasting feeding habits of post-larval and adult *Astyanax* cavefish. *Subterr. Biol.* **2017**, *21*, 1–17, doi:10.3897/subtbiol.21.11046.

24. Simon, V.; Elleboode, R.; Mahé, K.; Legendre, L.; Ornelas-Garcia, P.; Espinasa, L.; Rétaux, S. Comparing growth in surface and cave morphs of the species *Astyanax mexicanus*: Insights from scales. *EvoDevo* **2017**, *8*, doi:10.1186/s13227-017-0086-6.
25. Pierre, C.; Pradère, N.; Froc, C.; Ornelas-García, P.; Callebert, J.; Rétaux, S. A mutation in monoamine oxidase (MAO) affects the evolution of stress behavior in the blind cavefish *Astyanax mexicanus*. *J. Exp. Biol.* **2020**, doi:10.1242/jeb.226092.
26. Strecker, U.; Bermatchez, L.; Wilkens, H. Genetic divergence between cave and surface populations of *Astyanax* in Mexico (Characidae, Teleostei). *Mol. Ecol.* **2003**, *12*, 699–710, doi:10.1046/j.1365-294x.2003.01753.x.
27. Mathuru, A.S.; Kibat, C.; Cheong, W.F.; Shui, G.; Wenk, M.R.; Friedrich, R.W.; Jesuthasan, S. Chondroitin fragments are odorants that trigger fear behavior in fish. *Curr. Biol. CB* **2012**, *22*, 538–544, doi:10.1016/j.cub.2012.01.061.
28. Pfeiffer, W. [On the heredity of the fear reaction in *Astyanax* (Characidae, pisces)]. *Zeitschrift fur Vererbungslehre* **1966**, *98*, 97–105.
29. Parzefall, J.; Fricke, D. Alarm reaction and schooling in population hybrids of *Astyanax fasciatus* (Pisces, Characidae). *Memoires e Biospeologie* **1991**, *18*, 29–32.
30. VideoLan. VLC Media Player. 2006. Available online: <https://www.videolan.org/vlc/index.html> (accessed on 1st February 2010).
31. Pérez-Escudero, A.; Vicente-Page, J.; Hinz, R.C.; Arganda, S.; de Polavieja, G.G. idTracker: Tracking individuals in a group by automatic identification of unmarked animals. *Nat. Methods* **2014**, *11*, 743–748, doi:10.1038/nmeth.2994.
32. R Core Team. R: *A Language and Environment for Statistical Computing*; R Foundation for Statistical Computing: Vienna, Austria. 2017. Available online: <https://www.R-project.org/> (accessed on 1 February 2018).
33. RStudio Team. *RStudio: Integrated Development for R*; RStudio, PBC: Boston, MA, USA. Springer-Verlag: New York, NY, USA, 2020. Available online: <http://www.rstudio.com/> (accessed on 1 February 2018).
34. Alboukadel Kassambara rstatix: Pipe-Friendly Framework for Basic Statistical Tests. R package version 0.5.0. 2020. Available online: <https://CRAN.R-project.org/package=rstatix> (accessed on 1 February 2020).
35. Wickham, H. *ggplot2: Elegant Graphics for Data Analysis*; Springer-Verlag New York, NY, USA, 2016. ISBN 978-3-319-24277-4. 2016. Available online: <https://ggplot2.tidyverse.org> (accessed on 1 February 2020).
36. Wickham, H.; Averick, M.; Bryan, J.; Chang, W.; McGowan, L.D.A.; François, R.; Grolemund, G.; Hayes, A.; Henry, L.; Hester, J.; et al. Welcome to the tidyverse. *J. Open Sour. Softw.* **2019**, *4*, 1686.
37. Elipot, Y.; Legendre, L.; Père, S.; Sohm, F.; Rétaux, S. Astyanax transgenesis and husbandry: How cavefish enters the laboratory. *Zebrafish* **2014**, *11*, 291–299, doi:10.1089/zeb.2014.1005.
38. Hara, T.J. Olfaction and gustation in fish: An overview. *Acta Physiol. Scand.* **1994**, *152*, 207–217, doi:10.1111/j.1748-1716.1994.tb09800.x.
39. Hara, T.J. Feeding behaviour in some teleosts is triggered by single amino acids primarily through olfaction. *J. Fish. Biol.* **2006**, *68*, 810–825, doi:10.1111/j.0022-1112.2006.00967.x.
40. Friedrich, R.W.; Korschning, S.I. Combinatorial and chemotopic odorant coding in the zebrafish olfactory bulb visualized by optical imaging. *Neuron* **1997**, *18*, 737–752, doi:10.1016/s0896-6273(00)80314-1.
41. Frisch, K. Die Bedeutung des Geruchsinnes im Leben der Fische. *Süffert F Ed. Naturwissenschaften* **1941**, 321–333, doi:10.1007/BF01481736
42. Døving, K.B.; Lastein, S. The alarm reaction in fishes-odorants, modulations of responses, neural pathways. *Ann. N. Y. Acad. Sci.* **2009**, *1170*, 413–423, doi:10.1111/j.1749-6632.2009.04111.x.
43. Fricke, D. Reaction to Alarm Substance in Cave Populations of *Astyanax fasciatus* (Characidae, Pisces). *Ethology* **1987**, *76*, 305–308, doi:10.1111/j.1439-0310.1987.tb00691.x.
44. Kowalko, J. Utilizing the blind cavefish *Astyanax mexicanus* to understand the genetic basis of behavioral evolution. *J. Exp. Biol.* **2020**, *223*, doi:10.1242/jeb.208835.
45. Vitebsky, A.; Reyes, R.; Sanderson, M.J.; Michel, W.C.; Whitlock, K.E. Isolation and characterization of the laure olfactory behavioral mutant in the zebrafish, *Danio rerio*. *Dev. Dyn.* **2005**, *234*, 229–242, doi:10.1002/dvdy.20530.
46. Braubach, O.R.; Wood, H.-D.; Gadbois, S.; Fine, A.; Croll, R.P. Olfactory conditioning in the zebrafish (*Danio rerio*). *Behav. Brain Res.* **2009**, *198*, 190–198, doi:10.1016/j.bbr.2008.10.044.

47. Valentinčić, T.; Wegert, S.; Caprio, J. Learned olfactory discrimination versus innate taste responses to amino acids in channel catfish (*Ictalurus punctatus*). *Physiol. Behav.* **1994**, *55*, 865–873, doi:10.1016/0031-9384(94)90072-8.
48. Bradic, M.; Beerli, P.; García-de León, F.J.; Esquivel-Bobadilla, S.; Borowsky, R.L. Gene flow and population structure in the Mexican blind cavefish complex (*Astyanax mexicanus*). *BMC Evol. Biol.* **2012**, *12*, 9, doi:10.1186/1471-2148-12-9.
49. Avise, J.C.; Selander, R.K. Evolutionary genetics of cave-dwelling fishes of the genus astyanax. *Evol. Int. J. Org. Evol.* **1972**, *26*, 1–19, doi:10.1111/j.1558-5646.1972.tb00170.x.
50. Yoshizawa, M.; Jeffery, W.R. Evolutionary tuning of an adaptive behavior requires enhancement of the neuromast sensory system. *Commun. Integr. Biol.* **2011**, *4*, 89–91, doi:10.4161/cib.4.1.14118.
51. Espinasa, L.; Heintz, C.; Rétaux, S.; Yoshisawa, M.; Agnès, F.; Ornelas-Garcia, P.; Balogh-Robinson, R. Vibration Attraction Response (VAB) is a plastic trait in Blind Mexican tetra (*Astyanax mexicanus*), variable within subpopulations inhabiting the same cave. *J. Fish. Biol.* *in press*. doi: 10.1111/jfb.14586.
52. Breder, C.M. Descriptive ecology of La Cueva Chica, with especial reference to the blind fish, *Anoptichthys. Zoologica* **1942**, *27*, 7–15.
53. Hyacinthe, C.; Attia, J.; Rétaux, S. Evolution of acoustic communication in blind cavefish. *Nat. Commun.* **2019**, *10*, 4231, doi:10.1038/s41467-019-12078-9.
54. Peuß, R.; Box, A.C.; Chen, S.; Wang, Y.; Tsuchiya, D.; Persons, J.L.; Kenzior, A.; Maldonado, E.; Krishnan, J.; Scharsack, J.P.; et al. Adaptation to low parasite abundance affects immune investment and immunopathological responses of cavefish. *Nat. Ecol. Evol.* **2020**, doi:10.1038/s41559-020-1234-2.



© 2020 by the authors. Licensee MDPI, Basel, Switzerland. This article is an open access article distributed under the terms and conditions of the Creative Commons Attribution (CC BY) license (<http://creativecommons.org/licenses/by/4.0/>).

Annexe 2

***gdf6b* expression in fish gonads using *in situ* hybridization**

cDNA cloning

Total RNA was extracted from different staged Pachón cavefish embryos using TRIzol (Invitrogen, Carlsbad, USA) and chloroform, purified with isopropanol and 70% ethanol, and finally treated with DNase (Invitrogen, Carlsbad, USA). Following purification, total RNA concentration was measured with a NanoVue Spectrophotometer and stored at -80°C. Subsequently, 2 µg of RNA supplemented by 10 mM dNTP were reverse transcribed with random hexamer primers using AMV reverse transcriptase (Promega, Madison, USA) during 60 minutes at 37°C. *gdf6b* transcript sequence in *A. mexicanus* was identified by aligning sequences collected from Ensembl database (<http://www.ensembl.org/index.html>, release 93, July 2018) and Phylofish database (<http://phylofish.sigenae.org/index.html>) used with BLAST-based search (Pasquier et al., 2016). A 634 bp fragment was amplified in *A. mexicanus* and purified with Nucleospin Gel and PCR Clean-up (Machery-Nagel, Düren, Germany). Subsequently, PCR products were cloned into pGEM-T Easy Vector (Promega, Madison, USA) and purified using NucleoSpin plasmid DNA purification kit (Machery-Nagel, Düren, Germany) according to the supplier's indications. PCR products were sequenced by Sanger method before probe synthesis (<https://www.eurofinsgenomics.eu/en/custom-dna-sequencing/gatc-services/>).

Whole-mount in situ hybridization

For *in situ* hybridization (ISH), Pachón cave *A. mexicanus* of 16, 23, and 30 days post-fertilization (dpf) stage were collected. They were fixed in 4% paraformaldehyde (PFA) and phosphate buffer 0.12 M (PBS, pH7.4) at 4°C for 24 hours (h). Following fixation, specimens were thoroughly washed 5 times (10 min each) at room temperature in 1X PBS, then gradually dehydrated in increasing methanol concentration baths for 10 minutes (min) each (75% PBS/25% MeOH, 50% PBS/50% MeOH, 25% PBS/75% MeOH, and 100% MeOH), and finally stored in methanol 100% at -20°C until use. The expression patterns of *gdf6b* were analyzed in 16, 23, and 30 dpf fishes. A *gdf6b* RNA probe of 634 bp was obtained with the digoxigenin (Dig) RNA labelling mix kit from Roche from cDNA template with T7 polymerase and purified using Nucleospin RNA purification (Machery-Nagel, Düren, Germany). Cavefish specimens were progressively rehydrated by graded baths of PBS solution mixed with decreasing concentrations of MeOH and permeabilized by proteinase K concentrated at 100

μ g/ml (Sigma) during 40 min followed by a post-fixation step in 4% PFA. They were incubated overnight during 16 hr at 65 °C in a hybridization buffer containing the probes at 60 ng/ μ l. After stringent washes, the hybridized probes were detected by immunohistochemistry using an alkaline phosphatase-conjugated antibody against digoxigenin diluted at 1/6000 (Roche) and a NBT/BCIP chromogenic substrate (Roche).

Annexe 3

Additive transgenesis with *gdf6b* constructs

Based on the pool-seq data, we reconstituted the consensus sequences of *gdf6b-B* (containing 2231 bp of the proximal promoter and 1328 of the cDNA + 3'UTR) and *gdf6b-A* (encompassing 2144 bp of the proximal promoter and 1328 of the cDNA + 3'UTR). For both sequences, we added two restriction sites on both ends of the cDNA+3'UTR (Kpn1 to the 5'UTR end and Not1 to the 3'UTR end). Two meganuclease sites (ISceI) were also added on both ends of the whole construction (5'UTR and 3'UTR) (Figure 1). Both constructs were then synthesized separately and cloned in a pUC18 vector (GenScript).

Following these steps, both constructs were double digested in separate tubes containing 10 µg of each plasmid, 1X multiCore buffer (10X), 1.5 µl of Kpn1 (Promega), 2 µl of Not1 (Promega) and finally q.s to 60 µl total volume of nuclease-free water. The tubes were then incubated overnight at 37 °C. Subsequently, digestion products were electrophoresed in a 1.6 % agarose gel and resulting bands (cDNAs and pUC18+promoters) were purified separately using a NucleoSpin Gel and PCR clean up purification kit (Machery-Nagel, Düren, Germany) according to the supplier's indications. Following the purification step, *gdf6b-B*-cDNA + *gdf6b-A*-promoter and *gdf6b-A*-cDNA + *gdf6b-B*-promoter were ligated in two separate tubes containing 1 ng of DNA plasmids, 3 ng of each cDNA and 1µl of T4 DNA Ligase Buffer (10X), 1µl of T4 DNA ligase and q.s to 10 µl total volume of nuclease-free water, and finally incubated overnight at 4 °C. After ligation, plasmids were transformed into One Shot Top10 chemically competent cells (Invitrogen) according to the supplier's indications. After transformation, colonies with plasmid construct were selected on LB agar plates and purified using a NucleoSpin plasmid purification kit (Machery-Nagel, Düren, Germany) according to the supplier's indications. Cavefish embryos were microinjected at the one-cell stage with a mixture containing each construct at a concentration of 10 ng/µl, 2 µl ISceI buffer (Promega), 1 µl ISceI enzyme and 16 µl nuclease-free water.

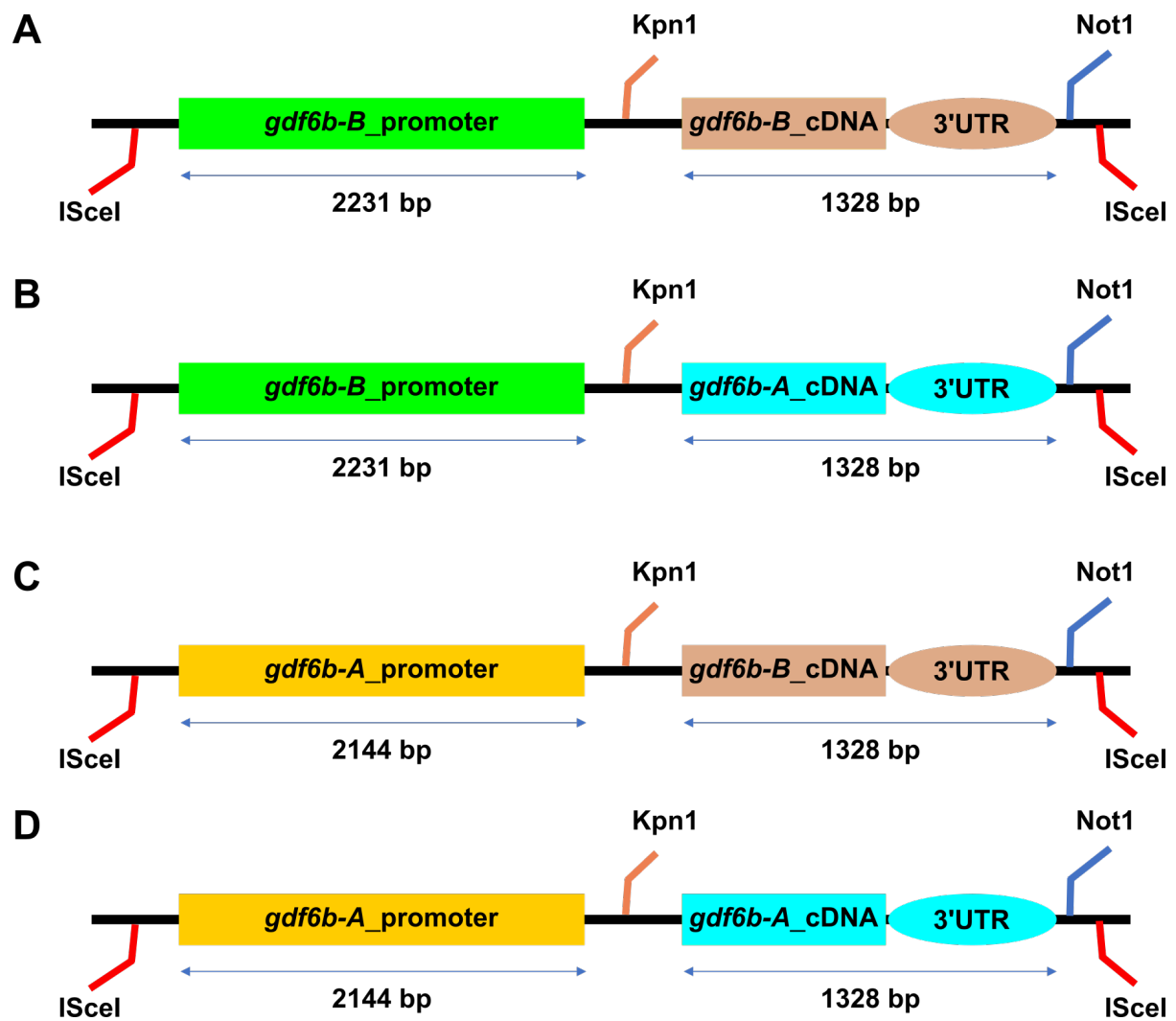


Figure 1. *gdf6b* constructs

Titre : Microévolution des déterminismes sexuels chez le poisson Tétra Mexicain, *Astyanax mexicanus*

Mots clés : Évolution, détermination du sexe, chromosomes B, chromosomes sexuels, *Astyanax mexicanus*, *gdf6b-B*

Résumé : L'évolution des mécanismes de détermination du sexe (SD), qui a souvent été abordée principalement dans un contexte macro-évolutif chez les poissons, montre une variabilité saisissante des gènes SD et de leurs chromosomes sexuels associés. En plus des chromosomes de type A, certaines espèces de poissons téléostéens contiennent des chromosomes B (Bs), qui sont parfois considérés comme des chromosomes sexuels. À ce titre, mon projet de thèse avait pour objectif d'explorer l'évolution des systèmes SD en lien avec les Bs chez le tétra Mexicain, *Astyanax mexicanus*, qui comporte de nombreuses populations cavernicoles (CF) ayant évoluées à partir d'une population ancestrale de surface (SF) il y a moins de 20 000 ans.

Nos travaux apportent des preuves fonctionnelles de l'existence d'un système de SD "original" reposant uniquement sur des chromosomes "B-sexuels" à dominance mâle avec *gdf6b-B* comme potentiel gène déterminant majeur du sexe chez les CF de la grotte Pachón. En parallèle, nous apportons des résultats qui suggèrent qu'il pourrait exister une transition évolutive rapide entre un système de type B-sex chromosome à dominance mâle fixe chez certaines populations vers un système plus complexe (probablement polygénique) ne reposant que partiellement sur le chromosome "B-sexuel" et ses loci *gdf6b-B* chez d'autres populations.

Title: Microevolution of sex determining mechanisms in the Mexican tetra, *Astyanax mexicanus*

Keywords: Evolution, sex determination, B chromosomes, sex chromosomes, cavefish, *gdf6b-B*

Abstract: Sex determining (SD) mechanisms in teleost fishes have been investigated mainly at a macro-evolutionary scale highlighting a high turnover of master SD genes and their associated sex chromosomes. Interestingly, in addition to the A chromosomes, supernumerary B chromosomes (Bs) have been detected in a number of species and even associated as sex chromosomes in some of them. As such, my thesis project aimed to investigate SD mechanisms evolution with respect to these Bs in the Mexican tetra, *Astyanax mexicanus*, in which many blind cave populations (CF) are known to have evolved from a surface ancestral population (SF) less than 20,000 years.

Our results provide functional evidences for the existence of an "unusual" SD system relying solely on male-dominant "B-sex" chromosomes with the *gdf6b-B* gene as a potential MSD gene in the Pachón CF. Furthermore, we also provide results suggesting a rapid evolutionary transition from a fixed male-dominant B-sex chromosome-type system in some populations toward a complex (probably polygenic) SD system relying only partly on the B-sex chromosome and their *gdf6b-B* loci in other populations.